The dose individualisation of oral anticoagulants

Shamin Mohd Saffian

A thesis submitted for the degree of

Doctor of Philosophy

at the University of Otago, Dunedin,

New Zealand.

July 2017

ABSTRACT

Oral anticoagulants are used to treat and prevent blood clots. All anticoagulants carry the risk of bleeding if the systemic exposure is too high, while inadequate exposure will increase the risk of thrombosis. Therefore, the safe and effective use of all oral anticoagulants will require dose individualisation and monitoring. The overarching goal of this thesis is to critically evaluate and explore dose individualisation methods for warfarin and dabigatran therapy to improve patient outcomes.

For warfarin, methods for predicting the maintenance dose were investigated. Specifically, Chapter 2 investigates the predictive performance of a Bayesian dose individualisation tool for warfarin. It was found that the maintenance dose was over-predicted especially in patients requiring higher daily doses and further studies into the source of bias were conducted. Chapter 3 further evaluates whether published warfarin maintenance dose prediction algorithms can accurately predict the observed maintenance dose in patients who require ≥7 mg daily (the upper quartile of dose requirements). A systematic review and meta-analysis was conducted to answer this question. It was found that all warfarin dosing algorithms included in the study under-predicted the maintenance dose in this group of patients.

One common metric to measure predictive performance of a model is the mean prediction error, which is a measure of bias. The work conducted in Chapter 2 and 3 suggests that the mean prediction error may not capture non-constant bias. This is when the predictions systematically deviate away from the line of identity in one direction in relation to the observed data. Chapter 4 proposes new method to assess predictive performance to analyse non-constant systematic deviation from the line of identity. The proposed method is not specific to warfarin, but can be applied to the analysis of predictive performance in general.

For dabigatran dosing, aspects of concentration monitoring as a means of determining a suitable dosing rate were explored. In Chapter 5, an assay using liquid chromatography coupled with tandem mass spectrometry (LC-MS/MS) was developed to measure all active entities of dabigatran concentrations in human plasma. The assay was used to measure dabigatran concentrations collected from a previous study. A *de novo* population pharmacokinetic model was not pursued in the first instance as the data were fairly sparse. Instead, the measured concentrations were used in Chapter 6 in a simulation based study to select an appropriate prior population pharmacokinetic model that might be used in a future Bayesian dose individualisation method for dabigatran. The overall intention of Chapter 6 was to develop a Bayesian dose individualisation method for dabigatran.

In conclusion, this thesis has identified the limitations of current methods for predicting warfarin maintenance dose and has explored dabigatran concentration monitoring as a means of improving dabigatran dosing. Models for predicting warfarin maintenance dose were critically evaluated and it was found that all existing models can not accurately predict the maintenance dose in patients requiring higher daily doses. An improvement in the method to assess predictive performance was proposed. The work conducted in this thesis on dabigatran dosing provides the basis for future research to individualise dosing and monitoring using population pharmacokinetic models.

ACKNOWLEDGMENTS

I would like to express my deepest gratitude to my supervisors, Dr Dan Wright, Professor Stephen Duffull and Dr Paul Chin for their patience in guiding me through this journey. The few words that I have to say about them do not do justice to their tireless contributions in supervising and mentoring me through research. All three of them have given their time freely and have been generous in sharing their knowledge. Their encouragement, enthusiasm, passion and bright insights have made my time spent on my research meaningful and fulfilling.

I would like to thank Berit, Mei Zhang and the team at Canterbury Health Lab for their invaluable help and guidance for the bioanalytical assay project. Berit and Mei Zhang have been instrumental towards my understanding of assay validation and LC-MSMS techniques.

Many thanks to all my colleagues in the Otago Pharmacometrics Group who were or are in the same boat – Hesh, Vittal, Tom & Shan, Jill, Mohammed, Derek, Vijay, Sudeep, Jaydeep, and Isabelle. Also to the others who have spent some time in the lab – Chihiro, Zheng Liu, Mathilde, Marion, Alina, Fabian, Juin, Natalie, Dharsh and others who have slipped my memory. Thank you for the good humour, free-flow coffee and lunches together. A special thanks to Qing Xi for being the lab mother, for helping me in understanding difficult concepts, for bouncing ideas with me and for printing my thesis.

I would also like to thank the staff members, both academic and administrative staff, and research students of school of Pharmacy for their friendship and assistance. You have all provided invaluable experience. Thanks to Brian and Tim for providing support for any hardware/software problems.

I am grateful to the Ministry of Higher Education Malaysia and The National University of Malaysia for their co-sponsorship of my PhD. I am also thankful to the School of Pharmacy for supporting my tuition fees and stipend in the last year of my study.

I would also like to express my greatest appreciation and admiration to my lovely wife, Hanisah, who have endured all my complains, grumpy days, late nights and weekends in the lab. My two little twins, Furqan and Nuha, have provided all the spirit and motivation for me to go on and to never give up.

I would also like to thank my dearest sister, Soraya, my brother, Gerald, and to my parents who have been very supportive of my studies in all ways they could have.

PUBLICATIONS

THAT HAVE ARISEN FROM WORK ASSOCIATED WITH THIS THESIS

Three papers are described in this thesis. Another paper was work completed prior to my PhD, but was published during my PhD candidature. A list of author contributions for each of the publication is provided in Appendix I.

International peer-reviewed journals described in this thesis

1. Saffian SM, Zhang M, Leong Chin PK, Jensen BP. *Quantification of dabigatran and indirect quantification of dabigatran acylglucuronides in human plasma by LC-MS/MS*. Bioanalysis 2015; 7: 957-66. (Bioanalysis Zone Editor's choice).

2. Saffian SM, Duffull SB, Roberts RL, Tait RC, Black L, Lund KA, Thomson AH, Wright DF. *Influence of Genotype on Warfarin Maintenance Dose Predictions Produced Using a Bayesian Dose Individualization Tool*. Therapeutic drug monitoring 2016; 38: 677-83.

3. Saffian, SM, Duffull SB, Wright DFB. *Warfarin dosing algorithms under-predict dose requirements in patients requiring ≥ 7mg daily: A systematic review and meta-analysis.* Clinical Pharmacology & Therapeutics 2017; 102(2):297-304.

Other International peer-reviewed journals not described in this thesis

1. Saffian SM, Wright DF, Roberts RL, Duffull SB. *Methods for Predicting Warfarin Dose Requirements.* Therapeutic Drug Monitoring 2015; 37: 531-8.

Oral Presentations

1. Saffian S, Wright D, Roberts R, Tait R, Black L, Lund K, Thomson A, Duffull S, (2014*). The influence of CYP2C9 and VKORC1 genotype on the predictive performance of a Bayesian forecasting method for warfarin therapy*. Population Approach Group in Australia and New Zealand (PAGANZ), Dunedin, New Zealand
2. Saffian S, Zhang M, Chin P, Jensen B (2014). *An LC-MS/MS assay for the indirect quantification of dabigatran acyl glucuronide*. The Australasian Society of Clinical and Experimental Pharmacologists & Toxicologists (ASCEPT), Queenstown, New Zealand.
3. Saffian S, Wright D, Duffull S, (2015). *A suggestion on determining systematic bias when measuring predictive performance*. Population Approach Group in Australia and New Zealand (PAGANZ), Melbourne, Australia
4. Saffian S, Duffull S, Tait R, Black L, Lund K, Thomson A, Wright D, (2015). *Current warfarin dose prediction tools do not accurately predict the maintenance dose of warfarin for patients requiring above 7mg/day*. The Australasian Society of Clinical and Experimental Pharmacologists & Toxicologists (ASCEPT), Queenstown, New Zealand
5. Saffian S, Duffull S, Wright D, (2016). *An evaluation of warfarin dose prediction methods*. The Australasian Society of Clinical and Experimental Pharmacologists & Toxicologists (ASCEPT), Nelson, New Zealand

Poster Presentations

1. Saffian S, Duffull S, Wright D, (2016). *Warfarin dose prediction tools do not work for patients who need it*. World Conference on Pharmacometrics (WCoP), Brisbane, Australia

TABLE OF CONTENTS

LIST OF FIGURES

LIST OF TABLES

LIST OF EQUATIONS

ABBREVIATIONS

AF	Atrial fibrillation
aPTT	Activated partial thromboplastin time test
BD	Twice daily
BIBR951	Dabigatran intermediate metabolite
BSA	Body surface area
BSV	Between subject variability
CES	Carboxylesterase
CI	Confidence interval
CL	Clearance
CLCR	Creatinine clearance
CV	Coefficient of variation
CYP	Cytochrome P450
CVA	Cerebrovascular accident
DAG	Dabigatran acyl glucuronide
DMSO	Dimethyl sulfoxide
dTT	Diluted thrombin time
DVT	Deep vein thrombosis
E	Drug effect
EC50	Drug concentration resulting in half maximal effect
ECT	Ecarin clotting time
EDTA	Ethylenediaminetetraacetic acid
EFF	Inhibitory effect on vitamin K epoxide reductase
EMA	European Medical Agency
ESI	Electrospray ionization
F	Fractional oral bioavailability
FDA	Food and Drug Administration
GGCX	Gamma-Glutamyl Carboxylase
HCL	Hydrochloric acid
HPLC	High performance liquid chromatography
HQC	High quality control
HVR	Heart valve replacement
INR	International normalised ratio
IQR	Interquartile range
ISI	International sensitivity index
k	A proportionality constant
Kg	kilogram
k_i	Inhibitory constant
KPD	Kinetic Pharmacodynamic

KS test	Kolmogorov-Smirnov test
L	Litre
LC-MS/MS	Liquid chromatography-tandem mass spectrometry/ mass spectrometry
LLOQ	Lower limit of quantification
LQC	Low quality control
MAP	Maximum a posteriori
MDR	Maintenance dose rate
MPE	Mean prediction error
MQC	Mid quality control
MSE	Mean squared error
mL	Millilitre
MTT	Mean transit time
NA	Not available
NAOH	Sodium hydroxide
ng	Nanogram
N_{max}	total number of bins
NPDE	Normalized prediction distribution error
NZ	New Zealand
OD	Once daily
OS	Orthopaedic Surgery
pcVPC	Prediction- and variability-corrected VPC
PE	Pulmonary embolism
P-gp	P-glycoprotein
QC	Quality control
RMSE	Root mean squared error
SD	Standard deviation
SNP	Single nucleotide polymorphism
TIA	Transient Ischaemic Attack
T_{max}	Time to reach maximum concentration
TTR	Percentage time within therapeutic range
V	Volume of distribution
VPC	Visual predictive check
VTE	Venous thromboembolism

INDICES AND SYMBOLS

B	Number of bound receptors
B_{max}	Maximum binding capacity
C_{free}	Concentration of dabigatran without alkaline hydrolysis
$C_{ss,ave}$	Average steady-state concentration
C_{total}	Concentration of dabigatran after alkaline hydrolysis
k_a	Absorption rate constant
K_d	Dissociation rate constant
k_e	Elimination rate constant
k_{off}	Rate of disassociation of a drug receptor complex
k_{on}	Rate of formation of a drug receptor complex
INR_{max}	Maximum theoretical INR
INR_{pred}	Predicted INR
$INR_{baseline}$	Baseline INR
γ	Hill coefficient
τ	Dosing interval
σ^2	Variance
θ	A vector of individual parameter estimates

STRUCTURE OF THE THESIS

The thesis is divided into six parts (Table P.1). **Part I** includes an introduction to dose individualisation methods, an overview of pharmacokinetics and pharmacodynamics and models for predicting drug responses, and a literature review on oral anticoagulants.

Part II focuses on methods to individualise warfarin maintenance dose. Chapter 2 investigates a Bayesian forecasting method for warfarin dosing. The predictive performance of warfarin dosing tools will be evaluated in Chapter 3.

Part III includes Chapter 4 which proposes a revision to the method for evaluating predictive performance using the mean prediction error.

Part IV focuses on exploring aspects of dabigatran concentration monitoring. Chapter 5 describes the development and validation of an assay to measure dabigatran and its active metabolite (dabigatran acyl glucuronide) in human plasma and measures plasma concentration available from a previous study. Chapter 6 uses concentration measurements obtained from Chapter 5 in a simulation based study to determine an appropriate model for dose individualisation of dabigatran in the future.

Part V concludes the thesis with a discussion of the findings and future research.

Part VI includes the appendices which provide contain additional material related to the individual chapters, including author contribution for published papers described in this thesis, figures, MATLAB® code, and references.

Table P.1 Overview of the thesis

Part I	**Introduction**
	Chapter 1. Introduction
Part II	**Warfarin dosing**
	Chapter 2. Investigating warfarin maintenance dose predictions using a Bayesian forecasting method
	Chapter 3. An evaluation of warfarin dosing tools in patients requiring ≥ 7mg daily
Part III	**Predictive performance**
	Chapter 4. An approach for testing non-constant deviation associated with the magnitude of the observation
Part IV	**Dabigatran dosing**
	Chapter 5. Quantification of dabigatran and dabigatran acyl glucuronides in human plasma by LC-MS/MS
	Chapter 6. Evaluation and selection of a prior dabigatran population pharmacokinetic model for dose individualisation
Part V	**Discussion and Conclusion**
	Chapter 7. Discussion and Conclusion
Part VI	**Appendices**
	Appendix 1. Appendices to Preface
	Appendix 2. Appendices to Chapter 3
	Appendix 3. Appendices to Chapter 4
	Appendix 4. Appendices to Chapter 6
	References

PART I

INTRODUCTION

Chapter 1: Introduction

1.1. Introduction to the thesis

Anticoagulants are used to treat and prevent blood clots. The physiological response to anticoagulant therapy is a prolonged clotting time. Therefore, the use of anticoagulants will carry an increased risk of bleeding if drug exposure is too high while inadequate exposure carries an increased risk of thrombosis. Hence, successful treatment with anticoagulant drugs requires the prescriber to select a maintenance dose rate that will balance the need for adequate anticoagulation without over- or under-anticoagulating the patient.

The overarching assumption of the work conducted in this thesis is that all anticoagulants will require monitoring of clotting times or drug exposure to ensure their safe and effective use. Two oral anticoagulants, warfarin and dabigatran, are examined in this thesis.

Warfarin has been used clinically for over 70 years. Despite this long history, the dosing of warfarin remains a challenge in the clinic. A large number of warfarin dosing aids have been developed to improve anticoagulation control. Bayesian forecasting methods have been proposed as a means of guiding dose selection using routinely collected anticoagulation response data, such as clotting time [1, 2]. Chapter 2 investigates the predictive performance of a Bayesian dosing tool for warfarin therapy.

Recent publications advocate for the *a priori* prediction of warfarin maintenance doses, using empirically-derived algorithms based on patient characteristics known to influence warfarin dosing requirements between patients [3, 4]. There have been a large number of dosing algorithms published over the past 10 years but there is a limited understanding of how these tools perform in routine clinical practice. In particular, there are few studies to date comparing the predictive performance of different warfarin dosing algorithms against each other. Work conducted in this thesis raises the concern that warfarin dosing aids may not perform well in patients who require larger daily doses. Chapter 3 presents a meta-analysis of published dosing algorithms with a

particular emphasis on the predictive performance in those patients who require doses greater than 7 mg daily (the upper quartile of dose requirements).

Chapter 4 presents a new methodology to evaluate the performance of tools designed to predict dose requirements. This method can be viewed as both an expansion of, and complimentary to, the method involving mean prediction error proposed by Sheiner and Beal [5].

Dabigatran is an oral anticoagulant first approved in October 2010 in the United States [6, 7] and in July 2011 in New Zealand [8, 9]. The manufacturer recommends a fixed dose for most patients, with dose modification based on patient characteristics such as renal function [9]. Importantly, the drug was marketed as an alternative to warfarin that did not require the monitoring of clotting time to evaluate anticoagulant response. There is evidence to suggest that the dosing guidelines for dabigatran may lead to over- or under-exposure of dabigatran and thus bleeding and thrombosis (treatment failure) [10], respectively. Therefore, this thesis will explore aspects of dabigatran dose individualisation, including the measuring and monitoring of plasma concentrations as a means of guiding dose selection. Specifically, Chapter 5 and 6 describe the development of an assay for dabigatran and its active metabolite and an evaluation of published dabigatran pharmacokinetic models as a means of predicting dose requirements.

1.1.1. Aims of the thesis

The overarching goal of this thesis is to critically evaluate and explore aspects of dose individualisation for warfarin and dabigatran therapy.

There are three specific objectives;

a. To critically evaluate dose prediction methods for warfarin therapy (Chapters 2 and 3)
b. To propose a method for evaluating the predictive performance of dose prediction methods (Chapter 4)

c. To explore aspects of dabigatran dose individualisation related to plasma drug concentration monitoring (Chapter 5 and 6).

1.1.2. Structure of the introduction

The introduction will present background material relevant to the experimental work conducted for this doctoral thesis as follows;

- Section 1.2 - Models for predicting dose requirements
- Section 1.3 - A conceptual framework for dose individualisation methods
- Section 1.4 - Anticoagulants considered in this thesis

1.2. Models for predicting dose requirements

1.2.1. A population pharmacokinetics-pharmacodynamics (PKPD) approach

This section briefly describes salient points of a model based approach to dosing that are investigated in this thesis. Note that estimation of model parameters will not be covered (a minor part of the thesis presented here).

Population pharmacokinetics-pharmacodynamic models provide a means of defining the typical time course of drug concentrations in the plasma, the time course of drug effects, and different sources of variability. In addition, a population model provides estimates of between subject variability in model parameters (e.g. clearance, volume), covariate effects, and random variability. This provides the basis for dose individualisation as it allows individual patient characteristics (i.e. covariates) that predict differences in drug response to be identified and accounted for.

1.2.1.1. Pharmacokinetic models

Pharmacokinetics describes the time course of drug concentrations in the body [11]. The simplest pharmacokinetic model is a one-compartment model where the drug is assumed to be distributed instantaneously throughout the compartment. The concentration at any time can be calculated as:

$$C(t) = \frac{D}{V} \times exp^{\left(-\frac{CL}{V} \times t\right)}$$

Equation 1.1 *Equation for one-compartment linear pharmacokinetic model after intravenous bolus*

where C is the plasma concentration as a function of t, D is the dose, V is the apparent volume into which the drug distributes, CL is the clearance and t is time. Clearance links the rate of elimination and concentration of drug in body and is related to functional capacity of the body to remove drugs [12]. Volume of distribution reflects structural aspects of the body and is related to body composition [12]. A secondary parameter, the elimination rate constant (k_e) is given by $\frac{CL}{V}$.

For oral dosing, the fraction that reaches the circulation is often less than the dose taken due to incomplete absorption and first pass metabolism in the liver. Therefore 2 more parameters are needed for oral dosing; bioavailability (F) and absorption rate constant (k_a) and the concentration as a function of time can be given by:

$$C(t) = \frac{D \times F \times k_a}{V \times (k_a - k_e)} \times (exp^{(-k_e \times t)} - exp^{(-k_a \times t)})$$

Equation 1.2 *The equation for a one compartment pharmacokinetic model with first-order absorption and elimination*

When the drug is taken repeatedly, the concentration will approach a steady-state where the amount of drug entering the body and the amount of drug leaving the body are equal. Under these conditions, the steady-state average concentration ($C_{ss,ave}$) can be calculated using Equation 1.3:

$$C_{ss,ave} = \frac{Dose \times F}{CL \times \tau}$$

Equation 1.3 *The equation for calculating steady-state concentration*

where τ is the dosing interval.

1.2.1.2. Pharmacodynamic models

Pharmacodynamics is the science that describes the relationship between drug concentrations and the observed pharmacological response [13]. Most drug action can be attributed to the binding of the drug to the receptor [14]. Mathematically, assuming 1:1 stoichiometry, the binding of drug to the receptor can be expressed using Equation 1.4 where the drug (D) binds to a receptor site (R) to form an activated drug-receptor complex (DR).

$$D + R \underset{k_{off}}{\overset{k_{on}}{\rightleftarrows}} DR$$

Equation 1.4 *Binding of a drug to a receptor*

where k_{on} is the association rate constant of a drug to the receptor and k_{off} is the dissociation rate constant.

At equilibrium, the dissociation constant (k_d) represents the inverse of the affinity of the drug for the receptor which is given by the ratio k_{off} and k_{on} as follows;

$$k_d = \frac{k_{off}}{k_{on}}$$

Equation 1.5 *Dissociation constant at equilibrium*

Subsequently, assuming that all receptors are available for the drug to bind, the receptor binding equation can be expressed as:

$$B = B_{max} \times \frac{C}{k_d + C}$$

Equation 1.6 *Receptor binding equation, the Bmax model*

where B is the number of bound receptors, C is the drug concentration, B_{max} is the maximum binding capacity when all receptors are occupied.

In clinical practice, receptor binding information is not available, but the pharmacological effect can be measured. If we assume the drug effect is

proportional to B [15], then drug effects (E) can be linked to B using a proportionality constant as follows:

$$E = k \times B$$

Equation 1.7 *Drug effect following receptor binding*

where k is a proportionality constant that links the receptor occupancy with effect (E).

Drug effect (E) can be described using the E_{max} model:

$$E = E_{max} \times \frac{C}{EC_{50} + C}$$

Equation 1.8 *An E_{max} model*

Here, two parameters of interest are E_{max} which is the maximum effect, and EC_{50} which is the concentration of drug at 50 % of maximum drug effect.

The E_{max} model can be generalised to allow different steepness of the slope of the concentration-effect relationship. This is called the sigmoidal E_{max} model where concentration is exponentiated with the Hill coefficient.

$$E = E_{max} \times \frac{C^{\gamma}}{EC_{50}^{\gamma} + C^{\gamma}}$$

Equation 1.9 *A sigmoidal E_{max} model*

Figure 1.1 depicts the sigmoidal E_{max} concentration-effect relationship with different Hill coefficients.

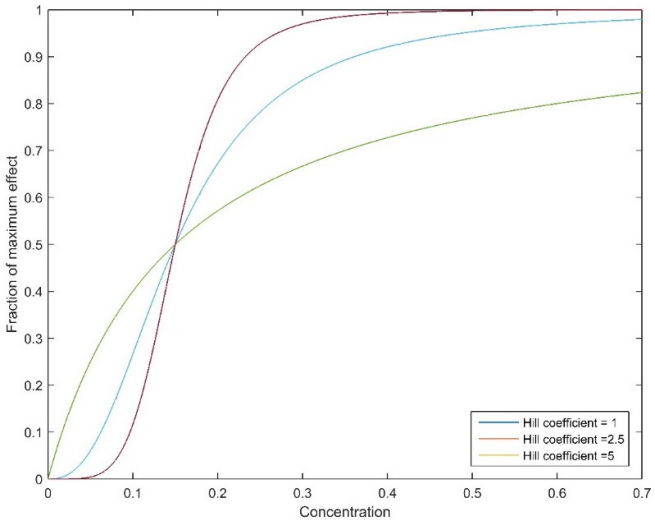

Figure 1.1 *The model showing the change in shape with different Hill coefficients. In this model* E_{max} *= 1,* $\boldsymbol{EC_{50}}$ *= 0.15 units/L.*

1.2.1.3. Pharmacokinetic-pharmacodynamic models

By linking pharmacokinetic and pharmacodynamic models, the time course of drug effect can be described. Figure 1.2 illustrates a concentration-time profile (pharmacokinetics), concentration-effect profile (pharmacodynamics) and effect-time profile which is a combination of pharmacokinetic and pharmacodynamic profile.

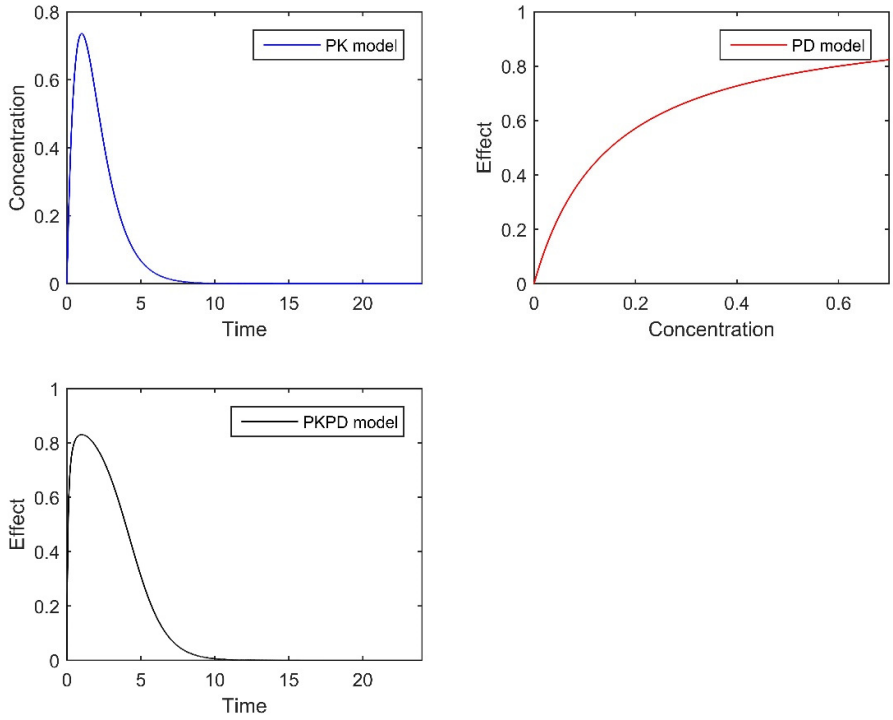

Figure 1.2 *An illustration of concentration-time profile pharmacokinetic model (A), concentration-effect profile pharmacodynamic model (B) and a combined effect-time profile pharmacokinetic-pharmacodynamic model (C).*

Two general forms of a PKPD model will be described here;

a) Immediate effects model
b) Delayed effects model

In an immediate effects model, the time to peak plasma concentration and the time to peak drug effect are considered to be essentially the same. In this scenario, the time course of drug effects can be described using a pharmacokinetic model linked to an E_{max} model, as shown in equation 1.8 or 1.9. Figure 1.3 illustrates the effect-time profile overlaid on the concentration-time profile of a hypothetical drug.

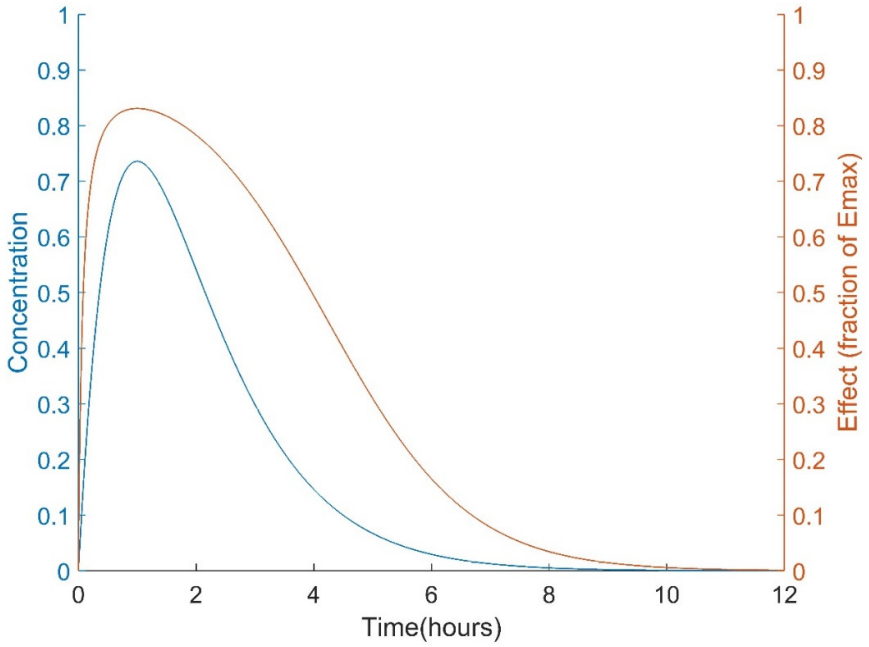

Figure 1.3 *The time course of concentrations (blue line) and drug effects (brown line) for an immediate effects model. The concentrations were generated using a one compartment model with first-order input. Dose = 10 units, CL = 5 L/hour, V = 5 L and ka= 1 hours. Emax= 1,* $\boldsymbol{EC_{50}}$*= 0.15 units/L.*

Delayed effects models are used to account for the delay in drug effect in relation to the plasma concentration. The delay in drug effect may reflect the time required for the drug to distribute from the plasma to the site of action (a pharmacokinetic phenomenon) or the slow turnover of a physiological intermediate. The mechanism of action for many drugs involves the activation or blockade of a receptor which, in turn, initiates a physiological response mediated by a series of secondary messengers or the turnover of biological intermediates. These physiological processes have a time course of their own and often constitute the rate-limiting step in the time course of drug effects. These models account for the delay in the observed drug effect with respect to the measured plasma concentration and are commonly referred to as 'turnover models (and sometimes 'indirect-response models') [16]. There are several methods proposed on how delayed effects can be modelled and several excellent reviews have been published [17, 18]. Therefore, delayed effect models will not be described in more detail here as they were not studied in this thesis. The

exception is a transit compartment model described in Chapter 2, which will be discussed below.

Transit compartments were first introduced to describe delays in drug absorption in pharmacokinetics studies [19]. It has been used to account for delayed response–time profile where the stimulus is transmitted through a series of transit compartments to produce the response. A practical application of transit compartment models is to account for the delay between warfarin plasma concentrations and the resulting inhibition of vitamin K-dependent clotting factor synthesis [20]. Here, transit compartments were used to represent the depletion of clotting factors linked in series. Figure 1.4 depicts the structure and mathematical equations of the transit compartment model by Hamberg *et al* [20]. This is the model used in Chapter 2.

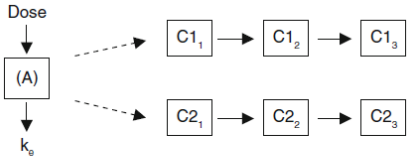

$$\frac{dA}{dT} = -k_e \bullet A$$

$$\frac{dC1_1}{dT} = (1 - EFF) \bullet \frac{3}{MTT_{C1}} - C1_1 \bullet \frac{3}{MTT_{C1}}$$

$$\frac{dC1_m}{dT} = C1_{m-1} \bullet \frac{3}{MTT_{C1}} - C1_m \bullet \frac{3}{MTT_{C1}}$$

$$\frac{dC2_1}{dT} = (1 - EFF) \bullet \frac{3}{MTT_{C2}} - C2_1 \bullet \frac{3}{MTT_{C2}}$$

$$\frac{dC2_m}{dT} = C2_{m-1} \bullet \frac{3}{MTT_{C2}} - C1_m \bullet \frac{3}{MTT_{C2}}$$

$$k_e = \frac{CL_s}{V_s}$$

$$DR = A \bullet k_e$$

$$EDK_{50} = CL_s \bullet EC_{50}$$

$$EFF = \frac{E_{max} \bullet DR^{\gamma}}{EDK_{50}^{\gamma} + DR^{\gamma}}$$

Figure 1.4 *A schematic of a transit compartment model. Reproduced from Wright et al [2] with permission from Springer. The initial condition for amount of drug in the body (A) was 0, for $C1_m$ was 1 and $C2_m$ was 1. $C1_m$ and $C2_m$ are the m^{th} compartment in the two transit chains, CL_s is the s-warfarin clearance and V_s is the volume of distribution, DR dose driving rate, EDK_{50} dose rate for 50 % inhibition of coagulation, EFF inhibitory effect on vitamin K epoxide reductase, E_{max} maximum inhibition of coagulation, k_e first-order elimination rate constant, MTT mean transit time, γ Hill coefficient.*

The transit compartment model in Figure 1.4 represents two transit compartment chains with three compartments each. C1 refers to the first transit chain and C2 the second transit chain. The inhibitory E_{max} model enters the model at the first transit compartment in each chain. The drug effect is then the average of the two chains (i.e. $C1_3$ and $C2_3$) as follows:

$$INR_{pred} = INR_{baseline} + INR_{max}\ (1 - \frac{C1_3 + C2_3}{2})$$

Equation 1.10 *INR calculation for the transit compartment*

where INR_{pred} is the predicted International Normalized Ratio (INR), $INR_{baseline}$ is the baseline INR before treatment, INR_{max} is the maximum theoretical INR (set to 20 as per Hamberg *et al* [20]).

Each transit compartment has an intercompartmental transit time, but the overall process is parameterized as the mean transit time (MTT) of each chain. The transit compartment rate constant (k_{tr}) is assumed to be the same for each compartment and assumed to be equivalent to k_e. The number of transit compartment and transit chains are usually empirically determined.

1.2.1.4. Models for heterogeneity and residual variability

Population pharmacokinetic and pharmacodynamic models include random effects parameters to describe the heterogeneity between individuals (termed between subject variability, BSV) of the corresponding population parameter, and measurement uncertainty (termed residual unexplained variability, RUV).

Consider an example of the model parameter for volume (V) in Equation 1.1 above (i.e. $C(t) = \frac{D}{V} \times exp^{-\left(\frac{CL}{V} \times t\right)}$); here V is the population average of V ($POPV$). The BSV for V can be modelled as follows:

$$V_i = POPV\ \times exp(\eta_i);\ \eta_i \sim N(0, \omega^2)$$

Equation 1.11 *A model to account for BSV of volume in the i^{th} individual*

where V_i is the individual's V estimate, η_i is the difference between individual parameter predictions for the i^{th} individual from the typical value for the population. η_i is assumed to be normally distributed over all individuals with a mean of zero and variance ω^2.

A population model includes a statistical model to account for the residual unexplained variability (RUV). Usually RUV is assumed to follow a normal distribution with a mean of zero and variance of σ^2 as follows;

$$\varepsilon_{ij} \sim N(0, \sigma^2)$$

Equation 1.12 *The distribution of* $\boldsymbol{\varepsilon_i}$

where ε_{ij} is the difference between model prediction to the j^{th} observation of the i^{th} individual.

1.2.2. Bayesian forecasting

Bayesian methodology provides the means of incorporating individual patient response data with prior knowledge of typical drug response in the population. Several Bayesian forecasting methods for dose individualisation have been published [1, 21-23]. A Bayesian forecasting approach involves predicting future responses for a given dose based on; 1) prior information about the patient's response to drug therapy, 2) an underlying population pharmacokinetic and pharmacodynamic model and 3) parameter values obtained from a prior population [23]. A Bayesian method estimates the parameter values that provide the relative balance between the prior information and the new observed data for the patient from a posterior distribution. A *maximum a posteriori* (MAP) estimator provides a point estimate of an unknown quantity that is equal to the mode of the posterior distribution. Individualised parameter estimates of a model can be obtained by minimizing the MAP objective function given by:

$$MAP_{obj} = \sum_{j=1}^{n} \frac{(y_j - g(\theta, x_j))^2}{\sigma_{y_j}^2} + \sum_{p=1}^{p} \frac{(ln\theta_p - ln\,\mu_{\theta_p})^2}{\omega_{\theta_p}^2}$$

Equation 1.13 *Maximum a posteriori objective function*

where MAP_{obj} is the MAP objective function, x_j is covariate of the jth patient, y_j is the jth observation, $g(\theta, x_j)$ is the model-predicted jth observation, θ is a vector of individual parameter estimates, $\sigma_{y_j}^2$ is the residual variance associated with the jth observation and calculated as $\sigma_{y_j}^2 = \sigma_{prop}^2 \times g(\theta, x_j)^2 + \sigma_{add}^2$, where σ_{prop}^2 is the proportional variance and σ_{add}^2 is the additive variance, $ln\,\theta_p$ is the natural log of the p^{th} parameter, $ln\,\mu_{\theta_p}$ is the natural log of the prior of the population value of the p^{th} parameter and $\omega_{\theta_p}^2$ is the log-normal inter-individual variance associated with the p^{th} parameter.

Note that when there is no information about the patient, the second term on the right-hand side of the equation disappears and the equation collapses to the prior population estimates. As more feedback about the drug response in the individual becomes available, the second term in the right-hand side equation dominates and predictions are based on more individualised posterior parameter estimates. This is an adaptive process which allows the Bayesian algorithm to incorporate new information. Theoretically, the more observations that is used, the more individualised the parameter estimates become and the more accurate the model predictions become.

1.2.3. A linear regression approach

This subsection relates to the work carried out in Chapter 3 where warfarin dosing algorithms developed using linear regression methods will be evaluated.

Linear regression is a statistical approach to find a relationship between a dependent variable and one or more independent variables. This approach has been used to find the relationship between the maintenance dose of warfarin and

variables that predict differences in dose requirements between individuals (see Gage *et al* [24] for an example).

Let y_j denote the dependent variable taken from the j^{th} covariate value of x_j, where $j = 1, \ldots\ldots, n$. A linear model can be written as follows:

$$y_j = f(x_j, \beta) + e_j$$

Equation 1.14 *A linear regression model*

where y is an $n \times 1$ vector of the dependent variable, β is the regression parameters coefficient, x is a vector of $n \times 1$ of the independent variable (or predictor) and e is the error. The goal is to find the best estimate of β (where β is the slope of the regression line). The notation above is for regression for a single variable but the regression equation can be extended to include multiple variables using the same principles. This is termed multilinear regression.

The standard assumptions of linear regression are that the independent variables are fixed and known with certainty. The errors in model prediction are uncorrelated with each other and are normally distributed with a mean zero and constant variance. These assumptions can be relaxed in some cases.

Linear regression models are empirical in nature and therefore, in theory, are limited in the ability to extrapolate beyond the data used to develop the model. It is noteworthy, however, that many linear regression equations developed for the purpose of dose prediction are explicitly designed to be used in patients in other clinical settings.

1.3. A conceptual framework for dose individualisation methods

Holford and Buclin [25] have described a framework for understanding drug dosing methods. They propose three general methods; 1) the population method, 2) group dosing, 3) dosing based on individual patient response. Population dosing refers to a fixed dose for all patients, i.e. the entire 'population'. Group dosing is used where the same dose is given to the same

group of patients, e.g. those with same renal function, body weight, or age. This method can also be referred to as 'covariate based' dosing. Dosing based on patient response requires feedback from the patient to adjust dosing.

In revised framework, a further refinement to the framework described by Holford and Buclin [25] will be proposed. In this case, dosing method will be divided into two categories: covariate based methods or response based methods. Response can be in the form of plasma concentration or can take the form of a biomarker for drug effect (e.g. INR for warfarin therapy). A biomarker is an objectively measured indicator of a biological, pathological or pharmacological response to drug therapy [26]. Biomarkers such as the INR are useful for guiding dosing if the long term clinical endpoint (e.g. stroke or bleed) can take years to manifest.

The following is a conceptual framework for dose individualisation that will be used in this thesis:

1. Population dosing

   All patients receive the same dose.
2. Covariate based dosing

   The dose is determined from patient characteristics that are known to influence dose requirements.

   i. Uni-dimension
      - Only single covariate is used to determine the dose
      - Example: weight-based dosing such as the initial dose of enoxaparin [27].

   ii. Multi-dimension
      - More than one covariate is used for dosing. Each covariate adds an extra dimension to the dose prediction allowing more flexibility to the final dose calculation.
      - Examples : dosing based on body surface area (i.e. weight and height) for cisplatin [28], several multilinear regression

algorithms to predict the maintenance dose of warfarin [24] (see Section 1.4.3.1.2).

3. Response based dosing

   Dosing based on response data (concentration or biomarker) as feedback

   i. Single feedback, no covariates, non-updating

      - Uses only the most recent response measure and does not account for previous response data
      - Example: Static INR nomograms (warfarin) by Tait and Sefcick [29]. This nomogram (see Figure 1.5) is specifically designed to be used in the first 8 days of therapy. It is based on a single INR response (hence 'static') and does not account for any covariate or previous INR measurement.

d5 INR	dose (for d5-7)	d8 INR	dose (from d8)
≤ 1.7	5mg	≤ 1.7	6mg
		1.8 - 2.4	5mg
		2.5 - 3.0	4mg
		> 3.0	3mg for 4 days
1.8 - 2.2	4mg	≤ 1.7	5mg
		1.8 - 2.4	4mg
		2.5 - 3.0	3.5mg
		3.1 - 3.5	3mg for 4 days
		> 3.5	2.5mg for 4 days
2.3 - 2.7	3mg	≤ 1.7	4mg
		1.8 - 2.4	3.5mg
		2.5 - 3.0	3mg
		3.1 - 3.5	2.5mg for 4 days
		> 3.5	2mg for 4 days
2.8 - 3.2	2mg	≤ 1.7	3mg
		1.8 - 2.4	2.5mg
		2.5 - 3.0	2mg
		3.1 - 3.5	1.5mg for 4 days
		> 3.5	1mg for 4 days
3.3 - 3.7	1mg	≤ 1.7	2mg
		1.8 - 2.4	1.5mg
		2.5 - 3.0	1mg
		3.1 - 3.5	0.5mg for 4 days
		> 3.5	omit for 4 days
> 3.7	0mg	< 2.0	1.5mg for 4 days
		2.0 - 2.9	1mg for 4 days
		3.0 - 3.5	0.5mg for 4 days

At day 15 (or day 12) check INR and make fine dose adjustment as appropriate

Figure 1.5 *An example of a nomogram by Tait and Sefcick [29] reproduced with permission from John Wiley and Sons*

ii. Single feedback, multi-dimension, non-updating
    - Combines information from response and patient covariates. Predictions cannot be updated.
    - Example: Warfarin algorithms that use a single INR response and multiple covariates to predict the maintenance dose fall into this group [30, 31].

iii. Multi-feedback, uni- or multidimension, non-updating
    - Dosing based on more than one feedback with one or more covariates. Predictions cannot be updated.
    - Example: Dosing based on creatinine clearance estimated using the Jelliffe and Jelliffe equation [32]. The equation is used in patients with unstable renal function and requires input of two serum creatinine concentrations (i.e. two feedbacks), body weight, and estimated creatinine production.

iv. Multi-feedback, multidimension, updating
    - Dosing based on multiple response data, multiple covariates and can update the predictions as more information becomes available.
    - Example: Bayesian forecasting methods for dose individualisation [1, 2, 33, 34].

1.4. Anticoagulants considered in this thesis

1.4.1. Introduction to the coagulation network

Anticoagulants modify haemostatic mechanisms resulting in a prolonged clotting time. Common clinical indications include atrial fibrillation/flutter, mechanical heart valve replacement, post-orthopaedic surgery, deep vein thrombosis or pulmonary embolism.

All anticoagulants inhibit thrombin production either directly, or indirectly by inhibiting the upstream activation of coagulation proteins. The physiological mechanism of thrombin production is complicated as it involves multiple feedback and feedforward mechanisms. Only a brief description of the coagulation network is presented here as more detailed description are available in textbooks and other excellent reviews [35, 36]. A schematic of the coagulation network is presented in Figure 1.6.

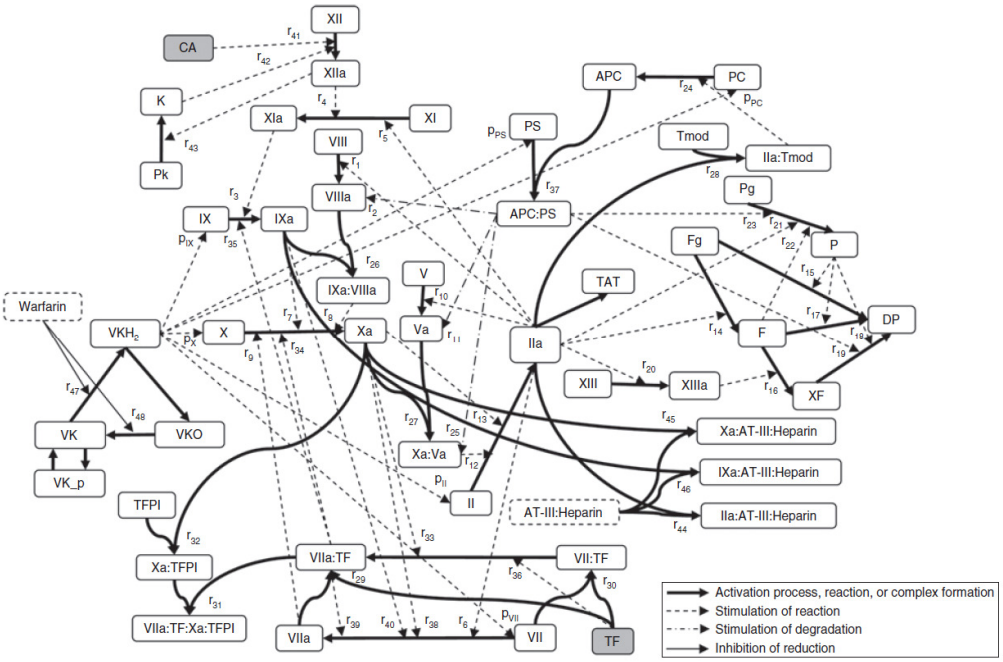

Figure 1.6 *A schematic of the coagulation network. The scheme of the coagulation network model. APC, activated protein C; AT-III, antithrombin-III; CA, activator for the contact system; DP, degradation product; F, fibrin; Fg, fibrinogen; II, prothrombin; IIa, thrombin; K, kallikrein; P, plasmin; PC, protein C; Pg, plasminogen; Pk, prekallikrein; PS, protein S; TAT, thrombin–antithrombin complex; TF, tissue factor; TFPI, tissue factor pathway inhibitor; Tmod, thrombomodulin; VK, vitamin K; VKH2, vitamin K hydroquinone; VKO, vitamin K epoxide; XF, cross-linked fibrin. Figure reproduced from Wajima et al. [36] with permission from John Wiley and Sons*

A clot formation starts as a response to an injury to the endothelium that lines the blood vessels. There are two pathways, classically known as contact activation (or intrinsic) pathway and tissue factor (or extrinsic) pathway. The contact activation pathway is activated when a negatively charged surface activator (labelled CA in a shaded box in Figure 1.6) activates factor XII. In the

tissue factor pathway, blood leaking through the endothelium activates the platelets and exposes subendothelial tissue factors to plasma Factor VII. In both pathways, there is a complex network of events that happen where each reaction takes place at very different time scales. Multiple blood proteins get activated and several co-factors (calcium, phospholipids and Vitamin K) participate and lead to the activation of factor X. Each molecule of factor Xa can catalyse (either directly or by forming a factor Xa:Va complex) the formation of approximately 1000 thrombin molecules [37, 38]. Thrombin can be viewed as the hub of the coagulation network where it has multiple pro-coagulation effects to stimulate a thrombin burst, and anticoagulant effects by activating plasminogen and protein C via cofactor thrombomodulin.

It is important to note that the variability in anticoagulation response is not only determined by the concentration of the anticoagulant in plasma but there is also innate variability in the sensitivity and concentration of clotting factors between individuals. This has been reviewed by Duffull 2012 [39]. It has been argued that all anticoagulants will have a narrow therapeutic range and will require monitoring to ensure a balance of antithrombotic effects and bleeding effects [39, 40]. This will be discussed further in section 6.1, and in Chapter 6.

1.4.2. Warfarin dose individualisation

Warfarin (3-α-acetonyl-benzyl)-4-hydroxycoumarin) is a synthetic analogue of bishydroxycoumarin (dicumarol) and is structurally related to natural coumarins found in many plants. Two other coumarins, phenprocoumon and acenocoumarol, are also used clinically in some European countries. Collectively, these are often referred to as 'vitamin K antagonists', although this is a misnomer as these drugs are inhibitors of the enzyme that reduces the oxidised form of vitamin (vitamin K epoxide reductase, VKOR) and not antagonizing the effects of vitamin K *per se*.

Warfarin is used to prevent ischaemic stroke and thromboembolism events. The most common indication of warfarin is nonvalvular atrial fibrillation where

the risk of stroke may be increased by 5-fold [41-44]. Clinical trials have repeatedly shown that warfarin is effective at preventing stroke in patients with atrial fibrillation with a relative risk reduction of 68% [45] and 59% [46] in two meta-analyses.

1.4.2.1. Clinical pharmacology

Warfarin is administered as a racemic mixture of *S*- and *R*- warfarin. Warfarin is almost completely absorbed from the gut with a reported bioavailability of nearly 100% [47]. Peak plasma concentrations occur 0.3 – 4 hours after administration [48]. The apparent volume of distribution of racemic warfarin has been estimated to be about 10L/70kg [49]. A range of 0.098-0.48 L/h/70kg has been reported for the oral clearance for racemic warfarin [49]. Racemic warfarin has an estimated half-life of approximately 36-42 hours, but given separately, *S*-warfarin has a shorter mean half-life (about 30 hours) compared to *R*-warfarin (about 45 hours) [48]. *S*-warfarin is about 2-5 times more potent than *R*-warfarin and is generally considered to be the enantiomer responsible for the anticoagulant effect [50]. Warfarin is eliminated almost entirely by hepatic metabolism, but clearance mechanisms differ for each enantiomer. *S*-warfarin is metabolized mainly by the cytochrome P450 (CYP) enzyme, CYP2C9, while *R*-warfarin is metabolised primarily by CYP2C19, CYP3A4, and CYP1A2. Following metabolism, hydroxylated metabolites are excreted in the faeces (20%) and urine (80%) [50].

The mechanism of action of warfarin involves inhibition of hepatic enzyme vitamin K epoxide reductase enzyme (VKOR) [51]. VKOR is required for the cyclic interconversion of vitamin K epoxide to a reduced form of vitamin K (Vitamin KH2) (see Figure 1.7). The reduced form of vitamin K is a cofactor for the post-translational carboxylation modification of vitamin K dependent precursor clotting factors II, VII, IX, X, and regulatory anticoagulation protein C and protein S. Carboxylation increases the affinity of the precursor clotting factors towards calcium, which is required for subsequent interaction with negatively charged phospholipid surfaces [35]. Depletion of carboxylated

clotting factors will prolong clotting time. However, since warfarin has no effect on fully carboxylated clotting factors, there is a delay between peak plasma warfarin concentrations and the peak effect on blood clotting. The time course of warfarin effect is therefore determined by the turnover of the circulating vitamin K dependent clotting factors.

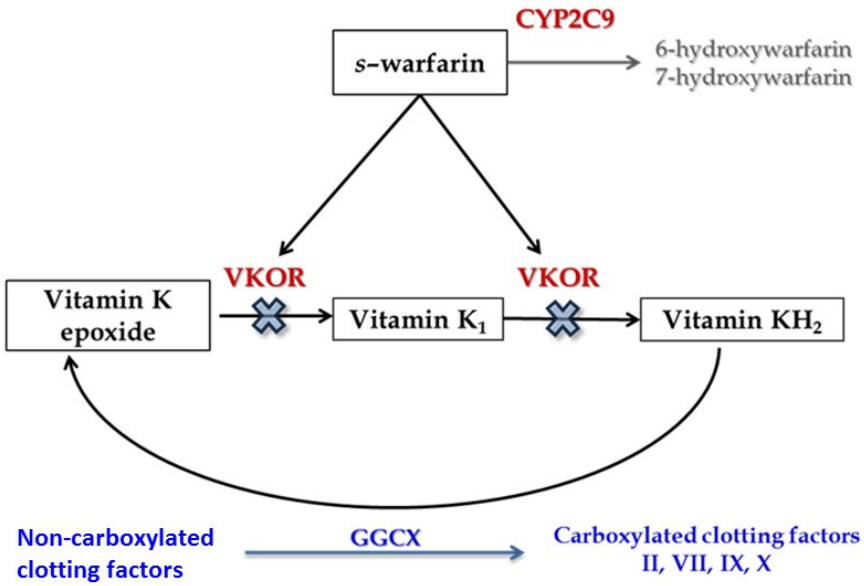

Figure 1.7 *Schematic of warfarin effect on the vitamin K cycle and the production of carboxylated clotting factors. VKOR, vitamin K epoxide reductase; GGCX, Gamma-Glutamyl Carboxylase.*

Several single nucleotide polymorphisms (SNP) have been found to influence the metabolism and sensitivity of warfarin. The most well described are SNPs in the *CYP2C9* and Vitamin K epoxide reductase complex subtype 1 (*VKORC1)* genes. The *CYP2C9* variants produce single base substitutions at residue 144 (Arginine to Cysteine) for *CYP2C9**2 and 359 (Isoleucine to Leucine) for *CYP2C9**3 resulting in an enzyme with reduced activity [52]. The enzyme VKOR is coded by the gene *VKORC1* and several polymorphisms in the promoter region of this gene have been found to significantly alter the amount of enzyme produced by the hepatocyte [53]. Most of these SNP appear to be in linkage disequilibrium (i.e. correlated) so most recent research has focused on the -1639G>A variant. Patients with the A allele have been demonstrated to

require lower warfarin doses compared to patients with GG allele in order to achieve the same INR [54].

1.4.2.2. Monitoring response and therapeutic range

The physiological response to warfarin therapy is a prolonged clotting time. Warfarin clotting time is measured using the prothrombin time (PT). The PT is an *ex vivo* test that measures the time for blood to form a fibrin clot in a test-tube after the addition of tissue factor and calcium. It is prolonged when there are deficiencies in factor II, VII, X. Thromboplastin reagent, which is a plasma protein, is also added to aid the conversion of prothrombin to thrombin. A normal PT is about 12-14 seconds but will vary depending on the sensitivity of the thromboplastin reagent used for the test. The PT is therefore commonly standardized to the INR. The equation for calculating INR is given as follows:

$$INR = \left(\frac{patient\ PT}{mean\ normal\ PT}\right)^{ISI}$$

Equation 1.15 *Equation to calculate the international normalised ratio*

where mean normal PT is the geometric mean of PT from at least 20 normal subjects from both sexes determined using the same test conditions, and ISI is the International Sensitivity Index of the thromboplastin reagent used in the local laboratory to perform PT tests. A lower ISI value denotes a more sensitive local thromboplastin reagent [55].

1.4.2.3. Defining the therapeutic range for warfarin

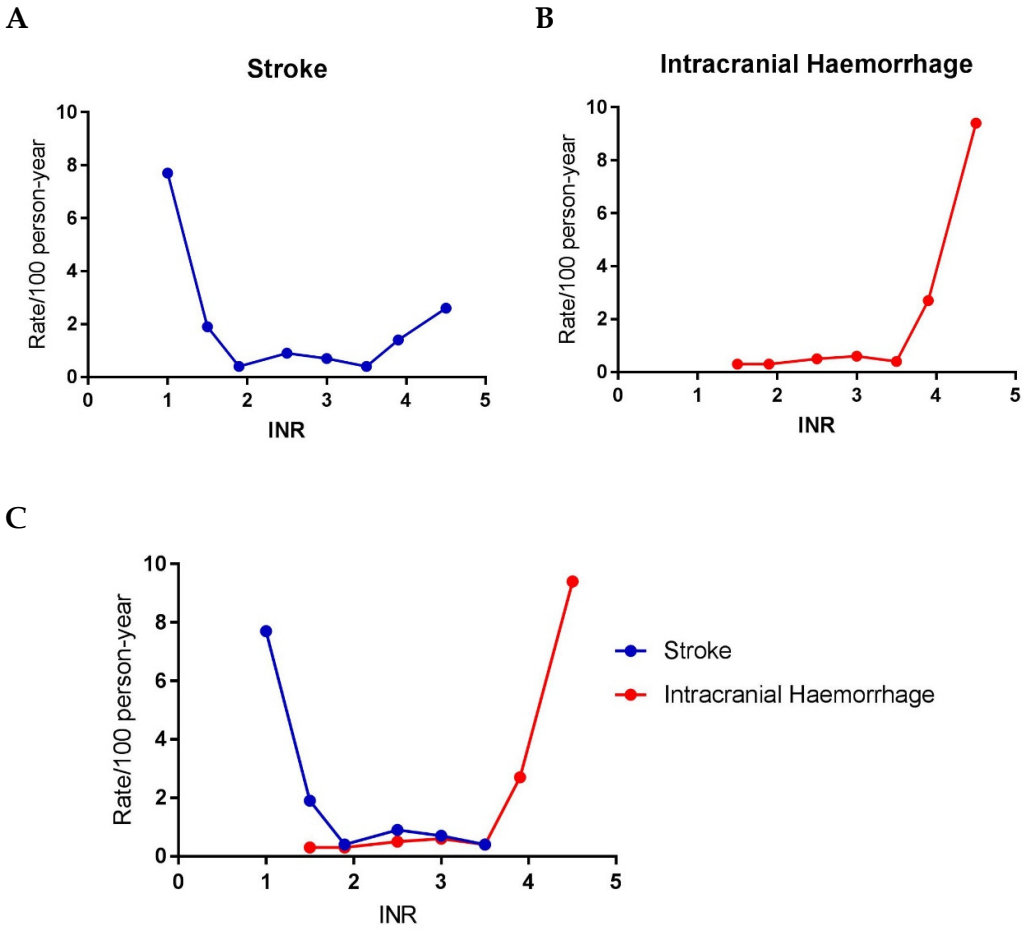

Figure 1.8 *Incidence rates of ischaemic stroke (A), intracranial haemorrhage (B) and combined data (C) among patients with nonvalvular atrial fibrillation who were taking warfarin versus to the INR at the time of the stroke produced based on data from Hylek et al 2003 [56]*

Figure 1.8 depicts a utility curve for warfarin therapy derived from a large published observational study [56]. Figure 1.8A represents the incidence of ischaemic stroke against the degree of anticoagulation. Figure 1.8B represents the incidence of haemorrhagic stroke as a function of the degree of anticoagulation. Both curves can then be combined to sum up the total thromboembolic and bleeding events which appear to be U-shaped (Figure 1.8C). The region with lowest incidence rates for both under- and over-anticoagulation can be targeted in practice. The example presented above

originates from a large observational data in patients who were taking warfarin [56], but as all anticoagulants carry the risk of bleeding this method of constructing a utility curve to define the therapeutic target generally applies.

The target anticoagulation response for warfarin has been well studied and multiple studies have found that the target INR to be within the range of 2-3 for atrial fibrillation [45, 57, 58] and for most other indications [59]. Some patients who are at higher risk of thrombosis, such as those with mechanical heart valves, an INR of 2.5 - 3.5 may be targeted [60].

1.4.2.4. Current dosing methods

In the absence of any dosing aids, warfarin dose adjustment will likely be largely heuristic (trial and error) where the adjusted maintenance dose for an individual patient is determined by the prescriber based on the magnitude of previously observed INR response. However, predicting the maintenance dose for a patient *a priori* is difficult as the INR response that is measured in the first 1-3 weeks of treatment, or after a dose change, will reflect non-steady state conditions. Thus, heuristic dosing requires the prescriber to have a working knowledge of the time course of warfarin dose-response and an understanding of the patient factors that influence dose requirements.

Several methods for improving INR control by predicting warfarin dose requirements have been described. For the purposes of this thesis (as outlined in Section 1.4) warfarin dosing methods are broadly divided into; 1) covariate-based dosing methods, and 2) response-based dosing method.

1.4.2.4.1. Covariate based dosing method

In recent years, there is increasing number of studies that are designed to identify patient characteristics that predict differences in warfarin dosing requirements between individuals [3, 61]. Typically, these studies regress the maintenance dose against patient characteristics using multi-linear regression methods. The resulting algorithms will include all patient factors (covariates)

that were found to have a statistically significant impact on warfarin maintenance doses in the population studied. The algorithms are therefore empirical by design and the covariates included in the regression algorithm may differ depending on the case mix and population included in the original study. Most published algorithms include *CYP2C9* and *VKORC1* genotypes, measures of body mass, age, warfarin indication, and, interacting drugs (e.g. amiodarone) [61]. In a recent review, Verhoef *et al* [4] identified 32 published algorithms for warfarin dosing. Similarly, Shin and Cao [61] found 34 warfarin dosing algorithms published between January 2004 to August 2009. In Chapter 3, a meta-analysis was conducted to pool the predictive performance from published dosing algorithms [62]. The large number of published algorithms may reflect the empirical nature of this method in that each algorithm is designed for use in either a particular population (e.g. Korean [63], Puerto Rican [64], Brazilian [65]) or for a particular indication (e.g. orthopaedic patients [31, 66]) or both (e.g. Korean patients with atrial fibrillation [67]).

An important limitation in many of the covariate based algorithms is that once therapy has initiated, these dosing tools have no further function in guiding dose adjustments. Most of the algorithms are designed to predict warfarin doses that will produce an INR between 2 to 3 (see Klein *et al.* (2009) [68]). In this case, there will be no means of adjusting the dose if a higher target INR is required. The result is that these algorithms may underestimate warfarin doses for patients who are at increased risk of clotting and require higher INR targets such as patients with mechanical heart valves [60]. Some recently published algorithms including those published by Gage *et al* [69] and [24] include a user-defined 'target INR' in the algorithm which allows for targeting unique INR values.

1.4.2.4.2. Response-based dosing method

a. Dosing based on single feedback without covariates

Dosing of warfarin based on a single INR response generally provide guidance for initial dose selection and for dose adjustment within the first few

days of therapy. These take the form of dosing tables or static nomograms (see an example in Figure 1.9), but can also include computerised decision-support tools such as the PARMA-5 system used in some European hospitals [70]. They are designed to standardise dose adjustment practices between prescribers and many (but not all, see Ryan et al 1989 [71]) are based on the assumption that warfarin dose and INR response are linearly related. This assumption does not hold true if the INR response lies outside the linear portion of the dose-response curve (<20% and >80% of maximum effect) which will likely be the case during warfarin initiation [72]. In addition, warfarin dosing nomograms do not account for differences in response between individuals and were designed with the implicit assumption that the magnitude of the INR response for a given warfarin dose is only dependent on warfarin dose and hence will be the same for each individual. For example, the nomogram in Figure 1.9 assumes that a 91-year-old patient who weighs 45 kg and takes several interacting drugs will respond to the same dose of warfarin as a 28-year-old patient with a deep vein thrombosis (DVT) who weighs 80 kg, or a 50-year-old patient with a mechanical heart value who is a poor metaboliser. According to this nomogram, the patient can be initiated using either the 5 mg or 10 mg nomogram depending on the rapidity required to reach target INR.

5-mg Warfarin Nomogram		
Day	INR	Dosage
1		5.0 mg
2	< 1.5 1.5 - 1.9 2.0 - 2.5 >2.5	5.0 mg 2.5 mg 1.0 - 2.5 mg 0.0
3	< 1.5 1.5 - 1.9 2.0 - 2.5 2.5 - 3.0 > 3.0	5.0 - 10.0 mg 2.5 - 5.0 mg 0.0 - 2.5 mg 0.0 - 2.5 mg 0.0
4	< 1.5 1.5 - 1.9 2.0 - 3.0 > 3.0	10.0 mg 5.0 - 7.5 mg 0.0 - 5.0 mg 0.0
5	< 1.5 1.5 - 1.9 2.0 - 3.0 > 3.0	10.0 mg 7.5 - 10.0 mg 0.0 - 5.0 mg 0.0
6	< 1.5 1.5 - 1.9 2.0 - 3.0 > 3.0	7.5 - 12.5 mg 5.0 - 10.0 mg 0.0 - 7.5 mg 0.0

10-mg Warfarin Nomogram		
Day	INR	Dosage
1		10.0 mg
2	< 1.5 1.5 - 1.9 2.0 - 2.5 > 2.5	7.5 - 10.0 mg 2.5 mg 1.0 - 2.5 mg 0.0
3	< 1.5 1.5 - 1.9 2.0 - 2.5 2.5 - 3.0 > 3.0	5.0 - 10.0 mg 2.5 - 5.0 mg 0.0 - 2.5 mg 0.0 - 2.5 mg 0.0
4	< 1.5 1.5 - 1.9 2.0 - 3.0 > 3.0	10.0 mg 5.0 - 7.5 mg 0.0 - 5.0 mg 0.0
5	< 1.5 1.5 - 1.9 2.0 - 3.0 > 3.0	10.0 mg 7.5 - 10.0 mg 0.0 - 5.0 mg 0.0
6	< 1.5 1.5 - 1.9 2.0 - 3.0 > 3.0	7.5 - 12.5 mg 5.0 - 10.0 mg 0.0 - 7.5 mg 0.0

Figure 1.9 *Two nomograms for initiating warfarin treatment by Crowther et al.* ***[73]*** *reproduced with permission from The American College of Physicians.*

b. Dosing based on single response and covariates

After accounting for all known covariates that influence warfarin dose requirements, only approximately 50% of dose variability can be explained [24, 68]. A small number of recent publications have added a single INR response in addition to covariates to improve the prediction of the maintenance dose [30, 74]. The INR measurement is a response measure that feeds back into the algorithm to capture further variability not accounted for by all the covariates and have been found to improve the predictive performance compared to algorithms without feedback [3].

c. Dosing based on Bayesian forecasting

Several studies have applied Bayesian forecasting methods to improve warfarin dosing [75-80], although it is unclear if any have been implemented in clinical practice. Wright and Duffull recently developed a Bayesian forecasting method for dosing warfarin [1, 2]. A more in-depth description of the underlying

model and details of the Bayesian dosing tool will be presented in Chapter 2. In a retrospective analysis, the Bayesian dosing tool was shown to provide precise and accurate predictions of INR response in a small cohort of patients (n=55) who were initiating warfarin [2]. Further work on this tool will be described in Chapter 2.

1.4.2.5. The need for improved dose prediction

Warfarin has been proven to be effective in preventing ischaemic strokes in patients with atrial fibrillation [45, 46]. However, predicting a suitable dose is problematic because the therapeutic range is narrow. The perceived difficulty in dosing warfarin has led some clinicians to avoid warfarin treatment in eligible patients. A Swedish study conducted in 2006 found that only 54% of eligible patients discharged from hospital with atrial fibrillation were appropriately treated with warfarin [81]. Amongst the reasons given for not prescribing warfarin were concerns about bleeding risk and a lack of understanding about the benefit of anticoagulation in stroke prevention. The lack of clear evidence-based guidelines regarding the optimal dosing method for warfarin has also been suggested as one of the reasons for not initiating warfarin in patients at risk of thrombosis [82].

The effectiveness and safety of warfarin treatment are currently measured by the time in the therapeutic range (TTR). It is a measure of how well a patient is anticoagulated within a specific time interval. TTR is increasingly viewed as a substitute for a clinical end point in clinical trials [83-85]. The TTR is derived by calculating the percentage of time the patient's INR remains within the therapeutic range and is commonly estimated using a linear interpolation described by Rosendaal *et al* [86]. Several studies have shown that patients with TTR above 70% have a low risk of thromboembolism and bleeding [87-89]. Similarly, patients with lower TTR are associated with increased risk of ischaemic stroke [90] and increase the incidence of venous thromboembolism and bleed [91]. The European Society of Cardiology Working Group on Thrombosis Anticoagulation Task Force have recommended that the individual

patient's TTR should be above 70% [92], however current dosing strategies appear to only achieve approximately 40-65% [93]. In large clinical trials where patients were highly selected, the average TTR has been found to be in the order of about 60% [94]. This thesis is predicated on the assumption that accurate and precise method of determining the dose of warfarin will improve the TTR.

1.4.3. Dabigatran dose individualisation

1.4.3.1. Clinical pharmacology

Dabigatran etexilate mesylate has low solubility in water (log P, pH 7.4 = 3.8) and high intrinsic passive permeability. It is the prodrug of dabigatran, a highly polar molecule (log P, pH 7.4 = -2.4). The bioavailability of dabigatran etexilate is approximately 3-7%. Absorption of dabigatran etexilate is pH dependent where an acidic environment is required to increase solubility. It is therefore formulated in pellets coated with tartaric acid. The mean peak plasma concentrations of dabigatran etexilate is approximately 2 hours (T_{max}). A high-fat diet can delay the T_{max} to approximately 4 hours but does not affect the extent of absorption [95].

Conversion from dabigatran etexilate to dabigatran requires hydrolysis of two esters; ethyl ester and carbamate ester (see Figure 1.10). Once absorbed, dabigatran etexilate is predominantly metabolised by carboxylesterase (CES) 2 in the intestine which hydrolyses the carbamate ester to form the intermediate metabolite BIBR951, which is then hydrolysed by CES 1 in the liver to form dabigatran. Another pathway, where both esters of dabigatran etexilate are hydrolysed by CES 1 and CES 2 in the liver is also possible [96]. CES1, which is present at higher concentrations in the liver than the intestine [97], can hydrolyse both carbamate and ethyl ester, but CES 2 can only hydrolyse the carbamate ester [96]. This sequential conversion will be almost complete within approximately 2 hours [98]. Intronic *CES 1* SNP at rs2244613 minor allele occurs in approximately a third of the population (in a phase III trial (RE-LY)) and has been associated with decreased exposure to dabigatran and bleeding risk [99]. Further studies

showed that another *CES1* SNP at rs71647871 (at residue 143 - glycine to glutamic acid) is a loss-of-function variant that can impair dabigatran etexilate conversion in humans [96].

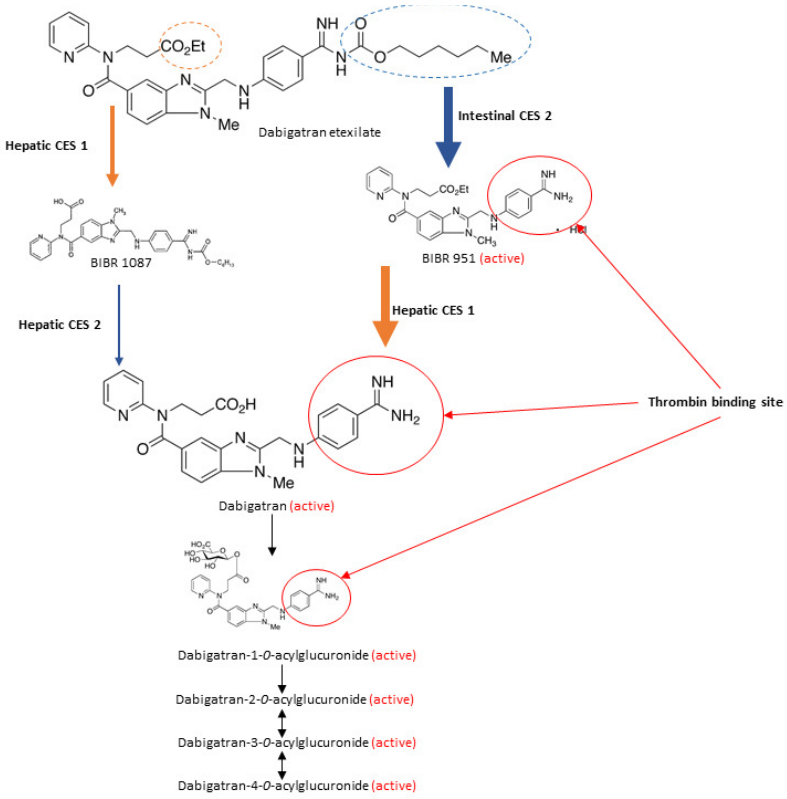

Figure 1.10 *A schematic of the metabolic pathway of dabigatran etexilate*

On average, approximately 20% (range 15-35%) of circulating dabigatran is glucuronidated and the remainder is excreted renally unchanged. There are other trace metabolites from oxidation but the contribution to dabigatran exposure is negligible [100]. Approximately 35% of dabigatran is protein bound [100]. Volume of distribution is 1 L/kg. Apparent clearance has been reported to be 0.12 L/hr/kg (values in healthy young adults). The terminal half-life of dabigatran is approximately 12-17 hours, which is increased in 15 to 34 hours in patients with mild renal impairment to end-stage renal disease on haemodialysis [101].

Inhibition of thrombin is achieved by the ionic interaction between Aspartate 189 and the benzamidine ring of dabigatran [102]. Hydrolysis of the

carbamate ester (see Figure 1.10) by CES1 exposes the binding site of dabigatran to thrombin. This explains why the intermediate metabolite (BIBR951) is also found to be active, although its overall anticoagulation contribution is small since the cleavage of the other ethyl ester to form dabigatran occurs rapidly within ~2hrs. Dabigatran 1-*O*-acylcluronide is the major metabolite of dabigatran which can further undergo three positional isomers (2-*O*, 3-*O* and 4-*O*) that are catalysed by basic pH and temperature (non-enzymatic isomerisation). As the conjugation of glucuronide does not block the thrombin binding site (benzamidine ring), dabigatran acylglucuronides has been shown to be equally potent at inhibiting thrombin as measured using activated partial thromboplastin time test (aPTT) [103].

Dabigatran inhibits circulating free thrombin, fibrin- and clot-bound thrombin, and thrombin-induced platelet aggregation. This, in turn, prevents the conversion of fibrinogen to insoluble fibrin which is the last step of the clot formation. As thrombin also provides positive feedback to amplify the coagulation activation, promotes cross-linking of fibrin monomers via activation of factor XIII, activates platelets and inhibits fibrinolysis, dabigatran inhibits these processes as well [104].

1.4.3.2. Monitoring dabigatran therapy

Current dosing guidelines for dabigatran do not recommend routine anticoagulation monitoring [9]. Nevertheless, there is a growing consensus that the concentration of dabigatran in the plasma could be used to guide therapy in patients at high risk of bleed or clotting [40, 105].

Concentrations of dabigatran can be measured using analytical chemistry methods such as liquid chromatography mass spectrometer/ mass spectrometer (LCMS/MS) or by inferring the concentration from a clotting time test. LCMS/MS assays are highly sensitive and specific but requires trained laboratory experience and instrument availability is often limited. An LCMS/MS

assay to measure dabigatran concentration in plasma and details on the principles of LCMS will be described in Chapter 5.

Several publications have studied the relationship between dabigatran exposure and clotting time tests [106-109], including the INR, activated partial thromboplastin time (aPTT), and thrombin time (TT) test. Less commonly used coagulation tests, such as the dilute thrombin time (dTT) and Ecarin clotting time (ECT) test, have also been studied. The latter two clotting time tests are not routinely available in many clinical settings. Figure 1.11 depicts the relationship between each clotting time test and dabigatran plasma concentrations.

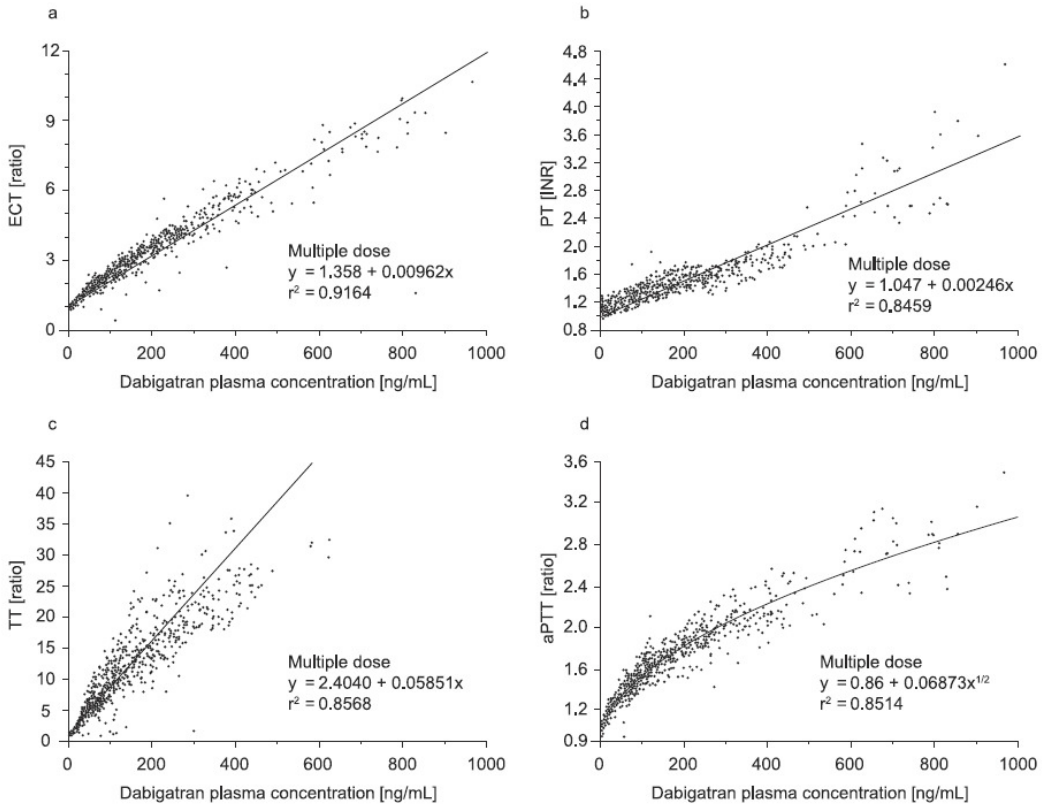

Figure 1.11 *Relationship of dabigatran plasma concentration and ECT ratio (a), INR (b), TT ratio (c) and aPTT (d). Reproduced from van Ryn et al 2010 [110] with permission from Schattauer.*

The INR test correlates poorly to dabigatran concentrations [111] and is therefore not recommended for measuring of dabigatran anticoagulation. The aPTT test has several drawbacks that make it unsuitable for routine monitoring including; 1) aPTT can be sensitive to preanalytical (sampling time, temperature etc), biological (reagent activities) and acquired factor deficiencies and therefore standardisation between laboratories is difficult [112], 2) the prolongation of aPTT does not predict bleeding events or thrombosis events well, 3) the relationship is curvilinear [113]. The aPTT test may be best suited for qualitative assessment of dabigatran response, but is less useful for defining a quantitative clotting time. The TT test is overly sensitive to thrombin inhibition by dabigatran [114]. The test will produce clotting times beyond the upper limit of the reporting time For example, dabigatran plasma concentrations above 60 ng/mL [115] and 90 ng/mL [116] have been reported to exceed the upper limit of reporting time of the TT test. A commercially available diluted version the TT test is the Hemoclot®. The Hemoclot® involves dilution (1 in 8 or 1 in 20 depending on protocol) of the test plasma with a normal pooled plasma. This compensates for the over sensitivity of TT and has been reported to show a good correlation to dabigatran concentration. However, since the dTT test involves dilution of a large pool of normal plasma, the impact of innate inter-individual variability, particularly fibrinogen concentrations, is not captured [107, 115]. ECT test correlates linearly with dabigatran concentrations [111]. The ECT test has historically been proposed as a general assay to measure concentrations of thrombin inhibitors [117]. The ECT test is sensitive to dabigatran thrombin inhibition but is expensive and there are currently no commercially available kits. This would require each laboratory to calibrate the test against measured dabigatran concentrations resulting in a standardisation between laboratories.

In summary, the TT test, dTT test, and ECT test have linear relationship with dabigatran concentrations and could be used to assess clotting time in patient receiving dabigatran therapy. However, currently, there is currently no utility curve for dabigatran. The use of plasma concentration monitoring to guide dosing requires that a therapeutic range to be defined, which can be

obtained from a utility curve. In limited studies to date, Chin *et al* [116] have proposed that the target steady state trough concentration of dabigatran to be between 30-130 ng/mL. This was derived by reanalysing published Phase III data – more details will be presented in Chapter 6.

1.4.3.3. Current dosing methods

The dabigatran product datasheet indicates that dabigatran etexilate can be prescribed as a fixed dose for many patients. Limited dose adjustments have been suggested at initiation which is based on covariates (i.e. renal function, age and concomitant P-gp inducer/inhibitor). The dosing recommendations also differ geographically. The drug labels published by the European Medical Agency (EMA) and Medsafe New Zealand include dosing recommendation for stroke prevention in atrial fibrillation and prophylaxis of venous thromboembolism following deep vein thrombosis/ pulmonary embolism, while the United States Food and Drug Administration (FDA) drug label does not distinguish between the two indications. Table 1.1 summarises current dosing guidelines for non-valvular atrial fibrillation by the FDA, EMA and Medsafe NZ.

Table 1.1 *Summary of current New Zealand Medsafe datasheet [9], FDA [118] and EMA [119] dosing guidelines for stroke prevention in atrial fibrillation*

Characteristics	Medsafe NZ	FDA	EMA
Standard maintenance dose	150 mg bd	150 mg bd	150 mg bd
CL_{Cr} 30-50 mL/min	110 mg bd	150 mg bd *	150 mg bd **
CL_{Cr} < 30 mL/min	Contraindicated	75 mg bd***	Contraindicated
Age > 80 y*	110 mg bd	Not specifically discussed	110 mg bd
P-gp inhibitors	Variable†	Not specifically discussed	110 mg bd

** Reduce to 75 mg bd co-administered with P-gp inhibitor*

*** Consider 110 mg bd if patient at high risk of bleeding)*

**** Avoid co-administration of P-gp inhibitors*

† In one part of the datasheet, no dose-adjustment is suggested when these are concomitantly prescribed, whereas in other parts, it is suggested that maintenance dose is reduced (strong P-gp inhibitors) or that the combination is avoided (P-gp inducers, and ketoconazole, a P-gp inhibitor)

CL_{Cr}, creatinine clearance; P-gp, P-glycoprotein; bd, twice daily

Alternative dosing methods have been proposed. Chin *et al* [120] have suggested an alternative *a priori* approach of dose adjustment based on a proportional increment or reduction of dose in relation to creatinine clearance (covariate based). The dosing frequency remained similar to the datasheet (once daily for VTE prophylaxis and twice daily for AF patients), but doses suggested were up to 220 mg twice daily [120]. In a more recent publication, Chin *et al.* further proposed dose adjustments using thrombin time as a measure of response [116].

1.4.3.4. The need for improved dose prediction

Dabigatran is claimed to have predictable pharmacokinetics [110] and therefore anticoagulation monitoring is not recommended. Yet published data have reported up to 7-fold variation of trough plasma dabigatran concentration between patients [114]. Table 1.2 summarizes trough concentrations from several studies.

Table 1.2 *Dabigatran trough concentration from several studies*

Dosing regimen	**Hawes *et al 2013 [114]***	**van Ryn *et al* 2010 (PETRO trial) [110]**	**Reilly *et al 2014 [10]***
110 mg twice daily			28.2-155 ng/ml (10-90th percentile)
150 mg twice daily	45–487 ng/mL peak (range)	31 to 225 ng/ml (5-95 percentile)	39.8-121.5 ng/mL (10-90th percentile)

It is noteworthy that a 5-fold variation in plasma concentration translates to approximately CV% of 40% across a patient population. This CV% has been proposed to be relatively 'normal' variation seen across many drugs [39, 121]. As noted above, it is argued that any drug that perturbs the coagulation network for the purposes of therapeutic anticoagulation will have a narrow therapeutic range and therefore warrants monitoring [39].

There have been published data that show a correlation between plasma dabigatran concentration and anticoagulation effect [10, 122]. The study by Reilly *et al* [10], found that renal function is the primary determinant of dabigatran plasma concentration and age is an important covariate. According to Cohen *et al* [123] the optimal dabigatran concentration should be between 40 ng/mL and 215 ng/mL, based on unpublished information from the RELY trial. Moore *et al* [124] have presented numerous reports from regulatory agencies worldwide indicating that current dosing practices result in bleeds particularly in older patients above 80. Another study by Eikelboom *et al* [125] also found that older patients on dabigatran are at higher risk of bleeding. Therefore, it could be argued that concentration monitoring, for patients at risk of thrombosis, should improve the safe and effective use of dabigatran. The possible therapeutic range for dabigatran compiled from several sources is presented in Table 1.3

Table 1.3 *Possible therapeutic range*

Source	Dabigatran concentration (ng/mL)
Unpublished emails between authors of Reilly *et al* [10] reported by Cohen et al [123]	40 – 215
Further internal author emails of Reilly *et al* [10] reported by Cohen et al [123]	40-200
EMA drug assessment report in 2010 [126]	48 - 200
Chin *et al* 2014 [116]	30-130 (trough concentration)

It is noted that dabigatran is currently only available in three dosage strength; 75, 110 and 150 mg. In New Zealand and Europe, all three dosage forms are available [9, 119, 127]. In the United State, the 110-mg capsule is not approved by the FDA for atrial fibrillation and hence is not available [128]. The primary concern, as stated in the summary review from the FDA's Center for Drug Evaluation and Research [129], is that the 110 mg capsule maybe over-utilised and therefore preventing some patients of the potential benefit from the higher 150 mg strength. Undoubtedly the restricted availability of dosage strength would limit the choice of dose adjustment.

PART II

WARFARIN DOSING

Part II of this thesis describes two studies that principally aim to improve warfarin dose predictions. Chapter II focuses on several investigations on the ability of a Bayesian forecasting method to predict the maintenance dose of warfarin and Chapter III evaluates the predictive performance of published warfarin dosing tools.

Chapter 2: Investigating warfarin maintenance dose predictions using a Bayesian forecasting method

This chapter is based on the following peer-reviewed publication:

Saffian SM, Duffull SB, Roberts RL, Tait RC, Black L, Lund KA, Thomson AH, Wright DF. Influence of Genotype on Warfarin Maintenance Dose Predictions Produced Using a Bayesian Dose Individualization Tool. Therapeutic drug monitoring. 2016 Dec;38(6):677-83

This chapter builds on work completed during my Postgraduate Certificate in Pharmacy (research). In my Postgraduate Certificate research work, the predictive performance of a Bayesian dosing tool was evaluated using a small sample of patients who were initiating warfarin therapy. This could be considered to be a pilot study. The work completed for this thesis extended this research into a full retrospective analysis of two datasets, including patients initiating warfarin from two different sites. The overarching aim of the thesis is to improve patient outcomes for patients receiving anticoagulation therapy. This chapter contributes to this aim by investigating whether a Bayesian forecasting method can be used to predict the maintenance dose of warfarin. The ultimate goal was to make this dosing method available for those involved in warfarin dosing and monitoring services.

2.1. Introduction

Warfarin has been the mainstay of oral anticoagulant therapy for the past seven decades and remains widely used for the treatment of thromboembolic diseases. The maintenance dose required to achieve therapeutic anticoagulation is difficult to predict and can vary by upwards of 15-fold between patients [68]. An additional challenge for prescribers is that each patient will have a relatively narrow range of doses that will produce safe and effective anticoagulation, usually monitored using the INR. Under- or over- dosing will result in INR values outside the target range (2-3 for most conditions) and may put the patient at risk of severe adverse outcomes such as bleeding or thromboembolism. Treatment is considered successful if the time that patients spend within the therapeutic range (TTR) is maximised. Conventional, heuristic, dosing methods have been found to result in a TTR of only 40-60% [130-133]. Not surprisingly, there is a large body of literature exploring strategies to improve warfarin dose prediction [3].

Bayesian forecasting methods for dosing warfarin have been proposed as a means of improving INR control [1]. In limited studies to date, Bayesian methods

show the potential to increase the TTR to 80% or more [2, 75, 134, 135]. In addition, Bayesian algorithms can easily be integrated with decision support tools for use in the clinic (see Hamberg et al. 2015 [136] for an example).

A published Bayesian forecasting method for warfarin therapy has been developed and implemented in a software called TCIWorks [1, 2]. The stated intention of the tool was to provide a means of predicting warfarin doses in individual patients in the clinic. In addition, the tool has been proposed as a means of predicting warfarin doses without the need for patient-specific genotype information, such as *CYP2C9* genotype which affects the metabolism of warfarin and *VKORC1* genotype which encode the enzyme that is responsible for recycling vitamin K [1]. An evaluation of the predictive performance of the Bayesian dosing tool in patients initiating warfarin (n=46) found that the maintenance doses predicted using the Bayesian dosing tool were unbiased on average [3]. However, in a *post-hoc* analysis it was found that doses for patients with *VKORC1* (-1639 G>A) GG genotype were positively biased by about 1 mg/day on average in some patients. In particular, it was noted that doses for patients with *VKORC1* (-1639 G>A) GG genotype and those taking more than about 7 mg daily were poorly predicted.

Bias in dose predictions of warfarin can have important clinical implications. In theory, a Bayesian dosing method, underpinned by population model for warfarin-dose response like the TCIWorks tool [20], should be able to predict warfarin response across a range of doses. A positive bias of 1 mg daily could result in an increased propensity for adverse effects depending on the actual dose requirements. Unbiased and precise maintenance dose predictions should improve patient outcome by increasing the time spent within the therapeutic range with lesser dose adjustments.

The source of the bias in warfarin doses produced by the published Bayesian dosing tool is not obvious. The following four possibilities can be hypothesised;

1. This is aberrant finding in a small single centre study
2. The bias is a dose effect, observable in those subjects who take more than about 7mg daily
3. The bias is a genotype effect
4. The prior population used to develop the Bayesian dosing tool was significantly different from the posterior population

2.2. Aims and objectives

This study aims to investigate the source of bias in warfarin maintenance dose predictions produced using a published Bayesian dosing tool.

There are four specific objectives:

(1) To determine if the previously observed bias in warfarin dose predictions could be replicated in a new cohort of patients from a different clinical setting,
(2) To explore the influence of maintenance dose on the predictive performance of the Bayesian tool
(3) To explore the influence of genotype on the predictive performance of the Bayesian dosing tool,
(4) To determine if the prior population used to develop the kinetic-pharmacodynamic (KPD) model underpinning the Bayesian dosing tool was sufficiently different from the test (posterior) population to account for the biased dose predictions.

2.3. Methods

2.3.1. Patient data

Data available for analysis in this study was collected previously as part of two published studies not directly related to this thesis [2, 137]. The current chapter concerns the reanalysis of the published data as a means of investigating the sources of bias in dose predictions.

The study data is described briefly here. The data consisted of warfarin dose and INR values from patients initiating warfarin therapy for any indication. INR values were recorded from the start of therapy until a stable INR had been achieved. A stable INR was defined as the second INR within 20% of the INR target (2.5 in most cases) as described elsewhere [3]. Patients were genotyped for *VKORC1* (–1639 G>A rs9923231) and *CYP2C9* *1, *2 (430C>T, rs1799853) and *3 (1075A>C, rs1057910) as described elsewhere [3, 138]. Ethical approval was obtained from the Lower South Regional Ethics Committee, New Zealand (LRS/10/11/056) and West of Scotland Research Ethics Service, Glasgow, Scotland. All participating patients gave written informed consent.

Data from a total of 153 patients from two centres were available for analysis. These are designed data set I and data set II as follows;

i. Data set I - Dunedin Hospital, Dunedin, New Zealand (n=55) [2]
ii. Data set II – Glasgow Royal Infirmary, Glasgow, Scotland (n=98) [137]

Thirteen of the original 153 patients were excluded from the analysis; 12 who were not genotyped and 1 who did not reach a stable INR. The demographic details of the remaining 140 patients are summarised in Table 2.1. The distributions of both genotypes were consistent with the Hardy-Weinberg equilibrium ($p>0.05$). Median (range) age was 62 years (23-87) and 65 years (15-85) for data sets I and II, respectively.

Table 2.1 *Patient characteristics and a summary of maintenance dose and stable INR*

		Data set I (n = 46)	Data set II (n = 94)	Combined data set (n =140)
Age (years)		62 (23-87)	65 (15-85)	64 (15-87)
Male/Female (number of patients)		19/27	48/46	67/73
Time to reach first stable INR (days)		38 (11-118)	24 (9-64)	28 (9-118)
Number of INR observations to reach stable INR		11 (6-21)	9 (6-24)	10 (6-24)
Stable INR value		2.4 (2 – 3.1)	2.3 (2-3)	2.4 (2-3.1)
Dose at stable INR (mg/day)		5 (1.5 – 11)	4 (0.75 - 10)	4.5 (0.75-11)
Interquartile range [Q1 – Q3]		[4-7]	[3-5.4]	[3-5.57]
CYP2C9 genotype (number (%) of patients)				
	*1*1	28 (61%)	60 (64%)	88 (63%)
	*1*2	8 (17%)	19 (20%)	27 (19%)
	*1*3	9 (20%)	10 (11%)	19 (14%)
	*2*2	-	2 (2%)	2 (1%)
	*2*3	-	2 (2%)	2 (1%)
	*3*3	1 (2%)	1 (1%)	2 (1%)
VKORC1(-1639 G>A, rs9923231) genotype, (number (%) of patients)				
	GG	23 (50%)	45 (48%)	68 (49%)
	AG	18 (39%)	38 (40%)	56 (40%)
	AA	5 (11%)	11 (12%)	16 (11%)

Values are expressed as median (range) unless specified otherwise
Data set I = patients recruited from Dunedin Hospital, Dunedin, New Zealand
Data set II = patients recruited from Glasgow Royal Infirmary, Glasgow, Scotland

2.3.2. Maintenance dose predictions

Details of the development of the Bayesian dosing tool (TCIWorks) have been published previously [1, 2]. The underpinning model that describes the warfarin dose and anticoagulant response is a KPD model developed by Hamberg et al. [20]. Briefly, a KPD model is a pharmacokinetic-pharmacodynamic model where the pharmacokinetic parameters are estimated solely from the pharmacodynamic data. This means that no warfarin concentration data are required to predict the INR response. The KPD model developed by Hamberg et al [20] consists of two transit compartment chains with three compartments in each chain to describe the time course of INR response. An E_{max} model was used to describe the link between pharmacokinetics and pharmacodynamics. The KPD model also included a covariate model for *VKORC1* on EC_{50} (concentration of s-warfarin at 50 % of maximum drug effect) and age and *CYP2C9* on clearance parameters. Note that genotype was not included as a covariate in the published Bayesian dosing tool examined for this chapter [1]. The model implemented in TCIWorks (Hamberg et al. [20]) used an additive model for residual variance on log-transformed data to remain consistent with the published model [20].

The full dosing history for each patient from warfarin therapy initiation to a stable INR and all measured INR observations up to the final dose change were entered into the TCIWorks software. The Bayesian dosing tool was then used to predict the daily dose required to achieve the observed stable INR for each patient. The patients were assumed to be taking their prescribed dose at 6 pm and INR was assumed to be sampled at 10 am.

2.3.3. The predictive performance of the Bayesian dosing tool

The predicted maintenance doses were compared to the observed maintenance doses using measures of bias (mean prediction error [MPE]) and imprecision (mean squared error [MSE] and root mean squared error [$RMSE$]). MPE, MSE, and $RMSE$ were calculated as follows:

$$MPE = \frac{1}{N}\sum_{i=1}^{N} PE_i,$$

***Equation* 2.1** *Mean prediction error*

$$MSE = \frac{1}{N}\sum_{i=1}^{N} (PE_i)^2,$$

***Equation* 2.2** *Mean squared error*

$$RMSE = \sqrt{MSE}$$

***Equation* 2.3** *Root mean squared error*

where MPE is the mean prediction error, N is the number of patients, PE_i is the prediction error (predicted minus observed maintenance dose) of the i^{th} individual. No statistical bias was concluded if the 95% confidence interval (CI) of the MPE included zero. MSE is the average of the sum of squared differences between predicted minus observed maintenance dose, and $RMSE$ is the square root of MSE. $RMSE$ provides an estimate of the variability of the prediction errors given in the same units as the predicted dose (mg/day).

2.3.4. Replication of bias in a new cohort of patients from a different clinical setting

Two data sets were used to evaluate the predictive performance of the Bayesian dosing tool. The first data set was a re-analysis of a data collected from Dunedin Hospital, New Zealand and reported previously [3]. In the original analysis, only the first four INR values were used for dose prediction. In this analysis, all measured INR observations up to the final dose change was used to predict the maintenance dose. The second data set was collected at Glasgow Royal Infirmary, Scotland. These data were used to confirm if bias in warfarin dose predictions was also observed in data collected from a different site.

Predictive performance in terms of MPE and $RMSE$ were assessed as above for each data set and as a combined data set.

2.3.5. The impact of dose requirement on the predictive performance of the Bayesian dosing tool

The data set was stratified by observed maintenance dose into two groups; those who required ≥ 7 mg/day and those who required < 7 mg/day. A cut off of 7 mg/day has been used in other studies [68, 139] to categorize patients requiring a higher than average daily dose and therefore was used here. MPE and $RMSE$ were assessed as above for each dose group.

2.3.6. The impact of genotype on the predictive performance of the Bayesian dosing tool

The influence of genotype on warfarin dose predictions was assessed by stratifying the study cohort into different *VKORC1* and *CYP2C9* genotypes. Three methods are used:

1.) by measuring MPE and $RMSE$, as above, for each genotype group,

2.) a scatter plot of the observed and predicted dose data according to *VKORC1* and *CYP2C9* genotype are plotted for visual comparison, and

3.) the influence of *VKORC1* genotype on Bayesian dose predictions was tested by altering the mean prior parameter values of EC_{50} to reflect the observed genotype in each patient. This is intended as a diagnostic aid to understand a possible source of bias and not how the Bayesian tool would normally be used. The prior parameter values were normally set to the wild-type (GG) value for all patients (see Wright and Duffull [1]). For the purposes of this analysis the mean EC_{50} was changed manually for each patient prior to predicting the maintenance dose. The parameter values chosen corresponded to the observed genotype effect reported in the published model by Hamberg et al [20], i.e. an EC_{50} of 4.01 mg/L for those with *VKORC1* GG genotype, 3.01 mg/L for

individuals with *VKORC1* GA genotype, and 1.92 mg/L for the *VKORC1* AA genotype. The initial parameter estimates of *CYP2C9* were set to the wild-type (*1*1) and was not changed. The influence of *CYP2C9* will only be tested further if there were any significant improvement in bias were observed by changing the *VKORC1* prior parameter estimates.

2.3.7. The impact of the prior population on predictive performance of the Bayesian dosing tool

The hypothesis that the bias may be caused by inherent differences in warfarin dose-response within the study population compared to the population used to develop the KPD model by Hamberg et al [20] was explored. To address this, the published KPD model was fitted to the data set using a nonlinear mixed effects modelling methodology in NONMEM (version 7.2 (Icon Inc. [PA, USA]). Initial parameter estimates were the values reported by Hamberg et al [20]. A non-parametric bootstrap was carried out to assess the precision of the parameter estimates. A total of 1000 bootstrap data sets were generated by randomly sampling the original data set and simulated from the model to obtain the 95% CI of each parameter estimate. The mean and 95% CI of the estimated model parameters from the study cohort were compared to the values from the published KPD model and considered not significantly different based on two criteria; 1) if the means were within 20% of the published values, and, 2) if the mean observed value fell within the 95% confidence interval of the bootstrap.

2.4. Results

2.4.1. Replication of bias in a new cohort of patients from a different clinical setting

A summary of the MPE and $RMSE$ results for each data set analysed separately and combined is presented in Table 2.2. The Bayesian dosing tool, on average, produced positively biased dose predictions (MPE mg/day [95% CI]; 0.32 [0.14, 0.50]). When analysed separately, dose predictions for both the

Dunedin (data set I) and Glasgow data sets (data set II) were also both positively biased (*MPE* mg/day [95% CI]; 0.53 [0.11, 0.94] and 0.22 [0.04, 0.39] respectively).

Table 2.2 *A summary of average bias (mean prediction error (95% CI) and root mean squared error (RMSE) of the dose predictions.*

	Data set I	*Data set II*	*Combined data set*
MPE (95% CI)	0.53 (0.11, 0.94)	0.22 (0.04, 0.39)	0.32 (0.14, 0.5)
RMSE	1.52	0.88	1.13

MPE mean prediction error (mg/day), *CI* confidence interval, *RMSE* root mean squared error (mg/day). Data set I = Dunedin, New Zealand (n=46); Data set II = Glasgow, Scotland (n=94); Combined data set (n=140);

2.4.2. The impact of dose requirement on the predictive performance of the Bayesian dosing tool

The *MPE* mg/day [95% CI] for patients requiring ≥7 mg/day was 1.15 [0.43, 1.87] which represents an average over-prediction of approximately 18%, while the *MPE* mg/day [95% CI] for patients requiring <7 mg/day was 0.18 [0.009, 0.34] (see Figure 2.1). *RMSE* values for patients requiring <7 mg/day and ≥7 mg/day were 0.94 mg/day and 1.90 mg/day, respectively.

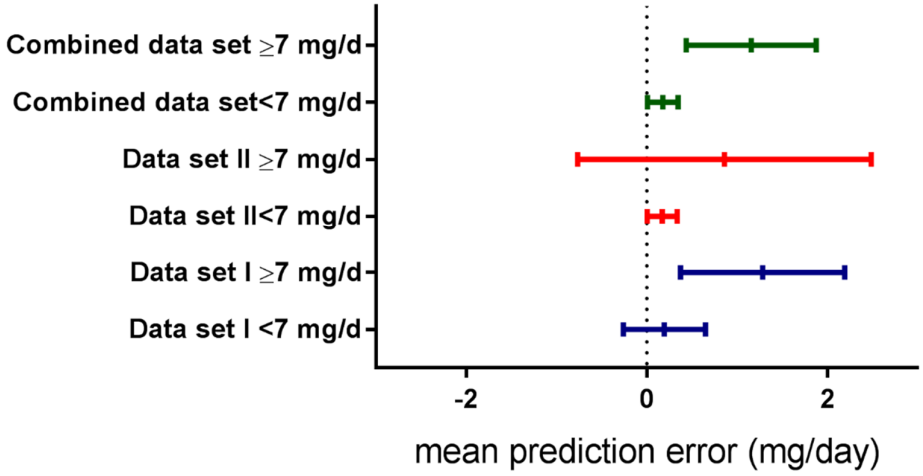

Figure 2.1 *Mean prediction error according to data set and magnitude of dose requirement. The horizontal lines represent 95% CI of the prediction error and the centre vertical line is the mean prediction error. The vertical dotted line indicates a prediction error of zero.*

2.4.3. The impact of genotype on the predictive performance of the Bayesian dosing tool

Dose predictions for patients with the *VKORC1* GG genotype in the combined data set were found to be positively biased (see Table 2.3). Dose predictions for patients with *VKORC1* AG and AA were unbiased. Visual plots of the observed versus prediction maintenance dose according to *VKORC1* is presented in Figure 2.2

Table 2.3 *A summary of average bias (mean prediction error (95% CI) and root mean squared error (**RMSE**) of the dose predictions according to VKORC1 genotype.*

VKORC1	Data set I		Data set II		Combined	
	MPE (95% CI)	*RMSE*	*MPE* (95% CI)	*RMSE*	*MPE* (95% CI)	*RMSE*
GG	1.13 (0.48, 1.77)	1.85	0.23 (-0.05, 0.52)	0.97	0.53 (0.21, 0.86)	1.34
AG	-0.05 (-0.67, 0.56)	1.21	0.23 (-0.03, 0.5)	0.84	0.14 (-0.11, 0.4)	0.97
AA	-0.13 (-0.68, 0.43)	0.42	0.08 (-0.37, 0.54)	0.65	0.02 (-0.28, 0.32)	0.59

MPE mean prediction error (mg/day), *CI* confidence interval, *RMSE* root mean squared error (mg/day). Data set I = Dunedin, New Zealand (n=46); Data set II = Glasgow, Scotland (n=94); Combined data set (n=140);

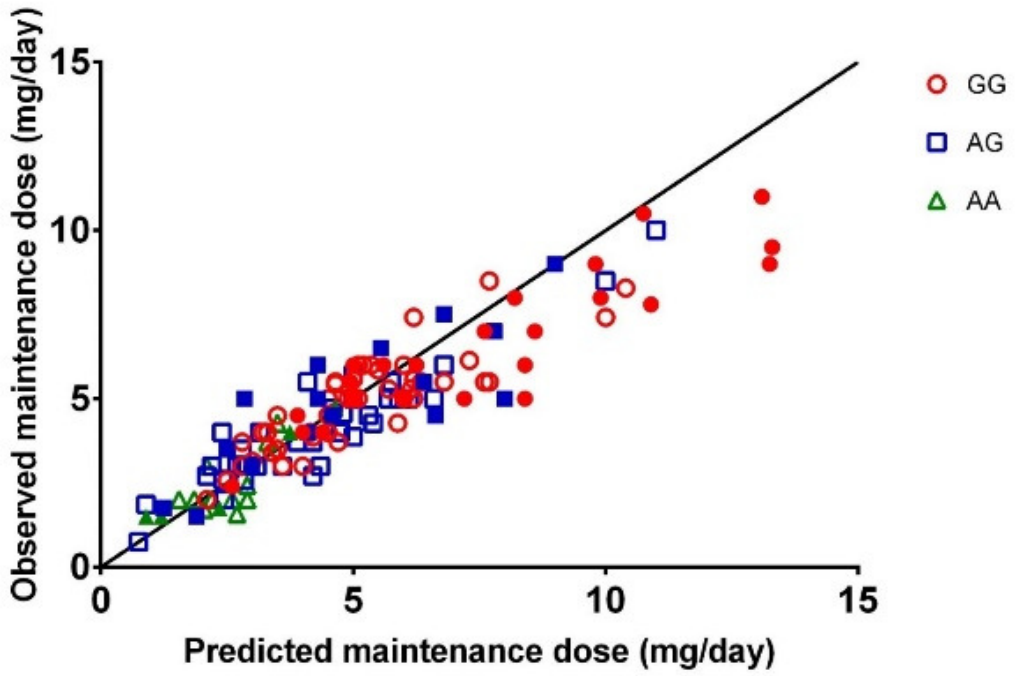

Figure 2.2 *Scatter plot of the observed versus predicted maintenance dose according to VKORC1 (-1639 G>A, rs9923231). The solid line is a line of identity. Filled symbols represent data set I (Dunedin, New Zealand) and open symbols represent data set II (Glasgow, Scotland)*

Dose predictions for patients with *CYP2C9* *1*1 were positively biased in the combined data set. Dose predictions for all other *CYP2C9* genotype combinations were unbiased in the combined data set (Table 2.4). A visual plot of the observed versus prediction maintenance dose according to *CYP2C9* is presented in Figure 2.3.

Table 2.4 *A summary of average bias (mean prediction error (95% CI) and root mean squared error (RMSE) of the dose predictions according to CYP2C9 genotype.*

CYP2C9	Data set I		Data set II		Combined	
	***MPE* (95% CI)**	***RMSE***	***MPE* (95% CI)**	***RMSE***	***MPE* (95% CI)**	***RMSE***
*1*1	0.46 (-0.13, 1.05)	1.56	0.32 (0.07, 0.57)	1.00	0.36 (0.12, 0.61)	1.21
*1*2	1.06 (-0.43, 2.56)	1.98	-0.1 (-0.37, 1.7)	0.55	0.24 (-0.22, 0.71)	1.17
*1*3	0.29 (-0.35, 0.93)	0.83	0.29 (-0.21, 0.79)	0.72	0.29 (-0.07, 0.65)	0.78
*2*2	-	-	0.25 (NA)	0.79	-0.5 (-9.3, 9.8)	0.79
*2*3	-	-	-0.18 (NA)	0.80	-0.18 (-10, 9.7)	0.80
*3*3	0.4 (NA)	0.40	0 (NA)	0	0.39 (-2.3, 2.7)	0.28

MPE mean prediction error (mg/day), CI confidence interval, RMSE root mean squared error (mg/day). Data set I = Dunedin, New Zealand (n=46); Data set II = Glasgow, Scotland (n=94); Combined data set (n=140); NA, not available

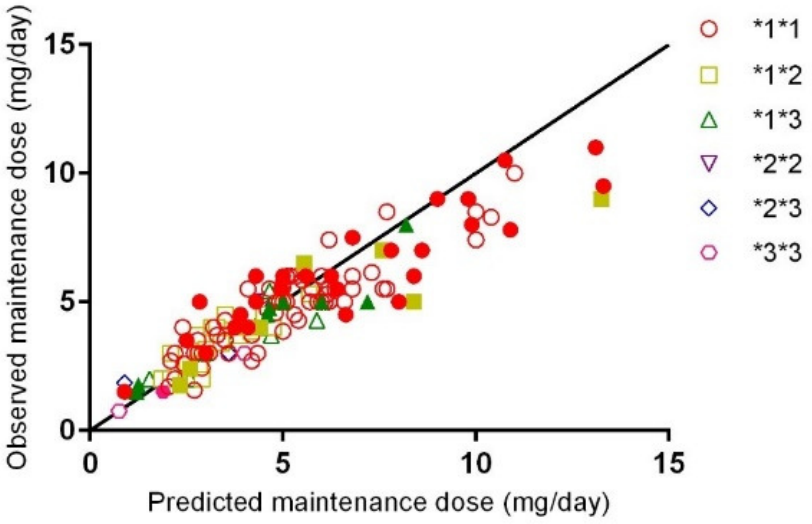

Figure 2.3 *Scatter plot of the observed versus predicted maintenance dose according to; CYP2C9. The solid line is a line of identity. Filled symbols represent data set I (Dunedin, New Zealand) and open symbols represent data set II (Glasgow, Scotland)*

To explore the influence of genotype further, the *MPE* for patients with *VKORC1* GG genotype who had *CYP2C9* *1*1 and those who were not *CYP2C9* *1*1 and found a positive bias for both combinations were compared. However, when patients with *CYP2C9* *1*1 patients who were not *VKORC1* GG were grouped, the dose predictions were not biased (Figure 2.4). This suggests that the source of the bias is more likely to be *VKORC1* genotype.

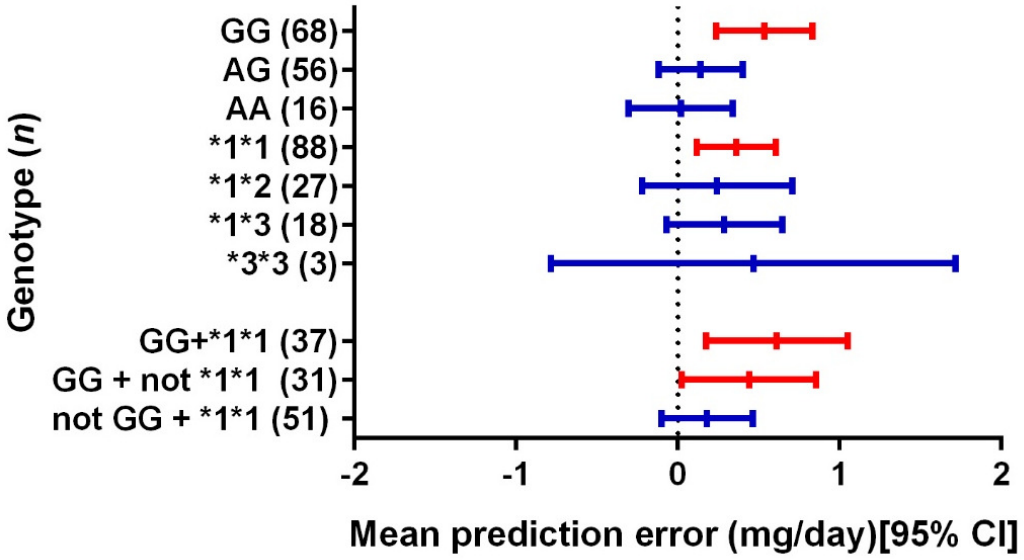

Figure 2.4 *Mean prediction error by subgrouping according to VKORC1 or CYP2C9 genotype combination. The horizontal lines represent 95% CI of the prediction error and the centre vertical line is the mean prediction error. The vertical dotted line indicates a prediction error of zero. Red horizontal lines indicate that the 95% CI of the prediction error does not cross zero (i.e. is biased).*

The Bayesian dose predictions conducted using individual values of EC_{50} for each patient, corresponding to their observed genotype, were found to produce positively biased results overall (Table 2.5). It is noteworthy that those subjects with reduced EC_{50} values (i.e. *VKORC1* AG and AA genotypes) had unbiased dose predictions. The *MPE* for the *VKORC1* GG genotype group remained the same since the wild-type values were used previously. Based on these results, the influence of prior parameter estimates of different individual's

CYP2C9 genotype (on clearance) were not tested as there was no improvement observed by using the values of EC_{50} that corresponds to the observed genotype of the patient.

Table 2.5 *A summary of **MPE** and **RMSE** using the individual's genotype to determine the prior value of EC_{50} used in the population model*

***VKORC1* (-1639 G>A) Genotype**	***MPE* (mg/day) [95% CI]**	***RMSE***
All data	0.28 (0.09, 0.46)	1.14
GG	0.53 (0.21, 0.86)	1.34
AG	0.08 (-0.18, 0.35)	1.01
AA	-0.11 (-0.46, 0.23)	0.65

2.4.4. The impact of the prior population on the predictive performance of the Bayesian dosing tool

The results of the estimated parameters and bootstrap runs using the model to estimate into a new population are summarized in Table 2.6. 93.8% of the bootstrap runs minimized successfully. Mean parameter estimates for EC_{50} (G allele and A allele) and between subject variability for EC_{50}, were within 20% of the published value. The mean published values for the parameters fell within the 95% CI of the bootstrap in all cases expect for MTT1 and proportion residual error. These parameters would not be considered likely to be a cause of bias in predictions because MTT1 partly describes the delay between pharmacokinetic and pharmacodynamic effect (as there is another MTT2 which describes delay in the second chain) and proportion residual error describes the individual differences between model prediction and individual patient. Both of these parameters are not expected to systematically deviate across the dosing requirements.

Table 2.6 *Parameter estimates from the published prior kinetic-pharmacodynamic (KPD) model (as a comparison) and bootstrap resampling*

Parameter	Published prior KPD model [95% CI]	Bootstrap mean estimate [95% CI]
EC_{50}G (mg/L)	2.05 [1.64, 2.46]	2.24 [1.32, 3.64]
EC_{50}A(mg/L)	0.96 [0.78, 1.14]	1.10 [0.63, 1.82]
MTT_1 (hours)	28.6 [27.25, 29.95]	34.92 [29.25, 45.50]
MTT_2 (hours)	118.30	64.86 [1.43, 140]
Proportional residual error (ε_{INR}) CV %	20.00	14.70 [13.50, 15.90]
γ	1.15 [1.05, 1.25]	1.51 [1.14, 2.01]
BSV EC_{50} (CV %)	34 [29.93, 38.07]	29.73 [25.78, 33.98]
BSV CL (CV %)	29.83 [17.9, 41.76]	44.18 [21.48, 67.72]
BSV V (CV %)	23.23 [10.17, 36.31]	49.46 [15.01, 79.96]

EC_{50}G and EC_{50}A concentration of s-warfarin at 50 % of maximum drug effect for G and A allele, MTT mean transit time, CV coefficient of variation, γ Hill coefficient, BSV between subject variability, K_{10} first-order elimination rate constant, CL clearance, V volume of distribution of *s*-warfarin

2.5. Discussion

In this study, the possible causes of bias in warfarin maintenance dose predictions with a Bayesian dosing tool were explored. A previously reported over-prediction of warfarin maintenance dose requirements was successfully replicated using two data sets from different clinical centres. Furthermore, dose predictions were carried out in the Bayesian dosing tool using all available INR measurements for each patient which should provide the most accurate estimate of the patient's response. The biased warfarin dose predictions were only observed in patients requiring ≥7 mg/day.

Several publications on the application of Bayesian methodologies to warfarin dose individualisation have been reported previously [75-80]. A summary of previous Bayesian dosing tools for warfarin and how they differ from the dosing tool in this study have also been reviewed [1, 2]. Vadher et al. [79] compared the observed dose to the predicted maintenance dose and found that their Bayesian dosing tool was negatively biased on average. A scatter plot

of the observed dose versus predicted dose reported by Vadher et al [79] also showed biased predictions in patients requiring higher daily doses, although in a different direction (under-prediction in higher dose patients). Other publications on Bayesian dosing tools for warfarin did not analyse the predictive performance of the dosing tool in a way that would allow comparison with this work.

Four possible explanations for the bias were explored in this study. First, the hypothesis that it was an aberrant finding only observed in a single population. This study found that the observed bias can be replicated in a different population and therefore suggests that the bias is not due to an aberrant population. The second and third hypothesis was that the bias is driven by a dose-effect relationship or due to the influence of *VKORC1* genotype. *VKORC1* was the primary focus since it was identified as a candidate in previous work [3] but in the present study it was found to have no influence on dose predictions. In addition, the direction of dose prediction error (i.e. over or under-predicted dose) in each patient requiring ≥ 7 mg/day was the same despite changing the EC_{50} priors to the values as per published prior model. This suggests that the influence of *VKORC1* is not a primary driver of the observed bias. Furthermore, the initial apparent association of bias and *VKORC1* GG may be explained by a higher proportion of patients with *VKORC1* GG in this dose category and therefore, the initial link between *VKORC1* GG and bias was more likely to be an association rather than a cause.

The possibility that the population used to derive the prior population parameter estimate for the KPD model had a different dose-response to our study population which would mean that the model could not be extrapolated to the study population was also explored. The results suggest that the prior and posterior populations were not sufficiently different to be a plausible cause of the observed bias.

As noted above, the bias in warfarin dose predictions was evident only for those patients taking ≥ 7 mg/day. The reason for this is not currently clear. Since

it was found that it is not likely to be the parameter values used as the basis of the prior, then this suggests it could be the structure of the prior model. It is known the coagulation network is complex [36]. It is therefore plausible that the use of empirical transit chain model to describe the time course of warfarin response may not be sufficiently flexible to account for the inherent feedback and feedforward mechanisms of the coagulation network. This being the case, bias may be apparent in those patients taking higher than average warfarin doses.

2.6. *Conclusion*

In two patient cohorts, the Bayesian dosing tool resulted in positively biased warfarin dose predictions. By combining both data sets, a positive bias dose prediction of 0.32 mg/day (95% CI; 0.14, 0.5) was found. Warfarin doses were over-predicted for patients requiring ≥ 7 mg/day by 1.15 mg/day on average. The bias in dose predictions was not found to be due to the influence of *VKORC1* genotype. The prior and posterior populations were not sufficiently different to be the source of bias.

Chapter 3: An evaluation of warfarin dosing tools in patients requiring ≥ 7mg daily

This chapter is based on the following peer-reviewed publication:

Saffian SM, Duffull SB, Wright DFB (2017) Warfarin dosing algorithms under-predict dose requirements in patients requiring ≥ 7mg daily: A systematic review and meta-analysis. Clinical Pharmacology & Therapeutics: 102(2): 297-304. DOI 10.1002/cpt.649

In the previous chapter, a Bayesian forecasting tool was found to produce biased dose predictions for those patients who required ≥ 7mg daily. While the source of the bias could not be determined, it was proposed that empirically-derived and semi-mechanistic models for warfarin dose-response may not adequately capture the complexity of the coagulation network and therefore cannot capture the warfarin-INR response at the extremes. This chapter examines other type of dosing tools that are designed to predict the maintenance dose of warfarin at initiation to learn if doses can be predicted accurately in patients requiring higher daily doses.

3.1. Introduction

There have been a large number of publications exploring strategies to improve INR control and to predict warfarin dose requirements. A variety of nomograms, computerised decision-support tools and Bayesian dose prediction tools have been proposed to aid dosing decisions in the clinic [76, 79, 140, 141]. In recent years, the use of patient characteristics to predict warfarin dosing requirements prior to the initiation of therapy has been advocated by researchers, clinicians, and the Food and Drug Administration (FDA). These algorithms are developed by regressing patient characteristics, including age, body size, ethnicity, concomitant drug use and genetic variability in warfarin metabolism (via *CYP2C9* genotype) or vitamin K recycling (via *VKORC1* genotype) [4, 24, 30, 68], against maintenance dose requirements. The algorithms therefore provide a means of rapidly predicting warfarin dosing requirements at the initiation of therapy [24, 68, 139, 143]. The algorithms have been shown to accurately predict dosing requirements for warfarin on average [30, 68], and have been implemented in some clinical settings [135, 144]. To date however, clinical trials have not consistently demonstrated that dose prediction using warfarin algorithms improves anticoagulant control or patient outcomes compared to other methods [84, 85, 145-149].

The average maintenance dose requirement for warfarin is reported to be 4-5 mg daily [68], with an interquartile range of 3-6 mg daily [68, 150]. The need for dose reduction in some patients due to factors such as increasing age [24], drug interactions [24, 30], and genetic factors [24, 68] are well documented. Factors that predict higher warfarin dose requirements are less well understood and the management of these patients presents a challenge for prescribers. This is particularly the case at the initiation of therapy when doses are being titrated to the anticoagulant response and the risk of over-anticoagulation has been found to be at its highest [150, 151]. Equally, overly cautious dose escalation for patients who require higher doses may unnecessarily prolong the time to reach stable anticoagulation, requiring extended periods of parenteral anticoagulant cover for patients with acute thromboembolism.

It could be argued that the patients who might receive the most benefit from the use of warfarin dosing aids in the clinic are those who require doses outside the normal dose range of 3-6 mg daily. However, published algorithms are developed largely using patient characteristics that predict a reduction in warfarin dose while factors associated with higher dose requirements are not considered or are restricted to smoking status, concomitant use of enzyme inducers, or African-American ethnicity (see Gage et al. [24] for an example).

In the previous chapter, a Bayesian dosing tool was found to produce biased maintenance dose predictions in patients requiring higher daily doses. There is published evidence to suggest that warfarin dosing algorithms under-predict dose requirements in those patients who require doses in the upper quartile of dose requirements [3, 152-154]. It is therefore unclear whether bias in dose prediction in this subgroup of patients (i.e. patients requiring ≥ 7 mg daily) are merely isolated problems with a few dosing tools or if a systematic bias may exist across different dosing tools.

3.2. Aim

To determine if warfarin dosing algorithms produce accurate maintenance dose predictions for those patients who require ≥ 7 mg daily.

3.3. Methods

3.3.1. Identifying published warfarin maintenance dose prediction algorithms

Medline (1946 – September 2015) and Embase (1947 – September 2015) was searched to identify all studies that evaluated the predictive performance of algorithms designed to predict the maintenance dose of warfarin. These included genotype-driven algorithms, Bayesian algorithms and warfarin decision-support tools. The Medline MeSH terms included: "warfarin", "algorithm*", "regression analysis", "statistical models", "Bayes theorem", "Dose-Response Relationship, Drug or dose response", "international normalized ratio", "pharmacogenetics" and keywords "dose predict*", "regression", and "dose calculation" were used. The search was limited to articles published in English and human studies. Key review publications were also identified and mined for further relevant studies. In addition, the reference lists from the identified studies were further examined for potentially relevant studies as well as citations of the studies identified.

3.3.2. Inclusion and exclusion criteria

Studies that were identified from the database search were screened based on the title and abstract. Full-text assessment was carried out on all studies that evaluated the ability of a dosing algorithm to predict the maintenance dose of warfarin. The unit of analysis in this meta-analysis was a unique algorithm.

Studies were included if they (1) provided an evaluation in the form of a scatterplot of observed versus predicted maintenance doses, and (2) the published scatterplot included observed doses from a validation data set. Here

the term 'validation data set' is used to refer to data external to the development of the algorithm.

Studies were excluded if (1) the published scatterplot was of insufficient resolution to allow the data to be extracted, and (2) there were less than five patients requiring ≥7 mg/day in the data set. Similar to the previous chapter, a cut off ≥7 mg/day was used to define patients requiring 'higher than average' dose as this definition has been used in several other large studies [68, 152].

3.3.3. Data extraction

For each scatterplot, data points for patients requiring ≥7mg/day were digitized using the MATLAB® script, GRABIT [155].

The reproducibility of the extracted data was evaluated by replicating the extracted data in a sample of 5 scatterplots (approximately a 10% sample). This was done by a researcher who was not involved in this study. The relative difference between the original and replicate of the extracted data points were compared. A difference of 10% was considered to be acceptable.

3.3.4. Meta-analysis

The null hypothesis was that dosing algorithms would produce unbiased dose predictions so that overall there would be an equal proportion of dose predictions on either side of the line of identity in the published scatterplots. Therefore, the null proportion of 0.5 (50% of predicted doses would be expected on either side of the line of identity) was used to test for bias. A minimum of 5 samples was required to obtain a binomial probability p value <0.05. This can be calculated using:

$$p(x): \binom{n}{x}\ p^x\ (1-p)^{n-x}$$

Equation 3.1 *The binomial probability*

where $p(x)$ is the binomial distribution for variable x, n is the number of trials (total number of patients requiring ≥7mg/day), x is the number of success (number of under-predicted doses), $n - x$ is the number of failures, p is the probability of success in any given trial (i.e. 0.5).

The proportion of over- and under-predicted doses was quantified. The primary outcome of interest for the meta-analysis was the proportion of over- or under-predicted warfarin doses for patients requiring a maintenance dose of 7 mg/day or more (the upper quartile of warfarin dosing requirements).

Several dosing algorithms were evaluated, and published, in more than one study was noted. This was considered to be a repeated measure.

The meta-analyses was performed using MedCalc for Windows, v15.10 (MedCalc Software, Ostend, Belgium) [156]. A random effects model was used given an *a priori* assumption of significant heterogeneity between studies [142]. The meta-analysis was conducted using a three-stage hierarchical meta-analytical model. Algorithms with repeated measure were first pooled across to provide an overall estimate for the individual algorithm. Then an estimate of n and p that would provide the same pooled proportion and 95% CI for each of the algorithm (with repeated measure) was obtained using a search algorithm in MATLAB® (see appendix A3.1). Herein, the algorithms with repeated evaluations are termed 'pooled' algorithms. The proportion of over and under-predicted doses for the pooled algorithms (i.e. with repeated measures) were then pooled with the rest of the whole population of algorithms. Therefore, stage one refers to the whole population of algorithms, stage two the individual algorithm and stage three the individual study.

Heterogeneity among studies were explored at the first stage using the I^2 statistic, where an I^2 of 25%, 50% and 75% is considered to have low, moderate and high heterogeneity respectively [157, 158]. Note that, since *a priori* a random effects model was used (to account for the various stages in the hierarchy), the analysis for heterogeneity is for descriptive purposes to quantify the homogeneity across algorithms.

3.3.5. Estimating the average prediction error

The average prediction error was calculated by dividing the sum of prediction error (predicted maintenance dose minus observed maintenance dose of each patient requiring ≥7 mg/day) by the total number of patients requiring ≥7 mg/day.

3.4. Results

3.4.1. Literature search results

Ninety-five studies that evaluated the predictive performance of warfarin dosing algorithms was found. Seventy-nine studies were excluded because they did not meet the inclusion/ exclusion criteria. Twenty-three evaluations were excluded on grounds that they were not evaluating dose predictions against external data, six evaluations had insufficient resolution to allow data extraction, and thirteen evaluations had no or less than five patients requiring doses ≥ 7mg/day (see Table 3.1). Figure 3.1 shows a flow diagram for the study selection process.

Table 3.1 *A breakdown of the excluded scatterplots from the meta-analysis*

Algorithm	Scatterplot	Reason for exclusion
Botton 2011 [159]	Botton 2011 [159]	Not evaluating against external data
Doi 2001 [160]	Doi 2001 [160]	Not evaluating against external data
Ekladious 2013 [161]	Ekladious 2013 [161]	Not evaluating against external data
Gong 2011 [162]	Gong 2011 [162]	Not evaluating against external data
Lazo-Langner 2009 [163]	Lazo-Langner 2009 [163]	Not evaluating against external data
Le Gal 2010 [164]	Le Gal 2010 [164]	Not evaluating against external data
Lenzini 2008[165]	Lenzini 2008 [165]	Not evaluating against external data
Lenzini 2010 [30]	Lenzini 2010 [30]	Not evaluating against external data
Michaud 2008 [166]	Michaud 2008 [166]	Not evaluating against external data
Millican 2007 [66]	Millican 2007 [66]	Not evaluating against external data
Pavani 2014 [167]	Pavani 2014 [167]	Not evaluating against external data
Perini 2010 [168]	Perini 2010 [168]	Not evaluating against external data
Roper 2010 [169]	Roper 2010 [169]	Not evaluating against external data
Santos 2015 [170]	Santos 2015 [170]	Not evaluating against external data
Schelleman 2008 [171]	Schelleman 2008 [171]	Not evaluating against external data
Suprianata 2011 [172]	Suprianata 2011 [172]	Not evaluating against external data
Takahashi 2006 [173]	Takahashi 2006 [173]	Not evaluating against external data
Vadher 1999 [79]	Vadher 1999 [79]	Not evaluating against external data
Voora 2010 [174]	Voora 2010 [174]	Not evaluating against external data
Wei 2012 [175]	Wei 2012 [175]	Not evaluating against external data
Wells 2010 [164, 176]	Wells 2010 [164, 176]	Not evaluating against external data
Yoshizawa 2009 [177]	Yoshizawa 2009 [177]	Not evaluating against external data
Zhu 2007 [178]	Zhu 2007 [178]	Not evaluating against external data
Gage 2008 [24]	Voora 2010 [174]	Insufficient resolution
Sconce 2005 [143]	Roper 2010 [169]	Insufficient resolution
Klein 2009 [68]	Roper 2010 [169]	Insufficient resolution
Roper 2010 [169]	Roper 2010 [169]	Insufficient resolution
Gage 2008 [24]	Roper 2010 [169]	Insufficient resolution
Saleh 2014 [179]	Saleh 2014 [179]	Insufficient resolution
Haug 2008 [180]	Harada 2010 [181]	no patients requiring doses ≥ 7mg/day
Harada 2010 [181]	Harada 2010 [181]	no patients requiring doses ≥ 7mg/day

Huang 2009 [182]	Wang 2012 [183]	no patients requiring doses ≥ 7mg/day
Kim 2009 [184]	Kim 2009 [184]	no patients requiring doses ≥ 7mg/day
Lu 2013 [185]	Lu 2013 [185]	no patients requiring doses ≥ 7mg/day
Sconce 2005 [143]	Sconce 2005 [143]	no patients requiring doses ≥ 7mg/day
Sconce 2005 [143]	Harada 2010 [181]	no patients requiring doses ≥ 7mg/day
Zhang 2010 [186]	Lu 2013 [161] *	no patients requiring doses ≥ 7mg/day
Tan 2012 [187]	Tan 2012 [187]	<5 patients requiring doses ≥ 7mg/day
Huang 2009 [182]	Huang 2009 [182]	<5 patients requiring doses ≥ 7mg/day
Sasaki 2009 [188]	Sasaki 2009 [188]	<5 patients requiring doses ≥ 7mg/day
Klein 2009 [68]	Lei 2012 [189]	<5 patients requiring doses ≥ 7mg/day

* had two evaluations

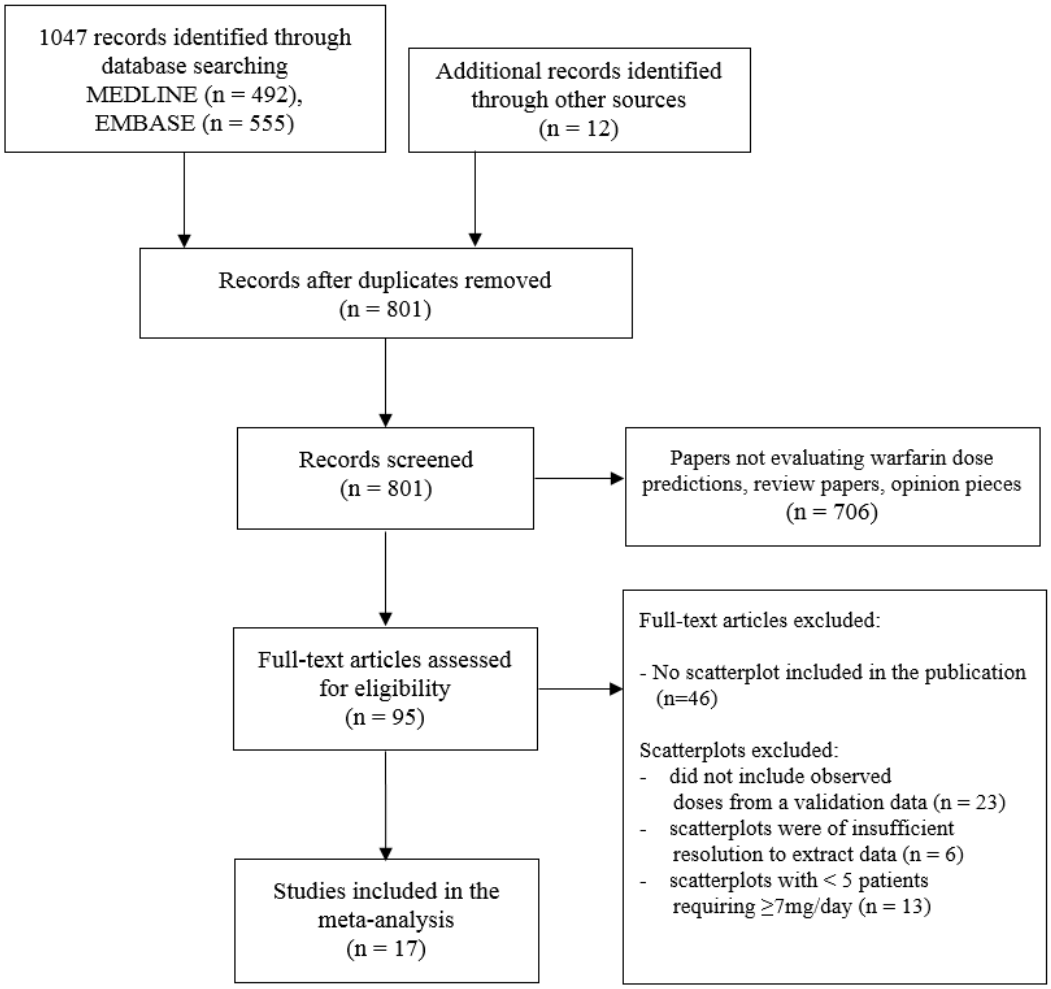

Figure 3.1 *Study selection process*

The final analysis included 47 evaluations of 22 unique algorithms [24, 30, 31, 64, 65, 68, 74, 143, 145, 159, 164, 167, 170, 178, 190-193] from 17 studies (scatterplots from [3, 31, 64, 68, 84, 167, 169, 170, 190, 192, 194-199]). Eleven algorithms [24, 30, 68, 143, 145, 164, 178, 190, 191] were evaluated in multiple studies (between 2-6 times).

3.4.2. Characteristics of the eligible studies

The study population included patients taking warfarin for atrial fibrillation, venous thromboembolism, heart valve replacement, transient ischaemic attack, and cardiomyopathy (Table 3.2). Patient characteristics used to predict dose requirements included measures of body size, age, race, co-medication, indication of warfarin use, and *CYP2C9* and *VKORC1* genotype information. Data from 1492 patients were available for analysis. On average, approximately 14% of all patients who were taking warfarin required doses ≥ 7 mg daily.

Table 3.2 *Summary of the studies and algorithms included in the meta-analysis*

Algorithm, year	Variables in the algorithm	Validation study‡, figure from which the data was extracted in the published article	Warfarin indication for patients in the validation cohort	n	Estimated number (%) of patients requiring ≥7 mg/day
Klein 2009 [68]	age, height, weight, *VKORC1*, *CYP2C9*, race, co-medications	Klein 2009 (S8) [68]	DVT/PE, AF, HVR, TIA, OS, Others	1008	125 (12.4)
		Pathare 2012, 3 [192]	AF, DVT/ PE, HVR	212	30 (14.15)
		Pavani 2014, 2C [167]	HVR	115	9 (7.83)
		Ramos 2012, 2B [64]	AF, PE, others	55	12 (21.82)
		Santos 2015, 4B [170]	AF, CVA, DVT/PE, HVR, others	133	8 (6.02)
		Saffian 2015, 1(G2) [3]	AF, DVT/PE	46	14 (30.43)
Sconce 2005 [143]	age, *CYP2C9*, *VKORC1*, and height	Francis 2014, 1 [194]	AF, DVT/PE, CVA, others	508	40 (7.87)
		Francis 2014, 2 [194]	AF, VTE	133	23 (17.29)
		Langley 2009, 1D [196]	NA	75	22 (29.33)
		Hatch 2008, 1B [195]	AF, DVT/PE, others	88	11 (12.5)

Zhu 2007 [178]	age, sex, weight, *VKORC1*, *CYP2C9*	Francis 2014, 1 [194]	AF, DVT/PE, CVA, others	508	40 (7.87)
		Francis 2014, 2 [194]	AF, VTE	133	23 (17.29)
		Langley 2009, 1C [196]	NA	75	22 (29.33)
		Linder 2009, 2 [197]	NA	137	18 (13.14)
Gage 2008 [24]	*VKORC1*, *CYP2C9*, BSA, target INR, co-medication, smoking status, race, indication	Gage 2008 in Corrigendum [24, 198]	AF, DVT/PE, others	295	73 (24.75)
		Shaw 2010, 1 [199]	AF, DVT/PE, others	71	27 (38.03)
		Saffian 2015, 1(G1) [3]	AF, DVT/PE	46	14 (30.43)
		Langley 2009, 1A [196]	NA	75	22 (26.67)
		Kimmel 2013, S4 [84]	AF, DVT/PE, others	514	97(18.87)
Wadelius 2009 [190]	*VKORC1*, *CYP2C9*, age, sex, co-medication	Francis 2014, 1 [194]	AF, DVT/PE, CVA, others	508	40 (7.87)
		Francis 2014, 2 [194]	AF, VTE	133	23 (17.29)
		Wadelius 2009, 1 [190]	AF, DVT/PE, HVR, TIA, others	181	27 (14.92)

Anderson 2007 [145]	*CYP2C9*, *VKORC1*, age, sex, weight	Francis 2014, 1 [194]	AF, DVT/PE, CVA, others	508	40 (7.87)
		Francis 2015, 2 [194]	AF, VTE	133	23 (17.29)
		Roper 2010, 3C [169]	AF, DVT/PE, HVR, others	974	108 (11.09)
Lenzini 2010 [30]	age, *VKORC1*, *CYP2C9*, BSA, target INR, race, indication, co-medication, diabetes, INR, previous doses	Ramos 2012, 2C [64]	AF, PE, others	55	12 (21.82)
		Saffian 2015, 1(G3) [3]	AF, DVT/PE	46	14 (30.43)
		Kimmel 2013, S4 [84]	AF, DVT/PE, others	514	97(18.87)
Le Gal 2010 [164]	cumulative dose, INR	Francis 2014, 1 [194]	AF, DVT/PE, CVA, others	508	40 (7.87)
		Francis 2014, 2 [194]	AF, VTE	133	23 (17.29)
Solomon 2004 [191]	age, total loading doses, INR, co-medication	Francis 2014, 1 [194]	AF, DVT/PE, CVA, others	508	40 (7.87)
		Francis 2014, 2[194]	AF, VTE	133	23 (17.29)
Gage 2008* [24]	BSA, age, race, target INR, smoking, indication, co-medication	Saffian 2015, 1(C1) [3]	AF, DVT/PE	46	14 (30.43)
		Kimmel 2013, S4 [84]	AF, DVT/PE, others	501	93(18.56)

Lenzini 2010* [30]	INR, age, target INR, BSA, indication, co-medication, race, previous doses, stroke, diabetes	Saffian 2015, 1(C3) [3]	AF, DVT/PE	46	14 (30.43
		Kimmel 2013, S4 [84]	AF, DVT/PE, others	501	93 (18.56)
Botton 2011 [159]	age, weight, co-medications, *CYP2C9*, *CYP4F2*, *VKORC1*	Santos 2015, 4A [170]	AF, DVT/PE, HVR, TIA, CVA, others	133	8 (6.02)
Klein 2009* [68]	age, height, weight, race, co-medication	Saffian 2015, 1(C2) [3]	AF, DVT/PE	46	14 (30.43)
Pathare 2012 [192]	age, weight, sex, indication, *CYP2C9*, *VKORC1*	Pathare 2012, 21 [192]	AF, DVT/PE, HVR	70	13 (18.57)
Pavani 2012 [167]	age, sex, BMI, *CYP2C9*, *VKORC1*, vitamin K intake	Pavani 2012, 23 [167]	AF, DVT, HVR	115	9 (7.83)
Perini 2008 [65]	age, weight, co-medication, *CYP2C9*, *VKORC1*, indication	Santos 2015, 4D [170]	AF, DVT/PE, HVR, TIA, CVA, others	133	8 (6.02)

Santos 2015 [170]	age, sex, weight, height, race, co-medication, *VKORC1*, *CYP2C9*	Santos 2015, 4A [170]	AF, DVT/PE, HVR, TIA, CVA, others	133	7 (5.26)
Wu 2008 [193]	*CYP2C9*, *VKORC1*, age, race, co-medication, sex, weight, height, smoking status	Langley 2009, 1B [196]	NA	75	22 (29.33)
Lenzini 2007 [31]	INR, blood loss, previous warfarin doses, co-medication	Lenzini 2007, 1 [31]	OS	105	17 (16.19)
Horne 2012 [74]	*VKORC1*, *CYP2C9*, co-medication, BSA, target INR, previous warfarin doses, INR, stroke, duration of therapy	Saffian 2015, 1(G4) [3]	AF, DVT/PE	46	14 (30.43)

Horne 2012* [74]	co-medication, BSA, target INR, previous warfarin doses, INR, stroke, duration of therapy	Saffian 2015, 1(C4) [3]	AF, DVT/PE	46	14 (30.43)
Ramos 2012 [64]	INR, previous warfarin dose, *VKORC1*, *CYP2C9*, indication, co-medication, age	Ramos 2012, 2A [64]	AF, PE, others	55	12 (21.82)

AF atrial fibrillation, VTE venous thromboembolism, HVR heart valve replacement, OS post orthopaedic surgery, TIA transient ischaemic attack, CVA cerebrovascular accident, DVT/PE deep vein thrombosis/pulmonary embolism, NA information was not available. ‡ validation study refers to an evaluation of dose predictions against external data. * denotes clinical algorithm.

3.4.3. Predictive performance of warfarin dosing tools in patients requiring ≥ 7 mg daily

Figure 3.2 presents a forest plot showing the proportion of warfarin doses that were under-predicted in patients requiring ≥ 7mg/day. Note that the analysis was indexed to each algorithm rather than to the study. The pooled proportions of under-predicted warfarin doses was 92.28% (95% CI 90.25 - 94.1) for these patients. Heterogeneity between the studies was low (I^2=23.99% [95% CI 0 - 54.89]). The average prediction error was found to be −2.32 mg/day. Scatter plots of the evaluations included in his study are reproduced in Appendix A3.2.

An evaluation of reproducibility of the extracted data is presented in Appendix Table A3.3. The deviation of the replicated data extraction from the originally extracted data was found to be between 0.8% to 5.9%.

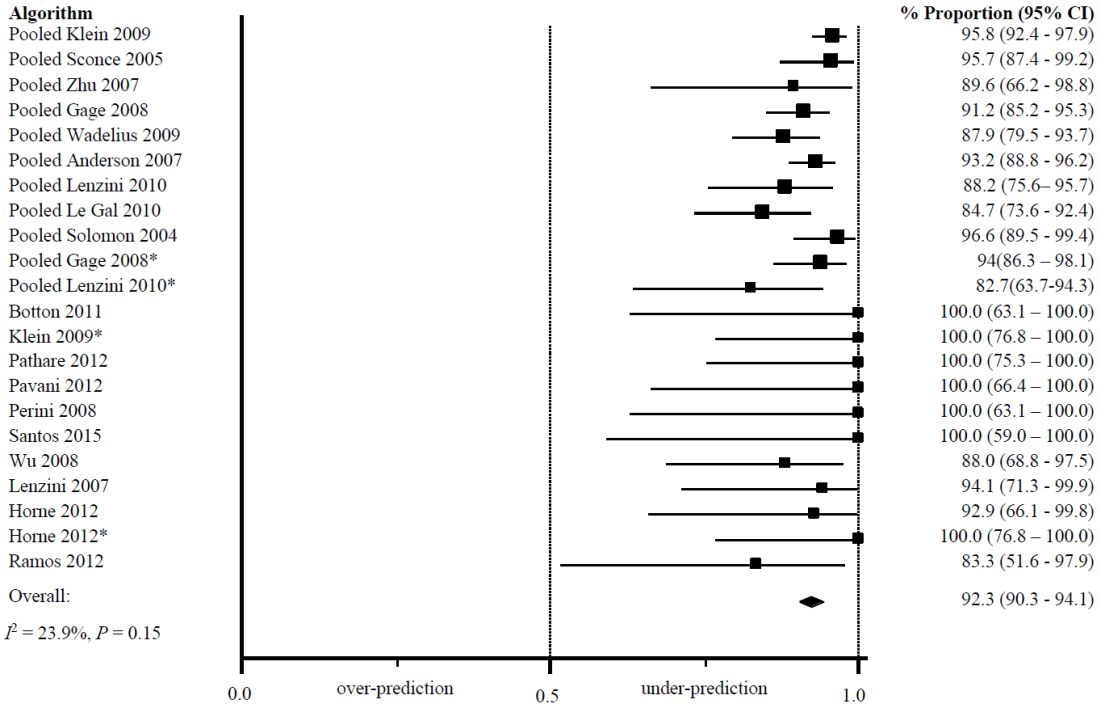

Figure 3.2 *Forest plot of included studies*

A sensitivity analysis was carried out to assess the impact of excluding 4 algorithms taken from studies with < 5 patients who required warfarin doses of 7mg daily or more [182, 187-189]. This was accomplished by pooling the data from the four excluded algorithms and including the pooled data in the estimation of the pooled proportion. The pooled proportion of under-predicted doses was 100% (95% CI 54.1 - 100) across the 4 algorithms. The inclusion of the pooled results in the meta-analysis did not change the overall pooled proportion of under-predicted doses (92.34, 95% CI 90.37 – 94.1 versus 92.28 95% CI 90.25–94.10).

3.5. Discussion

The ability of warfarin dosing algorithms to predict the observed maintenance doses in patients requiring higher than average daily doses was assessed in this study. The warfarin dosing algorithms included in this study were found to consistently under-predict the maintenance dose in patients requiring ≥ 7mg daily. This result was consistent across different algorithms, different clinical settings and in different patient populations. The choice of patient factors in the algorithm did not appear to influence the performance of the algorithm which includes several factors that have been associated with an increase in the dosing requirement such as *CYP4F2* polymorphism, ethnicity, inducing agents and smoking (see Botton et al 2011 [159] and Gage et al 2008 [24]). The average magnitude of the under-prediction is clinically important at approximately 2.3 mg/day or 26.5% relative bias for patients requiring ≥ 7 mg/day.

Several previous studies have also found that warfarin dosing algorithms perform poorly in patients requiring higher doses. Peng et al [153] compared the stable maintenance dose of 586 Chinese patients against maintenance doses predicted using nine algorithms. There were 6 patients requiring doses ≥ 7 mg/day in their study. Peng et al [153] found that the proportion of under-predicted doses in each of the algorithms were more than 80%. In another study,

Marin-LeBlanc et al [152] found that the proportion of under-predicted doses in all four algorithms tested requiring > 7 mg/day was > 61%.

The majority of published warfarin algorithms are designed to aid dose prediction at the initiation of therapy. Usually, an average population dose (often 5mg daily) would be used for all patients at the start of therapy and the dose adjusted heuristically according to INR response. In theory, algorithms that predict dose requirements prior to the initiation of therapy should minimise the need for dose adjustment and maximise the time in the therapeutic INR range. The results of this study suggest that patients in the upper quartile of dose requirements will not benefit from the use of these dosing tools and may be under-dosed which may unnecessarily delay attainment of a stable INR.

The cause of the bias observed in this study is not known. Of note, the direction of bias observed in this chapter is the opposite the observed bias in Chapter 2 (over-prediction). All of the dosing algorithms, but one [191], were developed using multi-linear regressions methods. Therefore, the algorithms will predict a response that follows a linear relationship across the full range of doses. Yet the dose-response relationship is only approximately linear in the central (20-80% of the maximum response) portion of the dose-response curve [200]. It is therefore possible that at higher doses the relationship between warfarin exposure and response reaches the non-linear portion of the curve (see Figure 3.3). If this were the case then, at higher doses, warfarin algorithms developed using linear regression techniques will under-predict dosing requirements by design.

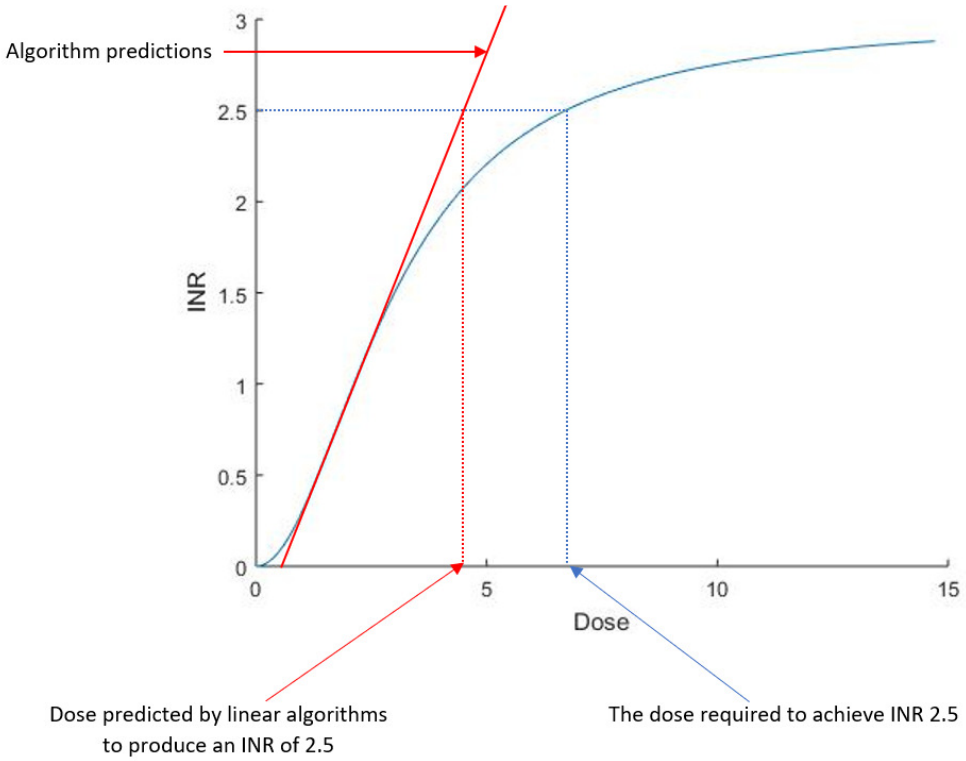

Figure 3.3 *A speculative relationship between warfarin dose and INR response. It is proposed that at higher doses, the warfarin dose-response relationship may flatten out. Therefore, algorithms that predict a linear relationship between dose and INR response would under-predict the dose required to achieve the target INR.*

The algorithms included in the analysis were all empirically derived by regressing dosing requirements against patient demographics. Using this methodology, the physiological and pharmacological mechanisms that underpin the warfarin-dose response are simplified into an empirical multilinear regression equation. Arguably, this will limit the ability of any given algorithm to generalize into new data, particularly data that extends past where the model was originally developed. Several warfarin dosing algorithms developed in a non-linear setting have been proposed including; support vector regression [201], boosted regression tree [202], artificial neural networks [191] and several other algorithms [203]. Li et al [154] evaluated several of these non-linear models and found that more than 59% of the maintenance doses were under-predicted

for patients requiring higher doses (defined as maintenance dose >30.66 mg/week).

This study reaffirms the assertion proposed in the previous chapter in that all current models to predict warfarin dose may be possibly too simple to capture the complexity of the coagulation network. A proposed solution might be a warfarin pharmacokinetic model linked to a systems pharmacology model for the coagulation network (see Wajima et al [36]). Further research to explore this mechanistic model is beyond the scope of this thesis.

There are several limitations to this study. Firstly, the extraction of data points depended on the clarity of the scatterplot. It was possible that overlapping data points were missed or digitised inaccurately. However, the error is expected to be relatively small overall and unlikely to have any significant influence on the results or conclusions. The three-stage hierarchical meta-analytic technique is not automated in the software used and incorporation of the repeated measures results included into the third stage of the hierarchy as a post-hoc step. In addition, the studies examined here did not consistently report adherence rates for the patients included. It is possible that some patients may have appeared to require larger doses because they were not adhering to the prescribed therapy. It is not possible in this setting to evaluate the impact of this on the findings.

3.6. Conclusion

Published warfarin dosing algorithms cannot be relied upon to accurately predict maintenance doses for patients who are likely to require higher than average daily doses. At therapy initiation, this is will not be known and hence the use of warfarin dosing tools may result in a prescribed dose that is 2.3 mg/day, on average, less than what is required to achieve therapeutic anticoagulation. This may increase the time to reach steady-state INR and may prolong the time below the therapeutic range with increase need of monitoring.

PART III

PREDICTIVE PERFORMANCE

Chapter 4: An approach for testing non-constant deviation associated with the magnitude of the observation

This chapter arose from a problem faced in the previous two chapters (in Figure 2.2 and Section 3.4.3). It was observed that dose predictions may appear to follow the line of identity quite well at lower values, but systematically deviate away from the line of identity in one direction at higher values. This chapter will propose an approach to evaluate bias associated with such data.

4.1. Introduction

When a mathematical model has been developed to predict observed data, a test of its predictive performance is warranted. It is typical to evaluate the model in terms of how close the model predictions are to the observed data and this may be achieved by plotting the observations against the model predictions. Here the observed data is considered the standard and is assumed to be an unbiased representation of the system, although will contain various levels of noise such as errors associated with imperfect measurement and imperfect study execution. A model that accurately captures the observed data, in some sense, is therefore the goal. There are of course situations in which the data are not an unbiased representation of the system, often due to confounding in the experiment, but this is not the case for consideration here. The differences between the predicted data and observed data are termed the residuals and in essence, the test of predictive performance of a model can be understood as a method for analysing residuals.

Several methods for analysing residuals have been proposed. One approach for analysing residuals is by fitting a smooth curve through the residuals using a non-parametric local regression known as lowess or loess [204, 205]. The lowess (or loess) curve are smoothing processes that can be understood as the moving average method where each of the smoothed values is determined only by the data points within a defined span. This approach is useful for visualizing the average scatter of residuals across the x-axis and therefore can be used to qualitatively assess where the residuals deviate systematically from the

line of identity. However, it lacks the ability to test whether the departure is statistically significant.

Another approach for analysing residuals is the Bland - Altman plot [206]. Although it was developed for a different purpose (i.e. agreement between two measurement methods), the method used in the Bland-Altman plot is similar in principle (i.e. analysis of residuals). In the Bland-Altman plot, the difference between the measurement of two methods are plotted against the mean of the two methods (on the x-axis). One advantage of the Bland-Altman plot is that it provides visualization of the relationship of the differences between measurements against the magnitude of measurement and therefore allows visual inspection of the existence of systematic difference between the two measurements. If there is no evidence that the differences between measurements are related to the magnitude of the measurements, then the mean of the difference between two measurements provide the measure of average bias between the two methods. In a later publication, Bland and Altman [207] further suggested an approach to test if bias is constant or not (the change in the difference between measurement of two methods is related to the magnitude of measurement). The approach involves regressing the difference between two measurement methods against the mean of the two measurements using linear regression. If the slope is significant, which was deliberately not defined by Bland and Altman [207], then the difference between measurements is estimated by the regression equation.

Perhaps the most common method for measuring the predictive performance of a model in clinical pharmacology is the method suggested by Sheiner and Beal in 1981 [5]. The method provides an estimate of bias using the mean prediction error (MPE) and imprecision using the mean squared error (MSE) or the root mean squared error ($RMSE$). In Chapter 2, bias was measured using the Sheiner and Beal 1981 [5] mean prediction error method. This chapter proposes an extension to the method of Sheiner and Beal to analyse bias that systematically deviates in relation to the magnitude of the predicted values.

4.2. The problem

The mean prediction error (MPE) is calculated using the following equation:

$$\boldsymbol{MPE = \frac{1}{N}\sum_{i=1}^{N} PE_i}$$

Equation 4.1 *Mean prediction error*

where PE_i is prediction error (the predicted data ($f(\theta, x_i)$), minus the observed data (y_i) for i^{th} experimental run (in this example it is an observation from an individual)), and N is the number of residuals. $f(\theta, x_i)$ is used to denote a model (linear or otherwise) that is defined by a $p \times 1$ vector the parameters (θ) and some independent variables x. Usually, the residuals are assumed to follow a normal distribution and therefore the 95% confidence interval is calculated using

$$\boldsymbol{95\%\ CI = MPE \pm 1.96 SE_{MPE}}$$

Equation 4.2 *Calculation of the 95% confidence interval of the MPE*

where SE_{MPE} is the asymptotic standard error of the mean prediction error. If the 95% CI includes zero, then no bias is concluded.

By reporting the MPE and its 95% CI, one can estimate the overall measure of bias as well as the direction of the bias (i.e. under- or over-prediction by the model). Inherently, the MPE measures the average prediction error across the entire observed data where, for the purposes of the calculation, the data are assumed to arise from a single bin and all residuals within a bin are exchangeable. However, a problem arises when the relationship between prediction error and the observed data is not random and itself shows a systematic trend over the range of the observations. An example of this situation is shown in Figure 4.1. During this thesis, examples of such scatter plots have been seen in Chapters 2 and 3. To illustrate this problem better, an example of a plot that is reproduced (see Figure 4.1) from a previous publication [3] that is not described in this thesis. The y-axis is the observed maintenance dose of warfarin

and the x-axis is the predicted dose using a dosing software. Further details of the study are omitted.

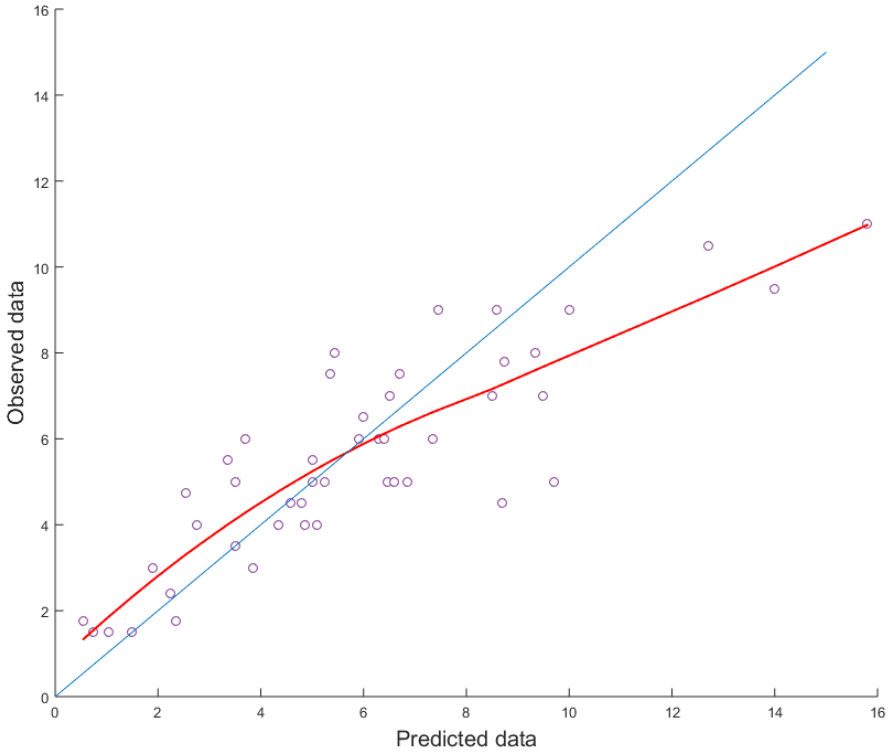

Figure 4.1 *Scatter plot showing systematic deviation from the line of identity as the magnitude of the data predictions increase. The red line is a loess smoothing function. Reproduced from Saffian et al. 2015 [3] with permission from Wolters Kluwer Health, Inc.*

The *MPE* for this analysis was +0.37 the lower and upper 95% CI was 0.89 and -0.15 respectively, which indicates that the dosing tool provides unbiased predictions. However, it is evident that dose predictions on the lower observed dose generally follow the line of identity, although visually, and based on the loess line, there is a suggestion of under-prediction. Predictions for the observed dose above a ~7mg were mostly over-predicted.

The aim of this chapter is to propose an approach that can be used to numerically test deviations that occur over regions of the observed data. The approach is based on a generalised form of the *MPE* method. The method

proposed in this paper is intended for use in situations in which there are no repeated measures over experimental runs.

4.3. A suggested approach

It is proposed that the single bin MPE of Sheiner and Beal 1981 (here on termed 'S&B method') can be extended to multiple bins which can then each be assessed for systematic deviation and formally for their asymptotic properties if we considered infinite bins.

The algorithm for the approach involves four steps which can be divided into two parts. Figure 4.2 depicts the flow chart of the suggested approach.

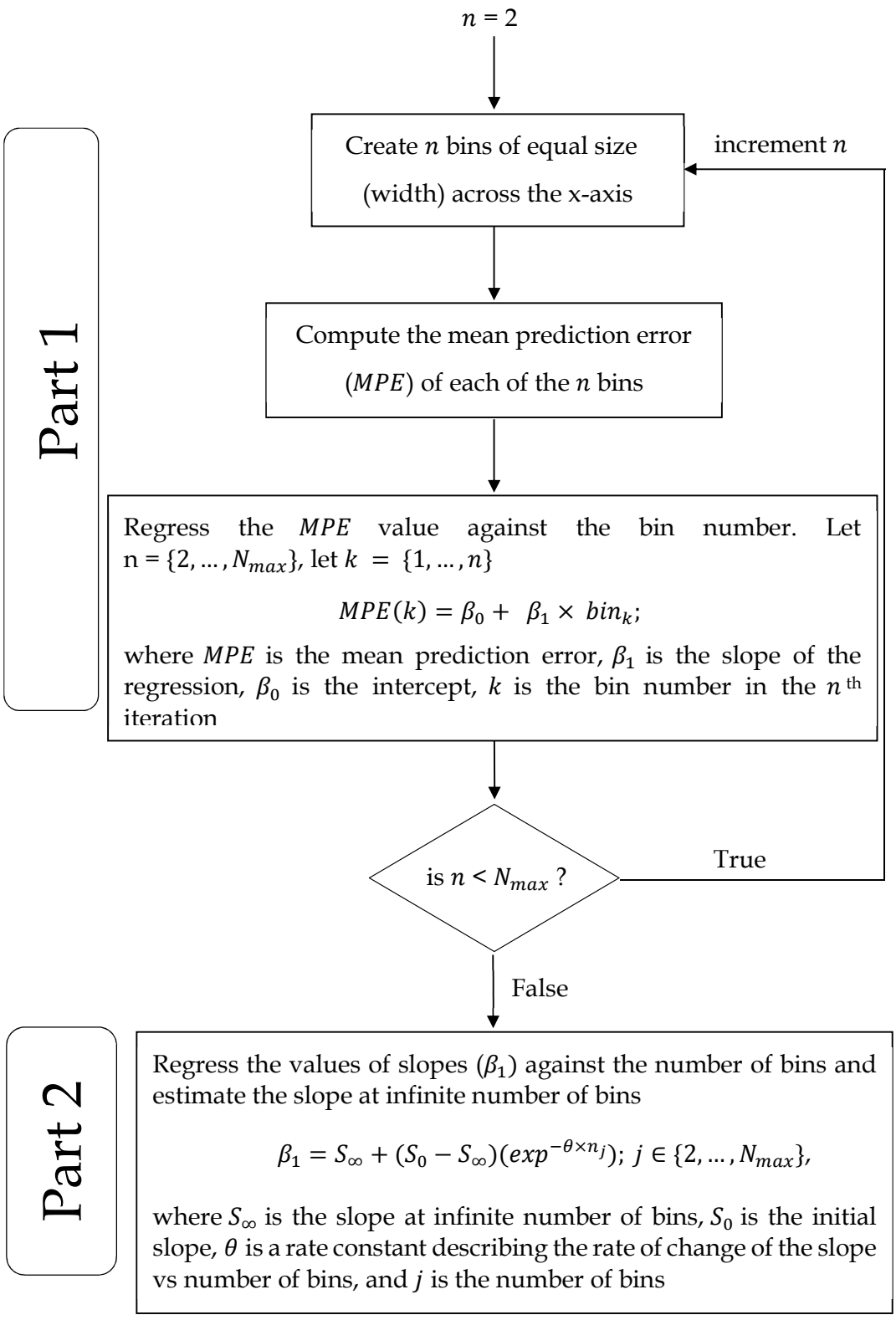

Figure 4.2 *Flow chart of the suggested approach*

n is a constant within an iteration and is the number of bins in a particular iteration. Since iterations start at 1, then n = 1 + iteration number. It is cycled through until the value of n equals the total number of allowable bins (N_{max}). For practicality, the choice of values of the vector n and total number of bins, N_{max}, may be optimised (not considered here). In Part 1, each iteration will provide a set of slope parameters (β_1). Here β_1 is now considered as if it were data and there are N_{max} – 1 values of β_1. If the value of β_1 is constant for all n, then no evidence of systematic trend in the bias of the residuals is concluded. However, in the presence of systematic bias the value of β_1 will change monotonically to an asymptotic value as n approaches ∞.

The second part is to fit an exponential model to the slope coefficients (β_1), and determine the asymptotic properties of the systematic bias in residuals. The value of S_∞ is the value of the asymptotic systematic bias. If the 95% CI of S_∞ includes zero, then this indicates that there is no systematic trend in the bias of the residuals. The 95% CI of S_∞ tests if there is bias in the residuals that is monotonically systematic. Further explanation with respect to the rationale of using the 95% CI of S_∞ to test for a systematic trend in the bias of the residuals will be presented in the Discussion (Section 4.6).

There are also occasions where the model produces bias, but the bias is not systematically related to the magnitude of the measurement and will described in the following section. See Table 4.1 for a step schematic of a setting with both systematic deviation of residuals versus not.

Table 4.1 *Step schematic of the proposed approach*

Description of the algorithm	Model prediction with no systematic deviation of residuals	Model prediction with systematic deviation in the residuals
1. Create n ($n > 1$) bins of equal size on the x-axis	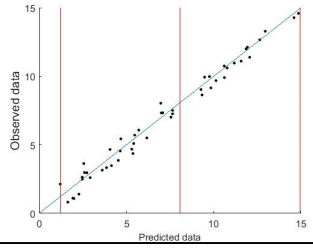	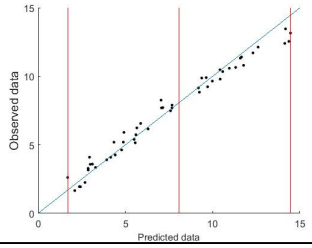
2. Compute the mean prediction error (MPE) of each of the n bins	MPE Single bin (S&B): -0.10 2 bins: bin 1 0.12, bin 2 0.10	MPE Single bin (S&B): 0.06 2 bins: bin 1 -0.24, bin 2 0.52
3. Regress the MPE value against the bin number	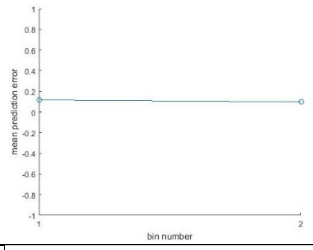	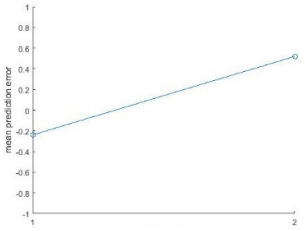
Increment n and repeat step 1 to step 3. Stop when $n > N_{max}$. In this example, N_{max} = 6 was used	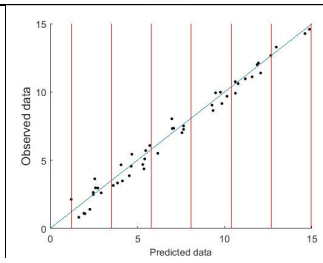 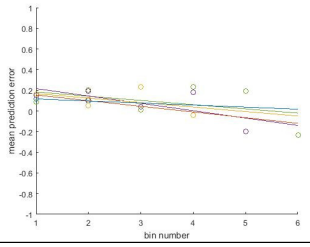	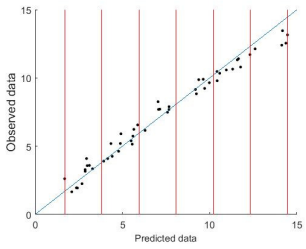 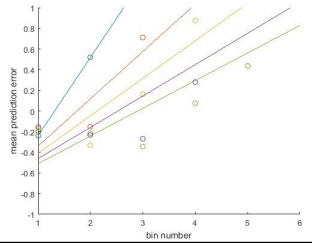

4. Fit an exponential model to the slope coefficients and determine the asymptotic properties of the systematic bias in residuals

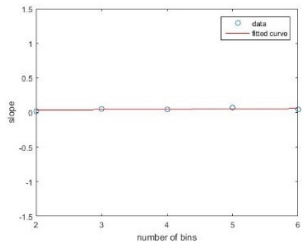

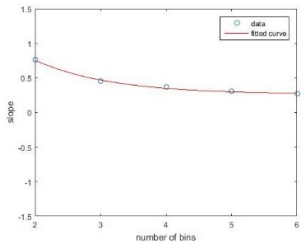

4.4. Evaluation of the Approach

This section will proceed by illustrating the suggested approach using simulated data. All data sets comprised 50 values of x and y and were generated using MATLAB® (2015a, The Math Works, Natick, MA). The MATLAB® code used to implement the scenarios this analysis is attached in Appendix A3.1.

Seven scenarios were considered as follows:

A. No systematic deviation of predicted from observed data,
B. Constant positive deviation of predicted from observed,
C. Proportional deviation of residuals (i.e. the value of the deviation of the residuals was proportional to the magnitude of the observations),
D. Nonlinear deviation of residuals associated with the magnitude of the observed data,
E. Nonlinear deviation of residuals associated with the inverse of the magnitude of the observed data,
F. A combination of constant and nonlinear deviation of residuals,
G. Curvilinear deviation of residuals.

Figure 4.3 depicts scenario A to G created without any noise so that readers can see the scenarios simulated. In the simulations, however, random noise was added by randomly generating 50 values using the following equation:

$$\varepsilon_i \sim N(0, \sigma^2)$$

Equation 4.3 *The distribution of random noise*

where ε_i is the residual error of the i^{th} data point, N is used to denote a normal distribution with a mean of zero and variance (σ^2). A σ^2 of 0.25 was used as this value was sufficient to provide random variability but still maintain the shape of bias. Each scenario was only simulated once.

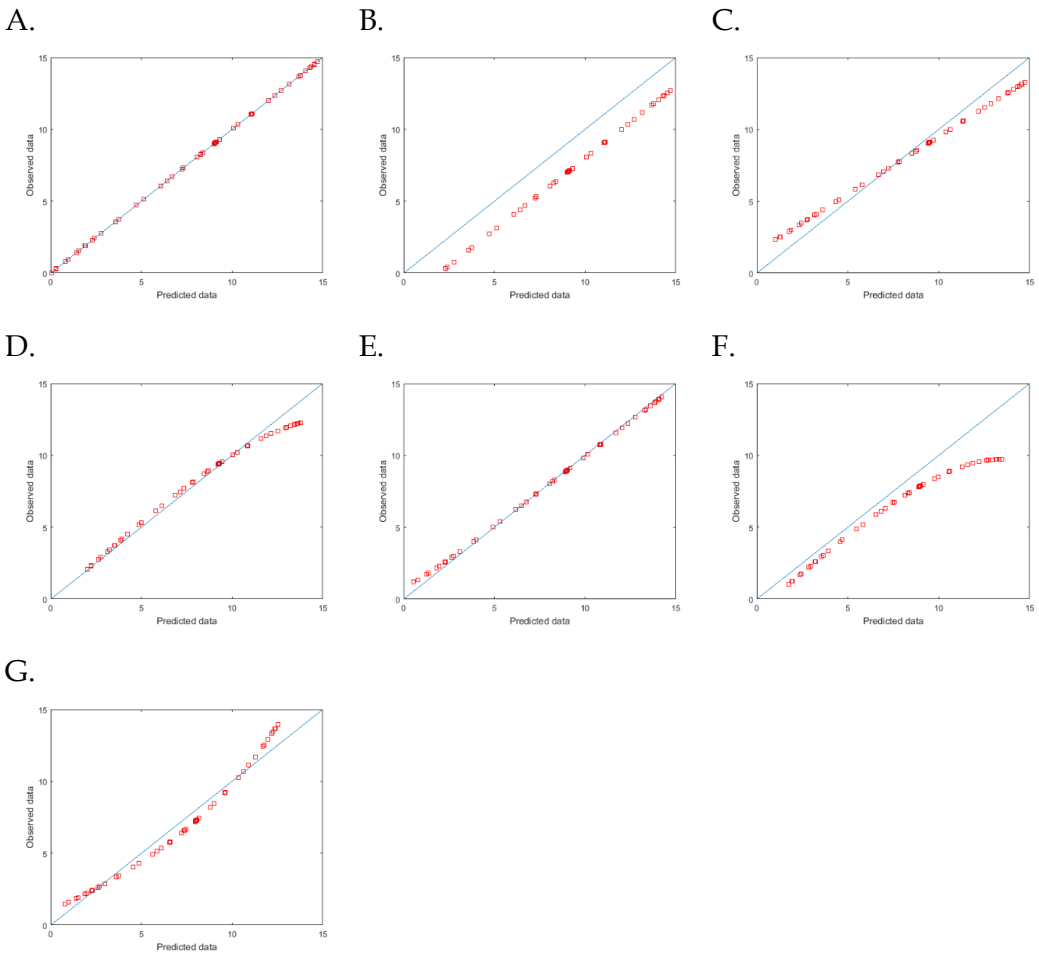

Figure 4.3 *Scatterplot of data created without noise to simulate six scenarios (scenario B to G) where deviation from the line of identity may be observed. Scenario A is where there is no deviation from the line of identity.*

In all 7 scenarios, the single bin MPE approach as suggested by Sheiner and Beal (1981) [5] will be analysed and compared with the suggested approach.

4.5. Results/ Application

The results for of calculating bias using the single bin MPE (S&B) approach versus the suggested approach for scenarios A – G are presented below. The full working for each scenario can be found in Appendix 3.2-3.8. For all the scenarios simulated below, the scatter plots are observed versus predicted data in arbitrary units, the blue line is the line of identity, MPE is the mean prediction error in arbitrary units and S_∞ is the asymptotic slope (at infinite number of bins).

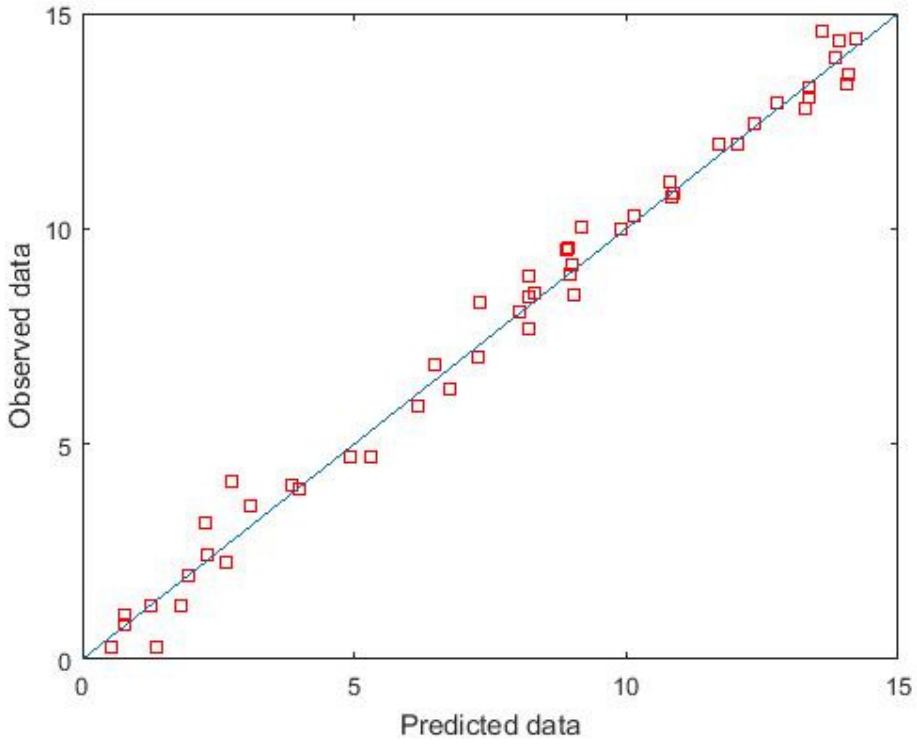

Figure 4.4 *Scatter plot with no systematic deviation of predicted from observed data*

A. In this scenario, the predicted values were randomly scattered around the line of identity. Visually, there is no evidence that the prediction values systematically deviate from the line of identity. MPE (S&B) [95% CI] was -0.06 [-0.2, 0.07] and s_∞ [95% CI] was -0.02 [-0.04, 0.01]. The total bias is the sum of MPE and S_∞, therefore when S_∞ is 0 (i.e. 95% CI includes zero)

then total bias is the MPE. The 95% CI MPE included zero, hence it can be interpreted as no bias and constant deviation in residuals.

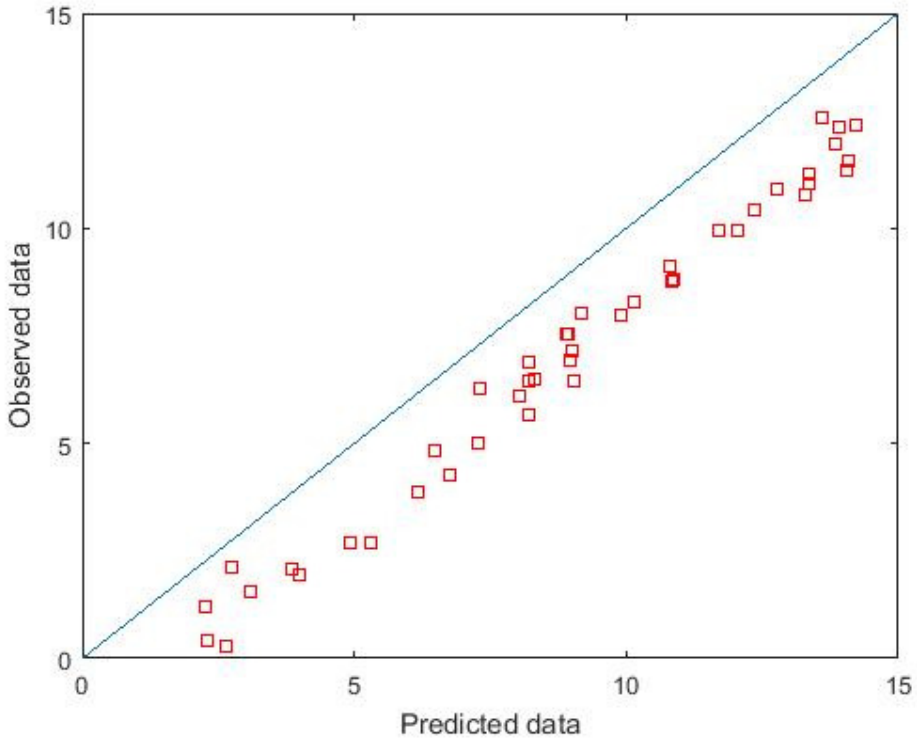

Figure 4.5 *Scatter plot of constant positive deviation of predicted from observed*

B. Scenario B is similar to scenario A, except that all of the predictions were shifted below the line of identity. Therefore, the deviation from the line of identity was constant across the magnitude of the observed data. The MPE (S&B) [95% CI] was 1.94 [1.80,2.07] and s_∞ [95% CI] was -0.015 [-0.04, 0.01]. As S_∞ is statistically not different from zero, the total bias is the MPE. This scenario can be interpreted as positive bias but the deviation is constant.

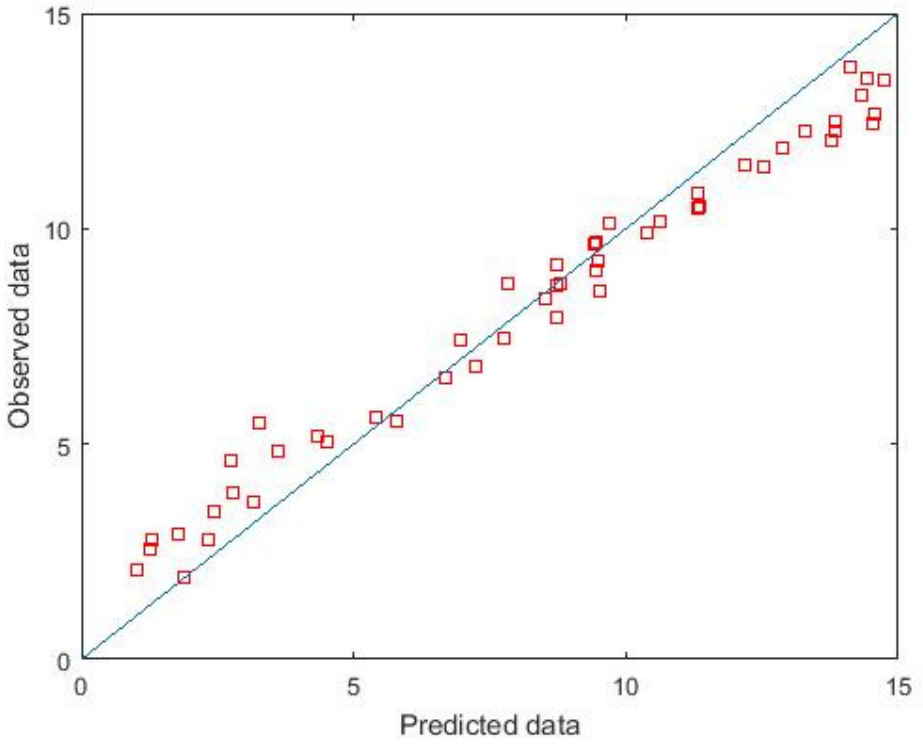

Figure 4.6 *Scatter plot with proportional deviation of residuals*

C. In this scenario, the predictions systematically deviated from the line of identity across the observed data. At lower observed values, the deviation from the line of identity is negative but at higher observed values the deviation is positive. Summing all the prediction error as a single bin may cancel out the overall bias as seen here where the MPE (S&B) [95% CI] was 0.11 [-0.16, 0.39]. When the data was binned, the S_{∞} [95% CI] was 0.25 [0.21, 0.30]. It can be interpreted as there is no bias on average, but there is a statistically significant systematic non-constant deviation associated with the magnitude of observation.

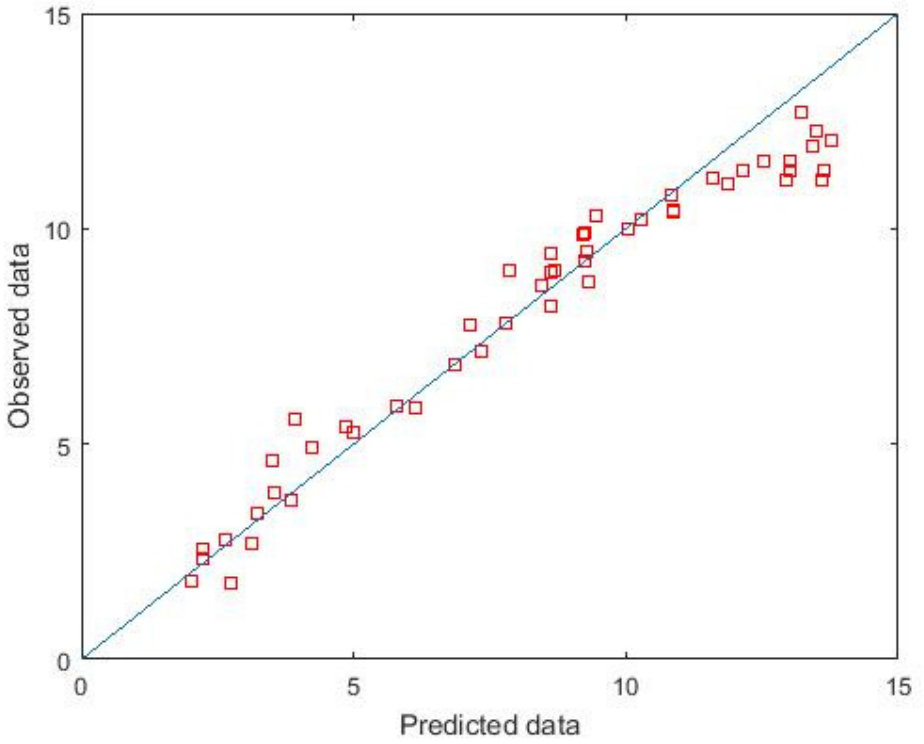

Figure 4.7 *Scatter plot of nonlinear deviation of residuals associated with the magnitude of the observed data*

D. The scenario that was simulated here shows a systematic deviation from the line of identity in a non-linear way that is related to the magnitude of the observed values. The MPE (S&B) [95% CI] was 0.21 [-0.03,0.46], which included zero and therefore it would be concluded that the model is unbiased. Yet from the scatterplot, it is apparent that lower x- and y-values followed the line of identity well, while as the y-axis values increase, the bias systematically shifts in one direction to under the line of identity. The S_{∞} [95% CI] was 0.11 [0.03, 0.19] which does not include zero. It can be interpreted as there is no bias in the residual on average, but there is non-constant bias.

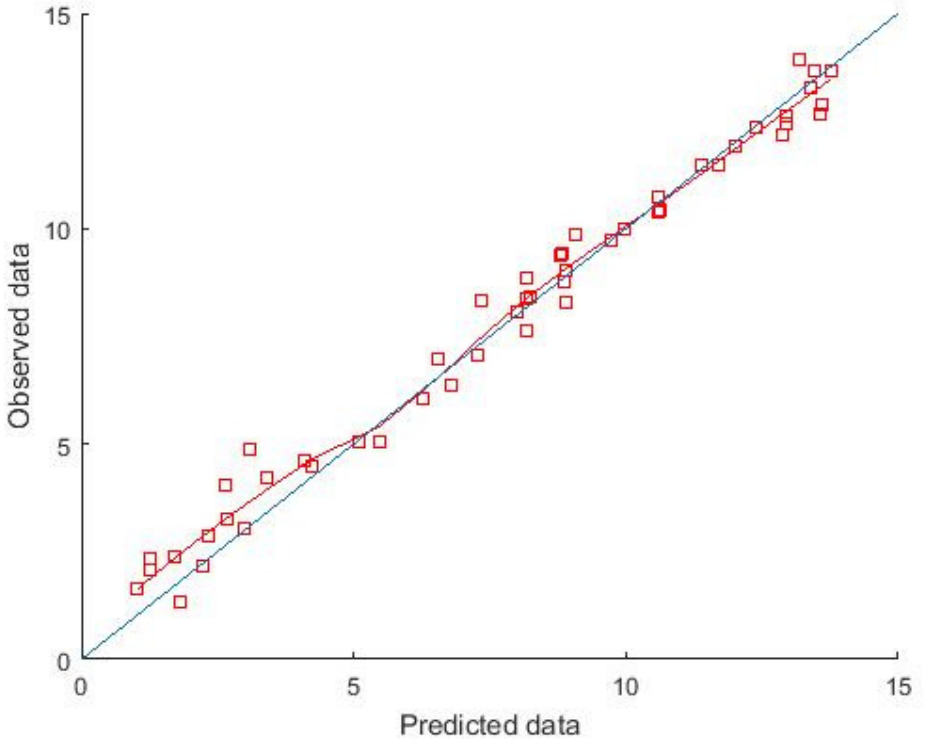

Figure 4.8 *Scatter plot of nonlinear deviation of residuals associated with the inverse of the magnitude of the observed data. The red line is a loess smoothing function*

E. Scenario E is similar to scenario D but is in the inverse order. Deviation above the line of identity is seen at the lower y-values, but as the y-value increased, the predictions followed the line of identity well. A loess smoothing function was added for this scenario as it is harder to see bias at lower values since the axes are naturally compressed due to the limited range that the data can deviate. The MPE (S&B) [95% CI] was -0.19 [-0.31, 0.001] and S_{∞} [95% CI] was 0.07 [0.02, 0.1]. It can be interpreted as there is no bias in the residual on average, but there is non-constant deviation that occurs systematically.

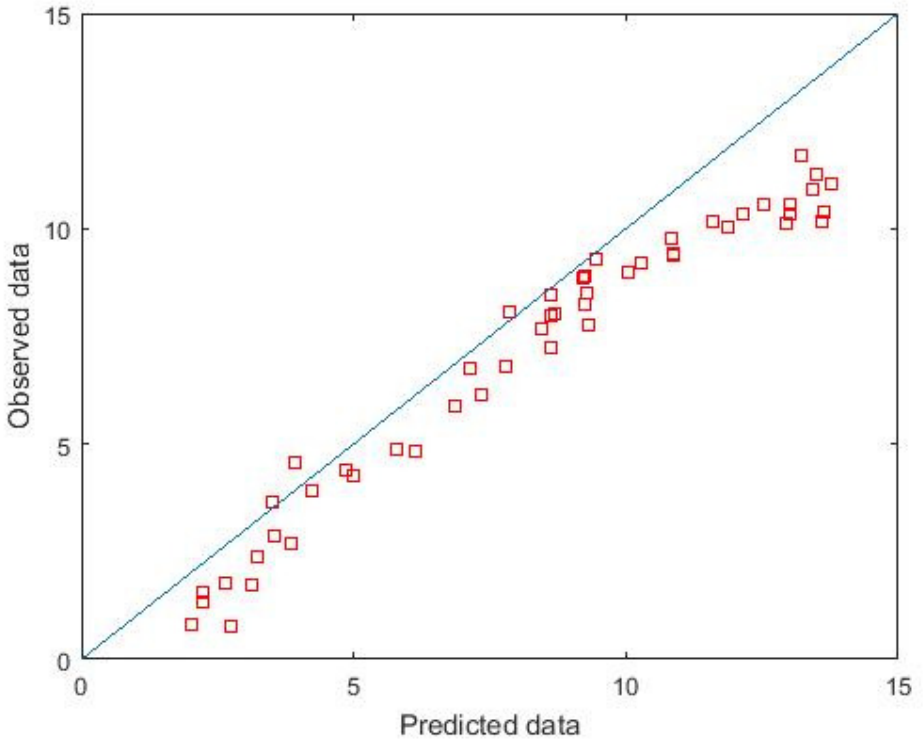

Figure 4.9 *Scatter plot of a combination of constant and nonlinear deviation of residuals*

F. This scenario is a combination of scenario B and D. The mean of all observations is below the line of identity (as in scenario B) and there is evidence of a nonlinear deviation that is related to the magnitude of the predictions. MPE (S&B) [95% CI] for this example was 1.21 [0.97, 1.46] and S_{∞} [95% CI] was 0.11 [0.03, 0.19]. It can be interpreted as positive bias in the residuals on average and the bias in the residuals is systematic.

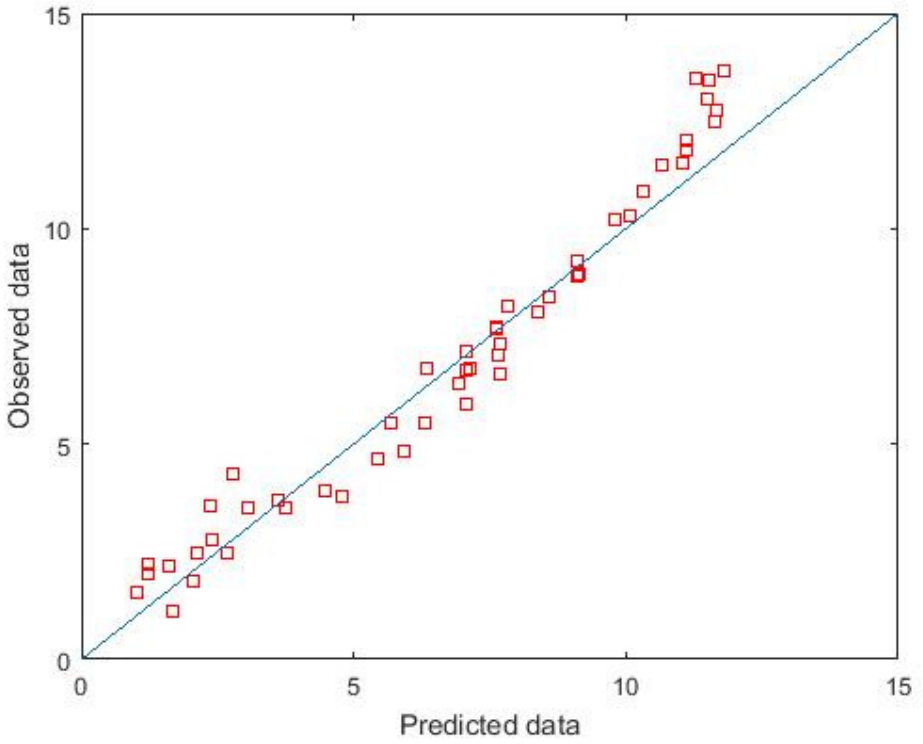

Figure 4.10 *Scatter plot of curvilinear deviation of residuals*

G. In this scenario, the deviation was non-monotonic (different direction across the lower and upper values). Y-values for the lower x-values were above the line of identity, values of y-variable in the middle region of the x-axis was under the line of identity while y-values on the upper x-values were above the line of identity. MPE (S&B) [95% CI] was -0.21 [-0.43, 0.01] and S_{∞} [95% CI] was 0.03 (-0.0039, 0.07). No bias on average and no systematic deviation from the line of identity, however visual plot provides a different interpretation.

4.6. Discussion

An approach to numerically test for non-constant deviation from the line of identity is presented in this chapter.

This work arose from a need for a different metric to measure bias. The approach principally builds on the mean prediction error approach outlined by Sheiner and Beal in 1981 [5] in which their method is considered to be a special case of the current work. The suggested approach generalises the Sheiner and Beal method by allowing the prediction error to be computed in multiple data bins. Increasing the number of bins from 1 to 2 allows the MPE to be computed in each bin and therefore provides the basis for assessing whether the bias is constant. Increasing the number of bins further allows a more granular assessment of how bias changes with changes in the magnitude of the predicted data. Regressing the MPE values over the bin number provides a measure of total bias. If there is no systematic bias, the regression line will remain constant as the number of bins is increased. The first step completely captures the presence of systematic magnitude-driven bias but does not capture its quantitative properties. The second step effectively determines the asymptotic slope of the bias if, in theory, an infinite number of bins had been chosen. This is performed by finding the slope of the linear slopes and its asymptotic properties. The assumption that the regression shape will reach a plateau when systematic deviation occurs was consistent with the finding of this study. The approach presented here is a proposed solution to test whether the deviation from the line of identity that is associated with the magnitude of observation is significant. Primarily, this approach can be used to improve analysis of predictive performance.

The method proposed in this chapter is able to capture monotonic departure from a specific linear model (in this case, the line of identity). The application of method proposed is therefore not limited to predictive performance analyses. The method of binning and regressing the residual slopes and estimating the slope under conditions of infinite bins (S_∞) can be applied to

other statistical methods to test for departure from linearity. For example, the Bland-Altman plot [207] analyses the difference between two measurements (y-axis) on a horizontal line (the mean of the two measurements) and the proposed binning method can be applied to test if the two measurements deviates in relation to the magnitude of the x-axis. The work completed in this chapter is effectively an alternative approach to the method suggested by Bland and Altman.

Several scenarios were simulated to provide examples of how the method will work. The chosen examples represent typical scenarios where deviations from the line of identity can occur. The motivating example comes primarily from the work in Chapter 2 where predictions appear to follow the line of identity for lower observed data, but deviate away from the line of identity at higher observed values. Likewise, predictions that deviate at the lower observed values, but follow the line of identity at higher observed data (Scenario E) can also be seen in publications. Several scenarios such as scenarios B and F are unlikely to be seen in publications as the standard MPE approach would have captured the bias and it is visually clear. However, the reader may be deceived if a regression line is plotted instead of the line of identity because the regression line measures the association between the x and y variable. The correlation between x and y may be good but it does not indicate good predictive performance. What is important is the association along the line of identity.

There are limitations to the current approach which can be divided into two types. The first relate to limitations to the method; 1) The approach does not capture non-monotonic deviation (Scenario G). It should be noted that the single bin MPE approach by Sheiner and Beal also does not capture non-monotonic bias. In this case, the researcher must visually assess the goodness of fit plot to find evidence of such deviation and a loess fitted function may be useful. 2) This approach does not work independent of the Sheiner and Beal single bin method, but rather is complementary. The flow diagram in Figure 4.11 below describes

how decisions would be made using the Sheiner and Beal single bin MPE method and S_∞. Note that the two metrics must be used in combination.

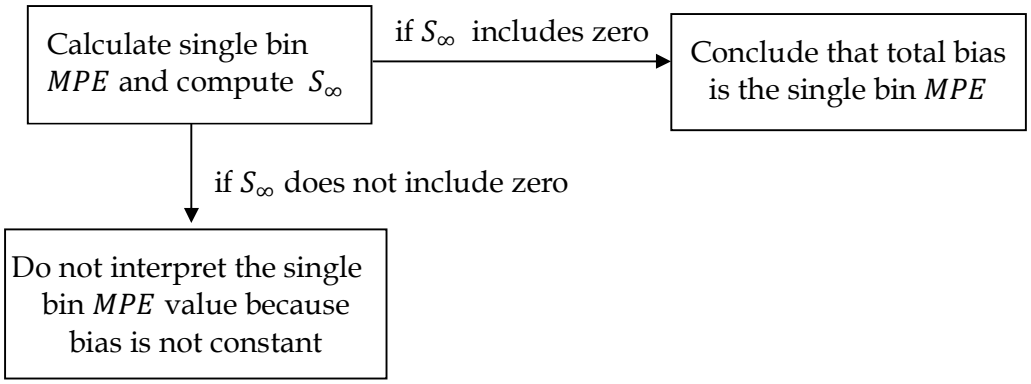

Figure 4.11 *Flow chart of how decision would be made using the suggested approach*

3) The s_∞ does not capture the magnitude or direction of non-constant bias (positive bias or negative bias). 4) The value of s_∞ does not capture in which region the bias deviates from the line of identity (Scenario D and E deviate at opposite ends but the 95% CI of s_∞ were positive for both scenarios) and hence provides a statistical interpretation only. 5)An adequate sample size is needed to provide a good estimate of s_∞. A sample size of at least 2 times N_{max} is needed for this approach to work because at least 2 data points are needed to calculate an average prediction error in each bin. 6) The number of bins (N_{max}) is user dependent, but may be optimized in the future. In the simulations above, it appears that 10 bins are sufficient to provide an estimate for s_∞ and increasing the number of bins does not change the inference. The second type of limitation relates to assessment of the proposed method. The current work only provides a theoretical evaluation of the proposed method. A wider range of scenarios should be tested for robustness and sensitivity of the proposed method.

4.7. Conclusion

A method for numerically testing non-constant systematic deviations from the line of identity based on a generalisation of the mean prediction error has been proposed. This proposed approach provides the first numerical test to assess for statistically significant non-constant systematic deviation and

therefore provides an additional interpretation to the standard single bin MPE approach. The method can be implemented easily in any statistical software.

PART IV

DABIGATRAN DOSING

Part III of this thesis describes two studies where the overarching aim is to explore dabigatran concentration monitoring as a means of guiding dose selection. Chapter 5 describes an assay to measure the concentration of dabigatran and its active metabolite, dabigatran acyl glucuronides, in human plasma. Chapter 6 describes a simulation study to select a suitable prior population pharmacokinetic model for individualising dabigatran dosing.

Chapter 5: Quantification of dabigatran and dabigatran acyl glucuronides in human plasma by LC-MS/MS

This chapter is based on the following peer-reviewed publication:

Saffian, S. M., et al. (2015). "Quantification of dabigatran and indirect quantification of dabigatran acyl glucuronides in human plasma by LC-MS/MS." Bioanalysis 7(8): 957-966

5.1. Introduction

Dabigatran is administered as the prodrug dabigatran etexilate that undergoes sequential hydrolysis in the intestine and liver via CES 1 and CES 2 to form the active drug dabigatran [98]. Approximately 80% of dabigatran is excreted renally unchanged while the remainder is primarily glucuronidated and excreted renally [111]. *In vitro* data indicate that dabigatran and all four isomeric forms of dabigatran acyl glucuronides (see Figure 5.1) have equivalent anticoagulant effect in terms of the activated partial prothrombin time (aPTT) [103]. It is therefore important to measure all active dabigatran entities when correlating plasma concentrations with clinical effects.

a. b.

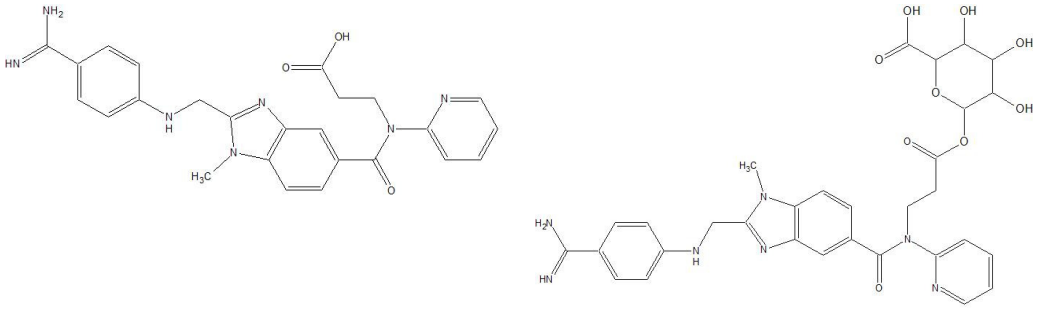

Figure 5.1 *Chemical structures. a. dabigatran; b. dabigatran 1-O-acyl glucuronide*

5.1.1. A brief introduction to acyl glucuronides

Conjugation by acyl glucuronide is a phase II metabolic pathway that is common for drugs containing a carboxylic acid functional group (—COOH) and it has been found to be the major metabolic pathway for elimination for dabigatran [103]. An ester bond is formed at the β-1-*O*- position when the enzyme uridine diphosphoglucuronyl transferases catalyses the transfer of a glucuronic acid, a five-carbon pyranose sugar molecule (molecular weight 176 g/mol), from uridine 5-diphosphoglucuronic acid to the carboxylic functional group of the drug molecule. Generally, acyl glucuronides increase the hydrophilicity of the drug to aid in excretion by the kidneys [208].

The ester bond of the acyl glucuronide conjugate is susceptible to nucleophilic attack which can lead to either hydrolysis or acyl migration, both *in vitro* and *in vivo* [208-210]. Hydrolysis occurs when water is the attacking nucleophile [208], which is catalysed by either high pH, high temperature or β-glucuronidase enzymes [208, 211] which consequently back-converts (or deconjugate) to the parent drug. When the attacking nucleophile is the neighbouring hydroxyl group (R—OH) in the glucuronic ring, the acyl group (RCO—) migrates from position 1-*O* to 2-, 3- and 4- sequentially and reversibly around the glucuronic ring in the β configuration (Figure 5.2).

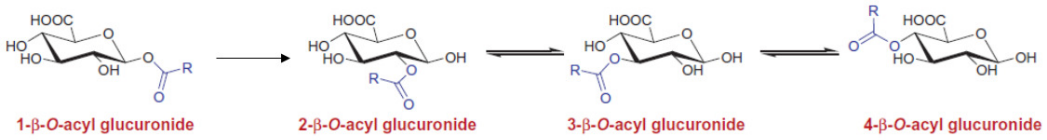

Figure 5.2 *Positional isomer formation of acyl glucuronide*

This reaction is called intramolecular acyl migration. The positional isomers 2-, 3- and 4- are more stable towards hydrolysis [212] and β-glucuronidase [208, 213]. Reformation back to the β-1-*O* position, although possible, is unlikely to occur due to the higher energy requirement for this reaction to occur [208]. In theory, the corresponding β migration isomers can mutarotate to form an α configuration and further undergo reversible acyl migrations [213]. This has been shown for a few drugs such as probenecid [214], zomepirac [215] and diflunisal [216], but has not been shown for dabigatran acyl glucuronide [100]. Furthermore it is rarely observed in biological fluids [217]. Acyl glucuronides can also covalently bind to endogenous proteins through a Schiff base reaction [210, 218]. Since this chapter does not consider any biological implication of dabigatran acyl glucuronides, and several excellent reviews have been published on the topic [209, 219-221], no further discussion is presented here.

5.1.2. Quantification of acyl glucuronides using liquid chromatography-tandem mass spectrometry/ mass spectrometry (LC-MS/MS)

LC-MS/MS is a technique in analytical chemistry that combines physical separation of a mixture of analytes in the liquid chromatography column (HPLC) and mass analysis in the mass spectrometer (MS). Measuring drug concentration in biological fluids using LC-MS/MS can be divided into three steps; 1.) removing inferences in biological matrices in the sample preparation, 2.) separation of analytes by high performance liquid chromatography and 3.) identification of individual components by mass analysis. Care must be taken to control hydrolysis and acyl migration as the reaction can occur at any stage of the analysis. Separation of acyl glucuronide from the parent compound is therefore a key step to ensure accurate quantification of the parent compound and a pre-requisite for direct quantification (see next section). In general, lowering the pH and temperature will decrease hydrolysis and acyl migration. This section will proceed with a brief description of principles of LC-MS/MS and methods to optimize quantification of acyl glucuronides.

Sample preparation for acyl glucuronides should be fast and simple. Samples should also be kept as cool as possible. This includes acquisition of sample from the patient, centrifuging to obtain plasma and storing in the freezer for analysis later. Although several sample preparation techniques such as solid phase extraction [222] and liquid-liquid extraction [223] has been used, protein precipitation is generally the preferred method due to its simplicity, and has also been the choice in other published dabigatran assay methods [224-226]. Acetonitrile is generally preferred as an extraction solvent when assaying acyl glucuronides as it is more inert. It has been reported that acyl glucuronides can react with solvents such as methanol and ethanol, possibly through methylation, leading to an increased rate of hydrolysis [227, 228].

Separation of acyl glucuronides from the parent drug using high-performance liquid chromatography is relatively easy to achieve as acyl glucuronides are often more polar. Separation of acyl glucuronides from its parent compound is important because acyl glucuronides can back-convert

usually in the ion source, which results in an over-estimate of the parent compound. In contrast, the resolution of the four migration isomers, which is required to accurately quantify all four positional isomers if a direct method is pursued (see next section), is more difficult. Separation of carboxylic acid containing compounds can often be achieved by manipulating the ionic strength and the pH of the mobile phase [229-231], while separation of the migration isomers can be further resolved by changing the solvent strength and mobile phase flow rate [230]. Several studies have repeatedly found that the order of elution of the positional isomers remain the same (in the order of retention time 4β < 1β < 3β < 2β in a reversed-phase column) irrespective of the structure of the parent compound [232-236].

Triple-quadrupole tandem mass spectrometer is a highly sensitive and highly specific technique in analytical chemistry. Figure 5.3 is a schematic of a triple-quadrupole mass spectrometer set up. After analyte separation by liquid chromatography, the sample is first ionized and the analyte of interest is selected based on the mass to charge ratio (m/z) which is called the precursor ion. The precursor ion is then fragmented in the collision chamber to produce product ions that is again selected based on the m/z ratio. Each precursor ion has a distinct fragmentation pattern which will provide structural information to specifically detect each compound.

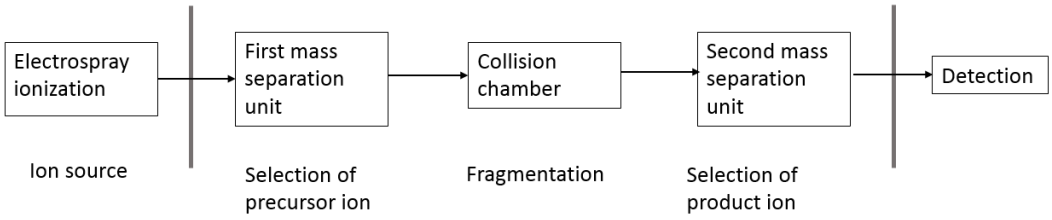

Figure 5.3 *A schematic of a triple-quadrupole mass spectrometer as used in this study.*

In the LC-MS/MS set up used in this study, two transition ions are monitored; one act as a qualifier and the other as a quantifier. Typically, the quantifier is often the product ion with highest response and product ion with the second highest product ion is used as a qualifier. The qualifier ratio is used

to confirm structural identification and should remain relatively constant between calibration samples and unknown samples (i.e. patient samples).

One drawback in LC-MS/MS analysis is in-source fragmentation which is the dissociation of glucuronic acid from the parent drug in the ion source of the mass spectrometer [217, 237]. In-source fragmentation will result in ions that are identical to the parent compound which results in an overestimation of the parent drug if the acyl glucuronides are not well resolved from the parent compound chromatographically. Typically, it occurs in molecules with weaker bonds such as the ester bond of acyl glucuronide. Several steps can be taken to minimize in-source fragmentation. This include controlling the ion source temperature, declustering potentials, cone voltage the ionization method [156, 217, 238, 239]. Electrospray ionization (ESI) is generally the preferred choice of ionization method compared to atmospheric pressure chemical ionization as it minimizes in-source fragmentation [240, 241].

5.1.3. Direct and indirect quantification of dabigatran acyl glucuronide

Dabigatran acyl glucuronides (DAG) can be quantified directly or indirectly. The direct method is where the parent dabigatran and dabigatran acyl glucuronides are simultaneously quantified from one aliquot. This is only possible if reference standards are available and the stability is controlled, as dabigatran 1-*O* acyl glucuronide has an *in vitro* half-life of 1 hour at 37°C, pH 7.4 [103]. DAG can also be indirectly quantified by dividing the samples into two aliquots; one aliquot to measure the free dabigatran concentration, and another aliquot that undergoes alkaline hydrolysis to release all the glucuronic acid from DAG. The post-hydrolysis dabigatran concentration (here termed 'total dabigatran') is the sum of dabigatran and the contribution from all DAG isomers. The DAG concentration can then be inferred from the difference between the concentrations of the two aliquots using the following equation:

$$Percentage\ of\ dabigatran\ acyl\ glucuronide = \frac{(C_{total} - C_{free})}{C_{total}} \times 100$$

Equation 5.1 *Calculation of dabigatran acyl glucuronide using indirect method*

where C_{total} is the concentration of dabigatran after alkaline hydrolysis (i.e. sum of conjugated and unconjugated dabigatran concentration) and C_{free} is the concentration of dabigatran without alkaline hydrolysis (i.e. unconjugated dabigatran).

5.1.4. Rationale for the study

Since dabigatran and all four isomeric forms of dabigatran acyl glucuronides have equivalent anticoagulant effect, an assay to measure dabigatran and dabigatran acyl glucuronide in human plasma was needed for a clinical study of correlating all active dabigatran entities in plasma with effect. At the time when this study was conducted, a few human plasma LC-MS/MS assays of dabigatran, with the indirect quantification of DAG, have been briefly described in several clinical papers [108, 242, 243]. None of them provide sufficient detail for method replication and validation data according to the FDA guidelines [244]. Furthermore, while there have been four publications for assays of free (unconjugated) dabigatran [224-226, 245], these did not evaluate the stability of DAG and its potential influence on the quantification of dabigatran. Further, none of these papers describe whether the impact of in-source fragmentation of DAG interferes with the quantification of dabigatran. The present work therefore demonstrates a simplified and rapid sample preparation for the analysis of dabigatran and dabigatran acyl glucuronide in human plasma.

5.2. Aims

The initial aim of this study was to develop a direct quantification method of all the isomeric forms of DAG simultaneously with free unconjugated dabigatran. The assumption was that all four isomers (dabigatran 1-*O*, 2-*O*, 3-*O* and 4-*O*-acyl glucuronide) could be quantified using the 1-*O* acyl glucuronide as the reference standard. This has been the assumption when developing assays for acyl glucuronides [217]. However, during development of the assay, it was discovered that although the 2-, 3- and 4-*O* isomers fragment to the same product ions as the 1-*O*-isomer, the product ion to precursor ratios were different (i.e. the

qualifier ion ratio between calibration samples and patient samples were different). Therefore, direct quantification would require reference standards for all four isomers, in addition to approaches to control isomerization of the samples and calibrators. As the reference standard for the dabigatran 1-*O* acyl glucuronide was the only standard that was commercially and readily available at the time when the study was conducted, an approach to indirectly quantify the DAG was pursued. In this paper, a validated assay for the quantification of free dabigatran and all active entities of dabigatran (total dabigatran) is presented. This allows for an indirect quantification of DAG. Further, data on the stability of DAG and measures taken to ensure that DAG hydrolysis does not interfere with free dabigatran measurement are presented.

There are 3 specific objectives of this study:

1. To develop and validate an LC-MS/MS assay for dabigatran and dabigatran acyl glucuronides in human plasma
2. To investigate the impact of temperature and pH on the stability of dabigatran 1-*O*-acyl glucuronide in human plasma
3. To analyse dabigatran concentrations in patient plasma samples collected from a previous clinical study

5.3. Methods

5.3.1. Chemicals & materials

Accurately weighed dabigatran and [$^{13}C_6$]-dabigatran internal standard (Figure 5.4) were purchased from Alsachim (Strasbourg, *France*) and dabigatran 1-*O* acyl glucuronide was purchased as dabigatran 1-*O*-acyl glucuronide trifluoroacetic acid salt from Toronto Research Chemicals (Toronto, Canada). The purity of dabigatran and [$^{13}C_6$]-dabigatran was 97% and dabigatran 1-*O* dabigatran acyl glucuronide 95%. HPLC-grade methanol was purchased from Merck (Darmstadt, Germany), HPLC-grade acetonitrile was purchased from VWR International (IL, USA) and formic acid (analytical grade, 98–100% pure) was purchased from BDH (Poole, UK). Analytical grade sodium hydroxide (NaOH) and hydrochloric acid (HCl) were purchased from Merck (Darmstadt, Germany) and reagent grade ammonium formate from Sigma-Aldrich (St Louis, MO, USA). Distilled, de-ionized water was produced in house by a Milli-Q Reagent Water System from Millipore Corp. (MA, USA). Blank human plasma from healthy volunteers was collected in BD Vacutainer® K_2 EDTA tubes for the preparation of calibration standards and quality controls.

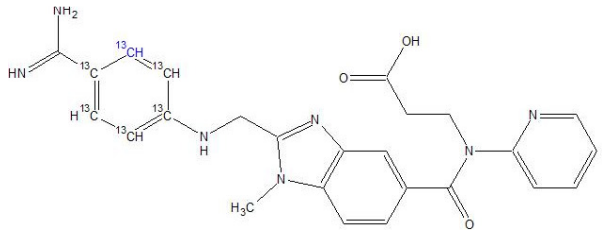

Figure 5.4 *Internal standard ($^{13}C_6$ -Dabigatran)*

5.3.2. Stock solutions, calibration standards and quality control samples

Two stock standard solutions of dabigatran (one for calibration samples and one for quality control (QC) samples) and internal standard [$^{13}C_6$]-dabigatran (2.0 mg/ml) were prepared by dissolving 10.0 mg of dabigatran or [$^{13}C_6$]-dabigatran in a mixture of dimethylsulfoxide (DMSO) & 50 mM aqueous HCl (95:5, v/v). Dabigatran 1-*O* acyl glucuronide stock standard solution (1 mg/ml) was prepared by dissolving 1.0 mg, accurately weighed, in DMSO. The stock standard solutions were aliquoted into smaller quantities and were stored at -30^{o}C. Intermediate standard solutions (one from calibration stock solution and one from QC stock solution) of dabigatran were prepared at 50 µg/ml in DMSO & 50 mM aqueous HCl (95:5, v/v). Serial dilutions were made from these and used to spike into drug-free K_2 EDTA plasma at concentrations of 0, 2.5, 10, 50, 100, 500 and 1000 ng/ml for calibration standards and 10, 100, and 1000 ng/ml for QC samples. The internal standard [$^{13}C_6$]-dabigatran (100 ng/ml) working solution was prepared in water and stored at 4^{o}C.

5.3.3. Sample preparation

For quantification of free unconjugated dabigatran (without alkaline hydrolysis):

In an Eppendorf tube, 50 µl of working internal standard solution was added to 50 µl of blank, standard, quality control or patient plasma sample. Then 50 µl of 0.2 M ammonium formate buffer pH 3.5 was added and the mixture was vortexed. For protein precipitation, 200 µl acetonitrile was added and the mixture was vortexed. After centrifugation at 15,000 g for 5 min at 22±1.0^{o}C, a 50 µl aliquot of clear supernatant was transferred to a 96-well plate and mixed with 200 µl of water. The 96-well plate was centrifuged at 3500 × g for 5 min before injecting 20 µl into the LC-MS/MS system.

For quantification of total dabigatran (with alkaline hydrolysis):

In an Eppendorf tube, 50 µl of working internal standard solution was added to 50 µl of blank, standard, quality control or patient plasma sample. For hydrolysis, 20 µl of 0.2 M NaOH was added and the mixture was vortexed thoroughly and incubated for 2 hours at 37°C. Then the mixture was left to cool for approximately 5 minutes and 30 µl of 0.2 M HCl was added. For protein precipitation, 200 µl acetonitrile was added and the mixture was vortexed. After centrifugation at 15,000 g for 5 min at 22±1.0°C, a 50 µl aliquot of clear supernatant was transferred to a 96-well plate and mixed with 200 µl of water. The 96-well plate was centrifuged at 3500 × g for 5 min before injecting 20 µl into the LC-MS/MS system.

5.3.4. LC–MS/MS conditions

An Agilent 6460 Triple Quadrupole LC/MS System, which consisted of an Agilent 1290 Infinity LC coupled to an Agilent 6460 Triple Quadrupole Mass Spectrometer with Agilent JetStream was used (Agilent Technologies, Santa Clara, CA, USA). A Poroshell 120 EC C18 2.7 µm, 50 × 3.0 mm column (Agilent Technologies, Santa Clara, CA, USA) equipped with a SecurityGuard C18 4.0 x 3.0 mm cartridge (Phenomenex) was used. Mobile phase A consisted of water containing 0.2% formic acid and 10 mmol/l ammonium formate and mobile phase B was acetonitrile. The flow rate was 0.6 ml/min. Chromatographic separation was achieved by a linear gradient of 1-10% mobile phase B within 3 mins. This was further increased from 10-20% B between 3 and 3.5 min followed by a steep increase to 90% B at 4 mins. This level was maintained for 1 min and returned to the initial condition from 5-5.2 mins and re-equilibrated for 1.8 min. Under these conditions, dabigatran eluted at 4.08 min and dabigatran acyl glucuronides at 3.5-3.9 mins. The total time for analysis was 7 min. The auto sampler was kept at 5°C.

The mass spectrometer was operated in the positive ion mode using electrospray ionization (ESI). Drying gas temperature and flow rate were 200°C

and 5 l/min, respectively, nebuliser gas pressure was 15 psi, capillary voltage was 3000 V, and sheath gas temperature and flow rate were 400°C and 10 l/min. The optimized precursor-to-product ion transitions monitored for dabigatran $[M + H]^+$ and $[^{13}C_6]$-dabigatran $[M + H]^+$ were *m/z* 472.0/289.1 and *m/z* 478.0/295.1, respectively, with a fragmentor voltage of 160 V, a collision energy of 26 V and a dwell time 100 milliseconds for both transitions. Qualifier ions were 472.0/324.1 for dabigatran and 478.0/330.1 for $[^{13}C_6]$-dabigatran with a collision energy of 18 V and a dwell time of 20 ms for both transitions. Two transitions of dabigatran 1-*O* acyl glucuronide $[M + H]^+$ were also monitored for completeness of hydrolysis and stability studies. The first transition (*m/z* 648.2/472.2) is specific to dabigatran 1-*O*-acyl glucuronide as the loss of 176 Da relates to the loss of glucuronic acid of 1-*O* but not the migration isomers [217]. The second transition (648.2/289.1) product ion is a fragment of dabigatran and thus nonspecific to DAG isomers (dabigatran 1-*O*, 2-*O*, 3-*O*, 4-*O* acyl glucuronide), but allowed for qualitative measurement of the migration isomers. MassHunter Workstation Software (B.06.00, Agilent Technologies, Santa Clara, CA, USA) was used for instrument control, data acquisition and analysis.

5.3.5. Assay validation

The validation was performed on both sample preparation procedures (with and without alkaline hydrolysis). Calibration curve samples and QC samples (n = 6 at each level) were prepared and analysed on three separate days to evaluate linearity, inter- and intra-day precision and accuracy, and recovery according to the US FDA guidelines for bioanalytical method validation for human studies [10]. Selectivity was evaluated by accessing the absence of interference from blank plasma samples obtained from six different individuals. The extraction recoveries and matrix effects were evaluated at the three QC levels (n = 6). Blank plasma from six different subjects was extracted and spiked to concentrations corresponding to the QC concentrations. Absolute extraction recovery was determined by comparing the peak areas of QC samples with those of the spiked extracted plasma blanks (representing 100% recovery). Matrix

effect was determined by comparing the peak areas of spiked extracted plasma blanks to peak area of samples spiked at corresponding concentration in a neat solution representing 100% (no matrix effect).

For test of completeness of alkaline hydrolysis of DAG to dabigatran, 13.7, 137 and 685 ng/ml DAG (the molar equivalent of 10, 100 and 500 ng/ml dabigatran) was spiked into blank plasma (n=3) and prepared with and without hydrolysis as described above.

Long-term stability of dabigatran in plasma was assessed by storing a set of samples spiked at three concentrations (n = 3 for 50, 200 and 1000 ng/ml) at -80ºC for 12 months. Evaluation of freeze–thaw and short-term stability were combined and was assessed by storing QC samples at -80ºC and thawing up to three cycles, after which samples were kept at room temperature for 4 hours prior to analysis. The stability samples for dabigatran were not acidified before freezing. The stability samples were analysed using free dabigatran sample preparation (without hydrolysis) and the results were compared with those of freshly prepared samples (n = 3 at each concentration). Post-preparative stability was evaluated by determining the concentrations of a set of QC samples and storing the samples in the 96-well plate at 5ºC in the auto sampler for 72 hours. The QC samples were reanalysed and the results compared with original values.

Long term stability of DAG towards hydrolysis was assessed by storing a set of samples spiked at two concentrations (n = 3 for 100 and 1000 ng/ml) at -80ºC for 70 days. Freeze-thaw stability was assessed at two concentrations (n = 3 for 50 and 500 ng/ml) by storing spiked samples at -80 ºC, thawing to room temperature and repeated in three cycles. These samples were analysed immediately. Samples for long term and free-thaw stability of DAG were not acidified before freezing. For short term stability, samples were prepared in triplicates in a cold room (4ºC) and then kept for 4 hours under the following conditions; 4ºC and 22ºC, with and without addition of 0.2 M ammonium formate buffer (pH 3.5) and compared with a control set that was analysed immediately. All samples were prepared without hydrolysis and the

concentrations of dabigatran were measured, allowing the percent hydrolysis of DAG to dabigatran to be calculated.

5.3.6. Assay application

The assay was used to analyse plasma samples from a previous clinical study. A total of 58 patients provided either one (2 hours post-dose), two (2 and 10-16 hours post-dose) or five (1, 2, 4, 8 and 10-16 hours post-dose) samples resulting in a total of 150 samples. The samples were collected in BD Vacutainer® K_2 EDTA tubes and centrifuged for 15 minutes at room temperature without delay and the plasma was immediately stored at -80^{o}C until analysis.

5.4. Results and Discussion

5.4.1. Assay development

The MS/MS parameters were optimized to produce the most abundant fragment ions for dabigatran using ESI in positive mode. The *m/z* transition of 472/289 produced the highest signal-to-noise ratio and was used for quantification, which was also the case in several other assays [108, 225, 246]. Representative chromatograms of dabigatran (without and after alkaline hydrolysis) are shown in Figure 5.5 and Figure 5.6. The MS/MS parameters were also optimised to reduce in-source fragmentation of DAG to dabigatran, which readily occurs due to the thermally unstable ester bond of the glucuronide. It was not possible to completely avoid in-source fragmentation as seen in Figure 5.7C where an earlier peak is seen in the dabigatran *m/z* 472/289 channel eluting at the same retention time (3.78 min) as DAG (Figure 5.7A and B). Chromatographic separation of dabigatran and DAG was therefore required to avoid overestimation of dabigatran due to in-source fragmentation. This was achieved by having a slow organic gradient from 0-3.5 mins.

Ammonium formate pH 3.5 was used in our study to stabilize DAG against hydrolysis to dabigatran. Acyl glucuronides, in general, have been reported to be substantially more stable against hydrolysis and acyl migration

when the samples are kept below pH 4 [208, 211]. Other acids have been used to reduce the pH and stabilize DAG against hydrolysis [208, 237], but were not tested in this study.

5.4.2. Assay validation

The dabigatran and [$^{13}C_6$]-dabigatran peaks were free of interference from endogenous substances present in drug-free plasma (Figure 5.5A, 5.5B and Figure 5.6A, 5.6B). Plasma standard curves of dabigatran were adequately fitted by 1/x weighted quadratic regressions (r > 0.999) over the concentration range of 2.5 to 1,000 ng/ml. The absolute extraction recoveries and matrix effects are presented in Table 5.1. Mean extraction recoveries were >98% for both sample preparation methods. Some ionization enhancement was observed for dabigatran. However, this was corrected for by the isotopically labelled internal standard and the internal standard normalised variation between individuals was <4% CV. Hemolysed and lipemic samples were not tested in this work. The use of an isotopically labelled internal standard and the generally low matrix effects observed (Table 5.1) indicate that the internal standard corrects for any matrix interferences. Accuracy was demonstrated with the mean values being within 101-114% of the spiked values. Imprecision was small, as indicated by both intra- and inter-day CV of <9% at all concentrations except at the lower limit of quantification, LLOQ (<11%, Table 5.2).

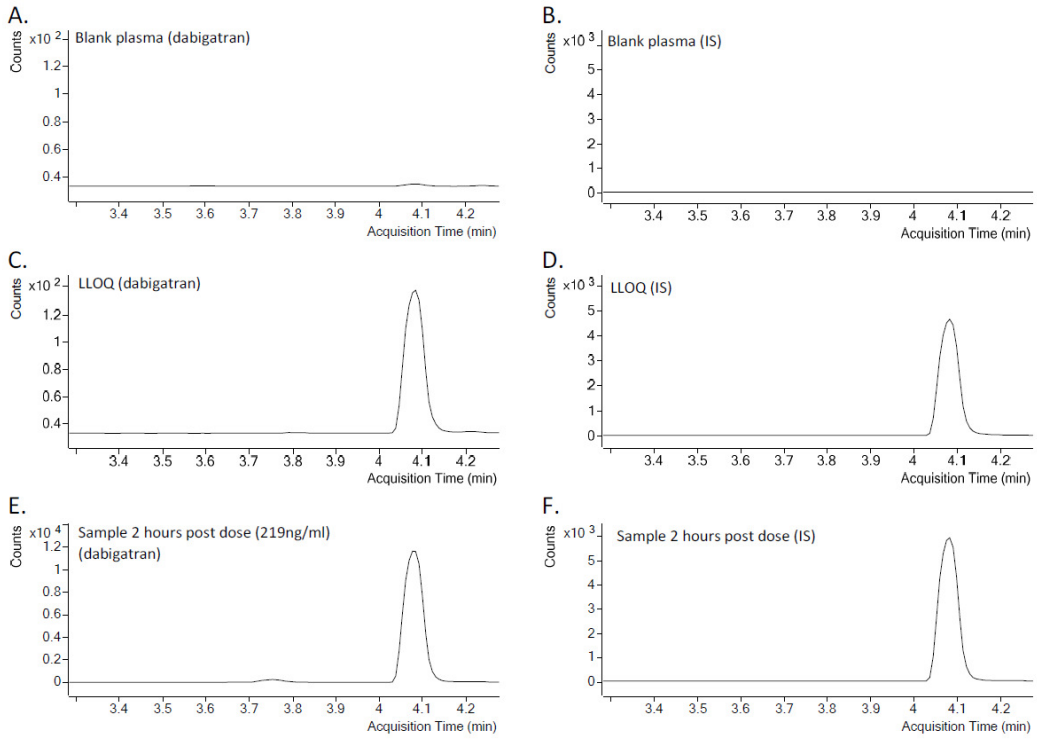

Figure 5.5 *Representative chromatograms of samples without alkaline hydrolysis. (A, B) Blank plasma. (C, D) LOQ = 2.5 ng/ml. (E, F) Patient sample 2 h post dose (219 ng/ml). A, C and E represent dabigatran chromatograms; B, D and F represent [$^{13}C_6$]-dabigatran chromatograms.*

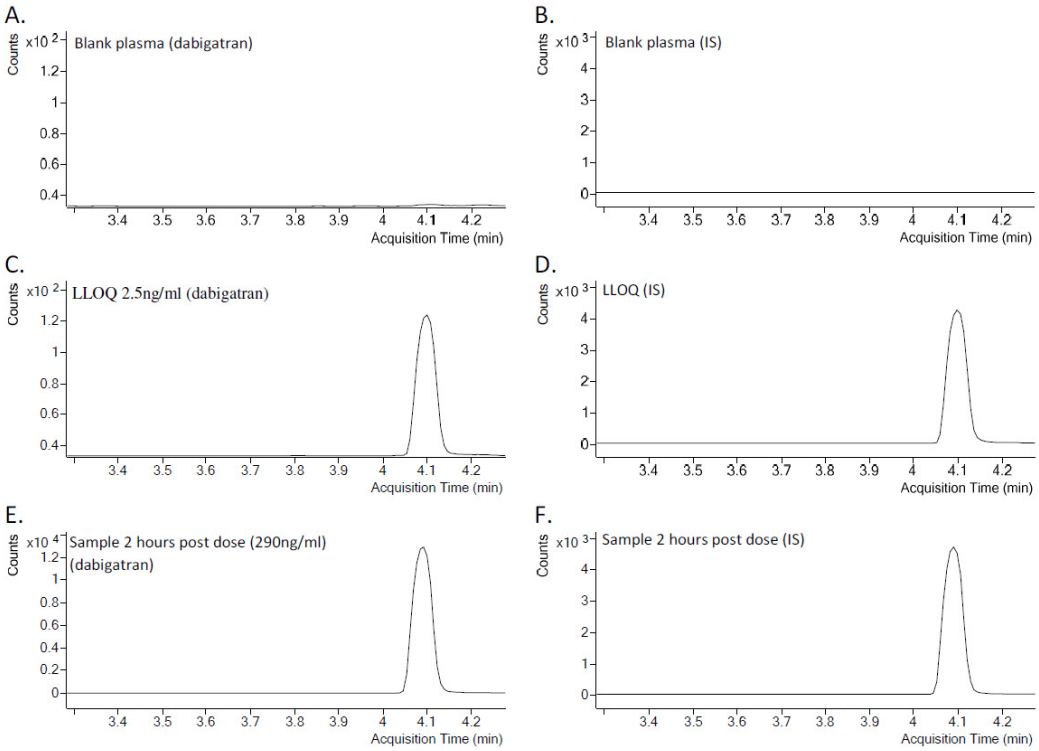

Figure 5.6 *Representative chromatograms of samples after alkaline hydrolysis. (A, B) Blank plasma. (C, D) LOQ = 2.5 ng/ml. (E, F) Patient sample 2 h post dose (290 ng/ml). A, C and E represent dabigatran chromatograms; B, D and F represent [$^{13}C_6$]-dabigatran chromatograms.*

QC samples that underwent alkaline hydrolysis (total dabigatran sample preparation) were within the limits of accuracy and precision observed for QC samples without alkaline hydrolysis (free dabigatran sample preparation). Therefore, a single standard curve prepared without alkaline hydrolysis could be used for both sample preparation methods.

The incubation conditions for alkaline hydrolysis were sufficient to hydrolyse off all DAG to yield free dabigatran (mean recoveries of 101%, 103% and 96% for concentrations 10, 100 and 500 ng/ml dabigatran). Figure 5.7 shows an example chromatogram before and after hydrolysis.

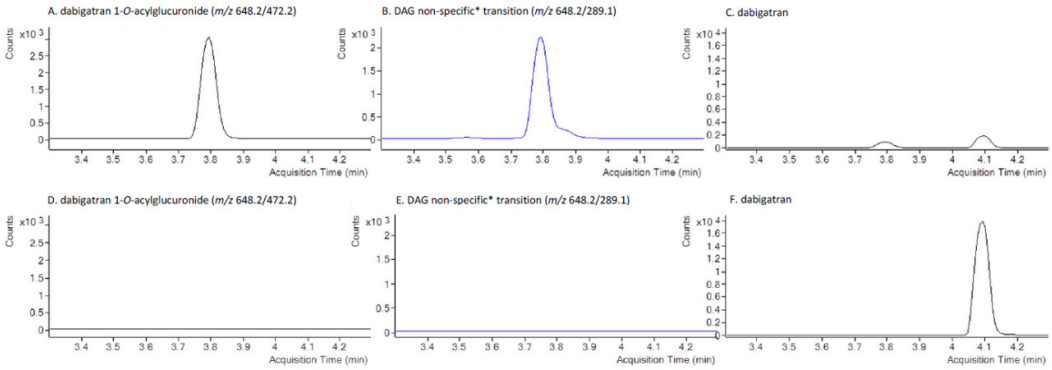

Figure 5.7 *Representative chromatograms before (top) and after (bottom) alkaline hydrolysis of 137 ng/ml dabigatran 1-O-Acyl glucuronide in plasma. *Non-specific refers to the four isomeric forms of dabigatran acyl glucuronide (dabigatran 1-O, 2-O, 3-O, 4-O Acyl glucuronide)*

Dabigatran was found to be stable (<10% deviation from nominal concentration) in plasma (Table 5.3) after three freeze-thaw cycles followed by 4 hours at room temperature and for 1 year at -80°C. The long-term stability data thus agrees with, and extends, dabigatran stability data reported previously [224-226]. The processed samples were stable for at least 72 hours at 5°C for both methods of sample preparation (hydrolysis and non-hydrolysis).

Table 5.1 *Extraction recovery and matrix effect for dabigatran without and after alkaline hydrolysis in 6 different individuals*

Analyte	Nominal Concentration (ng/ml)	% Recovery		% Matrix Effect	
		Mean ± SD	Internal standard normalised mean ± SD	Mean ± SD	Internal standard normalised mean ± SD
Dabigatran without alkaline hydrolysis					
LQC	10	104.9 ± 11.1	102.2 ± 5.8	112.7 ± 13.1	99.7 ± 4.0
MQC	100	98.0 ± 4.9	100.7 ± 0.8	116.2 ± 7.7	101.0 ± 0.5
HQC	1000	99.4 ± 10.7	99.4 ± 1.4	111.6 ± 4.1	99.8 ± 0.9
Dabigatran after alkaline hydrolysis					
LQC	10	107.6 ±10.8	111.6 ± 6.2	123.8 ± 14.0	100.3 ±1.1
MQC	100	98.7 ± 4.7	101.5 ± 1.0	124.3 ± 15.9	100.1±0.5
HQC	1000	97.8 ± 6.0	100.1 ± 2.9	105.4 ± 8.3	99.5±0.8

CV: Coefficient of variation; HQC: High quality control; LLOQ: Lower limit of quantification; LQC: Low quality control; MQC: Mid quality control; SD: Standard deviation

Table 5.2 *Intra- and inter-day accuracy and imprecision dabigatran without and after alkaline hydrolysis in human plasma.*

Sample	Nominal concentration (ng/ml)	Intraday			Interday		
		Mean concentration ± SD (ng/ml)	Imprecision (%CV)	Accuracy (%)	Mean concentration ± SD (ng/ml)	Imprecision (%CV)	Accuracy (%)
Dabigatran without alkaline hydrolysis							
LLOQ	2.5	2.9 ± 0.2	6.1	114.2	2.8 ± 0.3	10.9	110.2
LQC	10	10.5 ± 0.2	1.7	104.7	10.1 ± 0.8	7.5	101.4
MQC	100	105.5 ± 2.7	2.6	105.5	102.3 ± 6.9	6.7	102.3
HQC	1000	1105.3 ± 35.8	3.2	110.5	1049.2 ± 70.7	6.7	104.9
Dabigatran after alkaline hydrolysis							
LLOQ	2.5	2.7 ± 0.2	7.7	107.1	2.7 ± 0.2	8.6	108.8
LQC	10	9.5 ± 0.4	3.9	95.0	10.2 ± 0.9	8.4	102.0
MQC	100	98.6 ± 3.6	3.6	98.6	102.7 ± 4.4	4.3	102.7
HQC	1000	991.3 ± 35.3	3.6	99.1	1012.7 ± 38.6	3.8	101.3

CV: Coefficient of variation; HQC: High quality control; LLOQ: Lower limit of quantification; LQC: Low quality control; MQC: Mid quality control; SD: Standard deviation

Table 5.3 *Stability of dabigatran (n=3) in human plasma*

Long Term		**Freeze-thaw and short term**	
Nominal concentration (ng/ml)	1 year at -80°C (ng/ml)	Nominal concentration (ng/ml)	3 freeze-thaw cycles and 4 hours at 22°C (ng/ml)
50	47.3	10	9.1
200	200.2	100	94.7
1000	976.2	1000	929.1

Table 5.4 *Stability of dabigatran 1-O-acylglucuronide (n=3) in human plasma (expressed as % hydrolysis to dabigatran)*

Long term		**Freeze-thaw**		**Short term, 4 hours (%)**			
Concentration (ng/ml)	70 days, -80°C (%)	Concentration (ng/ml)	3 freeze-thaw 22°C (%)	4°C, pH 3.5	4°C	22°C, pH 3.5	22°C
100	6.9	50	3.2	0	5.1	1.0	16.9
1000	6.9	500	3.4	0.4	4.2	1.2	15.8

For DAG in plasma, ~7% hydrolysis was found after 70 days at -80ºC and ~3% hydrolysis was found after 3 freeze thaw cycles (Table 5.4). DAG readily hydrolysed at room temperature (~17% after 4 hours), but could be stabilised against hydrolysis by adding ammonium formate pH 3.5 and lowering the temperature to 4ºC. The DAG acyl migration can be qualitatively observed by monitoring the transition *m/z* 648/289. Figure 5.8 shows chromatograms of a sample that was left for 4 hours at room temperature, with and without ammonium formate pH 3.5. Figure 5.8E shows marked isomerization with multiple peaks that corresponds to the migration isomers. Besides protecting against hydrolysis, the addition of ammonium formate pH 3.5 also stabilises the 1-*O* isomer against acyl migration (Figure 5.8B).

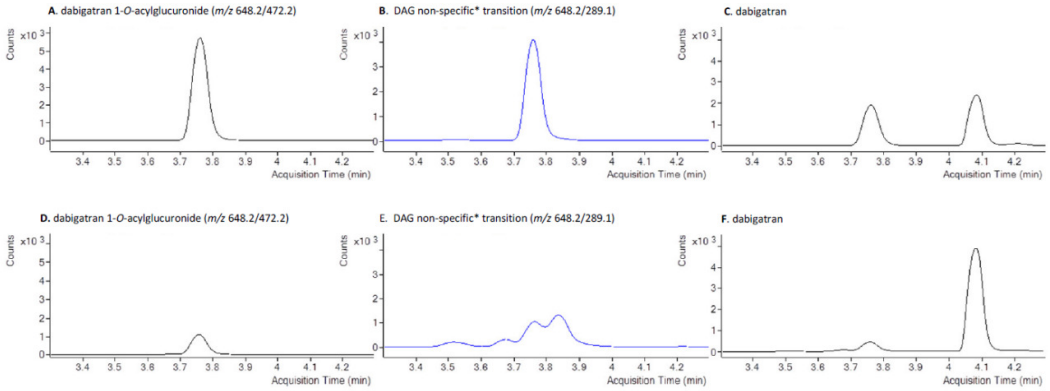

Figure 5.8 *Representative chromatograms of 500 ng/ml dabigatran 1-O-Acyl glucuronide in plasma incubated for 4 hours at 22°C with (top rows) and without (bottom rows) addition of 0.2 M ammonium formate pH 3.5. *Non-specific refers to the four isomeric forms of dabigatran acyl glucuronide (dabigatran 1-O, 2-O, 3-O, 4-O acyl glucuronide)*

The results for DAG are thus consistent with what is generally reported for acyl glucuronides, in that hydrolysis can occur when freezing and thawing [208] and that low temperature and pH play important roles in stabilising acyl glucuronides [228, 247]. Therefore, for accurate and precise quantification of free dabigatran, the samples should be cooled and measured as soon as possible with the fewest freeze-thaw cycles, and ideally with the addition of ammonium formate to lower pH. In other bioanalytical assay studies of dabigatran in plasma, acid was added during sample collection [108, 246, 248] or during sample preparation [225, 226, 249] while in one study, no acid was added [224].

5.4.3. Assay application

The mean total concentration of dabigatran in 150 patient samples measured in duplicates after alkaline hydrolysis was 124 ng/ml (range 0-427 ng/ml). Deviations on duplicate values were <20% for 96.7% of the samples (145/150). QC and calibration samples were within 15% CV and bias. A representative chromatogram from a sample taken 2 hours' post dose is shown in Figure 5.5E (without hydrolysis) and 5.6E (with alkaline hydrolysis).

A subset of 16 samples was measured without alkaline hydrolysis, with a mean free dabigatran concentration of 146 ng/ml (range 12-299 ng/ml) and total dabigatran concentration of 161 ng/ml (range 11-349 ng/ml) in this subset of patients. Deviations on duplicate values were <20% for 87.5% of the samples (16/18). The range of DAG indirectly quantified in this subset of samples was 0-39% of the post-hydrolysis (i.e. total) dabigatran concentration. However, due to the samples being collected prior to the development of the assay, the samples were not acid stabilized on collection. Therefore, the actual DAG concentration is likely to be underestimated, and the free dabigatran concentration overestimated. The remaining 132 samples were therefore not measured and the measurements obtained from this subset of 16 samples should be viewed only as an illustration of the indirect method for quantifying dabigatran acyl glucuronide. No inference can be made in terms of the relationship of free and total dabigatran concentrations from these data.

The analysis of the data obtained from this study will be reported in the next chapter (Chapter 6).

5.5. Conclusion

A sensitive LC–MS/MS assay with a simple plasma protein precipitation step was developed for the quantification of dabigatran, and the indirect quantification of dabigatran acyl glucuronide via alkaline hydrolysis. Data showing that DAG is unstable at room temperature if the pH is not lowered have been presented. It is therefore critical to lower the pH, preferably at sample collection, or at least during sample preparation for accurate determination of dabigatran. The assay was validated over the range of 2.5 to 1000 ng/ml dabigatran. It was found to give accurate and precise reproducible results and has been successfully applied to patient samples.

Chapter 6: Evaluation and selection of a prior dabigatran population pharmacokinetic model for dose individualisation

In the previous chapter, an LC-MS/MS assay for measuring dabigatran and dabigatran acyl glucuronide in plasma was developed. The assay was used to measure the sum of dabigatran and dabigatran acyl glucuronide (measured as dabigatran) from patient samples collected from a previous study. In this chapter, the measured dabigatran concentrations from Chapter 5 are used in a simulation based study designed to evaluate published population pharmacokinetic models for dabigatran. The purpose of this chapter is to select an appropriate prior model to be used for individualising dabigatran doses in a future setting.

6.1. Introduction

Dabigatran is an orally administered anticoagulant that acts by inhibiting thrombin. Dabigatran is a polar molecule (log P, pH 7.4 = −2.4). It is orally administered as a prodrug, dabigatran etexilate, which has low fractional oral bioavailability of approximately 7% [100]. The absorption of dabigatran etexilate is pH dependent and is increased in acidic conditions. In the formulation used clinically, dabigatran etexilate is coated onto a tartaric acid core to minimise the influence of pH at the absorption site [250].

The pharmacokinetics of dabigatran have been well summarised in several publications [95, 111, 113, 243, 246, 251, 252]. The peak concentration and total exposure was found to be proportional over the investigated dose range of 50 to 400 mg of dabigatran etexilate [111]. The terminal half-life of dabigatran is approximately 13 hours [113, 248] and a steady-state concentration is typically achieved after 3 days of twice-daily dosing [243, 253]. Approximately 20% of dabigatran is conjugated to form the pharmacologically active dabigatran acyl glucuronide [103]. Due to the difficulty in measuring dabigatran and dabigatran acyl glucuronide separately, as described in the previous chapter, many studies (see [111, 248, 251] for example), have measured the sum of (unconjugated) dabigatran and de-conjugated dabigatran acyl glucuronides (measured as dabigatran).

For the purposes of this chapter, unless stated otherwise, "dabigatran concentration" refers to the sum of dabigatran and dabigatran acyl glucuronides (measured as dabigatran).

Current dosing and monitoring guidelines by the manufacturer have been questioned by several authors [40, 254-257]. The contention is whether the existing variability between individuals in the dose-response is large enough to the extent that there are risks of side effects and treatment failure if the same dose is used for most patients. There have been calls for improved anticoagulation monitoring especially in patients with renal impairment, at the extremes body weight and those who are high risk of bleeding [40, 258]. There are published data that relates dabigatran concentrations to stroke and bleeding risk [10, 122], which suggests that monitoring and individualising the dose of dabigatran etexilate may improve the safety and efficacy of therapy.

To date, there is no consensus on what constitutes a safe and effective therapeutic range for dabigatran plasma concentrations. There have been limited published studies exploring this issue to date. Chin *et al* [116] have proposed a target range of steady-state trough concentration for patients with non-valvular atrial fibrillation. This target range was derived from secondary analysis of published of phase III data [10, 94, 125, 259]. Briefly, Chin *et al* [116] extracted the logistic regression curves for stroke/systemic embolic events and major bleeding risk published by Reilly *et al* [10] and the numbers of subtypes of events contributing to ischaemic stroke/systemic embolic events and major bleeding in the RE-LY study [10, 94, 125, 259]. They then applied weightings for adverse events according to the hazard ratios of death as described by Eikelboom *et al* [118]. The two curves were combined by adding the two equations to produce a combined weight-adjusted risk curve. The authors then assessed the combined risk curves with different bleed and stroke scores and suggested a general target trough dabigatran concentration range of 30 – 130 ng/mL. The steady-state trough concentration is therefore an exposure metric of interest to guide dosing

because it has been correlated with clinical outcomes including thromboembolic and bleeding events.

A population pharmacokinetic model that captures the time course and magnitude of drug exposure, and accounts for pharmacokinetic differences between individuals as well as the factors which determine these differences can be used to individualise dosing [260, 261]. This can be accomplished by using the model to predict the dose required to achieve a target exposure metric of interest, such as the steady-state trough concentration, in each patient. An example of a population model that was used to guide dosing is a tobramycin population pharmacokinetic model in paediatric cystic fibrosis patients by Hennig *et al* [262]. The study aimed to assess the need for a target concentration intervention approach in the group of patients studied. The authors developed a tobramycin population pharmacokinetic model and used it to simulate doses to achieve the target area under the curve with 80-125% variability of the target. The authors concluded that dose adjustments using a target concentration intervention approach is needed to maximize the pharmacokinetic/ pharmacodynamic relationship to achieve the target area under the curve and can be achieved using their model. Likewise, this strategy can be applied to dabigatran dosing where a population pharmacokinetic model of dabigatran is used to predict a dose to achieve a certain probability of hitting the target concentration.

Several population pharmacokinetic models of dabigatran have been published [263, 264]. These models were developed using 'total' dabigatran concentrations which is the same as the measured concentration from Chapter 5. Therefore, evaluation of the predictive performance of previously published models against our data is a logical first step in determining whether a model exists now that may be of value in dose-individualisation. Such a model may be able to replace the need for developing another population pharmacokinetic model of dabigatran *de novo* to be used as a prior for future dose individualisation. Note the data generated from Chapter 5 were fairly sparse and

there would be a significant risk of producing an under-determined population pharmacokinetic model.

The overarching goal of this chapter is to identify the best population pharmacokinetic model that adequately describes the data from Chapter 5. If such a model is identified, it can be used in future work to inform the dose individualisation using Bayesian methodology. There are at least two options of how this goal can be achieved. The first option is directly using a suitable prior model in a Bayesian forecasting method dosing software. In this case, the underlying prior model should have good predictive performance of the external data. The parameter estimates for the individual can then be updated from the prior as more feedback becomes available so that is more refined and individualised to that patient. Equipped with individualised patient parameters, an accurate dosing schedule can be selected. If the prior model does not have good predictive performance, the second option is to use the best model from the literature and apply as a prior for analysis of the current data in a fully Bayesian population analysis. This would provide population parameter estimates associated with the current data that are stabilised by prior work. Stability of the model is important for the identifiability of model parameters and reproducibility of the model (i.e. same objective function value) following small perturbations in the input data or starting parameter values. The subsequent model is then used as a prior in a Bayesian forecasting method for dose individualisation for future patients. Option two is therefore, a two-step process. Notwithstanding the choice of pharmacometric methods to utilise the prior model, there remains a need to identify a suitable prior model. This provides the impetus for this chapter where the predictive performance of the published dabigatran models will be evaluated against the data generated from Chapter 5.

The specific aims of this study are to identify all previously published population pharmacokinetic models of dabigatran and to evaluate the predictive performance of each model against the data set from Chapter 5. The prior model

with good predictive performance can then be used to aid in dose individualisation of dabigatran.

6.2. Methods

6.2.1. Identification of a population pharmacokinetic models

Medline and EMBASE databases were searched for published population pharmacokinetic models of dabigatran. The search terms included ("dabigatran or dabigatran etexilate") AND ("Models, Theoretical" OR "Models, Biological", "Models, Statistical" OR "algorithms" OR "population pharmacokinetics" OR "population analysis" OR "nonlinear mixed effects modelling" OR "NONMEM") AND ("pharmacokinetics" OR "Dose-Response Relationship, Drug"). The search was limited to articles published in English and human studies. Citation records were searched for potentially relevant papers. The inclusion criterion was population pharmacokinetic models for plasma total dabigatran concentration. Population models were excluded if there was insufficient information in the published paper to enable stochastic simulations of dabigatran plasma concentration.

6.2.2. Data source

Dabigatran concentrations were measured as described in Chapter 5. This is the test data set used in this chapter. The data set was sourced from a previous published study by Chin *et al* [109]. The publication included blood sample analysis from 52 patients. Additionally, data from 6 patients were collected as part of the study but not published. The aim of the study was to explore the relationship between plasma concentrations of parent (unconjugated) dabigatran and four coagulation assays (INR, aPTT, thrombin time and diluted thrombin time) and to examine the contribution of fibrinogen variability to the thrombin time test variability in relation to unconjugated dabigatran plasma concentration. The data collected included the prescribed dose dabigatran etexilate, the time since the last dose was taken, the duration since initiation of

dabigatran. Demographic data included weight, height, sex, indication for dabigatran and serum creatinine.

The total number of patients in the data set was 58. Six patients who were starting dabigatran (first dose) and these each contributed 5 plasma samples (at approximately 1, 2, 4, 8 and 10-16 hours post a morning dose). The remaining 52 patients had been on a specific dosing regimen of dabigatran for at least 10 days prior to sample collection and were assumed to be at steady state. Each patient either contributed one plasma sample (pre-morning dose, n=2), two plasma samples (pre-morning dose and 2 hours post morning dose, n=44) or five plasma samples (at approximately 1, 2, 4, 8 and 10-16 hours post a morning dose, n=6).

A summary of the key demographic and pharmacokinetic features of the patients providing data for this study is provided in Table 6.1. The indication of dabigatran for all patients in the data set was thromboprophylaxis for atrial fibrillation, although this was not an inclusion criterion for the study.

Table 6.1 *Characteristics of patients in the data set (n=58)*

Characteristics		**Median [IQR]*(range)****
Age, y		67 [58-75] *(38-94)*
Male, n (%)		44 (76)
Total body weight, kg		95 [82-109] *(56-187)*
Height, m		1.75 [1.7-1.8] *(1.55-1.93)*
Serum creatinine (µmol/L)		93 [83-102] *(64-125)*
Creatinine clearance (mL/min) #		64 [55-76] *(23-106)*
Dabigatran etexilate MDR at sampling		
75 mg twice daily, n (%)		5 (9)
110 mg twice daily, n (%)		25 (43)
150 mg twice daily, n (%)		28 (48)
Duration on dabigatran etexilate, weeks†		6.0 [4 – 9.5] *(0-52)*
Proton pump inhibitor use, n (%)		13 (22.4)
Drugs affecting P-glycoprotein function		
Amiodarone and/or verapamil, n (%)		10 (17.2)
Phenytoin and phenobarbitone, n (%)		1 (2)
Pre-dose plasma dabigatran concentration, ng/mL		68 [45-89] *(22-258)*
Number of samples per patient		
	1	2 (ss)
	2	44 (ss)
	5	12 (6 ss and 6 initiating)

** Unless stated otherwise*

† At the same dose-rate as at sampling

 # Creatinine clearance calculated using the method of Cockcroft and Gault

IQR, interquartile range; MDR, maintenance dose-rate; ss, steady-state

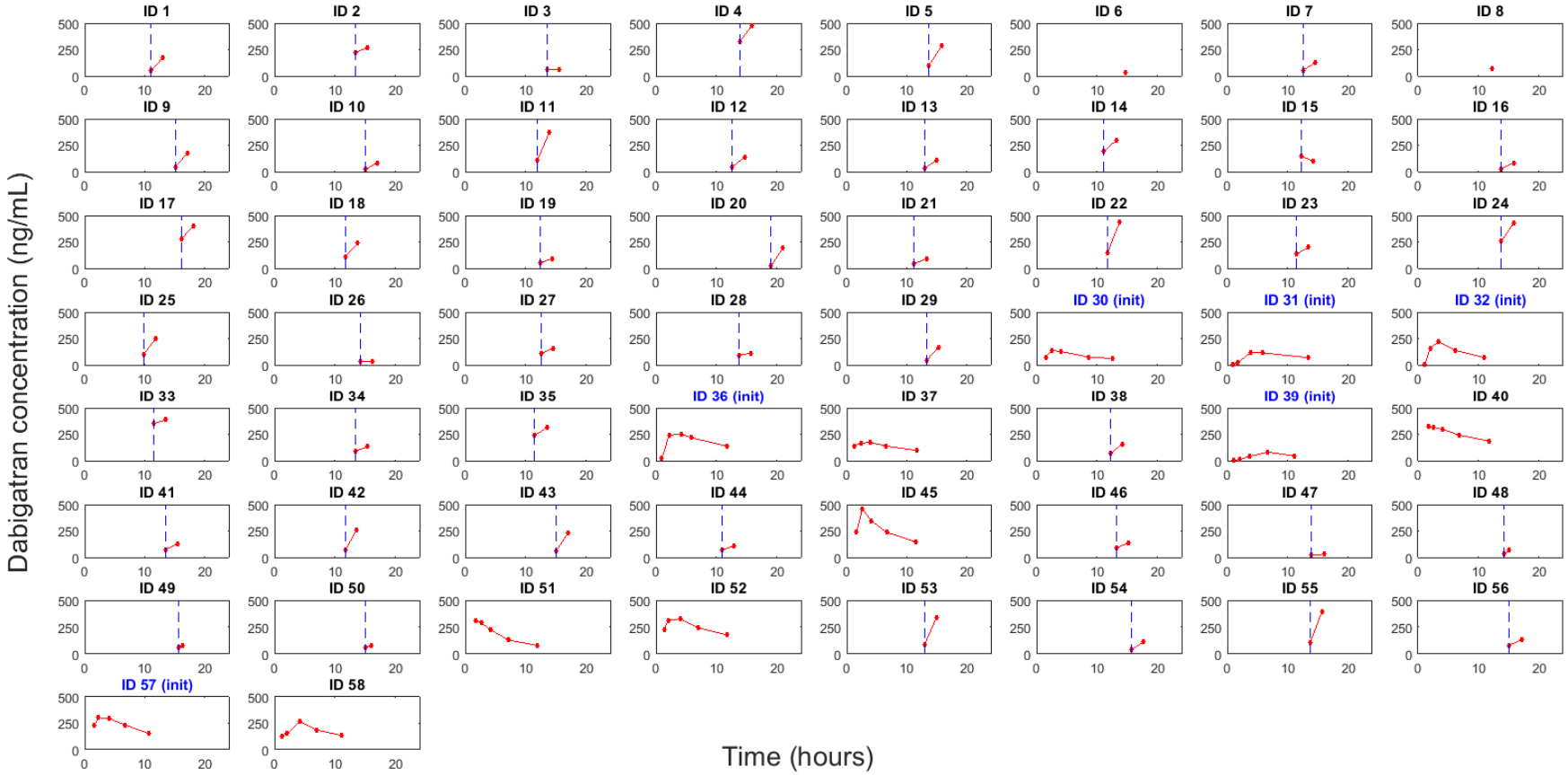

Figure 6.1 *Individual profiles of dabigatran concentration versus time after dose. ID is individual subject. IDs 30, 31, 32, 36, 39 and 57 were individuals who were newly initiated on dabigatran (first dose), other IDs were patients who have initiated dabigatran for >10 days and were assumed to have reached steady-state concentration. Vertical blue dashed lines are when a dose was taken for individuals who contributed two samples – note that there are two dosing intervals for these profiles. All concentration profiles were dose-referenced to 150mg twice daily*

6.2.3. Model evaluation

Each pharmacokinetic model was evaluated in terms of its ability to predict the observed concentrations from the test data set. For the purposes of this analysis, the test data set was divided into the following groups:

- Group A – All concentration data from patients initiating dabigatran. These patients contributed 5 plasma samples (n=6).
- Group B – All concentration data from patients assumed to be at steady-state, who contributed 5 plasma samples (n=6).
- Group C – All concentration data from patients who contributed one or two concentrations at steady state at either pre-dose and/or post-dose timing (n=52). Note that this includes part of the data from Group B.

Each of the population pharmacokinetic models were coded in MATLAB® (version 2015b, Mathwork, Natick, MA) using the same structural components, covariate relationships, error models and parameter values as the published model. For each model, one-thousand patients were simulated.

Covariates were sampled non-parametrically from the demographics of the test data set. Covariates that were used in the published models but not available in the test data set (e.g. gastrin concentration) were fixed to the null value (see Table 6.2 for details).

The input of the model is either a single dose or twelve doses of dabigatran etexilate 150 mg twice daily. Twelve doses were simulated to approximate steady-state.

There was no execution model in this study as adherence and protocol violations were not considered in this work.

For the purposes of comparison with simulated pharmacokinetic profiles, each observed concentration was dose-referenced to a 150-mg dabigatran etexilate twice daily dosing regimen.

The predictive performance of each model was assessed by a visual predictive check (VPC):

1. For Group A (full profile first-dose), the models were assessed using a VPC of concentration-time profile that covered the full dosing interval. The VPC was constructed with the median of the predicted and observed data and the 10th and 90th percentiles of the simulated data only. The 10th and 90th percentiles of the observed data were not included because the data were sparse.
2. For Group B (full profile at steady state), the models were assessed using a VPC of concentration-time profile that covered the full dosing interval. The VPC was constructed with the median of the predicted and observed data and the 10th and 90th percentiles of the simulated data only. The 10th and 90th percentiles of the observed data were not included because the data were sparse.
3. For Group C, the distribution and central tendency of the pre-dose and 2-hour post-dose concentrations of the simulated were compared to the binned observed concentrations using box plots. In addition, for Group C, a Kolmogorov-Smirnov test (KS test) for two samples was used to compare the cumulative density distributions (CDF) of the simulated and observed pre-dose and post-dose concentrations, separately. A p value <0.05 was chosen to reject the hypothesis that both simulated and observed data have the same distribution.

The simulation output and all statistical analysis were conducted using MATLAB® (version 2015b, MathWorks, Natick, MA). See Appendix IV, section A4.1-4.3 for details of the MATLAB® code used for this analysis.

6.2.4. Model selection

The primary model selection criteria was driven by how well the model predicted the steady-state pre-dose concentrations of the test data set (i.e. the trough concentration). Secondarily, consideration was given to VPCs of the overall concentration-time profile.

6.3. Results

6.3.1. Published population pharmacokinetic models

Five studies describing five dabigatran population pharmacokinetic models were found in the published literature. Two studies were excluded, (1) the population model by Delavene 2012 [265], excluded on the basis that the model was developed using only plasma unconjugated dabigatran concentrations, and (2) the population model by Liesenfeld 2013 [266], excluded on the basis that the model was developed from patients who were undertaking haemodialysis. The models required to describe extracorporeal elimination, are sufficiently different from our population to justify excluding this work. The excluded models are summarised in Appendix IV, Section A4.1 (Table A4.1).

Table 6.2 provides a summary of the three population pharmacokinetic models included in the current study. All three models were two-compartment disposition model with first-order absorption and elimination. Fractional oral bioavailability (F) was fixed to 1 in the models by Liesenfeld *et al* 2011 and Dansirikul *et al* 2012 although the between subject variability for F was estimated. The study by Trocóniz *et al* 2007 did not include estimates of absolute or relative F, or BSV on F. Note that this is equivalent to a fixed the value to 1. All three models found Cockcroft-Gault creatinine clearance (as an estimate of renal function) to be a significant covariate on clearance. Typical values for apparent oral clearance ranged from 82 L/h to 124 L/h. Other covariates that were reported to be significant in specific models were serum creatinine and gastrin concentrations (Trocóniz 2007 [267]), atrial fibrillation (Dansirikul [263]), heart failure and South Asian ethnicity (Liesenfeld 2011 [264]), body weight

(Dansirikul [263] and Liesenfeld 2011 [264]), blood haemoglobin (Liesenfeld 2011 [264]), sex (Liesenfeld 2011 [264] and Dansirikul [263]), age (Trocóniz 2007 [267], Dansirikul [263] and Liesenfeld 2011 [264]), sex (Liesenfeld 2011 [264] and Dansirikul [263]) and co-medication (proton pump inhibitor and P-gp inhibitors in Dansirikul [263]; proton pump inhibitor, amiodarone and verapamil in Liesenfeld 2011 [264]). In all three models, total dabigatran concentrations (dabigatran and dabigatran acyl glucuronide) were measured using LC-MS/MS. The study by Dansirikul *et al* 2012 was a population PKPD model, however only the pharmacokinetic component was used in this simulation. PK and PD parameters in this study were sequentially estimated.

Table 6.2 *Details of published dabigatran models*

Author	Study details	Structural model	Parameter estimates	Description
Trocóniz, 2007 [267]	Dose escalation in patients who have undergone orthopedic surgery study. Dose in mg (n): 12.5 od (27), 25 od (28), 50 od (30), 100 od (40), 150 od (29), 200 od (28), 300 bd (20), 150 od (41), 300 (46) qd. 4604 observations in total from 287 patients Note: The experimental tablet formulation did not contain tartaric acid).	PK (sum of dabigatran and dabigatran acyl glucuronide): 2-compartment First order input	Fixed effects (θs) k_a =0.265 h^{-1} $ALAG$=0.4 h Q/F=13.6 L h^{-1} V_2/F = 30.8L V_3/F=136L CL/F= 82.1 L h^{-1} Covariates (θs) $Gastrin$ = 0.633 S_{cr} = 0.363 Age = 0.447 BSV (CV%) CL/F = 46.04 k_a= 29.83 RUV (CV%) Additive (ng/mL) = 0.375 Proportional = 36.61	 First order absorption rate constant Absorption lag time Apparent intercompartmental CL Apparent volume of central compartment Apparent volume of peripheral compartment Apparent clearance (CL) Coefficient for serum gastrin concentration effect on CL/F ($Gastrin$ concentration was fixed to 34.58 pmol L^{-1} in this study) Coefficient for serum creatinine concentration effect on KA Coefficient for age effect on k_a BSV in the apparent clearance BSV in k_a Additive residual variability Proportional residual variability

Covariate relationship

$$CL/F = \theta_{CL} \times \frac{CL_{CR}}{76.17} \times 1 + (\theta_{Gastrin} \times \frac{Gastrin}{34.58})$$

$$k_a = \theta_{k_a} \times (1 - \theta_{Scr} \times \frac{Scr}{0.964}) \times (1 - \theta_{Age} \times \frac{Age}{66.97})$$

Liesenfeld 2011 **[264]**	Phase 3 (RE-LY) trial. Atrial fibrillation patients. n=9522 27 706 observations in total	PK (sum of dabigatran and dabigatran acyl glucuronide): 2-compartment First order input	Fixed effects (θs) k_a =0.754 h^{-1} $ALAG$ =0.634 h F=1 (fixed) $V_2/$F=673 L V_3/F=345 L Q/F =35.5 L h^{-1} CL/F =124 L h^{-1} Covariates (θs) $EC50$ = 56.7 (mL min^{-1}) $Power$ = 1.29 Age = −0.41 (% year^{-1}) $Ethn$ = 0.797 HF = 0.933 HGB = −3.99 (%) Sex = 0.917 PPI =0.875 $Amio$ =1.12 $Vera$ = 1.23	First order absorption rate constant Absorption lag time Bioavailability Apparent volume of central compartment Apparent volume of peripheral compartment Apparent intercompartmental CL Apparent clearance (CL) CL$_{CR}$ value at which half of the maximum clearance is reached Power coefficient of the E$_{max}$ CL$_{CR}$ and CL/F relationship Coefficient for age effect on CL/F Coefficient for South Asian ethnicity effect on CL/F Coefficient for heart failure effect on CL/F Coefficient for blood haemoglobin concentration effect on $V2/F$ (HGB concentration was fixed to 0.143 kg/L in this study) Coefficient for female effect on CL/F Coefficient for proton pump inhibitor effects on F Coefficient for amiodarone on F Coefficient for verapamil on F

BSV (CV%)

V_2/F = 20.5	BSV in the volume of central compartment
F = 44.3	BSV in the relative bioavailability

RUV (CV%)

Additive (ng/mL) = 6.68	Additive residual variability
Proportional = 32.8	Proportional residual variability

Covariate relationship

$$CL/F = (\theta_{CL} \times CLCR^{(\frac{\theta_{power}}{\theta_{EC50}{}^{\theta_{power}} + CLCR^{\theta_{power}}})} \times (1 + \theta_{age}[age - 72] \times \theta_{Ethn} \times \theta_{HF} \times \theta_{sex})$$

$$V2/F = \theta_{V2} \times (1 + \theta_{Wt} \times [Wt - 80.3]) \times (1 + [HGB - 14.3])$$

$$F = \theta_F \times \theta_{PPI} \times \theta_{Amiodarone} \times \theta_{Vera}$$

Dansirikul 2012 [263]	Data from 4 phase I and 4 phase II studies containing healthy and patient data set for PK, and PKPD data set Number of patients (observations): 80 (1031), 1965 (7931), 762 (7659) One of the trial data had different formulation to the final product. 3 of the source data were not published (internal report). Others were the same as final marketed product.	PKPD (sum of dabigatran and dabigatran acyl glucuronide): 2-compartment First order input	<u>Fixed effects (θs</u> k_a = 0.754 h^{-1} $ALAG$ = 0.634 h Q/F = 35.5 L h^{-1} F = 1(fixed) V_2/F=728 L V_3/F= 345 L CL/F = 111 L h^{-1} <u>Covariates (θs)</u> CL_{CR} = 0.00644 Wt = 0.0110 Age = –0.00662 PPI = 0.854 PgP = 1.150 AF = 0.939 $Female$ = 0.875	 First order absorption rate constant Absorption lag time Apparent intercompartmental CL Bioavailability Apparent volume of central compartment Apparent volume of peripheral compartment Apparent clearance (CL) Coefficient for CL_{CR} effect on CL/F Coefficient for weight effect on apparent volume of central compartment Coefficient for age effect on CL/F Coefficient for proton pump inhibitors effects on F Coefficient for P-glycoprotein inhibitors effects on F Coefficient for atrial fibrillation effects on CL/F Coefficient for female sex on CL/F

<u>BSV (CV%)</u>	
V_2/F= 26.1	BSV in the volume of central compartment
k_a = 95.3	BSV in the first order absorption rate constant
F = 44.7	BSV in the relative bioavailability
<u>RUV (CV%)</u>	
Proportional = 29.4	Proportional residual error
<u>Covariate relationship</u>	
If CL_{CR}>120mL/min: $CL/F = \theta_{CL}(1 + \theta_{age}[age - 68] \times \theta_{AF} \times \theta_{Female})$	
if CL_{CR}<120mL/min: $CL/F = \theta_{CL}(1 + \theta_{CLCR}[CLCR - 120]) \times (1 + \theta_{age}[age - 68] \times \theta_{AF} \times \theta_{Female})$	
$V2/F = \theta_{V2} \times (1 + \theta_{Wt}[Weight - 80])$	
$F = \theta_F \times \theta_{PgP} \times \theta_{PPI}$	

BSV, between subject variability; CV, coefficient of variation; RUV, residual unexplained variability, CL_{CR}, creatinine clearance; PK, pharmacokinetic

6.3.2. Model evaluation

6.3.2.1. Model performance against full-profile data from patients initiating dabigatran (Group A)

Figure 6.2 shows the VPC of patients in Group A. Post-dose trough concentrations were under-predicted by the models of Trocóniz *et al* 2007 and Liesenfeld *et al* 2011. The model of Liesenfeld *et al* 2011 appear to under-predict the overall concentration profiles. The VPC plots show that the model published by Dansirikul *et al* appears to capture all other data points well and importantly pre-dose concentration appears to be well predicted.

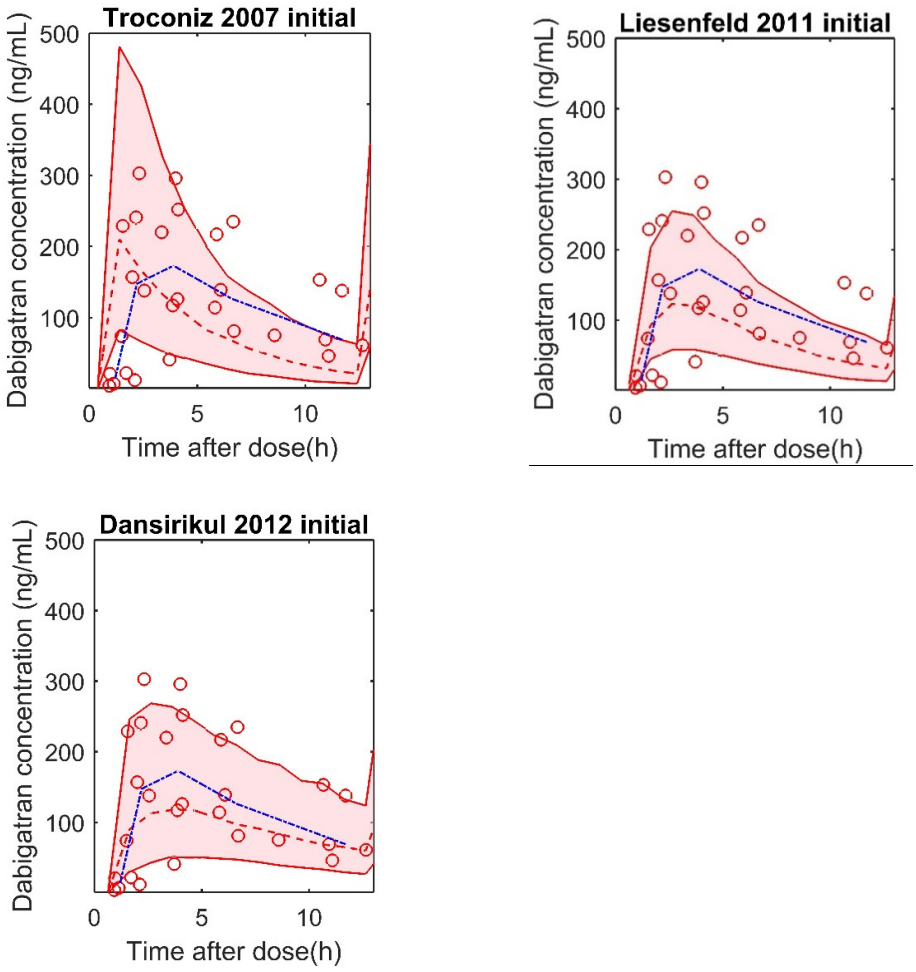

Figure 6.2 *A visual predictive check showing simulated concentrations at the first dose. The shaded area is the 10th to 90th percentile of the simulate and the dashed line in the middle is the median of the simulate, the blue line is median of the observed data. The dose-referenced observed concentrations are represented by red circles.*

6.3.2.2. Model performance against full profile data from patients at steady-state, who contributed 5 plasma samples (Group B)

Figure 6.3 shows the VPC plots for patients from Group B. Post-dose trough concentrations were under-predicted by the models of Trocóniz *et al* 2007 and Liesenfeld *et al* 2011. The model of Liesenfeld *et al* 2011 and Trocóniz *et al* 2007 both appear to substantially under-predict the overall concentration profiles. The VPC plots show that the model of Dansirikul *et al* appears to capture all data points well and the median of the post-dose trough concentrations were the closest to the observed data amongst the three models. However, there is greater spread of the between subject variability seen with the Dansirikul *et al* model.

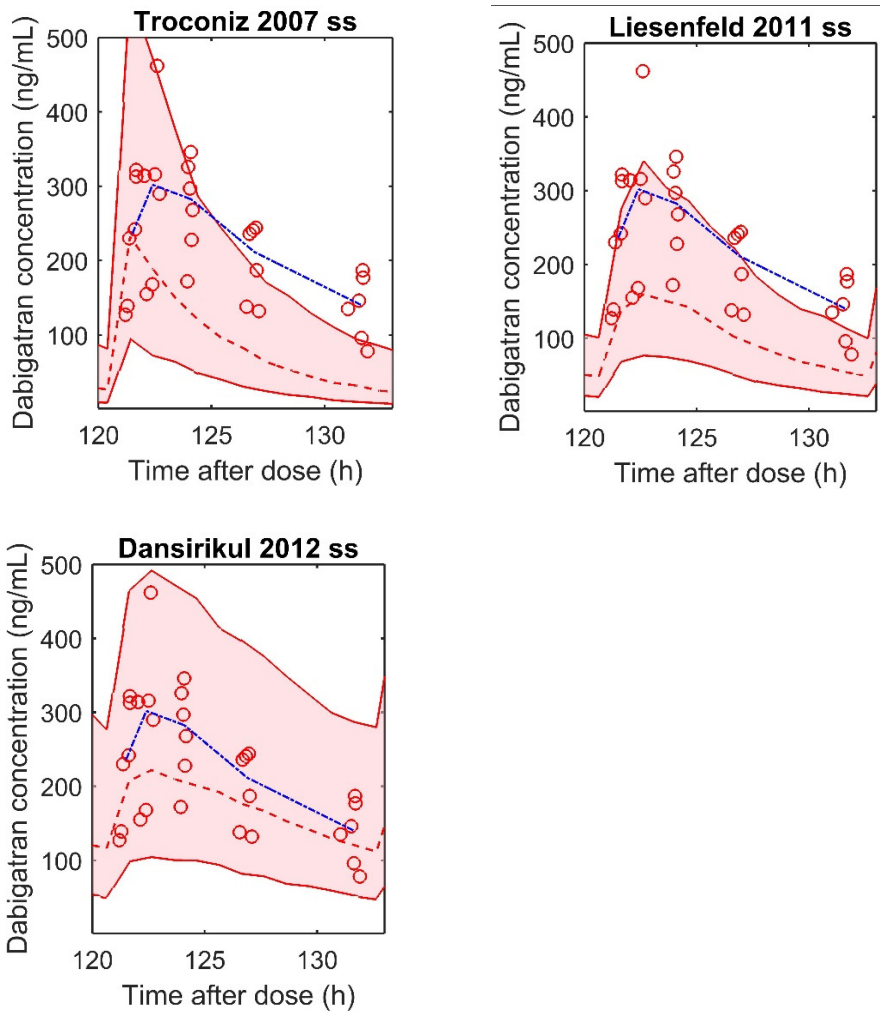

Figure 6.3 *A visual predictive check of concentration at steady state. The shaded area is the 10th to 90th percentile of the simulate and the dashed line in the middle is the median of the simulate, the blue line is median of the observed data. The dose-referenced observed concentrations are represented by red circles*

6.3.2.3. Model performance against data from patients who contributed one or two steady state concentrations at either pre-dose or post-dose or both (Group C)

Figure 6.4 shows a comparison of the predicted pre-dose concentration and 2 hours post-dose concentration against the test data set. Amongst the three models, the Dansirikul *et al* 2012 model appeared to predict the pre-dose concentration the best where the interquartile range overlapped the most out of the three models. The Trocóniz *et al* 2007 and Liesenfeld *et al* 2011 models appear to under-predict the pre-dose concentrations. There was generally close agreement between all model-predicted post-dose concentrations and the observed data for all three models.

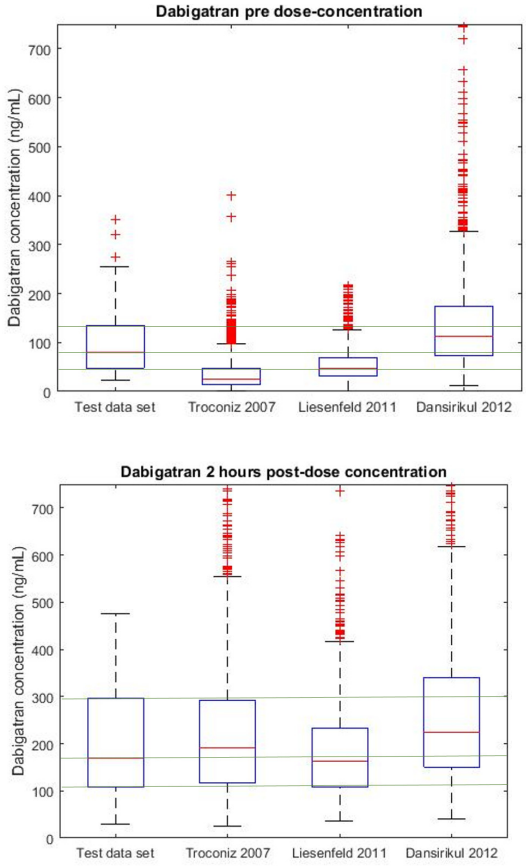

Figure 6.4 *Box plots of pre-dose (top) and 2-hour post-dose (bottom) concentrations of the test data set versus predictions of three published dabigatran pharmacokinetic model. Boxes represent the 25th and 75th percentiles and the centre red line is the median. The whiskers correspond to approximately +/–2.7σ of the data. The '+' symbols indicate outliers. The green horizontal line extends the 25th, 50th and 75th percentiles of the test data set.*

6.3.2.4. Kolmogorov-Smirnov test (KS test) for patients in Group C

The cumulative density distributions of the pre-dose concentrations for all three models were statistically different from the test data set (p<0.05). The distribution of the 2-hours post-dose concentration of the Dansirikul *et al* model was also significantly different from the test data set (p<0.05). The result of each KS test is provided in Table 6.3. Figure 6.5 shows the cumulative density function for pre-dose and post-dose concentration for each model compared to the test data set. The KS test appears to favour models where the IQR of the model predictions are incorporated within the IQR of the data. Hence the post-dose predictions preferred Trocóniz *et al* and Liesenfeld *et al*.

Table 6.3 *Results of the Kolmogorov-Smirnov test of predicted pre-dose and 2 hours post-dose concentrations of dabigatran PK models compared to the data*

	Trocóniz *et al* 2007		**Liesenfeld *et al* 2011**		**Dansirikul *et al* 2012**	
	Pre-dose	*Post-dose*	*Pre-dose*	*Post-dose*	*Pre-dose*	*Post-dose*
p-value	*<0.001*	*0.70*	*<0.001*	*0.26*	*0.01*	*0.01*

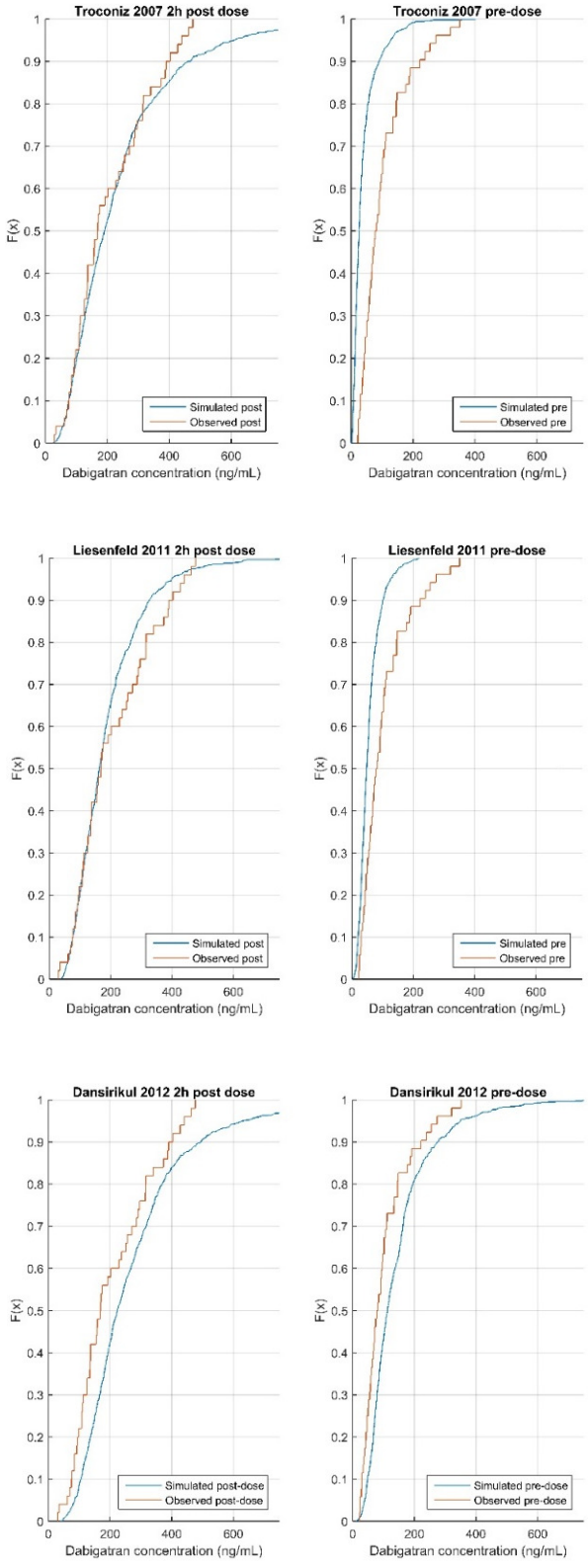

Figure 6.5 *The cumulative density function plot of predicted pre-dose and 2 hours post-dose concentrations of the three models compared to the observed concentrations of the test data set.*

6.3.3. Model selection

The primary measure was assessment of the trough concentrations. Visually the Dansirikul *et al* appeared superior to the other two models. The KS test however did not support any model. The secondary measures were the predictive performance over time, in these cases visually Dansirikul *et al* 2012 model was preferred. The post-dose concentration, however, was visually better predicted by Trocóniz and the KS test rejected Dansirikul *et al*. No model entirely adequately described the test data set. However, the key interest were the trough concentrations which supported the use of Dansirikul *et al* as an initial starting point.

6.4. *Discussion*

In this study, the predictive performance of three population pharmacokinetic model of dabigatran were evaluated against external data in a simulation based study. The selection of models was mainly driven by data from patients at steady-state because the goal is to predict the maintenance dose and not a loading dose, although data from patients initiating dabigatran was still used for visual assessment. Three forms of VPC diagnostics (concentration-time profiles, box plots and CDFs) were used to determine the best prior model. The KS test appear to reject pre-dose trough predictions from all three models. Based on the CDFs and box plots, the 2-hours post-dose concentrations were better predicted by Trocóniz *et al* 2007 and Liesenfeld *et al* 2011, however both models under-predicted the pre-dose trough concentrations.

The KS test has been used to assess predictive performance for model selection (see [268, 269]). It is a non-parametric test that is used to determine if two distributions (concentrations of the test data set and simulation in this case) are different. An advantage of the KS test is that it makes no assumption of the distribution of the data. One of the limitations of the KS test is that it tends to be more sensitive towards the differences at the center of the two CDFs compared to the tail ends. This is evident in Figure 6.5 where the CDFs of the post-dose

concentrations for the Trocóniz *et al* and Liesenfeld *et al* models were close to distribution of the test data set at the central region and hence the null hypothesis was not rejected.

In this study, none of the three models satisfactorily described the test data set. The Dansirikul *et al* model was selected on the basis of having the best predictive performance compared to the other two models at predicting the trough concentration, however the model does not adequately describe the entire concentration-time profile (specifically, the post-dose concentration). In light of this finding, an appropriate future direction for this research is to use the Dansirikul model in a full Bayesian population analysis with subsequent use of the resultant model as a prior in a Bayesian dosing tool (i.e. a two-step process).

The methods for assessing priors in this study were chosen because of the nature of the test data set. The majority of the data were from a sparse design. Only pre-dose concentration data were available from all patients and 2-hour post-dose concentrations were available from 56 out of 58 patients. Assessing a full VPC of the concentration-time profile alone was inadequate because only 6 patients per group provided five data concentration time points. This makes the VPC highly sensitive towards outliers. Box plots were useful as the pre-dose and post-dose observed concentrations had differences in the actual timing when the samples were collected. By binning, it allows easy comparison between the simulated concentrations and the observed concentration in the test data set.

There have been several similar studies where authors evaluate multiple population PK models to select the 'best prior model' for dose individualisation. Examples include publications by Wright and Duffull 2011 [1] (warfarin), Bloomfield *et al* 2016 [270] (tobramycin) and Zhao *et al* 2016 [271] (tacrolimus). Table 6.4 below summarizes the different techniques used by each study to evaluate and select the best model.

Table 6.4 *Methods used to select a prior model*

Author, year	Models evaluated	Diagnostic method
Bloomfield *et al* 2016 [270]	8 tobramycin models	MPE and RMSE VPC NPDE
Wright and Duffull 2011 [1]	5 warfarin models	VPC
Zhao *et al* 2016 [271]	16 tacrolimus models	% MPE pcVPC NPDE

MPE, mean prediction error; RMSE, root mean squared error; VPC, visual predictive check; NPDE normalized prediction distribution error; pcVPC, prediction- and variability-corrected VPC

As seen in Table 6.4, there are several methods used to select the 'best prior model'. There is no consensus on the preferred method [272]. The decision to select the best prior model is somewhat subjective and purpose-specific. An alternative approach to selecting the 'best model' is a hybrid model approach [273] which will be discussed in the next chapter in Section 7.1.2.3.

The model by Trocóniz *et al* 2007 was the first population pharmacokinetic model of dabigatran to be published. It was developed with 287 patients who had primary elective total hip replacement surgery. The data was from a phase IIa dose escalation study (BISTRO I [274]). As noted above, the dosage form of dabigatran etexilate in this study was different from the final product used clinically (not formulated with tartaric acid). The model prediction showed a distinctly sharper peak concentration with steep decline post-peak concentration which resulted in over-prediction the observed peak concentrations and under-prediction of the observed pre-dose concentrations. It is unclear if this could be due to the difference in the formulation used for this study.

Figure 6.6. is a deterministic simulation at the mean parameter values in each of all three models overlaid. The simulated concentrations appear to be higher in Dansirikul *et al* model compared to the other two models 4-hours post-dose onwards. This is mainly driven by differences in parameter estimates of clearance (67 L h^{-1} in Dansirikul model versus 89 L h^{-1} and 123 L h^{-1} L for Trocóniz

and Liesenfeld models respectively). This is likely to be the main difference that visually supports Dansirikul *et al* over the other models in terms of predicting into the test data set.

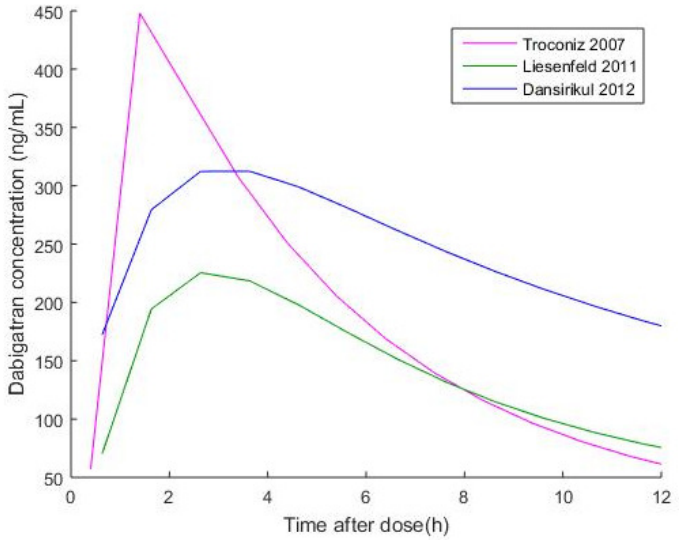

Figure 6.6 *A deterministic simulation at the mean parameter values of each model. Simulation was for a 67-year-old, male, weighing 95 kg, with creatinine clearance of 64 mL min^{-1}.*

The full model by Trocóniz *et al* 2007 include different k_a and CL/F parameter values for <24 hours, as patients who have recently undergone surgery manifest gastric stasis and flip-flop kinetics. The differences in gastric motility within the first 24 hours' post-surgery was reflected on pharmacokinetic parameters of absorption rate constant (K_a) (0.022 h^{-1} <24 hours versus 0.265 h^{-1} >24 hours) and CL/F (43.4 L h^{-1} <24 hours versus 82.1 L h^{-1} >24 hours). Figure 6.7 is a deterministic simulation of parameter values < 24 hours and flip-flop kinetics can be observed.

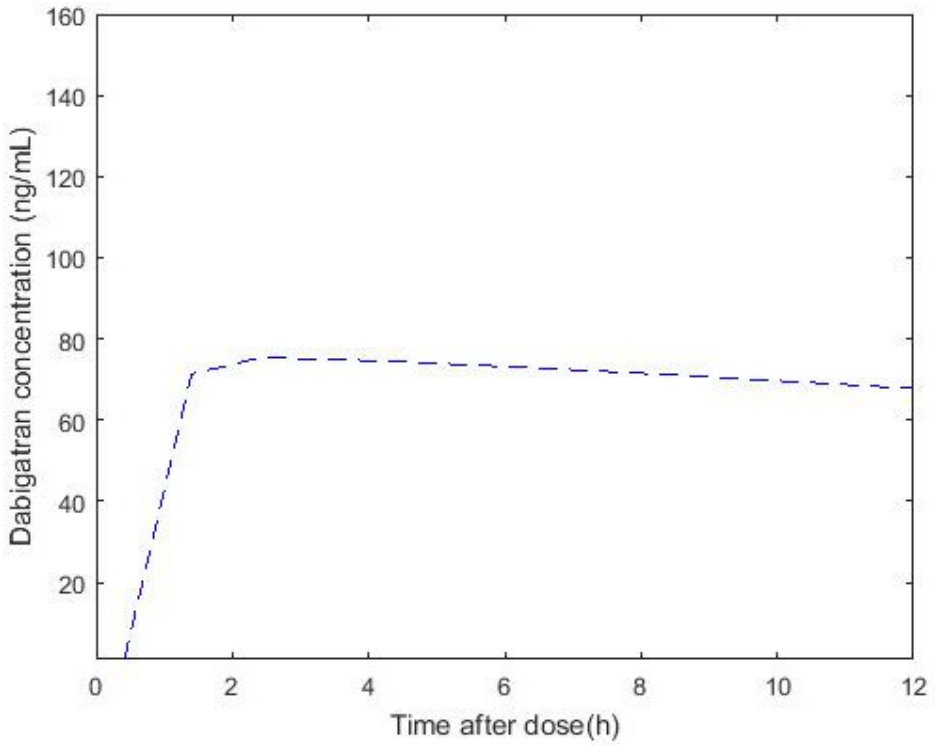

Figure 6.7 *A deterministic of simulation of the Trocóniz 2007 model. The plot shows dabigatran plasma concentration versus time profiles after the first dose of 150 mg.*

A proportional error model was used for <24 hours post-surgery, but a combined error model was used >24 hours post-surgery. For this study, only parameter values and error models for > 24 hours post-surgery were used as steady-state conditions were simulated.

The models published by Liesenfeld *et al* and Dansirikul *et al* were largely similar. Liesenfeld *et al* 2011 used the base model from the publication by Dansirikul *et al* 2012 in their model development. The Liesenfeld *et al* model was developed using the largest data set (n=9522) from a phase III (RE-LY) clinical trial in patients with atrial fibrillation [94] similar to patients in the test data set. In contrast, data for Dansirikul *et al* 2012 was sourced from 3 different data sets from eight phase I and phase II clinical trial studies, some of which included unpublished data from healthy volunteers and patients. Therefore, the heterogeneity in the data used to develop the Dansirikul *et al* model may have

captured the variability in the test data set which may explain why the Dansirikul *et al* 2012 model had the best predictive performance. Individual parameter estimates may be improved using Bayesian forecasting, however this is not within the scope of this thesis but may be explored in subsequent studies.

For patients who contributed two plasma samples, the samples were collected from two sequential dosing intervals. The median [range] of the first dosing interval was 13.3 [9.8-19] hours, and the median [range] of the post-dose samples were collected at 2.0 [0.7-2.2] hours. Evaluating the model performance using VPC is difficult, as the variability of the first dosing interval needed to be simulated and individual VPC would need to be generated and compared against the observed data. Therefore, this work was not done. Instead, the test data set was binned into pre-dose concentrations and 2-hours post dose concentrations and the model predictions were evaluated using box plots and the KS test. Binning the data may have resulted in some error, which is one of the limitations of this study.

There are several other limitations associated with this study. The study was based on data where adherence was not formally assessed. Several variables such as serum gastrin concentration (used in the Trocóniz *et al* model) and blood haemoglobin concentration (used in the Liesenfeld *et al* model) was not available in the test data set. Therefore, missing variables were fixed to the null value which may have introduced some error. The results of this study are based on the assumption that the model was correctly replicated in MATLAB®. The coded models were able to be modified and to simulate the data. This is a form of quality assurance that the model has been coded correctly for the purposes of this study. This study is also based on the assumption that the demographics of the data set was collected without error.

6.5. Conclusion

Three population pharmacokinetic models of dabigatran were evaluated against external data. The dabigatran model of Dansirikul *et al* 2012 was found to have the best predictive performance amongst the three models. However, the precision of the parameters can be improved by conducting a full Bayesian population analysis. Therefore, this model will be used as a prior model in a full Bayesian population analysis before implementation in a Bayesian dosing tool for future dose prediction.

PART V

DISCUSSION AND CONCLUSION

Chapter 7: Discussion and Conclusion

7.1. Discussion

7.1.1. Synopsis of the thesis

In this thesis, methods for predicting the maintenance dose of warfarin were evaluated and aspects of dabigatran concentration monitoring were explored. The overarching premise of this thesis was that all anticoagulants will require dose individualisation and monitoring to ensure that the use of anticoagulants are safe and effective. The research questions addressed in this thesis were focused on the challenges that arise when attempting to predict the maintenance dose requirements for warfarin and dabigatran. Each drug presents a slightly different issue in terms of predicting a safe and effective dose. For warfarin, the target INR range has been well established and therefore this research focuses on dosing techniques to achieve the target INR. For dabigatran, a therapeutic range has been proposed but has not been well established. The research conducted in this thesis is an effort to provide dosing guidance if a target therapeutic range exist in the future.

Chapters2 and 3 of this thesis explored the ability of current models to accurately predict the maintenance dose of warfarin. In Chapter 2, the predictive performance of the Bayesian dosing tool was assessed using data from two cohorts of patients. In both data sets, doses were over-predicted in patients requiring ≥7mg/day and the source of bias was not found to be a *VKORC1* genotype effect, nor was the posterior population sufficiently different from the prior population to be the driving force for the bias. In Chapter 3, the analysis was expanded to include a meta-analysis of all published warfarin dosing algorithms. It was found that all dosing algorithms studied, under-predicted the maintenance dose in patients requiring ≥7mg/day. It was proposed that a sufficiently mechanistic systems model is required to accurately and precisely predict the maintenance dose over the entire dose range.

Chapter 4 presented a revised method for assessing the predictive performance of a dosing tool. This was a modification of the method for

measuring predictive performance originally suggested by Sheiner and Beal in 1981 [5]. The motivation for this research can be found in Chapter 2 of this thesis and a previous work not described in this thesis [3] where the predicted doses of warfarin using a Bayesian method were found to be unbiased on average using mean prediction error. This was despite an observable systematic deviation at higher dose levels. A proposal to numerically test the significance of this deviation was described in Chapter 4.

Chapter 5 describes an assay to measure dabigatran and dabigatran acyl glucuronide concentrations in human plasma. The sum of dabigatran and dabigatran acyl glucuronides is expected to have a better correlation with anticoagulation intensity of the patient and thus clinical outcomes. The assay was used to analyse plasma samples that were available from a previous study [109]. The concentration measurements were used in the subsequent chapter. In Chapter 6, the predictive performance of published population pharmacokinetic models for dabigatran were evaluated against the observed plasma concentration data generated in Chapter 5. The goal was to select a prior model that could be used in a fully Bayesian forecasting tool in the future.

7.1.2. This thesis in the context of other works

7.1.2.1. Warfarin dosing

The use of mathematical models to aid in dosing warfarin dates back to early computerised models developed by Nagashima [275] and Sheiner [276] in 1969. Subsequently, several other strategies have been proposed to improve dose predictions.

Warfarin dosing nomograms are commonly used in the clinic to guide dosing during initiation. They are simple to use and provide the basis for standardising between clinical practice. However, as described in the introduction of this thesis, nomograms are usually fairly simple dose adjustment guides, usually assuming a linear relationship between warfarin dose and anticoagulation effect.

In recent years, the research on warfarin dosing has focussed on using individual patient genotype (mainly *CYP2C9* and *VKORC1*) to predict the maintenance dose. Several published genetic algorithms have been developed and published using multilinear regression methods. The systematic review of the literature conducted in Chapter 3 included 22 separate dosing algorithms. These were generally designed to predict warfarin maintenance dose *a priori*, before therapy is initiated. Seven algorithms included the ability to update the dose prediction using a single INR measurement [30, 64, 74, 164, 191]. Several of these algorithms [30, 74] have been found to provide more precise and less biased dose predictions [3].

There is conflicting evidence about whether the use of genetic algorithms for warfarin to predict the maintenance dose would result in improved INR control and patient outcomes (see Pirmohammed *et al* [85] and Kimmel *et al* [84]). From the research conducted in this thesis, it was found that multi-linear regression algorithms cannot accurately predict the maintenance dose for patients requiring higher daily doses. It was proposed in Chapter 3 that models developed that assume a linear relationship between dose and response are too empirical and not sufficiently mechanistic to allow extrapolation into new settings. In addition, these models do not appear to predict doses outside of the linear portion of the dose-response curve (>80% of maximal effect or < 20%). It is contended that a sufficiently mechanistic model, such a warfarin PK model that is tied into a lumped model of the coagulation network [36] is needed to predict the maintenance dose across the entire range of dosing requirements [see Section 7.2.1].

Recently, Xue *et al* [277] developed a warfarin PKPD model. The model accounts for the influence of *CYP2C9, VKORC1* and *CYP4F2* genotype, body size and composition. The pharmacokinetics of warfarin was described by a one-compartment model. A sigmoid E_{max} model was used to describe the inhibition of prothrombin complex activity (a composite of all clotting factors) as a function of S-warfarin concentration to predict INR. The model is based on the theory that

the time to reach a certain concentration of fibrin so that a clot can form will be inversely proportional to the concentration of coagulation factors and consequently to prothrombin complex activity [278]. Therefore, this model has mechanistic flavours. Furthermore, the model was tied into a Bayesian forecaster and can be used to predict the INR or dose. The model has been implemented in a dosing software that is freely available online at https://www.nextdose.org/.

There are several limitations to the research on warfarin dosing conducted in this thesis. The models were evaluated in terms of how well they predict the observed maintenance dose. However, the maintenance dose may not be the only 'ideal' dose. It may be better thought as a point estimate of an 'ideal' dose because there may be a range of maintenance doses that would achieve an INR within the therapeutic range of 2-3 for most patients. Furthermore, the maintenance dose definition varies between individual studies in Chapter 3. The data used in both studies do not account or control for adherence. It is possible that patients who are not compliant or are vitamin-K depleted may have difficulty maintaining a stable INR and require larger maintenance dose.

7.1.2.2. Dabigatran assay

A bioanalytical assay for measuring dabigatran in human plasma was described in Chapter 5 [279]. To date, the research in Chapter 5 is still the only publication that fully describes an assay for dabigatran and dabigatran acyl glucuronides in human plasma. Additionally, the study provided important data on the (in)stability of dabigatran acyl glucuronides which has not been previously reported. Several additional assays for dabigatran have been recently been proposed [226, 280-284] as this remains an active research area. All of the assays measure parent dabigatran and none of the published assays account for the instability of dabigatran acyl glucuronide which has been shown to affect the concentration of dabigatran [279]. Assays that do not account for dabigatran acyl glucuronide will lead to underestimation of the anticoagulant moieties associated with use of dabigatran etexilate. It has been reported that the fraction of glucuronide conjugate can be high (exceeding 50% in individual patients

[101]), which is why it is important to account for the glucuronides when measuring dabigatran concentrations. Hence, an assay that properly determines total concentrations of dabigatran (i.e. dabigatran and dabigatran acyl glucuronide) was developed. The total dabigatran concentrations are expected to have a better correlation with anticoagulation intensity of the patient and thus clinical outcomes. It is expected that a clotting screen (such as the thrombin time or diluted thrombin time) will predict clinical outcomes better than total dabigatran concentrations. However, currently, there are only data correlating clinical outcomes with total dabigatran concentrations, but not clotting times. When one or more coagulation assays are standardised between laboratories for dabigatran (as per warfarin and INR), then clotting times may be used. At present, dabigatran concentrations are the best metric to guide dosing.

A direct quantification of dabigatran acyl glucuronide is potentially better than the indirect method as the assay errors with the indirect method may result in negative dabigatran acyl glucuronide concentrations. However, the major challenge to the development of a direct method is the acquisition of the reference standards for all four isomers of dabigatran acyl glucuronide and controlling the stability of dabigatran acyl glucuronide against hydrolysis and isomerization during sample storage and preparation.

7.1.2.3. Dabigatran population PK models

Chapter 6 explores the ability of pharmacometric models for dabigatran to predict into data from a new population. It may appear as a contradiction to the findings on warfarin dosing conducted in this thesis, where all current models for predicting warfarin doses do not work. In this instance, it is proposed that a model that is tied into a Bayesian framework (such as a *MAP* estimator or a full Bayesian forecasting method) may provide accurate and precise individual parameter estimates and therefore will extrapolate well into a new clinical setting.

In Chapter 6, three published population PK models of dabigatran were evaluated and the model that provided the best prediction of the test data was selected for future work. It is not uncommon for several population pharmacokinetic models to be published for the same drug. There are several reasons for performing repeated population analysis. This includes to quantify a specific source of potential variability (e.g. Liesenfeld *et al* 2013 assessed the influence of haemodialysis [266] on clearance) and to describe the pharmacokinetics in different populations (e.g. Karlsson et al 2009 [285] developed a population PK model of voriconazole in paediatric patients). Duffull and Wright 2016 [260] have discussed the benefit of repeated population analysis and what value it might add. The authors concluded that the PK of the drug is often well characterized within the first few population analysis and that future work on the base and covariate model may not be helpful, however, studies on special population will continue to add value.

For this thesis, a *de novo* population pharmacokinetic model for dabigatran was not developed. The data available was sparsely sampled (see Chapter 6) and a model would have been under-determined. In this case, one way to avoid developing an under-determined model is to collect more concentration data from more patients which will incur cost, consume time, and ethics need to be considered. Therefore, the work conducted in Chapter 6 provide the means to accelerate research towards understanding of the needs for dose individualisation of dabigatran using published models.

McDougall *et al* [273] proposed an alternative approach using a 'hybrid' model. A 'hybrid' model incorporates as much information as possible from all prior models in a biologically plausible manner. Instead of selecting one 'best' model, the authors combined 6 prior models of voriconazole by averaging parameter values across studies. Several parameters could not be averaged due to variability in parameterisation and therefore authors had to handle each case separately. Covariate selection was based on biology and availability of data in a clinical setting as the model was intended for use in the hospital. This technique

of hybridising population models appears to be practical means of incorporating information from multiple population studies and is comparable to a meta-analysis. This technique could be explored in the future.

The main limitation of the research pertaining to dabigatran dosing in this thesis is that there is no consensus of a therapeutic range. If, from the work of Chin *et al* [116] or others, a therapeutic range exists for dabigatran, the development of a Bayesian forecasting method for dabigatran should reduce the probability of overdosing, resulting in bleeding, and the risk of under dosing, leading to potential treatment failures. Secondly, dabigatran etexilate dosage forms that exist in the market currently will limit the ability to individualise dosing. More clinical studies will be needed to warrant the need for availability of different dosage strengths in the future.

7.1.3. Who benefits the most from dose individualisation tools?

Dose individualisation in the clinic is a non-trivial process as it requires research into defining a therapeutic target and methods to achieve the target. Often, there is a paucity of information about improving patient outcomes with dose individualisation strategies.

The main reason for individualising drug doses is that a standard dose will not be effective to all patients or will cause harm to some patients. In this regard, patients who are significantly different in terms of their dosing requirements (i.e. significantly smaller or larger than the average dose in the population) can be understood as those who would benefit the most from the use of tools to aid doing since these may minimise adverse drug reactions and avoid treatment failure. Therefore, methods that can accurately and precisely predict the dose for patients who require significantly smaller or larger than the average dose are likely to be the ones who would benefit the most. If a dosing tool works well at predicting doses for patients who require an average dose but fails to identify patients who require extreme doses, then it can be thought that it is a shortcoming of its application to those who really need the dosing tool. The

findings from Chapter 2 and 3 suggests that all current models for dosing warfarin cannot accurately predict the dose in patients at the upper quartile of the dose requirement, and therefore patients who need warfarin dosing tools the most do not benefit from any of the currently available dosing tools.

7.2. Future work

7.2.1. Future work on the dose individualisation of warfarin

Future work to understand the dose-response relationship specifically in patients requiring higher doses is needed. The cause of bias in dose predictions in higher dose patients is unknown. It was hypothesized empirically based model is not sufficiently flexible to predict the dose. It is known that warfarin affects coagulation factors II, VII, XI, X and co-factors protein C and protein S. Each of these coagulation proteins has different half-lives and therefore the time course of effects on INR are different. It is plausible that the application of a single E_{max} model when used across a large range of dose–response values (as seen in the underlying model in Chapter 2) may not be sufficiently flexible to account for the inherent feedback and feedforward mechanisms of the coagulation network, which may be more apparent in patients requiring larger doses. It is proposed that a fully mechanistic is needed to capture the complex relationship between warfarin, clotting factors and INR. A mechanistic model is where the model is built on known biological and physiological mechanisms in which drives the observed drug effects [286]. Because of that, mechanistic models are usually better at extrapolation and may be able to account for the differences in patients requiring higher doses.

The development of a mechanistic model for warfarin was not done in this thesis, but there has been work that was recently published by our research group towards achieving this goal. Ooi *et al* [287] developed separate models to describe the depletion of carboxylated clotting factor (II, VII, IX, X, protein C and S) concentrations following warfarin initiation. Each individual model was then combined to produce a single joint model. Currently, the model describes the

relationship between warfarin dose and the concentration of all six clotting factors. The link between depletion of clotting factor concentrations to INR has yet to be modelled.

There are two other coumarins used clinically, which are phenprocoumon and acenocoumarol. The genotype influence on the metabolism and sensitivity of phenprocoumon and acenocoumarol is also an active research area. Several multilinear algorithms have been developed to predict the maintenance dose of phenprocoumon [288-290] and acenocoumarol [290-297]. The same technique of evaluating the predictive performance of dosing algorithms as conducted in this thesis can be applied for phenprocoumon and acenocoumarol dosing algorithms. If the same problem exists (i.e. bias at higher doses), this may indicate that there may be issues with the vitamin-K cycle of patients requiring higher doses that have not been explored.

7.2.2. Future work on the approach for testing non-constant deviation associated with the magnitude of the observation

Chapter 4 provides a metric for statistical assessment of non-constant systematic deviation from the line of identity. This is the first such metric and provides significant value in the assessment of prediction equations. Currently, this method must be used in conjunction with the Sheiner and Beal single bin MPE method as described previously in Section 4.6.

The future would warrant a single method that incorporates the Sheiner and Beal single bin MPE metric and the S_∞ metric in one overall metric. The method should also include a single metric that provides the location of the start of the deviation and direction of deviation. Additionally, a method to assess non-monotonic non-constant systematic deviation would be desirable. Furthermore, it would be preferable if the method is automated.

7.2.3. Future work on dose the dose individualisation of dabigatran

The need for an adaptive dosing system must be further established. There is evidence that the current covariate based dosing method would result in treatment failure and adverse drug effect, but further research is needed.

Future research that builds on the work conducted in this thesis includes pharmacometric research to incorporate the selected pharmacokinetic model to be used as a prior and to be applied to the data in a fully Bayesian population analysis. The prior model is then tied into a Bayesian forecaster that can then be used to determine an appropriate dose to achieve the proposed target concentration with a certain level of probability.

Another research route would be to link the dabigatran model to the coagulation network model [36]. The coagulation model can then be used to identify a suitable clotting time assay that is sensitive not only to the concentrations of dabigatran but also the concentrations and sensitivity of clotting factors. This is likely to be a modification of the thrombin time assay which will need to be modelled into an existing coagulation model [36]. The coagulation network model may need to be simplified (i.e. lumped down) in order to estimate the parameters.

There is a need for studies to clarify the contribution of anticoagulation effect of dabigatran acyl glucuronide. To date, very little information has been published about the pharmacodynamics of dabigatran acyl glucuronide. Only two publications [100, 103] that specifically studied aspects of dabigatran acyl glucuronide could be found. Both were conducted by the manufacturer during drug development [100, 103]. Blech *et al* [100] studied dabigatran metabolism and Ebner *et al* [103] studied the formation, *in vitro* stability and pharmacological activity of dabigatran acyl glucuronide. Ebner *et al* [103] reported equal pharmacological activity of dabigatran acyl glucuronide to the parent dabigatran, however these were measured using clotting activity assay (aPTT) and not receptor binding assays. There has not been any report on the inhibitory constant (k_i) values for dabigatran acyl glucuronides. If the k_i of the individual isomers of dabigatran acyl glucuronide have different k_i values, or dabigatran acyl glucuronide and unconjugated dabigatran k_i values are different, then measuring total concentrations of

dabigatran as done here and in other studies will not be appropriate and each acyl glucuronide isomer and unconjugated dabigatran should be treated as separate species.

There is an urgent need of a specially designed study to define the target concentration for dabigatran. Serial measurements of dabigatran concentrations leading up to adverse events (stroke or bleed) or at least at the time of adverse event would be helpful to define the therapeutic range.

A longitudinal study where concentrations of dabigatran are measured after several months of therapy will be useful to understand the inter-occasion variability. This has been explored in a small study [298], but larger studies or in a different clinical setting is needed. Furthermore, if new plasma samples are collected, measurements of dabigatran and dabigatran acyl glucuronide can be obtained and a parent-metabolite model can be developed. This can help improve the understanding of the pharmacokinetics of all active entities of dabigatran. If dabigatran acyl glucuronides were eliminated by biliary excretion and not renally, as reported by the manufacturer [104, 252], understanding the pharmacokinetics of the glucuronide may be useful in events such as biliary obstructions where the model can be used to predict increased glucuronide concentrations that may potentially increase the risk of bleeding.

7.3. Conclusions

This thesis has identified the limitations of current warfarin dosing methods and have explored dabigatran concentration monitoring as a means of improving dose individualisation. It was found that all current warfarin dose prediction models poorly predict the maintenance dose for patients requiring higher than average daily doses. Neither methods based on Bayesian forecasting nor methods based on multi-linear regression were found to be able to accurately predict the maintenance dose of these patients. While the reason for the poor prediction remains unknown, it was hypothesised that all current models to predict warfarin dose were conceivably too empirical, and therefore inadequate to capture the complexity of the coagulation network in patients requiring higher

than average maintenance dose. It was proposed that a mechanistic model is needed to accurately predict warfarin doses in the future.

Studies on the evaluation of the predictive performance of warfarin dosing tools identified a specific problem where the common metric used to measure predictive performance may not capture. This is where deviations from the line of identity are associated with the magnitude of observation. An approach to analyse such data was proposed and the method can easily be implemented into any statistical software.

An assay for quantifying dabigatran and dabigatran acyl glucuronide in human plasma has been developed. It was found that the metabolite of dabigatran, dabigatran acyl glucuronide, was highly unstable and prolonged storage and improper handling of plasma samples will affect the accuracy of dabigatran concentrations as the dabigatran acyl glucuronides back-convert to form dabigatran. Given that the glucuronide is thought to have a similar anticoagulation activity to dabigatran, the sum of dabigatran and dabigatran acyl glucuronide should be measured to inform clinical decisions.

The predictive performance of published population pharmacokinetic models of dabigatran was evaluated. A population pharmacokinetic model for dabigatran which adequately quantified the variability in the magnitude and time course of concentration in an external data set was identified. The selected pharmacokinetic model can provide a means of predicting the dose of dabigatran required to achieve the target concentration range and therefore provides a scientific basis of individualising the dose of dabigatran in the future.

PART VI

APPENDICES

Appendix 1: Appendices to Preface

A1.1 Author contributions of International peer-reviewed journal described in Chapter 2

Saffian SM, Duffull SB, Roberts RL, Tait RC, Black L, Lund KA, Thomson AH, Wright DF. Influence of Genotype on Warfarin Maintenance Dose Predictions Produced Using a Bayesian Dose Individualization Tool. Therapeutic drug monitoring 2016; 38: 677-83.

Initials	Wrote the manuscript	Revised the manuscript	Designed the research	Performed the analysis	Collected the data
SMS	✓	✓	✓	✓	
SBD	✓	✓	✓		
RLR		✓			
RCT		✓			✓
LB		✓			✓
KAL		✓			✓
AHT		✓			✓
DFBW	✓	✓	✓		✓

A1.2 Author contributions of international peer-reviewed journal described in Chapter 3

Saffian SM, Duffull SB, Wright DFB. Warfarin Dosing Algorithms Under-predict Dose Requirements in Patients Requiring ≥7 mg Daily: A Systematic Review and Meta-analysis. Clinical Pharmacology & Therapeutics 2017; 102: 297-304

Initials	Wrote the manuscript	Revised the manuscript	Designed the research	Performed the analysis	Collected the data
SMS	✓	✓	✓	✓	✓
SBD	✓	✓	✓		
DFBW	✓	✓	✓		

A1.3 Author contributions of international peer-reviewed journal described in Chapter 5

Saffian SM, Zhang M, Leong Chin PK, Jensen BP. Quantification of dabigatran and indirect quantification of dabigatran acyl glucuronides in human plasma by LC-MS/MS. Bioanalysis 2015; 7: 957-66.

Initials	Wrote the manuscript	Revised the manuscript	Designed the research	Analysed the samples	Collected the data
SMS	✓	✓	✓	✓	
MZ		✓	✓		
PKCL	✓	✓	✓		✓
BPJ	✓	✓	✓		

Appendix 2: Appendices to Chapter 3

A 2.1 *MATLAB® code for estimating proportion and 95% CI of a binomial test*

Estimating number of success (p) and number of trials (n) that was output by MedCalc

Run_file

```
%% Finding n and p that would give the exact proportion and CI as
calculated by MedCalc software
% Shamin warfarin_meta-analysis March 2016
clc
clear all

theta= [10 10]; % initial estimates for p and n

[theta, fval] = fminsearch(@pkfun, theta)% the search function

p = theta (1) % returns the estimated number of success (p)
n = theta (1) + abs (theta (2)) % returns the estimated sample size (n)

phat = p/n; % to calculate the 'calculated' proportion
LCI_hat= betaincinv(0.025, p,n-p+1); % to calculate the 'calculated' lower
CI
UCI_hat= betaincinv(0.975, p+1,n-p); % to calculate the 'calculated' upper
CI
```

pkfun_file

```
function objv=pkfun(theta)

prop = _____; % enter the proportion (p/n)
LCI  = _____; % enter the lower CI calculated by MedCalc
UCI  = _____; % enter the upper CI calculated by MedCalc

p_hat= abs(theta(1)); % estimated success
n_hat= abs(theta(2))+p_hat; % estimated trials

obj1 = p_hat/n_hat - prop; % estimate the proportion
obj2 = betaincinv(0.025,p_hat,n_hat - p_hat+1) - LCI; % estimate the lower
CI
obj3 = betaincinv(0.975,p_hat+1,n_hat - p_hat)- UCI; % estimate the upper
CI

objv= obj1^2 + obj2^2 + obj3^2; % minimize the sum of squares
```

A 2.2 Scatter plots of the studies included in the meta-analysis

Table A2.1 are studies and figures from which the data were extracted. Unless specified as per requirement of the copyright holder, all the figures included in Table A2.1 were reproduced with the permission from the copyright holder. All scatter plots were included except for evaluation by Wadelius et al [190] due to an inability to obtain permission to reproduce the figure from the publisher.

Note that in the text of the chapter, the analysis was indexed according to each unique algorithm. Here, the figure is arranged according the published study from which the data was extracted from.

Table A2.1 *Scatter plots of the studies included in the meta-analysis*

Description	Scatter plot
Study: Kimmel 2013 [84] Algorithms evaluated: Clinical and genotype driven algorithms by Gage 2008 [24] and Lenzini 2010 [30].	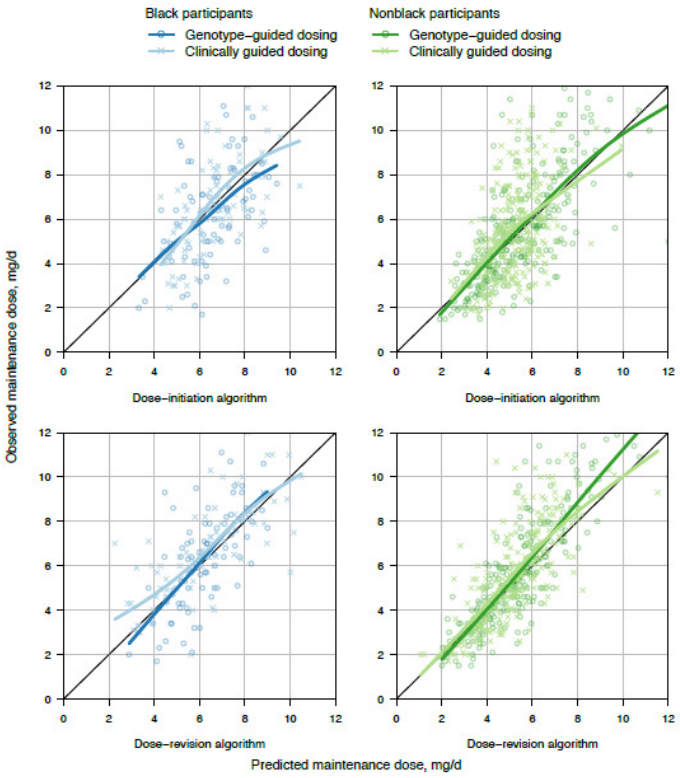 *Reproduced from Kimmel et al 2013, with permission from Copyright Massachusetts Medical Society*
Study: Langley 2009 [196] Algorithms evaluated: Gage 2008 [24], Wu 2008 [193], Zhu 2007 [178] and Sconce 2005 [143]	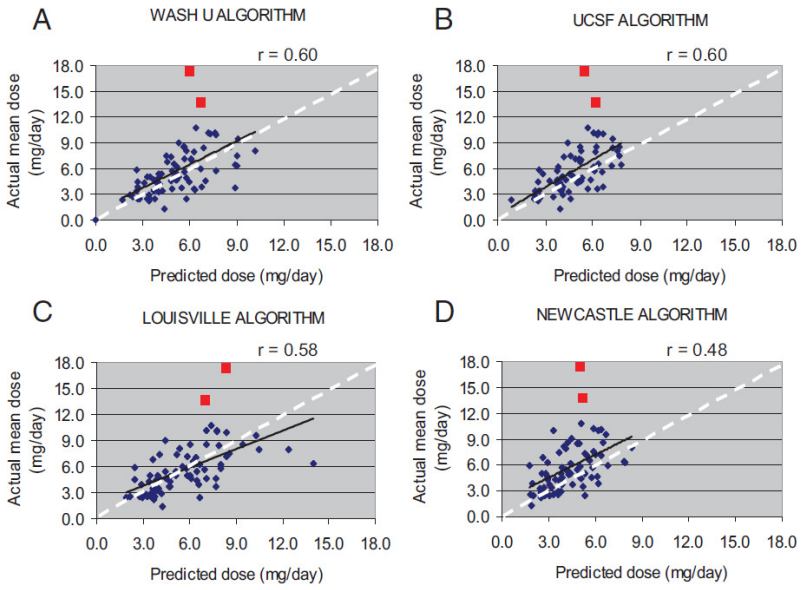

Study: Francis 2014 [194]

Algorithms evaluated:

Solomon 2004 [191]

Le Gal 2010 [164]

Anderson 2007 [145]

Zhu 2007 [178]

Sconce 2005 [143]

Wadelius 2009 [190]

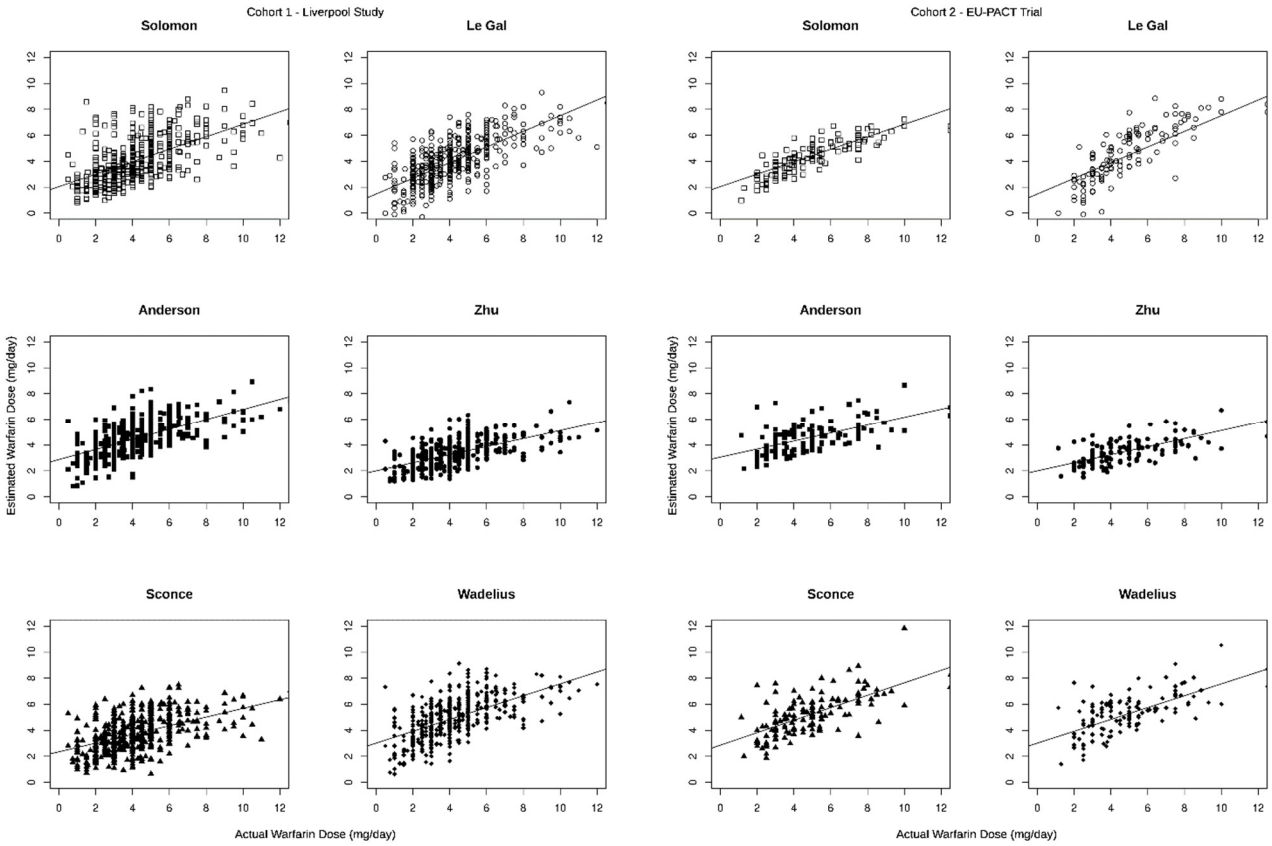

Reproduced with permission from (Francis et al 2014), PLoS ONE 9(12): e114896. doi: 10.1371/journal.pone.0114896

Study: Santos 2015 [40]

Algorithms evaluated:

Santos 2015 [40], Klein 2009 [6], Botton 2011 [36] and Perini 2008 [39]

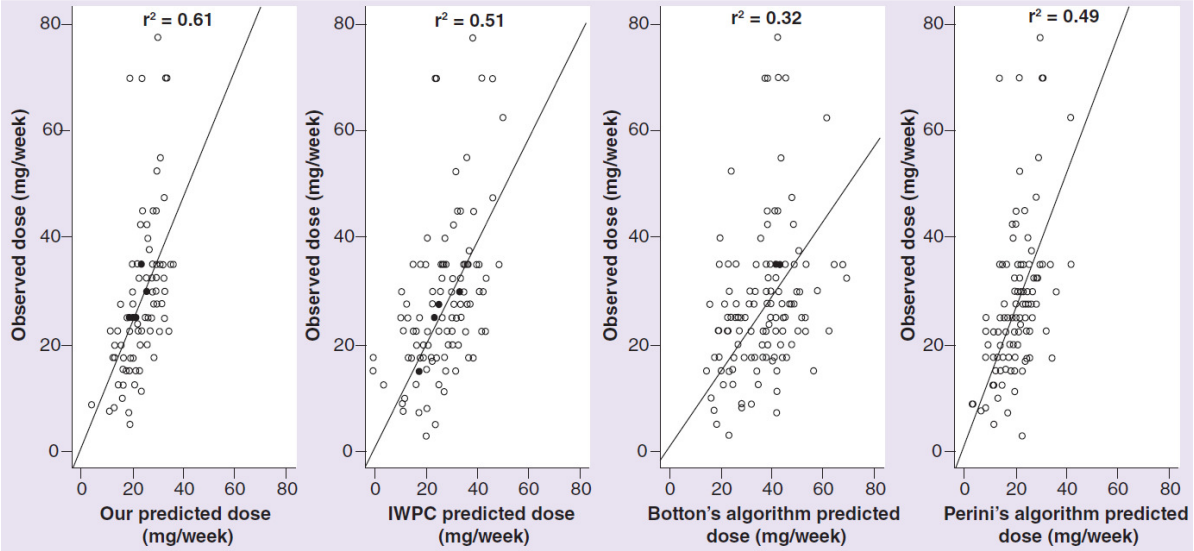

Study: Saffian 2015 [3]

Algorithms evaluated:

Clinical and genotype driven algorithms by Gage 2008 [24], Klein 2009 [69], Lenzini 2010 [30] and Horne 2012 [74]

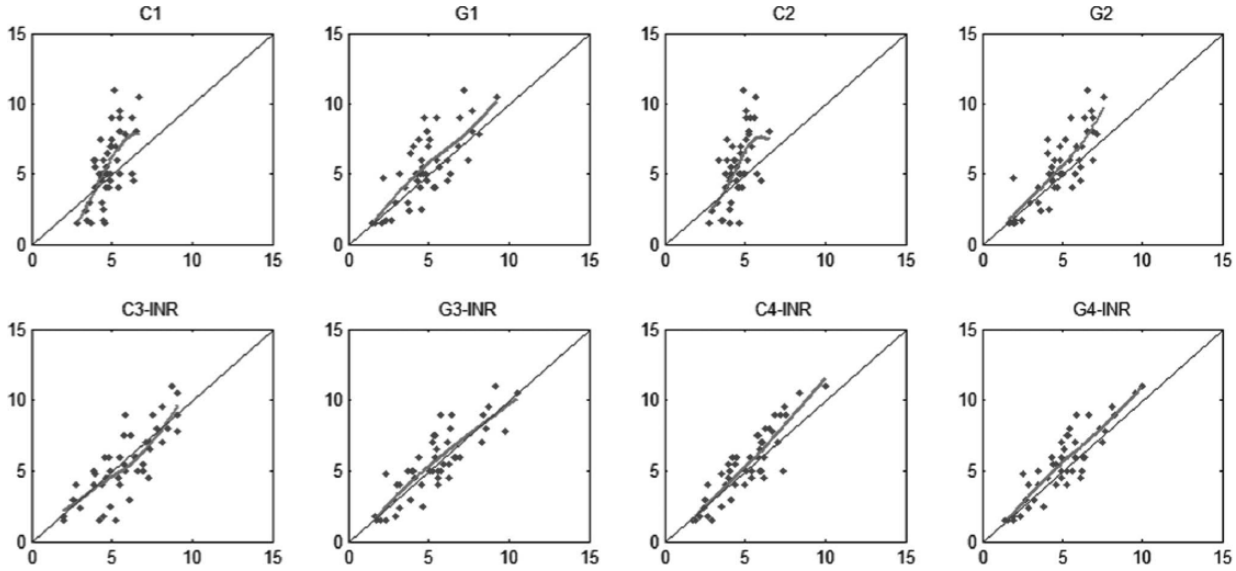

Study: Ramos 2012 [64]

Algorithms evaluated:

Ramos 2012 [64], Lenzini 2010 [30] and Klein 2009 [68]

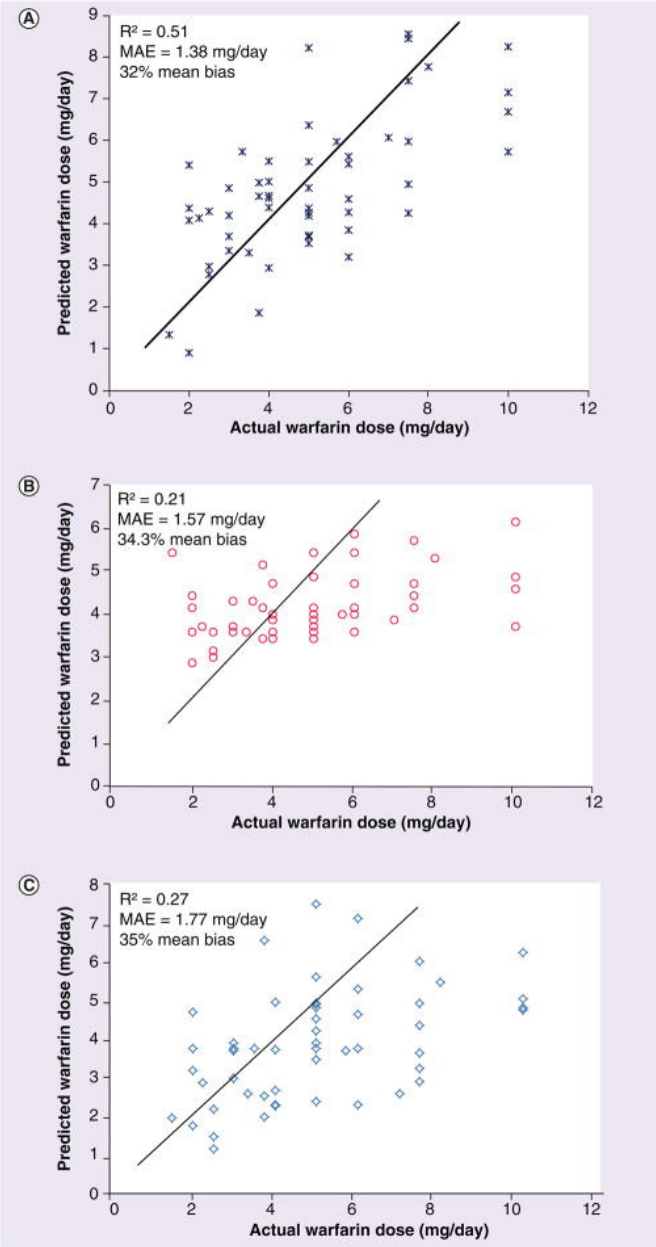

Study: Pavani 2012 [167]

Algorithm evaluated:

Pavani 2012 [167]

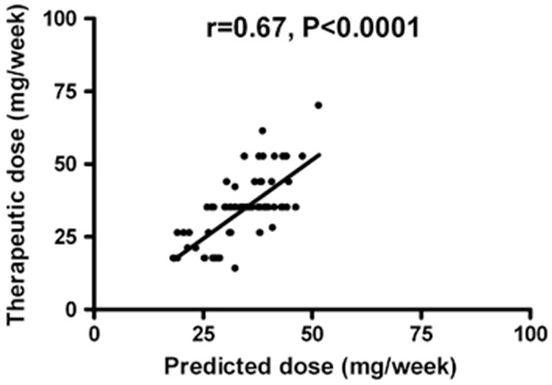

Study: Klein 2009 [68]

Algorithm evaluated:

Klein 2009 [68]

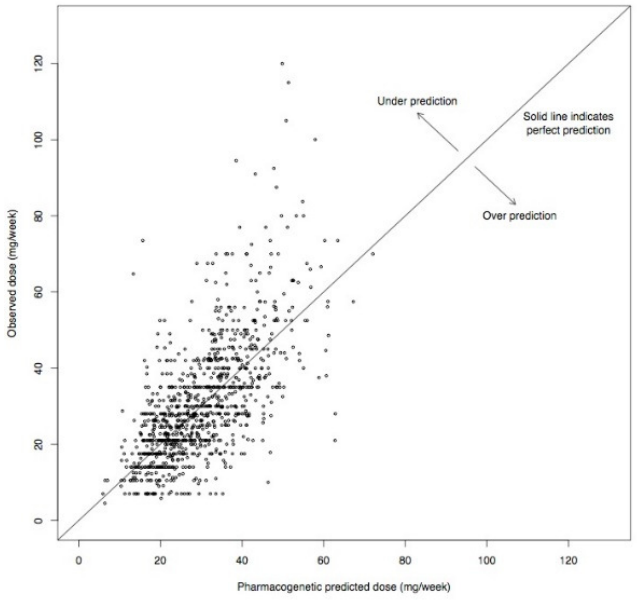

Reproduced with permission from (Klein et al 2009), Copyright Massachusetts Medical Society

Study: Gage 2008 [24]

Algorithm evaluated:

Gage 2008 [24]

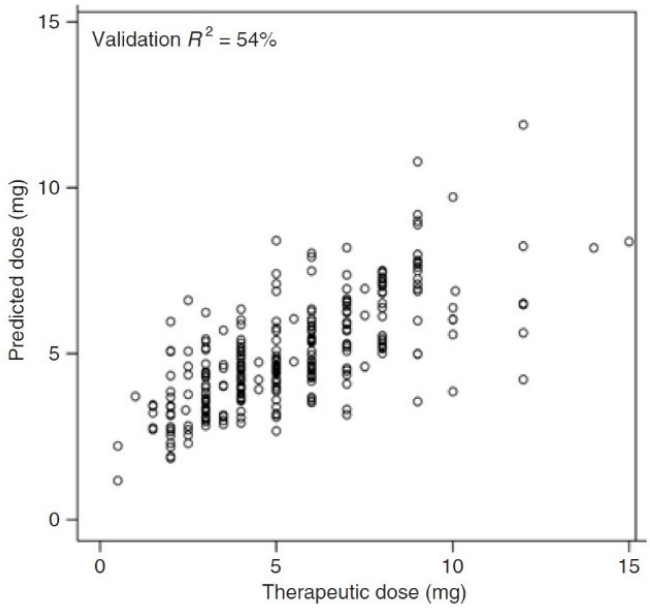

Study: Linder 2009 [197]

Algorithm evaluated:

Zhu 2007 [178]

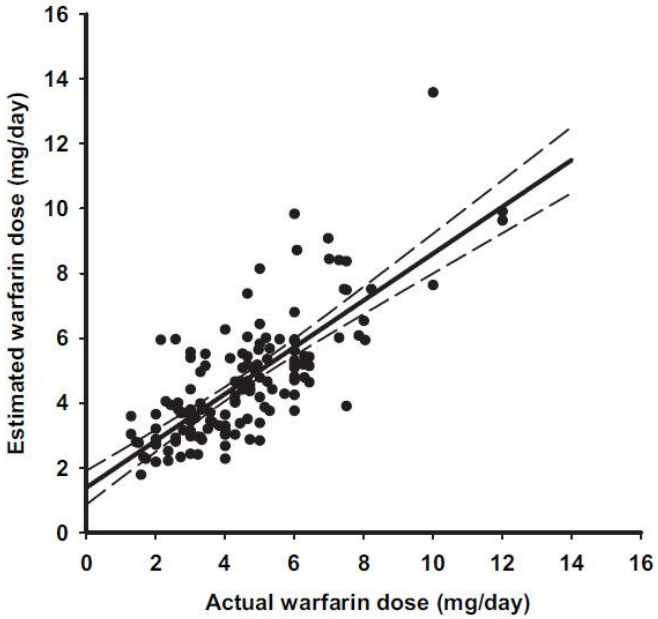

Study: Shaw 2010 [199]

Algorithm evaluated:

Gage 2008 [24]

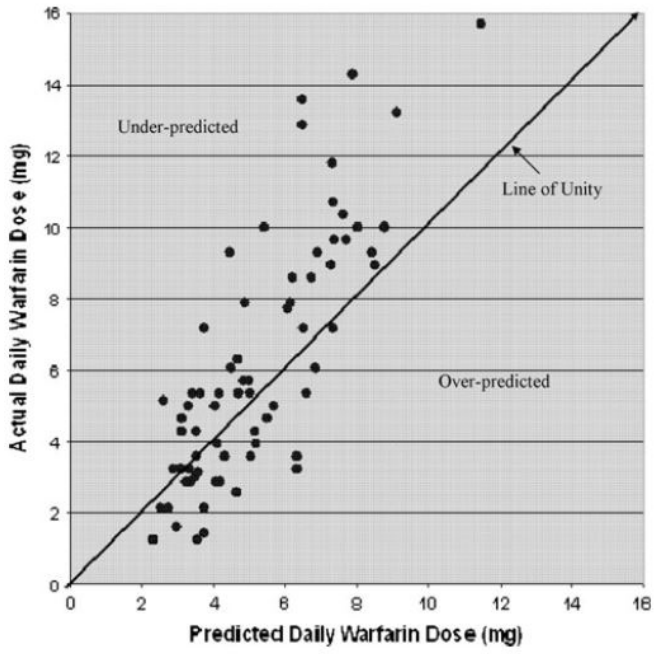

Study: Roper 2010 [169]

Algorithm evaluated:

Anderson 2007 [145]

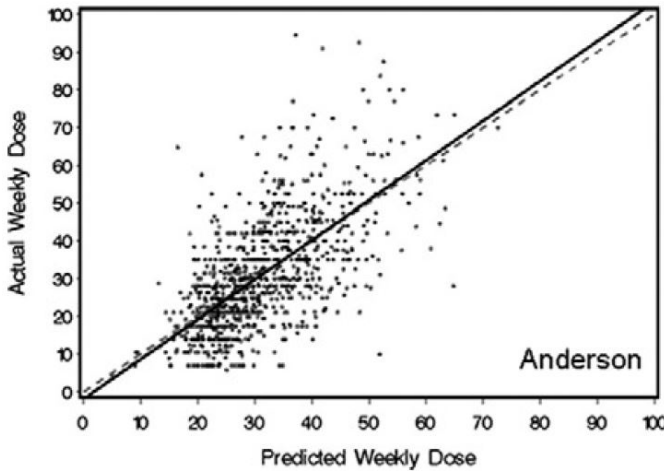

Study: Lenzini 2007 [31]

Algorithm evaluated:

Lenzini 2007 [31]

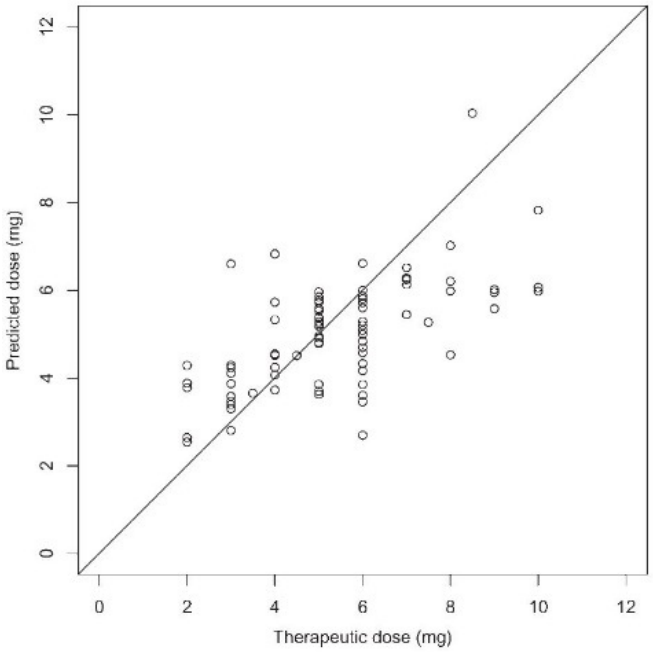

Study: Pathare 2012 [192]

Algorithm evaluated:

Klein 2009 [68] and

Pathare 2012 [192]

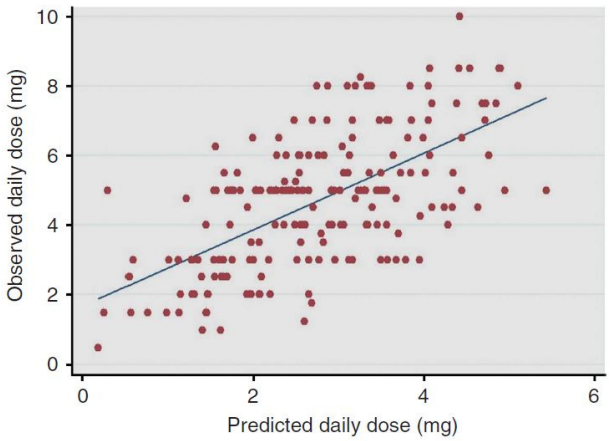

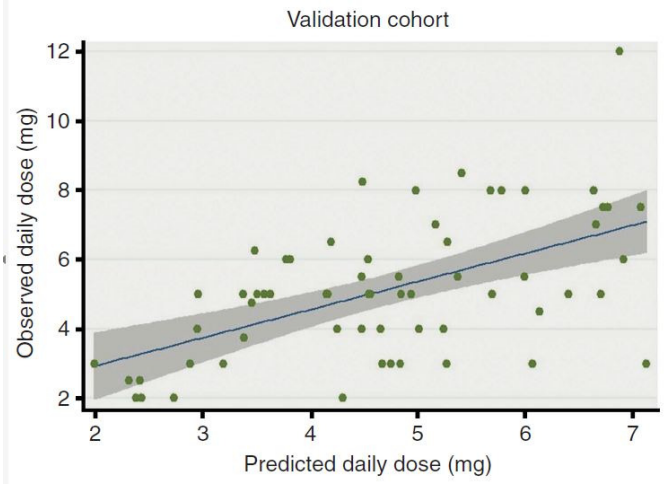

Study: Sconce 2005 [143]

Algorithm evaluated:

Hatch 2008 [195]

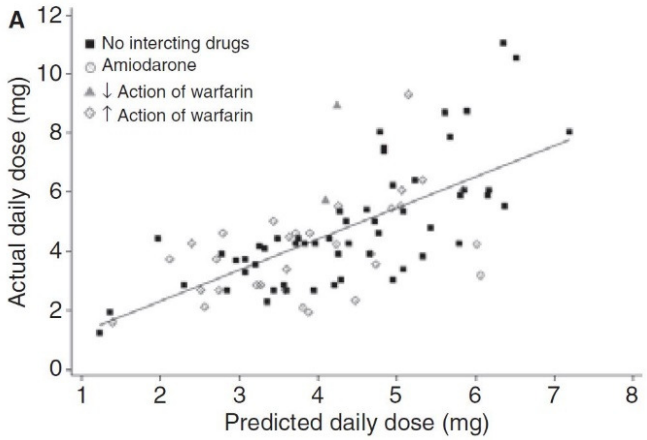

Study: Pavani 2014 [299]

Algorithm evaluated:

Klein 2009 [68]

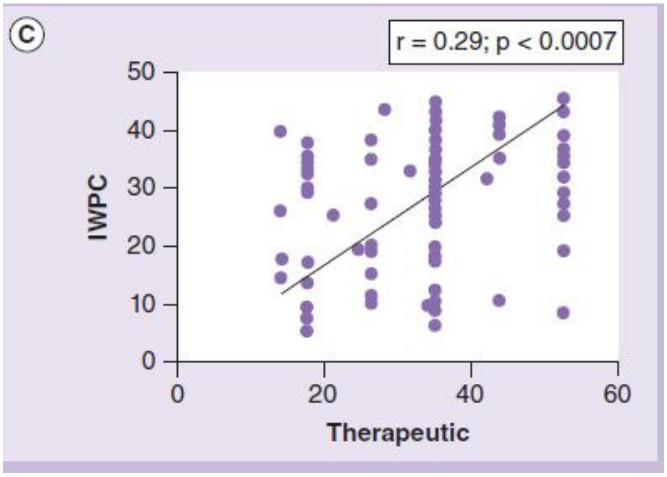

A 2.3 *Replication and evaluation of the extracted warfarin data from a sample of 5 scatter plots*

The accuracy of data extraction was evaluated by replicating the data extraction for 5 scatterplots (approximately a 10% sample) which by another researcher who was not part of the study (Table A2.2). The relative difference between the original and replicated data extraction were compared. A relative difference of less than 10% and was considered acceptable.

Table A2.2 *Replication and evaluation of the extracted scatter plot of warfarin data*

Scatterplot, figure from which the data was extracted in the published article	**Original data extraction**		**Replicated data extraction**	
	Proportion of under-predicted doses	**Average prediction error (mg/day)**	**Proportion of under-predicted doses**	**Average prediction error (mg/day)**
Klein 2009, S8 [68]	0.94	-2.55	0.94	-2.53
Roper 2010, 3C [169]	0.98	-2.56	0.93	-2.46
Gage 2008 [24] in Corrigendum [198]	0.97	-2.16	0.95	-2.20
Francis 2011, 1F [194]	0.93	-2.07	0.93	-2.05
Francis 2011, 1D [194]	1	-4.22	1	-3.97

Appendix 3: Appendices to Chapter 4

A3.1 MATLAB® code to test for systematic deviation from the line of identity

```
% Code for analysing systematic deviation from the line of identity
% Shamin Saffian
% last updated 22/02/2017
clear; clc; clear all; close all;

%% Create data
n=50; % observations
rng (63)

%% Simulate scenario
Scenario_A % no bias
% Scenario_B % non-systematic +ve bias
% Scenario_C % off set, and systematic bias
% Scenario_D % systematic deviation at the top (motivating example)
% Scenario_E % systematic deviation at the bottom
% Scenario_F % +ve bias systematic deviation at the top
% Scenario_G % non-monotonic bias
% Scenario_1a % no bias
% Scenario_1b % systematic bias
%% defining bin edges

topEdge = max(x)+0.0001; % define top edge limits (a small value is
added...
                         % so that values that lie exactly on the bin
Edges are included)
botEdge = min(x); % define bottom edge limits

nbins = 2; % start with 2 bins
tnbins =10; % total number of bins

%% Single bin MPE
PE = x-y; % prediction error
MPE = sum(PE)/n % mean prediction error
se= (std(PE))/(sqrt(length(PE))); % std error of each bin
quantile = se * 1.96; % for 95% confidence interval
Up_Lim95CI=MPE+quantile % Upper limit
LowLim95CI=MPE-quantile % lower limit

%% Infinite bin MPE approach

% Step 1 and 2 - Create n number of bins and calculate MPE in each bin
for j = 1:(tnbins-1)% we start with 2 bins, so tnbins-1
    binEdges = linspace(botEdge, topEdge, nbins+1); % defined the bin
edges - linearly spaced vector
    [h,whichBin] = histc(x, binEdges); % this sorts x-values according
to the bin

   for i = 1:nbins
    flagBinMembers = (whichBin == i);% flagging bin members
    binMembers     = PE(flagBinMembers);% calculate the PE in each bin
    binMean(i)     = mean(binMembers);% gives MPE of each bin (Step 2)
   end

MPE_bin=binMean';  % MPE of each bin
bin_number=(1:nbins)';% bin numbers
```

```
%% Step 3 regress MPE by bins

X = [ones(size(bin_number)) bin_number];
beta = regress (MPE_bin,X); % regress MPE vs bins

figure(3)
hold on
plot(bin_number,MPE_bin,'o');lsline % regression line
set(gca,'xtick',0:1:tnbins); xlim([1,tnbins]);ylim([-1 1]);
xlabel('bin number'); ylabel('mean prediction
error');%saveas(gcf,'Fig3.jpg')
%% Step 4 - increment n and repeat the loop (Step 1 - 3)
nbins = nbins + 1; % increment n until it reaches tnbins

slope(j)=beta(end);% keeping the slopes as a vector (for Step 5)
end
hold off

figure(2)% plot data with bin edges
    hold on
    plot (x,y,'k.','markersize',10);% Plotting x y
    set(gca,'fontsize',12)
    line([0,16],[0,16]);
    ylabel('Observed data','fontsize',15); xlabel('Predicted
data','fontsize',12)
    xlim([0 15]);ylim([0 15])
for x_edge = binEdges % putting lines on the binEdges
        plot([x_edge,x_edge],[0,16],'r');
end
hold off

%% Step 5 - regress slope vs bins

bins=(2:tnbins)'; % bins
slope= slope';% slope

% K is the rate constant which is equal to the reciprocal to the x
axis units

myfittype = fittype('s_inf+(s_init+s_inf)*exp(-
theta*bins)','dependent',{'slope'},'independent',{'bins'},'coefficient
s',...
    {'theta','s_inf','s_init'});% defining model, dependent,
independent variables, and parameters
myfit2 = fit(bins,abs(slope),myfittype)

%% Plotting
figure(4)%plot for slope vs bins
plot(myfit2,bins,abs(slope),'o')
xlabel('number of bins'); ylabel('slope');ylim([-1.5 1.5]);
set(gca,'xtick',0:1:tnbins);%saveas(gcf,'Fig4.jpg')
```

Scenario_A

```
noise = randn(n,1); % artificial noise
x = 0.5+rand(n,1) *14; % random numbers
y = x+0.5*noise; % Data with noise
y2= x; % Data without noise
```

Scenario_B

```
noise = randn(n,1); % artificial noise
x = 0.5+rand(n,1) *14; % random numbers
y = x+0.5*noise-2; % Data with noise
y2= x-2; % Data without noise
```

Scenario_C

```
noise = randn(n,1); % artificial noise
x = 1+rand(n,1) *14; % random numbers
y = 0.8*x+noise*0.5+1.5; % Data with noise
y2= 0.8*x+1.5; % Data without noise
```

Scenario_D

```
noise = randn(n,1); % artificial noise
x = 2+rand(n,1). *12; % random numbers
y = 1.25*x-0.5*exp(x). ^0.175+0.5*noise+0.25; % Data with noise
y2= 1.25*x-0.5*exp(x). ^0.175+0.25; % Data without noise
```

Scenario_E

```
noise = randn(n,1); % artificial noise
x = 1+rand(n,1) *13; % random numbers
y = x-log10(x)+0.5*noise+0.9; % Data with noise
y2= x-log10(x)+0.9; % Data without noise
```

Scenario_F

```
noise = randn(n,1); % artificial noise
x = 2+rand(n,1). *12; % random numbers
y = 1.25*x-0.5*exp(x). ^0.175+0.5*noise-0.75; % Data with noise
y2= 1.25*x-0.5*exp(x). ^0.175-0.75; % Data without noise
```

Scenario_G

```
noise = randn(n,1); % artificial noise
x = 1+rand(n,1). *11; % random numbers
y = exp(x*0.25). ^0.75+0.35*x+0.5*noise+0.25; % Data with noise
y2= exp(x*0.25). ^0.75+0.35*x+0.25; % Data without noise
```

Plot_data

```
%% code to plot data
figure(2)
% subplot(2,3,1)
plot(x,y,'s','Color','r')
ylim([0,15]);xlim([0,15]);xlabel('Predicted data'); ylabel('Observed
data')
line([0,15],[0,15]);
saveas(gcf,'Fig2A.jpg')

figure(1)
% subplot(2,3,4)
plot(x,y2,'s','Color','r')
ylim([0,15]);xlim([0,15]);xlabel('Predicted data'); ylabel('Observed
data')
line([0,15],[0,15]);saveas(gcf,'Fig1A.jpg')
```

A3.2 Workings for Scenario A

No systematic deviation of predicted from observed data

Data

x	y
9.89	9.97
8.97	8.92
6.17	5.87
8.03	8.09
14.05	13.35
1.27	1.27
13.27	12.78
12.36	12.45
13.84	13.96
0.54	0.27
13.35	13.05
12.03	11.96
8.22	8.90
10.82	11.11
13.61	14.59
4.00	3.95
14.24	14.40
8.31	8.49
7.32	8.29
8.91	9.52
8.94	9.56
9.00	9.17
14.07	13.58
9.18	10.04
5.30	4.71
3.10	3.54
12.78	12.91
11.70	11.94
2.75	4.14
10.86	10.81
10.83	10.75
1.95	1.93
2.65	2.27
0.77	0.81
7.26	7.02
9.02	8.45
10.14	10.29
1.83	1.23
13.35	13.26
0.79	1.04
8.21	7.68
4.91	4.68
6.75	6.26
8.22	8.43
13.92	14.36
1.38	0.28
2.26	3.18
6.48	6.83
2.29	2.41
3.84	4.07

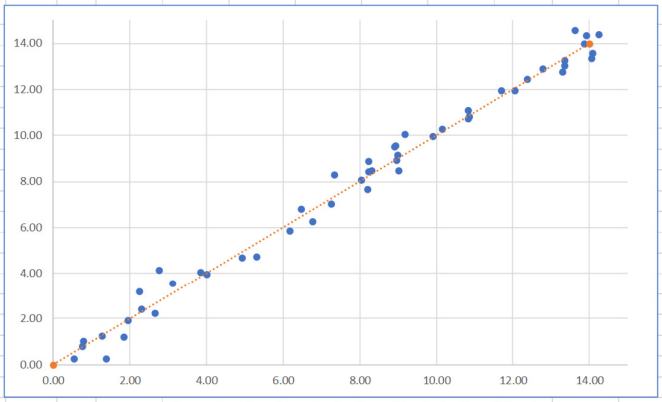

Figure A4.1 Plot of Y vs X. The dotted line is the line of identity

Mean Prediction Error (MPE) vs bins

Number of bins

MPE in bin number	2	3	4	5	6	7	8	9	10	Single bin
1	-0.02	-0.05	-0.08	-0.07	-0.03	0.07	0.24	0.24	0.28	S&B (MPE [95% CI])
2	-0.09	-0.11	0.08	0.16	-0.10	-0.32	-0.45	-0.50	-0.41	-0.06 [-0.2, 0.07]
3		-0.02	-0.19	-0.09	0.05	0.38	0.29	0.02	-0.09	
4			-0.01	-0.19	-0.21	-0.13	-0.05	0.18	0.41	
5				0.00	-0.10	-0.24	-0.14	-0.07	-0.05	
6					0.02	-0.06	-0.37	-0.22	-0.12	
7						0.01	-0.07	-0.08	-0.25	
8							0.02	-0.09	-0.08	
9								0.02	-0.10	
10									0.04	

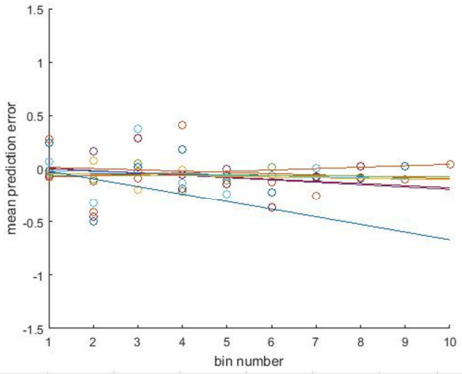

Figure A4.2 Linear regression of MPE vs bin number

Slope vs Number of bins

number of bins	Slope
2	-0.07
3	0.01
4	-0.01
5	-0.02
6	0.00
7	-0.01
8	-0.02
9	0.00
10	-0.01

Parameters of the fitted equation

θ = 5.7 (-2.753e+05, 2.753e+05)

S_∞ = -0.01485 (-0.04043, 0.01074)

S_0 = -7.022 (-3.874e+06, 3.874e+06)

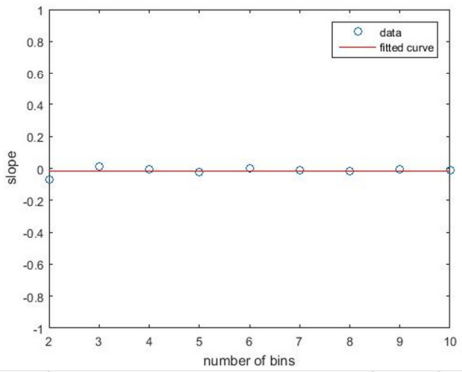

Figure A4.3 Regression of slope vs number of bins

A 3.3 Workings for Scenario B

Constant positive deviation of predicted from observed

Data

x	y
9.89	7.97
8.97	6.92
6.17	3.87
8.03	6.09
14.05	11.35
1.27	-0.73
13.27	10.78
12.36	10.45
13.84	11.96
0.54	-1.73
13.35	11.05
12.03	9.96
8.22	6.90
10.82	9.11
13.61	12.59
4.00	1.95
14.24	12.40
8.31	6.49
7.32	6.29
8.91	7.52
8.94	7.56
9.00	7.17
14.07	11.58
9.18	8.04
5.30	2.71
3.10	1.54
12.78	10.91
11.70	9.94
2.75	2.14
10.86	8.81
10.83	8.75
1.95	-0.07
2.65	0.27
0.77	-1.19
7.26	5.02
9.02	6.45
10.14	8.29
1.83	-0.77
13.35	11.26
0.79	-0.96
8.21	5.68
4.91	2.68
6.75	4.26
8.22	6.43
13.92	12.36
1.38	-1.72
2.26	1.18
6.48	4.83
2.29	0.41
3.84	2.07

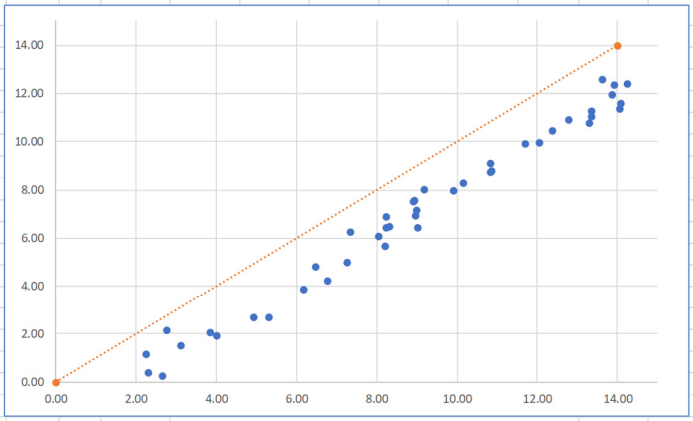

Figure A4.4 Plot of Y vs X. The dotted line is the line of identity

Mean Prediction Error (MPE) vs bins

Number of bins

MPE in bin number	2	3	4	5	6	7	8	9	10	Single bin
1	2.0	2.0	1.9	1.9	2.0	2.1	2.2	2.2	2.3	S&B (MPE [95% CI])
2	1.9	1.9	2.1	2.2	1.9	1.7	1.5	1.5	1.6	1.94 [1.80,2.07]
3		2.0	1.8	1.9	2.1	2.4	2.3	2.0	1.9	
4			2.0	1.8	1.8	1.9	1.9	2.2	2.4	
5				2.0	1.9	1.8	1.9	1.9	1.9	
6					2.0	1.9	1.6	1.8	1.9	
7						2.0	1.9	1.9	1.7	
8							2.0	1.9	1.9	
9								2.0	1.9	
10									2.0	

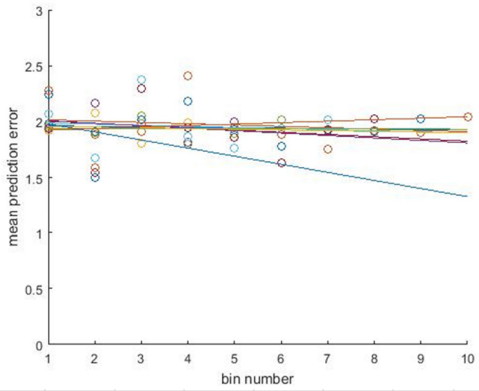

Figure A4.5 Linear regression of MPE vs bin number

Slope vs Number of bins

number of bins	Slope
2	-0.07
3	0.01
4	-0.01
5	-0.02
6	0.00
7	-0.01
8	-0.02
9	0.00
10	-0.01

Parameters of the fitted equation

θ = 5.7 (-2.748e+05, 2.748e+05)
S_∞ = -0.015 (-0.04, 0.01)
S_0 = -7.02 (-3.874e+06, 3.874e+06)

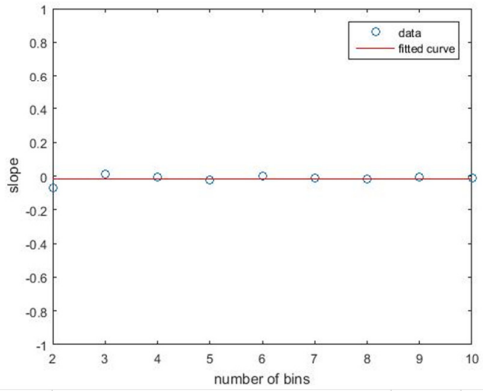

Figure A4.6 Regression of slope vs number of bins

A 3.4 Workings for Scenario C

Proportional deviation of residuals (i.e. the value of the deviation of the residuals is proportional to the magnitude of the observations)

Data

x	y
10.4	9.9
9.5	9.0
6.7	6.5
8.5	8.4
14.5	12.4
1.8	2.9
13.8	12.0
12.9	11.9
14.3	13.1
1.0	2.1
13.8	12.3
12.5	11.5
8.7	9.2
11.3	10.8
14.1	13.8
4.5	5.0
14.7	13.5
8.8	8.7
7.8	8.7
9.4	9.6
9.4	9.7
9.5	9.3
14.6	12.7
9.7	10.1
5.8	5.5
3.6	4.8
13.3	12.3
12.2	11.5
3.3	5.5
11.4	10.5
11.3	10.5
2.5	3.4
3.2	3.6
1.3	2.6
7.8	7.5
9.5	8.6
10.6	10.2
2.3	2.8
13.8	12.5
1.3	2.8
8.7	7.9
5.4	5.6
7.3	6.8
8.7	8.7
14.4	13.5
1.9	1.9
2.8	4.6
7.0	7.4
2.8	3.9
4.3	5.2

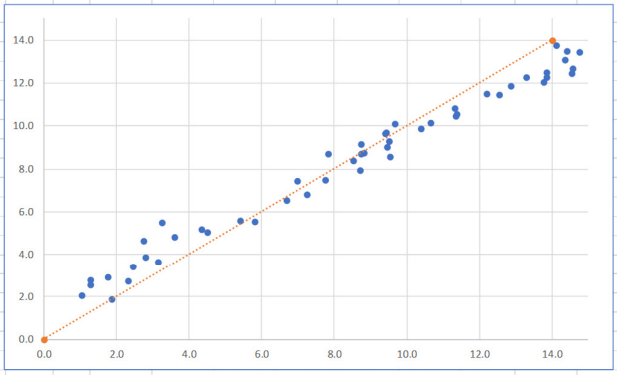

Figure A4.7 Plot of Y vs X. The dotted line is the line of identity

Mean Prediction Error (MPE) vs bins

Number of bins

MPE in bin number	2	3	4	5	6	7	8	9	10	Single bin
1	-0.72	-0.99	-1.09	-1.11	-1.10	-1.04	-0.92	-0.92	-0.90	S&B (MPE [95% CI])
2	0.72	0.07	-0.12	-0.33	-0.70	-1.07	-1.29	-1.38	-1.31	0.11 [-0.16,0.39]
3		1.08	0.18	0.01	-0.04	0.07	-0.16	-0.53	-0.70	
4			1.15	0.35	0.12	0.00	-0.10	-0.02	0.03	
5				1.25	0.64	0.21	0.18	0.00	-0.10	
6					1.30	0.79	0.18	0.12	0.12	
7						1.32	0.82	0.62	0.18	
8							1.35	0.92	0.66	
9								1.35	0.95	
10									1.39	

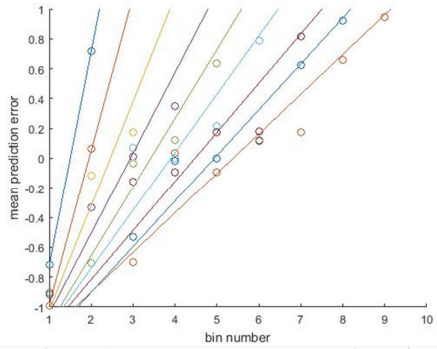

Figure A4.8Linear regression of MPE vs bin number

Slope vs Number of bins

number of bins	Slope
2	1.43
3	1.04
4	0.70
5	0.54
6	0.46
7	0.39
8	0.33
9	0.31
10	0.27

Parameters of the fitted equation

θ = 0.45 (0.39, 0.51)
S_∞ = 0.25 (0.21, 0.30)
S_0 = 2.70 (2.37, 3.02)

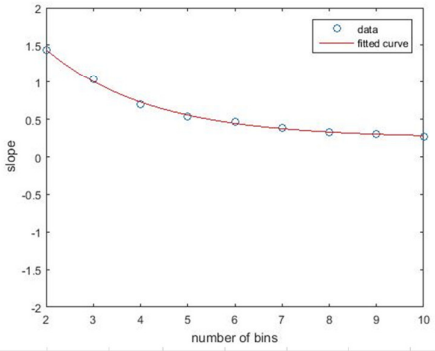

Figure A4.9 Regression of slope vs number of bins

A 3.5 Workings for Scenario D

Nonlinear deviation of residuals associated with the magnitude of the observed data

Data

x	y
10.1	10.0
9.3	9.3
6.9	6.9
8.5	8.7
13.6	11.1
2.7	2.8
12.9	11.1
12.2	11.3
13.4	11.9
2.0	1.8
13.0	11.3
11.9	11.0
8.6	9.4
10.8	10.8
13.2	12.7
5.0	5.2
13.8	12.1
8.7	9.0
7.8	9.0
9.2	9.9
9.2	9.9
9.3	9.5
13.6	11.4
9.4	10.3
6.1	5.8
4.2	4.9
12.5	11.6
11.6	11.2
3.9	5.6
10.9	10.4
10.9	10.4
3.2	3.4
3.8	3.7
2.2	2.3
7.8	7.8
9.3	8.8
10.3	10.2
3.1	2.7
13.0	11.5
2.2	2.6
8.6	8.2
5.8	5.9
7.4	7.1
8.6	9.0
13.5	12.3
2.8	1.8
3.5	4.6
7.1	7.8
3.5	3.9
4.9	5.4

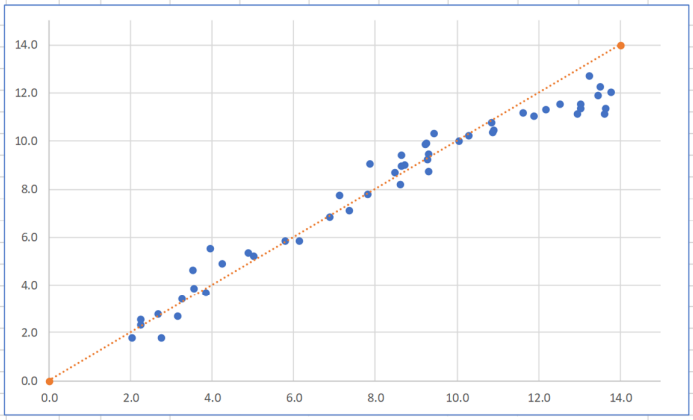

Figure A4.10 Plot of Y vs X. The dotted line is the line of identity

Mean Prediction Error (MPE) vs bins

Number of bins

MPE in bin number	2	3	4	5	6	7	8	9	10	Single bin
1	-0.23	-0.24	-0.25	-0.23	-0.18	-0.06	0.13	0.13	0.18	**S&B (MPE [95% CI])**
2	0.54	-0.27	-0.21	-0.15	-0.39	-0.59	-0.69	-0.73	-0.63	0.21 [-0.03,0.46]
3		1.05	-0.24	-0.30	-0.23	0.06	-0.02	-0.29	-0.38	
4			1.17	-0.07	-0.29	-0.33	-0.33	-0.12	0.09	
5				1.36	0.25	-0.22	-0.23	-0.30	-0.33	
6					1.44	0.45	-0.25	-0.30	-0.27	
7						1.50	0.51	0.22	-0.26	
8							1.56	0.70	0.26	
9								1.56	0.76	
10									1.63	

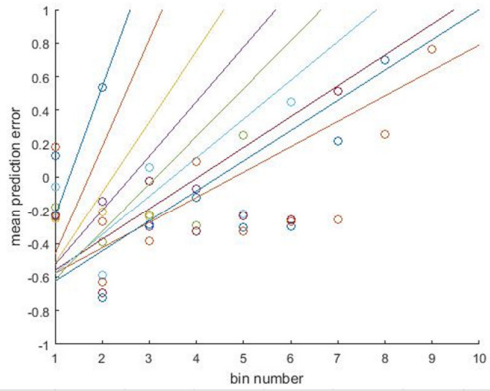

Figure A4.11 Linear regression of MPE vs bin number

Slope vs Number of bins

number of bins	Slope
2	0.77
3	0.64
4	0.42
5	0.33
6	0.29
7	0.23
8	0.18
9	0.18
10	0.15

Parameters of the fitted equation

θ = 0.35 (0.23, 0.47)

S_∞ = 0.11 (0.03, 0.19)

S_0 = 1.50 (1.14, 1.84)

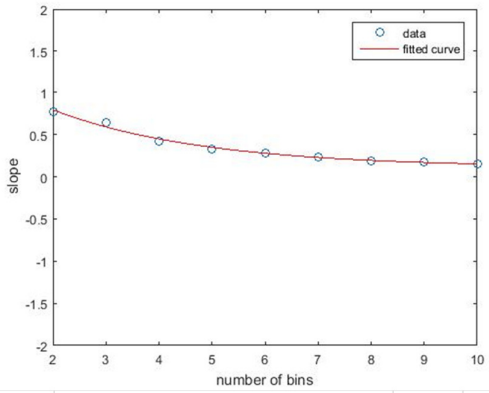

Figure A4.12 Regression of slope vs number of bins

A 3.6 Workings for Scenario E

Nonlinear deviation of residuals associated with the inverse of the magnitude of the observed data

Data

x	y
9.72	9.72
8.86	8.77
6.27	6.07
7.99	8.05
13.58	12.65
1.71	2.38
12.86	12.16
12.01	11.92
13.39	13.28
1.03	1.66
12.93	12.42
11.71	11.47
8.17	8.84
10.58	10.75
13.17	13.93
4.25	4.47
13.76	13.68
8.25	8.42
7.33	8.33
8.81	9.38
8.83	9.42
8.89	9.01
13.60	12.88
9.06	9.87
5.46	5.03
3.41	4.22
12.40	12.34
11.40	11.48
3.09	4.89
10.62	10.44
10.60	10.38
2.35	2.86
3.00	3.04
1.25	2.09
7.28	7.07
8.91	8.30
9.95	10.01
2.23	2.19
12.93	12.63
1.27	2.32
8.16	7.61
5.10	5.06
6.80	6.38
8.17	8.37
13.46	13.68
1.81	1.35
2.63	4.04
6.55	6.98
2.67	3.26
4.10	4.61

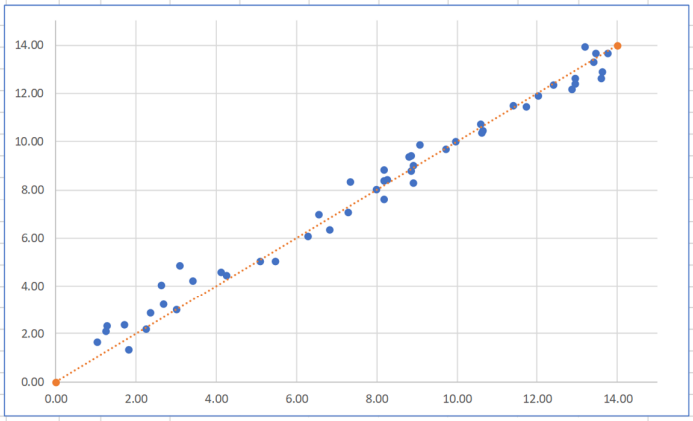

Figure A4.13 Plot of Y vs X. The dotted line is the line of identity

Mean Prediction Error (MPE) vs bins

Number of bins

MPE in bin number	2	3	4	5	6	7	8	9	10	Single bin
1	-0.41	-0.57	-0.64	-0.65	-0.64	-0.58	-0.46	-0.46	-0.45	S&B (MPE [95% CI])
2	0.03	-0.12	-0.04	-0.07	-0.38	-0.68	-0.86	-0.93	-0.86	-0.19 [-0.31, 0.001]
3		0.16	-0.15	-0.11	-0.03	0.22	0.08	-0.23	-0.37	
4			0.18	-0.11	-0.17	-0.15	-0.12	0.07	0.23	
5				0.21	0.02	-0.18	-0.11	-0.11	-0.12	
6					0.23	0.08	-0.29	-0.19	-0.11	
7						0.23	0.08	0.04	-0.20	
8							0.24	0.08	0.04	
9								0.24	0.08	
10									0.26	

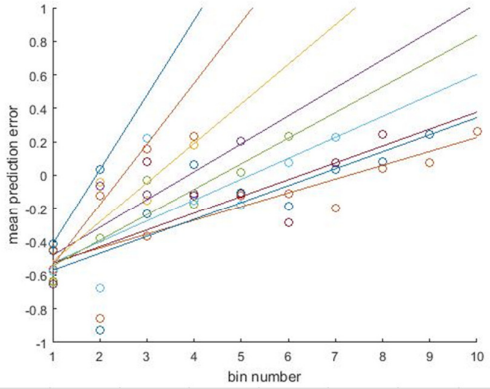

Figure A4.14 Linear regression of MPE vs bin number

Slope vs Number of bins

number of bins	Slope
2	0.45
3	0.36
4	0.24
5	0.17
6	0.15
7	0.13
8	0.10
9	0.10
10	0.08

Parameters of the fitted equation

θ = 0.39 (0.25, 0.53)

S_∞ = 0.07 (0.02, 0.1)

S_0 = 0.79 (0.59, 0.98)

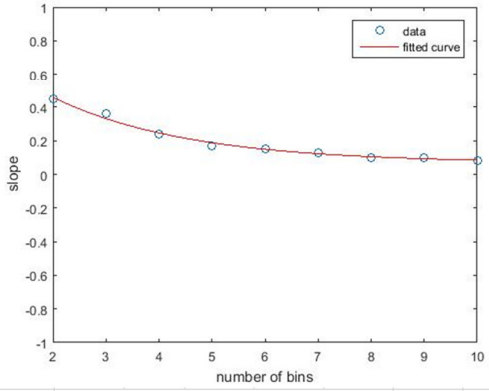

Figure A4.15 Regression of slope vs number of bins

A 3.7 Workings for Scenario F

A combination of constant and nonlinear deviation of residuals

Data

x	y
10.05	8.99
9.26	8.25
6.86	5.86
8.45	7.68
13.61	10.15
2.66	1.78
12.95	10.12
12.16	10.34
13.44	10.92
2.03	0.81
13.01	10.34
11.88	10.03
8.62	8.45
10.84	9.76
13.24	11.71
5.00	4.25
13.78	11.06
8.70	8.01
7.85	8.05
9.21	8.87
9.23	8.90
9.28	8.49
13.63	10.37
9.44	9.30
6.12	4.85
4.23	3.93
12.52	10.56
11.60	10.18
3.93	4.56
10.88	9.44
10.86	9.39
3.24	2.40
3.85	2.69
2.23	1.34
7.79	6.79
9.30	7.77
10.27	9.22
3.14	1.71
13.01	10.55
2.25	1.57
8.61	7.22
5.78	4.87
7.36	6.14
8.62	7.97
13.50	11.27
2.75	0.78
3.51	3.63
7.12	6.76
3.54	2.86
4.86	4.38

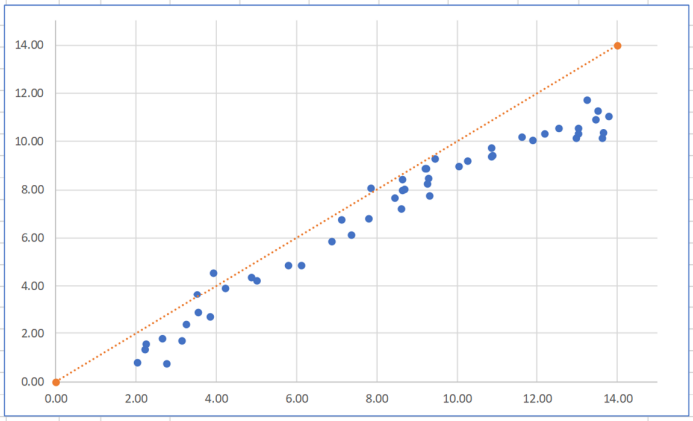

Figure A4.16 Plot of Y vs X. The dotted line is the line of identity

Mean Prediction Error (MPE) vs bins

Number of bins

MPE in bin number	2	3	4	5	6	7	8	9	10	Single bin
1	0.77	0.76	0.75	0.77	0.82	0.94	1.13	1.13	1.18	**S&B (MPE [95% CI])**
2	1.54	0.73	0.79	0.85	0.61	0.41	0.31	0.27	0.37	1.21 [0.97, 1.46]
3		2.05	0.76	0.70	0.77	1.06	0.98	0.71	0.62	
4			2.17	0.93	0.71	0.67	0.67	0.88	1.09	
5				2.36	1.25	0.78	0.77	0.70	0.67	
6					2.44	1.45	0.75	0.70	0.73	
7						2.50	1.51	1.22	0.74	
8							2.56	1.70	1.26	
9								2.56	1.76	
10									2.63	

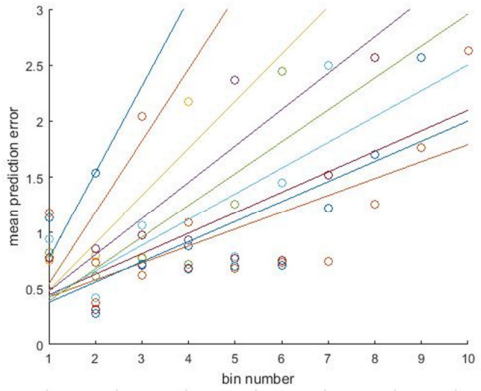

Figure A4.17 Linear regression of MPE vs bin number

Slope vs Number of bins

number of bins	Slope
2	0.77
3	0.64
4	0.42
5	0.33
6	0.29
7	0.23
8	0.18
9	0.18
10	0.15

Parameters of the fitted equation

θ = 0.35 (0.23, 0.47)

S_∞ = 0.11 (0.03, 0.19)

S_0 = 1.50 (1.14, 1.84)

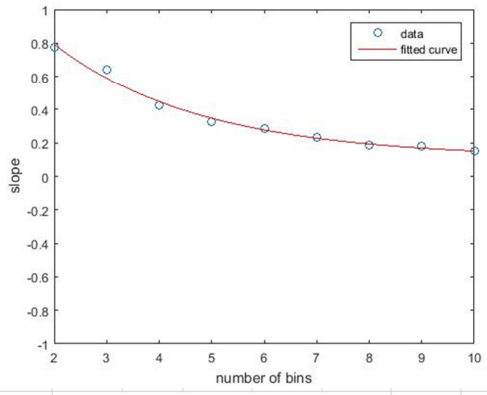

Figure A4.18 Regression of slope vs number of bins

A 3.8 Workings for Scenario G

Curvilinear deviation of residuals

Data

x	y
8.38	8.08
7.65	7.08
5.46	4.64
6.92	6.39
11.65	12.50
1.60	2.16
11.04	11.54
10.32	10.87
11.48	13.00
1.03	1.56
11.10	11.84
10.06	10.30
7.07	7.17
9.11	9.24
11.30	13.50
3.75	3.53
11.79	13.67
7.14	6.74
6.36	6.74
7.61	7.69
7.63	7.73
7.68	7.32
11.66	12.75
7.82	8.18
4.77	3.78
3.04	3.53
10.65	11.47
9.80	10.20
2.77	4.29
9.14	8.95
9.12	8.88
2.14	2.47
2.69	2.46
1.21	1.97
6.31	5.48
7.70	6.61
8.58	8.40
2.04	1.83
11.10	12.05
1.23	2.19
7.06	5.94
4.47	3.89
5.91	4.85
7.07	6.70
11.54	13.44
1.69	1.11
2.38	3.57
5.70	5.50
2.41	2.78
3.62	3.72

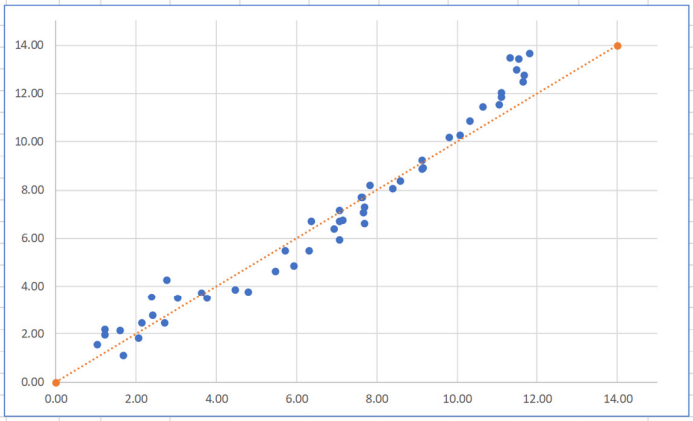

Figure A4.19 Plot of Y vs X. The dotted line is the line of identity

Mean Prediction Error (MPE) vs bins

Number of bins

MPE in bin number	2	3	4	5	6	7	8	9	10	Single bin
1	-0.07	-0.33	-0.45	-0.48	-0.47	-0.44	-0.34	-0.34	-0.34	S&B (MPE [95% CI])
2	-0.31	0.43	0.54	0.43	0.05	-0.33	-0.57	-0.67	-0.61	-0.21 [-0.43,0.01]
3		-0.72	0.33	0.48	0.59	0.80	0.60	0.23	0.06	
4			-0.84	0.20	0.34	0.45	0.50	0.67	0.79	
5				-1.05	0.06	0.24	0.41	0.51	0.50	
6					-1.11	-0.07	0.04	0.32	0.46	
7						-1.18	-0.15	0.15	0.25	
8							-1.25	-0.40	0.12	
9								-1.25	-0.50	
10									-1.29	

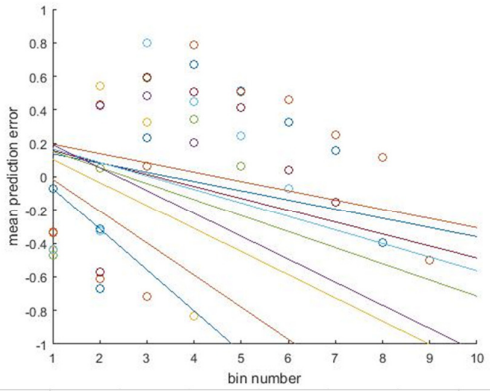

Figure A4.20 Linear regression of MPE vs bin number

Slope vs Number of bins

number of bins	Slope
2	-0.24
3	-0.19
4	-0.14
5	-0.14
6	-0.10
7	-0.08
8	-0.07
9	-0.06
10	-0.06

Parameters of the fitted equation

θ = 0.28 (0.16, 0.41)

S_∞ = 0.03 (-0.0039, 0.07)

S_0 = 0.34 (0.28, 0.40)

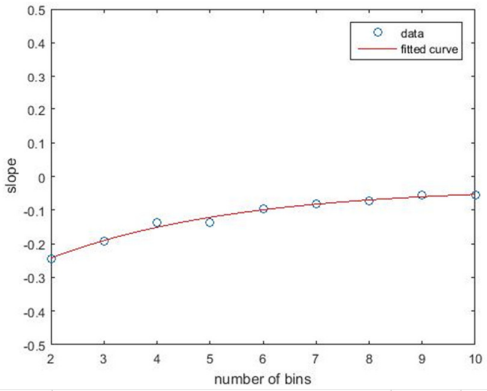

Figure A4.21 Regression of slope vs number of bins

Appendix 4: Appendices to Chapter 6

A4.1 Models for dabigatran population pharmacokinetics not evaluated in Chapter 6

Table A4.1 *Summary of published population pharmacokinetic models for dabigatran not already summarised in Chapter 6*

Author	Study details	Structural model	Parameter estimates	Description
Liesenfeld 2013 [266]	Data from Phase I dialysis [300] n = 7 A population PK model to quantify the influence of various haemodialysis parameters on dabigatran concentration.	2 compartment pharmacokinetic model First order input	<u>Fixed effect (θs)</u> KA =0.821 h^{-1} $ALAG$=1.67 h $ALAG_{3rd}$=1.67 h Q/F=152L h^{-1} V_2/F = 531 L V_3/F=499 L CL/F= 12.4 L h^{-1} F= 1 $EC50_{foodtime}$= 0.556 h $F_{\min\_foodtime}$= 0 $Hill_{foodtime}$= 6.10 K_0A= 313 mL min^{-1}	 First order absorption rate constant Absorption lag time Absorption lag time of the third dose (fasted) Apparent intercompartmental CL Apparent volume of central compartment Apparent volume of peripheral compartment Apparent total body clearance (CL) Absolute bioavailability Time between dose administration and food intake at which the effect on bioavailability is half of the maximum effect Minimum bioavailability when time between dose administration and food intake (fixed) Hill factor describing the steepness of the relation between time to food intake and the relative bioavailability Hemodialyzer mass transfer-area coefficient

	BSV (CV%)	
	CL/F = 40.4	BSV in the apparent total body clearance
	V_2/F = 14.3	BSV in the apparent volume of distribution of the central compartment
	IOV (CV%)	
	KA =64	Interoccasion variability in the relative first-order absorption rate constant
	F =48	Interoccasion variability in the relative bioavailability
	RUV (CV%)	
	Proportional = 8.5	Proportional residual variability
	Covariate relationship	
	$\boldsymbol{CL_{total}/F = CL_{dialysis}/F + \theta_{CL/F}}$	
	$F_{3rd\_dose} = \theta_{Fmin\_food\_time} + (1 - \theta_{Fmin\_food\_time}) \times food_{time}{}^{\theta_{Hill\_foodtime}} / (\theta_{EC50foodtime}{}^{\theta Hillfoodtime} + food\_time^{\theta Hillfoodtime})$	

Delavene 2012 [265]	Healthy volunteers n=11 Crossover 300mg DE or 300mg DE + 500mg Clarithromycin A PKPD model to study on the interaction of dabigatran etexilate and clarythromycin. Parent dabigatran concentration was used to develop this model.	2 compartment PK Inverse Gaussian absorption given by $f_A(t) = DF\sqrt{\frac{MAT}{2\pi CV_D{}^2 t^3}} \times exp^{\frac{-(t-MAT)^2}{2CV^2 MAT_t}}$ where $f_A(t)$ represents the quantity of dabigatran etexilate that passes into the central compartment during the time interval dt, D is the dose administered at time t	<u>Fixed effect</u> (θs) MAT=1.65 h CV_D=0.622 F=0.065 $F*$=0.101 V_2=48.3 L V_3=68.7 L Q=20.6 L h^{-1} CL=14.8 L h^{-1} <u>BSV (SD)</u> MAT=0.0722 CV=0.152 F=0.386 $F*$=0.725 V_2=0.105 L <u>RUV</u> Proportional=0.105 Additive=4.65	Mean absorption time Relative dispersion of absorption time Bioavailability (fixed) Bioavailability in presence of clarithromycin Volume of central compartment Volume of peripheral compartment Intercompartmental clearance Clearance BSV in the mean absorption time BSV in the relative dispersion of absorption time BSV in the bioavailability BSV in the bioavailability in presence of clarithromycin BSV in the volume of central compartment Proportional residual variability Additive residual variability

CV, coefficient of variation; SD, standard deviation, BSV, between subject variability, RUV, residual unexplained variability

A4.1 A MATLAB® code for simulating dabigatran population PK models

1. MATLAB® code for simulating the Troconiz 2007 model

Run file (go_dabi_Troconiz.m)

```
%% simulating dabigatran popPK model by Troconiz et al 2007
clear all; close all; clc; tic
rng(63) % random number generator seed
rep=1000;% number of patients to simulate

data_ori = xlsread('data_dabi_all.csv');%original data set
[rows, columns] = size(data_ori);
ID = datasample(1:rows,rep,'Replace',true);%resample 1000 IDs with
replacement
data = data_ori(ID,:);% resampled dataset
[rows1, columns1] = size(data);
%% dosing
dose=150*10^3; % in mcg
dose_number=12;% dose number
di=12;
options = odeset('RelTol',1e-6,'AbsTol', 1e-6);% ignore

%% run the model
init_PK_param_dabi_troco % initialises PK parameters

   for i=1:rep;% first loop through each patient
    pt_data = data(i,:);
    get_patient % simulates a patients' PK parameter

    start=1;% start 1 dose
    D =[dose 0 0];% dosing in gut compartment
    inits = [dose 0 0];% initial condition in the compartment also can
code as inits = D;
    time_dose=0+ALAG(i); % start dose 1

    for jj=1:dose_number % loops through each dose and calculates the
concentration

        TT=[0:1:di];% this is to tell MATLAB to solve the ODE for each
TT
        stop=start+length(TT)-1;% defining when to stop
        sol=ode45(@ode_dabigatran,[0
di],[inits],options,KA(i),CL(i),V2(i),Q(i),V3(i));% differential
equation solver nonstiff, medium accuracy
        A2=deval(sol,TT,2); % amount in compartment 2

        conc=A2./V2(i); % concentration of dabi
        inits=deval(sol,di)'+D;% updates inits and adds another dose
in the gut compartment

%         EPS1=normrnd(0,sigma1,size(conc));% prop error <24hrs
        EPS2=normrnd(0,sigma2,size(conc));% prop error >24hrs
        EPS3=normrnd(0,sigma3,size(conc));% add error >24hrs
```

```
% if jj<3
%         C2(i,start:stop)=conc+conc.*exp(EPS1); %adding in prop RUV
to concentration
% else
        C2(i,start:stop)=conc.*exp(EPS2)+EPS3; %adding in prop RUV to
concentration
% end
        T(i,start:stop)=TT+time_dose;% time

        if jj==12
            C_post=C2(i,start+2);
            C_peak(i,:)=C_post;
        end

        start=stop;% updates the start point for the next iteration
starting from where it stops
        time_dose=time_dose+di;% add the next dose time

        if jj==11
            C_pre=C2(i,stop);
            C_trough(i,:)=C_pre;
        end
    end
   end

   plot_graph % calls plotting code
   stats2 % calls statistics code

% xlswrite('Percentiles_Troco.xlsx', Conc3);
% xlswrite('Time_Troco.xlsx', T);
toc
```

Initialisation file (init_PK_param_troco.m)

```
%% Defining THETA AND ETA
THETA=[0.022 0.4 13.6 30.8 136 43.4 0.265 82.1];% KA, ALAG, Q, F, V2,
V3, CL KA24 CL24
MEANETA=[0 0 0 0 0 0 0 0];
OMEGA_parTroco=[ 0 0 0 0 0 0 0       0        0; % KA
                 0 0 0 0 0 0 0       0        0; % ALAG
                 0 0 0 0 0 0 0       0        0; % Q
                 0 0 0 0 0 0 0       0        0; % V2
                 0 0 0 0 0 0 0       0        0; % V3
                 0 0 0 0 0 0 1.086^2 0        0;% CL <24
                 0 0 0 0 0 0 0       0.2983^2 0;% KA>24
                 0 0 0 0 0 0 0       0        0.4604^2];% CL

ETA = mvnrnd(MEANETA,OMEGA_parTroco,rep);

%% variance
sigma1=0.669; % Proportional error <24hr
sigma2=0.3661; % Proportional >24hr
sigma3=0.375;% Additive error >24hr
```

get_patient file (get_patient_troco.m)

```
%% simulating PK parameters
ID_COL=1; SEX_COL=3; AGE_COL=4; WT_COL = 5; PPI_COL=6; AMIO_COL=7;
VERA_COL=8; CLCR_COL=10; SCR_COL=11; DI_COL=19;

%% Other covariates thetas
THETA_AGE=0.447;
THETA_SCR=0.363;

%% Simulating individual parameters
% if jj<3
%     KA=THETA(1)*exp(ETA(:,1));
% else
    KA=THETA(7)*exp(ETA(:,7))*(1+THETA_AGE*pt_data(AGE_COL)/66.97)*(1-
THETA_SCR*(pt_data(SCR_COL)/88.42)/0.964);
% end

ALAG=THETA(2)*exp(ETA(:,2));
Q=THETA(3)*exp(ETA(:,3));
V2=THETA(4)*exp(ETA(:,4));
V3=THETA(5)*exp(ETA(:,5));
%
%% GAST is fixed to the null value
GAST=34.58;

% if jj<2
%     CL=THETA(6)*exp(ETA(:,6))*(1+0.633*GAST/34.58);
% else

CL=THETA(8)*pt_data(CLCR_COL)./76.17*(1+0.294*GAST/34.58)*exp(ETA(:,8)
);
% end

PK=[KA(i) ALAG(i) Q(i) V2(i) V3(i) CL(i)];
mat(i,:)=PK;% to check simulated PK parameters
```

ODE solver (ode_dabigatran.m)

```
function dAdt=ode_dabigatran(t,A,KA,CL,V2,Q,V3)

k20=CL/V2;
k23=Q/V2;
k32=Q/V3;

dAdt=[-KA*A(1)% central compartment
      KA*A(1)-k20*A(2)+k32*A(3)-k23*A(2)%intercompartments
      k23*A(2)-k32*A(3)];
```

2. *MATLAB® code for simulating the Liesenfeld 2011 model*

Run file (go_dabi_Liesen.m)

```
%% simulating dabigatran popPK model by Lisenfeld 2011
clear all; close all; clc; tic; warning off;
rng(63);

rep=1000;% number of patients to simulate

data_ori = xlsread('data_dabi_all.csv');% original data set
[rows, columns] = size(data_ori);
ID = datasample(1:rows,rep,'Replace',true);% resample 1000 IDs with
replacement
data = data_ori(ID,:);% resampled dataset

%% dosing
dose=150*10^3; % in mcg
dose_number=12;% doses to simulate
di=12; % dosing interval
options = odeset('RelTol',1e-3, 'AbsTol', 1e-6);% ignore

%% run model
init_PK_param_dabi % initialises PK parameters

for i=1:rep;% for each patient, create 'rep' number of realizations
(virtual pts)
    pt_data = data(i,:);% indexing to each row

    get_patient % simulates a patients' PK parameter
    start=1;% start 1 dose

    time_dose=0+ALAG(i); % start time dose 1
    D =[dose*F(i) 0 0];% dosing in gut compartment
    inits = [dose*F(i) 0 0];% initial condition in the compartment

    for jj=1:dose_number % loops through each dose and calculates the
concentration

        TT=[0:1:di];% this is to tell MATLAB to solve the ODE for each
TT
        stop=start+length(TT)-1;% defining when to stop
        sol=ode45(@ode_dabigatran,[0
di],[inits],options,KA(i),CL(i),V2(i),Q(i),V3(i));% differential
equation solver nonstiff, medium accuracy
        A2=deval(sol,TT,2); % amount in compartment 2

        conc=A2./V2(i); % concentration of dabi

        inits=deval(sol,di)'+D;% updates inits and adds another dose
in the gut compartment

        EPS1=normrnd(0,var_Liesen(1),size(TT));% prop RUV
        EPS2=normrnd(0,var_Liesen(2),size(TT));% add RUV

        C2(i,start:stop)=conc.*exp(EPS1)+EPS2; %adding in prop RUV to
concentration
```

```
        T(i,start:stop)=TT+time_dose;% time

         if jj==12
            C_post=C2(i,start+2);
            C_peak(i,:)=C_post; % Collect 2h post dose
        end

        start=stop;% updates the start point for the next iteration
starting from where it stops
        time_dose=time_dose+di;% add the next dose time

        if jj==11
            C_pre=C2(i,stop);
            C_trough(i,:)=C_pre; % Collect pre-dose
        end
    end
end

plot_graph % calls plotting code
stats2 % calls boxplot, KS test and CDF plot

% xlswrite('Percentiles_Liesen.xlsx', Conc3);
% xlswrite('Time_Liesen.xlsx', T);
    toc
```

Initialisation file (init_PK_param_liesen.m)

```
%Fixed effect

THETA=[0.754 0.634 35.5 1 673 345 124]; % KA(1/h), ALAG(h), Q(L/h), F,
V2(L), V3(L), CL(L/hr)

%% Random effects
MEANETA=[0 0 0 0 0 0 0];
OMEGA_parLiesen=   [0 0 0       0        0 0 0;
                    0 0 0       0        0 0 0;
                    0 0 0       0        0 0 0;
                    0 0 0 0.443^2        0 0 0; % F
                    0 0 0       0  0.205^2 0 0; % V2
                    0 0 0       0        0 0 0;
                    0 0 0       0        0 0 0];

ETA = mvnrnd(MEANETA,OMEGA_parLiesen,rep);

%% variance
var_Liesen=[0.328 6.68];
```

get_patient file (get_patient_Liesen.m)

```
%% simulating PK parameters

patient_data % this reads in the data set

%% Individual parameters
KA=THETA(1)*exp(ETA(:,1));
ALAG=THETA(2)*exp(ETA(:,2));
```

```
Q=THETA(3)*exp(ETA(:,3));
F=THETA(4)*THETA_PPI*THETA_AMIO*THETA_VERA*exp(ETA(:,4));
V2=THETA(5)*(1+THETA_WT*(pt_data(WT_COL)-80.3))*(1+THETA_HGB*(HGB-
14.3))*exp(ETA(:,5));
V3=THETA(6)*exp(ETA(:,6));
CL=THETA(7)*pt_data(CLCR_COL).^THETAPWRCLCR./(THETAEC50^THETAPWRCLCR
+pt_data(CLCR_COL)^THETAPWRCLCR)*(1+THETA_AGE*(pt_data(AGE_COL)-
72))*THETA_ETHN*THETA_HF*THETA_SEX.*exp(ETA(:,7));

PK=[KA(i) ALAG(i) Q(i) F(i) V2(i) V3(i) CL(i)];
mat(i,:)=PK;% matrix of simulated PK parameters
```

get_covariate(patient_data.m)

```
ID_COL=1;
SEX_COL=3;
AGE_COL=4;
WT_COL = 5;
PPI_COL=6;
AMIO_COL=7;
VERA_COL=8;
CLCR_COL=10;
SCR_COL=11;
DI_COL=19;

%% SEX
 if pt_data(SEX_COL)==0
     THETA_SEX=1;
 elseif pt_data(SEX_COL)==1
     THETA_SEX=0.917;
 end

%% AMIODARONE
 if pt_data(AMIO_COL)==0
     THETA_AMIO=1;
 elseif pt_data(AMIO_COL)==1
     THETA_AMIO=1.12;
 end

 %% VERAPAMIL
  if pt_data(VERA_COL)==0
     THETA_VERA=1;
 elseif pt_data(VERA_COL)==1
     THETA_VERA=1.23;
  end
```

```
 %% PPI
 if pt_data(PPI_COL)==0
     THETA_PPI=1;
 elseif pt_data(PPI_COL)==1
     THETA_PPI=0.875;
 end

HGB=14.3;
%% Liesenfeld's model

THETA_HGB=-3.99/100;% change to %
THETA_AGE=-0.41/100;% change to %
THETA_WT=0.77/100;% change to %

THETAPWRCLCR=1.29;
THETAEC50=56.7*60/1000; % %change units from mL min-1 to L/h
THETA_ETHN=1; % none of the pts were South Asian. value of 0.797 for
South Asian
THETA_HF=1;% None of the pts were Heart Failure, otherwise 0.933
```

ODE solver (ode_dabigatran.m)

```
function dAdt=ode_dabigatran(t,A,KA,CL,V2,Q,V3)

k20=CL/V2;
k23=Q/V2;
k32=Q/V3;

dAdt=[-KA*A(1)% central compartment
       KA*A(1)-k20*A(2)-k23*A(2)+k32*A(3)%intercompartments
       k23*A(2)-k32*A(3)];
```

A 4.3 MATLAB® code for simulating Dansirikul 2012 model

Run file (go_dabi_Dansirikul.m)

```
%% simulating dabigatran popPK model by Dansirikul et al 2012
% Shamin last updated May 2017
clear all; close all; clc; tic
rng(63)
rep=1000;% number of replicates

%% reads data and resamples 1000 patients
data_ori=xlsread('data_dabi_all.csv');
[rows1, columns] = size(data_ori);
ID = datasample(1:rows1,rep,'Replace',true)';%resample IDs with
replacement
data = data_ori(ID,:);% resampled dataset

%% dosing
dose=150*10^3; % dose in mcg
dn=12;% dose number
di=12;% dosing interval
options = odeset('RelTol',1e-3, 'AbsTol',1e-3);% ignore
%% run PK model
init_PK_param_dabi_dansirikul % initialises PK parameters

for i=1:rep;% first loop - for each patient, simulate rep profiles
    pt_data = data(i,:);% indexing pt_data to ith row
    patient_data % this reads in the data set
    get_patient % simulates the patient

    start=1;% start 1 dose
    time_dose=0+ALAG(i); % start dose 1

    A0 = [dose*F(i) 0 0];% initial condition in each compartment;
    D = A0; % dosing in gut compartment

    for jj=1:dn % loops through each dose and calculates the
concentration
%         disp([i,jj])% displays what simulation it is doing right now

        TT=[0:1:di];% this is to tell MATLAB to solve the ODE for each
TT
        stop=start+length(TT)-1;% defining when to stop
        sol=ode45(@ode_dabigatran,[0
di],[A0],options,KA(i),CL(i),V2(i),Q(i),V3(i));% differential equation
solver nonstiff, medium accuracy

        A2=deval(sol,TT,2); % amount in central    compartment 2

        conc=A2./V2(i);
        A0=deval(sol,di)'+D;% updates inits and adds another dose in
the gut compartment

        EPS=normrnd(0,sigma_RUVJoy,size(conc));%RUV

        C2(i,start:stop)=conc.*exp(EPS); %adding in prop RUV to
concentration
```

```
        T(i,start:stop)=TT+time_dose;% time

        if jj==12
            C_post=C2(i,start+2);
            C_peak(i,:)=C_post;
        end

        start=stop;% updates the start point for the next iteration
starting from where it stops
        time_dose=time_dose+di;% add the next dose time

        if jj==11
            C_pre=C2(i,stop);
            C_trough(i,:)=C_pre;% collecting simulated trough
concentrations
        end
    end% end for dosing loop
end% end for patient loop

stats2
plot_graph % calls plotting code

% xlswrite('Percentiles_Joy.xlsx', Conc3);
% xlswrite('Time_Joy.xlsx', T);

 toc
```

Initialisation file (init_PK_param_dansirikul.m)

```
%% Defining THETA AND ETA

THETA=[0.754 0.634 35.5 1 728 345 111];% KA, ALAG, Q, F, V2, V3, CL
MEANETA=[0 0 0 0 0 0 0];
OMEGA_parJoy=[0.953^2  0 0       0       0   0 0; % KA
                    0  0 0       0       0   0 0; % ALAG
                    0  0 0       0       0   0 0; % Q
                    0  0 0 0.447^2       0   0 0; % F
                    0  0 0       0 0.261^2   0 0; % V2
                    0  0 0       0       0   0 0; % V3
                    0  0 0       0       0   0 0];% CL

ETA = mvnrnd(MEANETA,OMEGA_parJoy,rep);

%% variance
sigma_RUVJoy=0.294; %
```

ODE solver (ode_dabigatran.m)

```
function dAdt=ode_dabigatran(t,A,KA,CL,V2,Q,V3)

k20=CL/V2;
k23=Q/V2;
k32=Q/V3;

dAdt=[-KA*A(1)% central compartment
```

```
      KA*A(1)-k20*A(2)-k23*A(2)+k32*A(3)%intercompartments
      k23*A(2)-k32*A(3)];
```

get_patient file (get_patient_Dansirikul.m)

```
%% simulating PK parameters
% Individual parameters

KA=THETA(1).*exp(ETA(:,1));
ALAG=THETA(2).*exp(ETA(:,2));
Q=THETA(3).*exp(ETA(:,3));
F=THETA(4)*THETA_PGP*THETA_PPI.*exp(ETA(:,4));
V2=THETA(5)*(1+THETA_WT*(pt_data(WT_COL)-80)).*exp(ETA(:,5));
V3=THETA(6).*exp(ETA(:,7));

if pt_data(CLCR_COL)>120
    CL = THETA(7)*(1+THETA_AGE*(pt_data(AGE_COL)-
68))*THETA_AF*THETA_SEX.*exp(ETA(:,7));% 'Healthy' patient
else
    CL = THETA(7)*(1+THETA_CLCR*(pt_data(CLCR_COL)-
120))*(1+THETA_AGE*(pt_data(AGE_COL)-
68))*THETA_AF*THETA_SEX.*exp(ETA(:,7));% 'Unhealthy' pt
end

PK=[KA(i) ALAG(i) Q(i) F(i) V2(i) V3(i) CL(i)];
mat(i,:)=PK;
```

get_covariate (patient_data.m)

```
ID_COL=1; SEX_COL=3; AGE_COL=4; WT_COL = 5; PPI_COL=6; AMIO_COL=7;
VERA_COL=8; CLCR_COL=10; SCR_COL=11; DI_COL=19; flag_COL=2;

 if pt_data(AMIO_COL)==0
     THETA_PGP=1.150;
 elseif pt_data(AMIO_COL)==1
     THETA_PGP=1;
 end

 if pt_data(PPI_COL)==0
     THETA_PPI=1;
 elseif pt_data(PPI_COL)==1
     THETA_PPI=0.854;
 end

 if pt_data(SEX_COL)==0
     THETA_SEX=1;
 elseif pt_data(SEX_COL)==1
     THETA_SEX=0.875;
 end

THETA_CLCR=0.00644;
THETA_WT=0.0110;
THETA_AGE=-0.00662;
THETA_AF=0.939;
```

A4.4 Generic MATLAB® code for plotting VPC

Plotting (plot_graph.m) – this is a generic code for plotting VPC

```
%% plotting percentiles
time_range=120:145;
Time3=T(i,time_range);
pink=[1 0.78 0.80];% RGB for pink
hold on
figure(1)
prct=[10 50 90];% percentile
Conc3=prctile(C2,prct);% median

%% plotting data
flag_COL=2;
flag_DUR=13;
[rows1, columns1] = size(data);
for i=1:rows1
pt_data = data(i,:);

if pt_data(flag_COL)== 5 && pt_data(flag_DUR)> 1; % patients at
steady-state with 5 samples
    TIME_COL2(i,:) = data(i,14:18);
    CONC_COL2(i,:) = data(i,19:23);

elseif   pt_data(flag_COL)== 5 && pt_data(flag_DUR)== 0;% patients
initiating with 5 samples
    TIME_COL3(i,:) = data(i,14:18);
    CONC_COL3(i,:) = data(i,19:23);

end
end
TIME_ind=[];
DV_ind=[];

subplot(2,3,1)% 5 samples init
time_range2=1:25;% columns for init pts
jbfill(T(1,time_range2),Conc3(3,time_range2),Conc3(1,time_range2),pink
,pink,0,0.5);
hold on
plot(T(1,time_range2),Conc3(1,time_range2),'r');plot(T(1,time_range2),
Conc3(2,time_range2),'--
r');plot(T(1,time_range2),Conc3(3,time_range2),'r')
plot(TIME_COL3,CONC_COL3,'ro','markersize',5)
ylim([1 500]);
xlim([0 13]);
title('Liesenfeld 2011 initial');
xlabel('Time after dose(h)');
ylabel('Dabigatran concentration (ng/mL)')
hold off

subplot(2,3,2)% 5 samples SS
jbfill(T(1,time_range),Conc3(3,time_range),Conc3(1,time_range),pink,pi
nk,0,0.5);
hold on
plot(T(1,time_range),Conc3(1,time_range),'r');plot(T(1,time_range),Con
c3(2,time_range),'--r');plot(T(1,time_range),Conc3(3,time_range),'r')
plot(TIME_COL2+120,CONC_COL2,'ro','markersize',5)
ylim([1 500]);xlim([120 133]);
```

```
title('Author Year ss');
xlabel('Time after dose (h)');
ylabel('Dabigatran concentration (ng/mL)')
hold off

% print('-r900', '-djpeg', 'Author Year graph2')
```

A4.5 Generic MATLAB® code for K-S test and boxplots

Statistics (plot_graph.m) – this is a generic code for the box plots and Kolmogorov-Smirnov test

```
% statistical analysis of simulations

%% To get pre and post dose pt and simulate
data_ss=xlsread('data_dabi_ss.csv');
[rows, columns] = size(data_ss);

flag_COL=2;
flag_DUR=13;
pt_pre_2=19;
pt_post_2=20;
pt_pre_5=23;
pt_post_5=20;

for i=1:rows
pt_data = data_ss(i,:); % pt data

if pt_data(flag_COL)== 5 && pt_data(flag_DUR)> 1;% patients with 5
samples
    pt_pre(i,:) = data_ss(i,pt_pre_5);
    pt_post(i,:) = data_ss(i,pt_post_5);
elseif pt_data(flag_COL)== 2% patients with 2 samples
    pt_pre(i,:) = data_ss(i,pt_pre_2);
    pt_post(i,:) = data_ss(i,pt_post_2);
else pt_data(flag_COL)== 1;% patients with 1 sample
    pt_pre(i,:) = data_ss(i,pt_pre_2);
    pt_post(i,:) = nan;
end
end

%% Kolmogorov-Smirnov test
% Null hypothesis = two samples were drawn from populations with the
same distribution
% If h = 1 ;reject the null hypothesis

[h_post, p_post, ks2stat_post] = kstest2(C_peak,pt_post);%
[h_pre, p_pre, ks2stat_pre] = kstest2(C_trough,pt_pre);

%% Plotting CDF
figure(3)
subplot(1,2,1)
hold on
cdfplot(C_peak); cdfplot(pt_post);xlim([0 750])
legend('Simulated post','Observed post','Location','SE')
xlabel(['Dabigatran concentration (ng/mL)']);
title('Author Year 2h post dose')
```

```
hold off

subplot(1,2,2)
hold on
cdfplot(C_trough); cdfplot(pt_pre);xlim([0 750])
legend('Simulated pre','Observed pre','Location','SE')
xlabel(['Dabigatran concentration (ng/mL)']);
title(' Author Year pre-dose')
hold off
% print('-r900', '-djpeg', ' Author Year CDF')

%% boxplots
hold on
figure(2)
post_pre=[C_peak;pt_post;C_trough;pt_pre];
g = [ones(size(C_peak));
2*ones(size(pt_pre));3*ones(size(C_peak));4*ones(size(pt_post))];
boxplot(post_pre,g,'Labels',['Simulated post','Observed
post','Simulated pre', 'Observed pre'], 'positions', [1,2,4,5]);
ylabel(['Dabigatran concentration (ng/mL)']);
title('Author Year ss')
ylim([0 750])
hold off
% print('-r900', '-djpeg', 'Author Year boxplot')
```

REFERENCES

References

1. Wright DFB, Duffull SB. Development of a bayesian forecasting method for warfarin dose individualisation. Pharmaceutical Research 2011; 28: 1100-11.
2. Wright DFB, Duffull SB. A bayesian dose-individualization method for warfarin. Clinical Pharmacokinetics 2013; 52: 59-68.
3. Saffian SM, Wright DF, Roberts RL, Duffull SB. Methods for Predicting Warfarin Dose Requirements. Therapeutic Drug Monitoring 2015; 37: 531-8.
4. Verhoef TI, Redekop WK, Daly AK, van Schie RM, de Boer A, Maitland-van der Zee AH. Pharmacogenetic-guided dosing of coumarin anticoagulants: algorithms for warfarin, acenocoumarol and phenprocoumon. British journal of clinical pharmacology 2014; 77: 626-41.
5. Sheiner LB, Beal SL. Some suggestions for measuring predictive performance. Journal of pharmacokinetics and biopharmaceutics 1981; 9: 503-12.
6. Southworth MR, Reichman ME, Unger EF. Dabigatran and postmarketing reports of bleeding. The New England journal of medicine 2013; 368: 1272-4.
7. van Ryn J, Goss A, Hauel N, Wienen W, Priepke H, Nar H, et al. The discovery of dabigatran etexilate. Frontiers in pharmacology 2013; 4: 12.
8. PHARMAC. 'Game-changing' anti-clotting treatment funded. In, 2011.
9. Boehringer Ingelheim (N.Z.) Limited. Pradaxa: New Zealand Datasheet. In, 3/5/2013 Edition: Medsafe, 2013.
10. Reilly PA, Lehr T, Haertter S, Connolly SJ, Yusuf S, Eikelboom JW, et al. The Effect of Dabigatran Plasma Concentrations and Patient Characteristics on the Frequency of Ischemic Stroke and Major Bleeding in Atrial Fibrillation Patients: The RE-LY Trial (Randomized Evaluation of Long-Term Anticoagulation Therapy). Journal of the American College of Cardiology 2014; 63: 321-28.
11. Holford NH. Clinical Pharmacokinetics and Pharmacodynamics: The Quantitative Basis for Therapeutics. In: Melmon and Morrelli's Clinical Pharmacology: Basic Principles in Therapeutics, 3rd Edition, edsMelmon K, Morrelli H, Nierenberg D, Hoffman B, New York: McGraw-Hil, 1992.
12. Green B, Duffull SB. What is the best size descriptor to use for pharmacokinetic studies in the obese? British Journal of Clinical Pharmacology 2004; 58: 119-33.
13. Holford NH, Sheiner LB. Kinetics of pharmacologic response. Pharmacology & therapeutics 1982; 16: 143-66.
14. Bourne HR, Roberts JM. Drug receptors and pharmacodynamics. Basic and Clinical Pharmacology 1995: 9-32.
15. Ariens EJ, Van Rossum JM, Simonis AM. Affinity, intrinsic activity and drug interactions. Pharmacological reviews 1957; 9: 218-36.

16. Jusko WJ, Ko HC. Physiologic indirect response models characterize diverse types of pharmacodynamic effects. Clinical pharmacology and therapeutics 1994; 56: 406-19.
17. Csajka C, Verotta D. Pharmacokinetic-pharmacodynamic modelling: history and perspectives. Journal of pharmacokinetics and pharmacodynamics 2006; 33: 227-79.
18. Al-Sallami HS, Pavan Kumar VV, Landersdorfer CB, Bulitta JB, Duffull SB. The time course of drug effects. Pharmaceutical statistics 2009; 8: 176-85.
19. Savic RM, Jonker DM, Kerbusch T, Karlsson MO. Implementation of a transit compartment model for describing drug absorption in pharmacokinetic studies. Journal of pharmacokinetics and pharmacodynamics 2007; 34: 711-26.
20. Hamberg AK, Wadelius M, Lindh JD, Dahl ML, Padrini R, Deloukas P, et al. A pharmacometric model describing the relationship between warfarin dose and INR response with respect to variations in CYP2C9, VKORC1, and age. Clinical Pharmacology and Therapeutics 2010; 87: 727-34.
21. Duffull SB, Kirkpatrick CMJ, Begg EJ. Comparison of two Bayesian approaches to dose-individualization for once-daily aminoglycoside regimens. British Journal of Clinical Pharmacology 1997; 43: 125-35.
22. McCune JS, Bemer MJ, Barrett JS, Scott Baker K, Gamis AS, Holford NH. Busulfan in infant to adult hematopoietic cell transplant recipients: a population pharmacokinetic model for initial and Bayesian dose personalization. Clinical cancer research : an official journal of the American Association for Cancer Research 2014; 20: 754-63.
23. Sheiner LB, Beal SL. Bayesian individualization of pharmacokinetics: Simple implementation and comparison with non-Bayesian methods. Journal of Pharmaceutical Sciences 1982; 71: 1344-48.
24. Gage BF, Eby C, Johnson JA, Deych E, Rieder MJ, Ridker PM, et al. Use of pharmacogenetic and clinical factors to predict the therapeutic dose of warfarin. Clinical pharmacology and therapeutics 2008; 84: 326-31.
25. Holford NH, Buclin T. Safe and effective variability-a criterion for dose individualization. Therapeutic drug monitoring 2012; 34: 565-8.
26. Group BDW. Biomarkers and surrogate endpoints: preferred definitions and conceptual framework. Clin Pharmacol Ther 2001; 69: 89-95.
27. Sanofi-Aventis New Zealand Ltd. Clexane® and Clexane® Forte: data sheet. 25 October 2013 [online] [cited 21 June 2017]; Available from: http://www.medsafe.govt.nz/profs/datasheet/c/clexaneinj.pdf.
28. Higuchi K, Tanabe S, Shimada K, Hosaka H, Sasaki E, Nakayama N, et al. Biweekly irinotecan plus cisplatin versus irinotecan alone as second-line treatment for advanced gastric cancer: a randomised phase III trial (TCOG GI-0801/BIRIP trial). European journal of cancer (Oxford, England : 1990) 2014; 50: 1437-45.
29. Tait, Sefcick. A warfarin induction regimen for out-patient anticoagulation in patients with atrial fibrillation. British Journal of Haematology 1998; 101: 450-54.

30. Lenzini P, Wadelius M, Kimmel S, Anderson JL, Jorgensen AL, Pirmohamed M, et al. Integration of genetic, clinical, and INR data to refine warfarin dosing. Clinical Pharmacology and Therapeutics 2010; 87: 572-78.
31. Lenzini PA, Grice GR, Milligan PE, Gatchel SK, Deych E, Eby CS, et al. Optimal initial dose adjustment of warfarin in orthopedic patients. The Annals of pharmacotherapy 2007; 41: 1798-804.
32. Jelliffe RW, Jelliffe SM. A computer program for estimation of creatinine clearance from unstable serum creatinine levels, age, sex, and weight. Mathematical Biosciences 1972; 14: 17-24.
33. Duffull SB, Begg EJ, Robinson BA, Deely JJ. A sequential Bayesian algorithm for dose individualisation of carboplatin. Cancer chemotherapy and pharmacology 1997; 39: 317-26.
34. Duffull SB, Kirkpatrick CM, Begg EJ. Comparison of two Bayesian approaches to dose-individualization for once-daily aminoglycoside regimens. British Journal of Clinical Pharmacology 1997; 43: 125-35.
35. Furie B, Furie BC. Molecular and Cellular Biology of Blood Coagulation. New England Journal of Medicine 1992; 326: 800-06.
36. Wajima T, Isbister GK, Duffull SB. A comprehensive model for the humoral coagulation network in humans. Clinical Pharmacology and Therapeutics 2009; 86: 290-8.
37. Mann KG, Brummel K, Butenas S. What is all that thrombin for? Journal of Thrombosis and Haemostasis 2003; 1: 1504-14.
38. Ansell J. Factor Xa or thrombin: is factor Xa a better target? Journal of thrombosis and haemostasis : JTH 2007; 5 Suppl 1: 60-4.
39. Duffull SB. Is the ideal anticoagulant a myth? Expert review of clinical pharmacology 2012; 5: 231-6.
40. Duffull SB, Wright DF, Al-Sallami HS, Zufferey PJ, Faed JM. Dabigatran: rational dose individualisation and monitoring guidance is needed. The New Zealand medical journal 2012; 125: 148-54.
41. Bogousslavsky J, Van Melle G, Regli F, Kappenberger L. Pathogenesis of anterior circulation stroke in patients with nonvalvular atrial fibrillation: The lausanne stroke registry. Neurology 1990; 40: 1046-50.
42. Britton M, Gustafsson C. Non-rheumatic atrial fibrillation as a risk factor for stroke. Stroke 1985; 16: 182-87.
43. Manning WJ, Silverman DI, Waksmonski CA, Oettgen P, Douglas PS. Prevalence of Residual Left Atrial Thrombi Among Patients With Acute Thromboembolism and Newly Recognized Atrial Fibrillation. Archives of Internal Medicine 1995; 155: 2193-97.
44. Wolf PA, Abbott RD, Kannel WB. Atrial fibrillation as an independent risk factor for stroke: The framingham study. Stroke 1991; 22: 983-88.
45. Atrial Fibrillation Investigators: Atrial Fibrillation AAS, Boston Area Anticoagulation Trial for Atrial Fibrillation S, Canadian Atrial Fibrillation Anticoagulation S, Stroke Prevention in Atrial Fibrillation S, Veterans Affairs Stroke Prevention in Nonrheumatic Atrial Fibrillation S. Risk Factors for Stroke and Efficacy of Antithrombotic Therapy in Atrial

Fibrillation: Analysis of Pooled Data From Five Randomized Controlled Trials. Archives of Internal Medicine 1994; 154: 1449-57.
46. Hart RG, Benavente O, McBride R, Pearce LA. Antithrombotic therapy to prevent stroke in patients with atrial fibrillation: A meta-analysis. Annals of Internal Medicine 1999; 131: 492-501.
47. Breckenridge A, Orme M. Kinetics of warfarin absorption in man. Clinical Pharmacology and Therapeutics 1973; 14: 955-61.
48. Kelly JG, O'Malley K. Clinical pharmacokinetics of oral anticoagulants. Clinical Pharmacokinetics 1979; 4: 1-15.
49. Holford NHG. Clinical pharmacokinetics and pharmacodynamics of warfarin. Understanding the dose-effect relationship. Clinical Pharmacokinetics 1986; 11: 483-504.
50. Ufer M. Comparative pharmacokinetics of vitamin K antagonists warfarin, phenprocoumon and acenocoumarol. Clinical Pharmacokinetics 2005; 44: 1227-46.
51. Whitlon DS, Sadowski JA, Suttie JW. Mechanism of coumarin action: significance of vitamin K epoxide reductase inhibition. Biochemistry 1978; 17: 1371-77.
52. Gardiner SJ, Begg EJ. Pharmacogenetics, drug-metabolizing enzymes, and clinical practice. Pharmacological reviews 2006; 58: 521-90.
53. Voora D, McLeod HL, Eby C, Gage BF. The pharmacogenetics of coumarin therapy. Pharmacogenomics 2005; 6: 503-13.
54. Daly AK, King BP. Pharmacogenetics of oral anticoagulants. Pharmacogenetics 2003; 13: 247-52.
55. Poller L. International Normalized Ratios (INR): The first 20 years. Journal of Thrombosis and Haemostasis 2004; 2: 849-60.
56. Hylek EM, Go AS, Chang Y, Jensvold NG, Henault LE, Selby JV, et al. Effect of Intensity of Oral Anticoagulation on Stroke Severity and Mortality in Atrial Fibrillation. New England Journal of Medicine 2003; 349: 1019-26.
57. Blackshear JL, Baker VS, Rubino F, Safford R, Lane G, Flipse T, et al. Adjusted-dose warfarin versus low-intensity, fixed-dose warfarin plus aspirin for high-risk patients with atrial fibrillation: Stroke prevention in Atrial Fibrillation III Randomised Clinical Trial. Lancet 1996; 348: 633-38.
58. Hylek EM, Skates SJ, Sheehan MA, Singer DE. An analysis of the lowest effective intensity of prophylactic anticoagulation for patients with nonrheumatic atrial fibrillation. New England Journal of Medicine 1996; 335: 540-46.
59. Holbrook A, Schulman S, Witt DM, Vandvik PO, Fish J, Kovacs MJ, et al. Evidence-based management of anticoagulant therapy: Antithrombotic Therapy and Prevention of Thrombosis, 9th ed: American College of Chest Physicians Evidence-Based Clinical Practice Guidelines. Chest 2012; 141: e152S-84S.
60. Hirsh J, Fuster V, Ansell J, Halperin JL. American Heart Association/American College of Cardiology Foundation guide to warfarin therapy. Journal of the American College of Cardiology 2003; 41: 1633-52.

61. Shin J, Cao D. Comparison of warfarin pharmacogenetic dosing algorithms in a racially diverse large cohort. Pharmacogenomics 2011; 12: 125-34.
62. Saffian SM, Duffull SB, Wright DFB. Warfarin dosing algorithms under-predict dose requirements in patients requiring ≥ 7mg daily: A systematic review and meta-analysis. Clinical Pharmacology & Therapeutics 2017: n/a-n/a.
63. Choi JR, Kim J-O, Kang DR, Yoon S-A, Shin J-Y, Zhang X, et al. Proposal of pharmacogenetics-based warfarin dosing algorithm in Korean patients. Journal of Human Genetics 2011; 56: 290-5.
64. Ramos AS, Seip RL, Rivera-Miranda G, Felici-Giovanini ME, Garcia-Berdecia R, Alejandro-Cowan Y, et al. Development of a pharmacogenetic-guided warfarin dosing algorithm for Puerto Rican patients. Pharmacogenomics 2012; 13: 1937-50.
65. Perini JA, Struchiner CJ, Silva-Assuncao E, Santana ISC, Rangel F, Ojopi EB, et al. Pharmacogenetics of warfarin: development of a dosing algorithm for brazilian patients. Clinical pharmacology and therapeutics 2008; 84: 722-8.
66. Millican EA, Lenzini PA, Milligan PE, Grosso L, Eby C, Deych E, et al. Genetic-based dosing in orthopedic patients beginning warfarin therapy. Blood 2007; 110: 1511-15.
67. Cho H-J, On Y-K, Bang OY, Kim J-W, Huh W, Ko J-W, et al. Development and comparison of a warfarin-dosing algorithm for Korean patients with atrial fibrillation. Clinical Therapeutics 2011; 33: 1371-80.
68. Klein T, Altman R, Eriksson N, Gage B, Kimmel S, Lee M, et al. Estimation of the warfarin dose with clinical and pharmacogenetic data. New England Journal of Medicine 2009; 360: 753-64.
69. Gage BF, Eby C, Milligan PE, Banet GA, Duncan JR, McLeod HL. Use of pharmacogenetics and clinical factors to predict the maintenance dose of warfarin. Thrombosis and Haemostasis 2004; 91: 87-94.
70. Poller L, Keown M, Ibrahim S, Lowe G, Moia M, Turpie AG, et al. A multicentre randomised clinical endpoint study of parma 5 computer-assisted oral anticoagulant dosage. British Journal of Haematology 2008; 143: 274-83.
71. Ryan P, Gilbert M, Rose P. Computer control of anticoagulant dose for therapeutic management. Bmj 1989; 299: 1207-09.
72. Holford NH. Clin Pharmacol Ther [Abstract] 1986; 39: 199.
73. Crowther MA, Harrison L, Hirsh J. Reply: Warfarin: Less May Be Better. Annals of Internal Medicine 1997; 127: 333.
74. Horne BD, Lenzini PA, Wadelius M, Jorgensen AL, Kimmel SE, Ridker PM, et al. Pharmacogenetic warfarin dose refinements remain significantly influenced by genetic factors after one week of therapy. Thrombosis and Haemostasis 2012; 107: 232-40.
75. Motykie GD, Mokhtee D, Zebala LP, Caprini JA, Kudrna JC, Mungall DR. The use of a Bayesian forecasting model in the management of warfarin therapy after total hip arthroplasty. The Journal of arthroplasty 1999; 14: 988-93.

76. Boyle DA, Ludden TM, Carter BL, Becker AJ, Taylor JW. Evaluation of a Bayesian regression program for predicting warfarin response. Therapeutic Drug Monitoring 1989; 11: 276-84.
77. Pitsiu M, Parker EM, Aarons L, Rowland M. A Bayesian method based on clotting factor activity for the prediction of maintenance warfarin dosage regimens. Therapeutic Drug Monitoring 2003; 25: 36-40.
78. Svec JM, Coleman RW, Mungall DR, Ludden TM. Bayesian pharmacokinetic/pharmacodynamic forecasting of prothrombin response to warfarin therapy: Preliminary evaluation. Therapeutic Drug Monitoring 1985; 7: 174-80.
79. Vadher B, Patterson D, Leaning M. Prediction of the international normalized ratio and maintenance dose during the initiation of warfarin therapy. British journal of clinical pharmacology 1999; 48: 63.
80. White RH, Mungall D. Outpatient management of warfarin therapy: comparison of computer-predicted dosage adjustment to skilled professional care. Therapeutic Drug Monitoring 1991; 13: 46-50.
81. Friberg L, Hammar N, Ringh M, Pettersson H, Rosenqvist M. Stroke prophylaxis in atrial fibrillation: who gets it and who does not? Report from the Stockholm Cohort-study on Atrial Fibrillation (SCAF-study). European heart journal 2006; 27: 1954-64.
82. Pradhan AA, Levine MA. Warfarin use in atrial fibrillation: A random sample survey of family physician beliefs and preferences. The Canadian journal of clinical pharmacology = Journal canadien de pharmacologie clinique 2002; 9: 199-202.
83. Lind M, Fahlen M, Kosiborod M, Eliasson B, Oden A. Variability of INR and its relationship with mortality, stroke, bleeding and hospitalisations in patients with atrial fibrillation. Thrombosis research 2012; 129: 32-5.
84. Kimmel SE, French B, Kasner SE, Johnson JA, Anderson JL, Gage BF, et al. A Pharmacogenetic versus a Clinical Algorithm for Warfarin Dosing. New England Journal of Medicine 2013; 369: 2283-93.
85. Pirmohamed M, Burnside G, Eriksson N, Jorgensen AL, Toh CH, Nicholson T, et al. A randomized trial of genotype-guided dosing of warfarin. New England Journal of Medicine 2013; 369: 2294-303.
86. Rosendaal FR, Cannegieter SC, van der Meer FJ, Briet E. A method to determine the optimal intensity of oral anticoagulant therapy. Thrombosis and haemostasis 1993; 69: 236-9.
87. Gallego P, Roldan V, Marín F, Romera M, Valdés M, Vicente V, et al. Cessation of oral anticoagulation in relation to mortality and the risk of thrombotic events in patients with atrial fibrillation. Thrombosis and Haemostasis 2013; 110: 1189-98.
88. Sjögren V, Grzymala-Lubanski B, Renlund H, Friberg L, Lip GYH, Svensson PJ, et al. Safety and efficacy of well managed warfarin: A report from the Swedish quality register Auricula. Thrombosis and Haemostasis 2015; 113: 1370-77.
89. Wan Y, Heneghan C, Perera R, Roberts N, Hollowell J, Glasziou P, et al. Anticoagulation control and prediction of adverse events in patients with

atrial fibrillation: A systematic review. Circulation: Cardiovascular Quality and Outcomes 2008; 1: 84-91.
90. Connolly SJ, Pogue J, Eikelboom J, Flaker G, Commerford P, Franzosi MG, et al. Benefit of oral anticoagulant over antiplatelet therapy in atrial fibrillation depends on the quality of international normalized ratio control achieved by centers and countries as measured by time in therapeutic range. Circulation 2008; 118: 2029-37.
91. Veeger NJ, Piersma-Wichers M, Tijssen JG, Hillege HL, van der Meer J. Individual time within target range in patients treated with vitamin K antagonists: main determinant of quality of anticoagulation and predictor of clinical outcome. A retrospective study of 2300 consecutive patients with venous thromboembolism. British journal of haematology 2005; 128: 513-9.
92. De Caterina R, Husted S, Wallentin L, Andreotti F, Arnesen H, Bachmann F, et al. Vitamin K antagonists in heart disease: Current status and perspectives (Section III): Position paper of the ESC working group on thrombosis - Task force on anticoagulants in heart disease. Thrombosis and Haemostasis 2013; 110: 1087-107.
93. Lader E, Martin N, Cohen G, Meyer M, Reiter P, Dimova A, et al. Warfarin therapeutic monitoring: Is 70% time in the therapeutic range the best we can do? Journal of Clinical Pharmacy and Therapeutics 2012; 37: 375-77.
94. Connolly SJ, Ezekowitz MD, Yusuf S, Eikelboom J, Oldgren J, Parekh A, et al. Dabigatran versus Warfarin in Patients with Atrial Fibrillation. New England Journal of Medicine 2009; 361: 1139-51.
95. Stangier J, Eriksson BI, Dahl OE, Ahnfelt L, Nehmiz G, Stahle H, et al. Pharmacokinetic profile of the oral direct thrombin inhibitor dabigatran etexilate in healthy volunteers and patients undergoing total hip replacement. Journal of Clinical Pharmacology 2005; 45: 555-63.
96. Shi J, Wang X, Nguyen JH, Bleske BE, Liang Y, Liu L, et al. Dabigatran etexilate activation is affected by the CES1 genetic polymorphism G143E (rs71647871) and gender. Biochemical Pharmacology 2016; 119: 76-84.
97. Imai T. Human Carboxylesterase Isozymes: Catalytic Properties and Rational Drug Design. Drug Metabolism and Pharmacokinetics 2006; 21: 173-85.
98. Laizure SC, Parker RB, Herring VL, Hu ZY. Identification of carboxylesterase-dependent dabigatran etexilate hydrolysis. Drug Metabolism and Disposition 2014; 42: 201-06.
99. Paré G, Eriksson N, Lehr T, Connolly S, Eikelboom J, Ezekowitz MD, et al. Genetic determinants of dabigatran plasma levels and their relation to bleeding. Circulation 2013; 127: 1404-12.
100. Blech S, Ebner T, Ludwig-Schwellinger E, Stangier J, Roth W. The metabolism and disposition of the oral direct thrombin inhibitor, dabigatran, in humans. Drug Metabolism and Disposition 2008; 36: 386-99.
101. Stangier J, Rathgen K, Stahle H, Mazur D. Influence of renal impairment on the pharmacokinetics and pharmacodynamics of oral dabigatran etexilate: an open-label, parallel-group, single-centre study. Clinical Pharmacokinetics 2010; 49: 259-68.

102. Hauel NH, Nar H, Priepke H, Ries U, Stassen JM, Wienen W. Structure-based design of novel potent nonpeptide thrombin inhibitors. Journal of medicinal chemistry 2002; 45: 1757-66.
103. Ebner T, Wagner K, Wienen W. Dabigatran acylglucuronide, the major human metabolite of dabigatran: In vitro formation, stability, and pharmacological activity. Drug Metabolism and Disposition 2010; 38: 1567-75.
104. Hankey GJ, Eikelboom JW. Dabigatran etexilate: a new oral thrombin inhibitor. Circulation 2011; 123: 1436-50.
105. ten Cate H. Monitoring new oral anticoagulants, managing thrombosis, or both? Thrombosis and Haemostasis 2012; 107: 803-05.
106. Antovic JP, Skeppholm M, Eintrei J, Boija EE, Soderblom L, Norberg EM, et al. Evaluation of coagulation assays versus LC-MS/MS for determinations of dabigatran concentrations in plasma. European journal of clinical pharmacology 2013; 69: 1875-81.
107. Douxfils J, Mullier F, Robert S, Chatelain C, Chatelain B, Dogne JM. Impact of dabigatran on a large panel of routine or specific coagulation assays. Laboratory recommendations for monitoring of dabigatran etexilate. Thrombosis and haemostasis 2012; 107: 985-97.
108. Douxfils J, Dogne JM, Mullier F, Chatelain B, Ronquist-Nii Y, Malmstrom RE, et al. Comparison of calibrated dilute thrombin time and aPTT tests with LC-MS/MS for the therapeutic monitoring of patients treated with dabigatran etexilate. Thromb Haemost 2013; 110: 543-9.
109. Chin PK, Patterson DM, Zhang M, Jensen BP, Wright DF, Barclay ML, et al. Coagulation assays and plasma fibrinogen concentrations in real-world patients with atrial fibrillation treated with dabigatran. British journal of clinical pharmacology 2014; 78: 630-8.
110. van Ryn J, Stangier J, Haertter S, Liesenfeld KH, Wienen W, Feuring M, et al. Dabigatran etexilate--a novel, reversible, oral direct thrombin inhibitor: interpretation of coagulation assays and reversal of anticoagulant activity. Thrombosis and haemostasis 2010; 103: 1116-27.
111. Stangier J, Rathgen K, Stahle H, Gansser D, Roth W. The pharmacokinetics, pharmacodynamics and tolerability of dabigatran etexilate, a new oral direct thrombin inhibitor, in healthy male subjects. British Journal of Clinical Pharmacology 2007; 64: 292-303.
112. Douxfils J, Mani H, Minet V, Devalet B, Chatelain B, Dogne JM, et al. Non-VKA Oral Anticoagulants: Accurate Measurement of Plasma Drug Concentrations. BioMed research international 2015; 2015: 345138.
113. Stangier J. Clinical pharmacokinetics and pharmacodynamics of the oral direct thrombin inhibitor dabigatran etexilate. Clinical Pharmacokinetics 2008; 47: 285-95.
114. Hawes EM, Deal AM, Funk-Adcock D, Gosselin R, Jeanneret C, Cook AM, et al. Performance of coagulation tests in patients on therapeutic doses of dabigatran: a cross-sectional pharmacodynamic study based on peak and trough plasma levels. Journal of thrombosis and haemostasis : JTH 2013; 11: 1493-502.

115. Hapgood G, Butler J, Malan E, Chunilal S, Tran H. The effect of dabigatran on the activated partial thromboplastin time and thrombin time as determined by the Hemoclot thrombin inhibitor assay in patient plasma samples. Thrombosis and haemostasis 2013; 110: 308-15.
116. Chin PKL, Wright DFB, Patterson DM, Doogue MP, Begg EJ. A proposal for dose-adjustment of dabigatran etexilate in atrial fibrillation guided by thrombin time. British Journal of Clinical Pharmacology 2014; 78: 599-609.
117. Nowak G. The ecarin clotting time, a universal method to quantify direct thrombin inhibitors. Pathophysiology of haemostasis and thrombosis 2003; 33: 173-83.
118. Eikelboom JW, Connolly SJ, Hart RG, Wallentin L, Reilly P, Oldgren J, et al. Balancing the benefits and risks of 2 doses of dabigatran compared with warfarin in atrial fibrillation. Journal of the American College of Cardiology 2013; 62: 900-8.
119. European_Medical_Agency. Pradaxa: European public assessment report - Summary for the public, http://www.ema.europa.eu/docs/en_GB/document_library/EPAR_-_Summary_for_the_public/human/000829/WC500041060.pdf Accessed: 15 June 2017. In, 2013.
120. Chin PKL, Vella-Brincat JWA, Barclay ML, Begg EJ. Perspective on dabigatran etexilate dosing: why not follow standard pharmacological principles? British Journal of Clinical Pharmacology 2012; 74: 734-40.
121. Al-Sallami HS, Cheah SL, Han SY, Liew J, Lim J, Ng MA, et al. Between-subject variability: should high be the new normal? European journal of clinical pharmacology 2014; 70: 1403-4.
122. Eriksson BI, Dahl OE, Buller HR, Hettiarachchi R, Rosencher N, Bravo ML, et al. A new oral direct thrombin inhibitor, dabigatran etexilate, compared with enoxaparin for prevention of thromboembolic events following total hip or knee replacement: the BISTRO II randomized trial. Journal of thrombosis and haemostasis : JTH 2005; 3: 103-11.
123. Cohen D. Dabigatran: How the drug company withheld important analyses. BMJ (Online) 2014; 349.
124. Moore TJ, Cohen MR, Mattison DR. Dabigatran, bleeding, and the regulators. BMJ : British Medical Journal 2014; 349.
125. Eikelboom JW, Wallentin L, Connolly SJ, Ezekowitz M, Healey JS, Oldgren J, et al. Risk of bleeding with 2 doses of dabigatran compared with warfarin in older and younger patients with atrial fibrillation: an analysis of the randomized evaluation of long-term anticoagulant therapy (RE-LY) trial. Circulation 2011; 123: 2363-72.
126. Srinivasan K, Nouri P, Kavetskaia O. Challenges in the indirect quantitation of acyl-glucuronide metabolites of a cardiovascular drug from complex biological mixtures in the absence of reference standards. Biomedical chromatography : BMC 2010; 24: 759-67.
127. Boehringer Ingelheim Pharma GmbH & Co. KG. Pradaxa. Summary of Product Characteristics. In: European Medicines Agency.

128. Beasley BN, Unger EF, Temple R. Anticoagulant options--why the FDA approved a higher but not a lower dose of dabigatran. The New England journal of medicine 2011; 364: 1788-90.
129. US Food and Drug Administration. Application Number: 22-512, Summary Review. In, 2010.
130. Chiquette E, Amato MG, Bussey HI. Comparison of an anticoagulation clinic with usual medical care: Anticoagulation control, patient outcomes, and health care costs. Archives of Internal Medicine 1998; 158: 1641-47.
131. Matchar DB, Jacobson A, Dolor R, Edson R, Uyeda L, Phibbs CS, et al. Effect of home testing of international normalized ratio on clinical events. New England Journal of Medicine 2010; 363: 1608-20.
132. van Walraven C, Jennings A, Oake N, Fergusson D, Forster AJ. Effect of study setting on anticoagulation control: A systematic review and metaregression. Chest 2006; 129: 1155-66.
133. Witt DM, Sadler MA, Shanahan RL, Mazzoli G, Tillman DJ. Effect of a centralized clinical pharmacy anticoagulation service on the outcomes of anticoagulation therapy. Chest 2005; 127: 1515-22.
134. White RH, Hong R, Venook AP, Daschbach MM, Murray W, Mungall DR, et al. Initiation of warfarin therapy: comparison of physician dosing with computer-assisted dosing. Journal of general internal medicine 1987; 2: 141-8.
135. Harper P, Harper J, Hill C. An audit of anticoagulant management to assess anticoagulant control using decision support software. BMJ Open 2014; 4: e005864.
136. Hamberg AK, Hellman J, Dahlberg J, Jonsson EN, Wadelius M. A Bayesian decision support tool for efficient dose individualization of warfarin in adults and children. BMC Medical Informatics and Decision Making 2015; 15.
137. Black L, Wright DFB, Thomson AH, MacTavish P, Tait C, McIntosh T. Bayesian forecasting: can TCIWorks accurately predict INR response to warfarin dosing? . In: The UK Clinical Pharmacy Association National Conference, Manchester, UK, 2014.
138. Lund K, Gaffney D, Spooner R, Etherington AM, Tansey P, Tait RC. Polymorphisms in VKORC1 have more impact than CYP2C9 polymorphisms on early warfarin International Normalized Ratio control and bleeding rates. British Journal of Haematology 2012; 158: 256-61.
139. Finkelman BS, Gage BF, Johnson JA, Brensinger CM, Kimmel SE. Genetic warfarin dosing: tables versus algorithms. Journal of the American College of Cardiology 2011; 57: 612-8.
140. Tait RC, Sefcick A. A warfarin induction regimen for out-patient anticoagulation in patients with atrial fibrillation. British Journal of Haematology 1998; 101: 450-54.
141. Fennerty A, Dolben J, Thomas P, Backhouse G, Bentley DP, Campbell IA, et al. Flexible induction dose regimen for warfarin and prediction of maintenance dose. British medical journal (Clinical research ed) 1984; 288: 1268-70.

142. Borenstein M, Hedges LV, Higgins JPT, Rothstein HR. Introduction to Meta-Analysis. United Kingdon: Wiley, 2009.
143. Sconce EA, Khan TI, Wynne HA, Avery P, Monkhouse L, King BP, et al. The impact of CYP2C9 and VKORC1 genetic polymorphism and patient characteristics upon warfarin dose requirements: Proposal for a new dosing regimen. Blood 2005; 106: 2329-33.
144. Nieuwlaat R, Hubers LM, Spyropoulos AC, Eikelboom JW, Connolly BJ, Van Spall HG, et al. Randomised comparison of a simple warfarin dosing algorithm versus a computerised anticoagulation management system for control of warfarin maintenance therapy. Thrombosis and haemostasis 2012; 108: 1228-35.
145. Anderson JL, Horne BD, Stevens SM, Grove AS, Barton S, Nicholas ZP, et al. Randomized trial of genotype-guided versus standard warfarin dosing in patients initiating oral anticoagulation. Circulation 2007; 116: 2563-70.
146. Burmester JK, Berg RL, Yale SH, Rottscheit CM, Glurich IE, Schmelzer JR, et al. A randomized controlled trial of genotype-based Coumadin initiation. Genet Med 2011; 13: 509-18.
147. Caraco Y, Blotnick S, Muszkat M. CYP2C9 genotype-guided warfarin prescribing enhances the efficacy and safety of anticoagulation: A prospective randomized controlled study. Clinical Pharmacology and Therapeutics 2008; 83: 460-70.
148. Hillman MA, Wilke RA, Yale SH, Vidaillet HJ, Caldwell MD, Glurich I, et al. A prospective, randomized pilot trial of model-based warfarin dose initiation using CYP2C9 genotype and clinical data. Clinical medicine & research 2005; 3: 137-45.
149. Jonas DE, Evans JP, McLeod HL, Brode S, Lange LA, Young ML, et al. Impact of genotype-guided dosing on anticoagulation visits for adults starting warfarin: a randomized controlled trial. Pharmacogenomics 2013; 14: 1593-603.
150. Kimmel SE. Warfarin therapy: in need of improvement after all these years. Expert Opinion on Pharmacotherapy 2008; 9: 677-86.
151. Landefeld CS, Goldman L. Major bleeding in outpatients treated with warfarin: incidence and prediction by factors known at the start of outpatient therapy. The American journal of medicine 1989; 87: 144-52.
152. Marin-Leblanc M, Perreault S, Bahroun I, Lapointe M, Mongrain I, Provost S, et al. Validation of warfarin pharmacogenetic algorithms in clinical practice. Pharmacogenomics 2012; 13: 21-29.
153. Peng Q, Huang S, Chen X, Yuan Y, Yu Y, Tao L, et al. Validation of warfarin pharmacogenetic algorithms in 586 Han Chinese patients. Pharmacogenomics 2015; 16: 1465-74.
154. Li X, Liu R, Luo ZY, Yan H, Huang WH, Yin JY, et al. Comparison of the predictive abilities of pharmacogenetics-based warfarin dosing algorithms using seven mathematical models in Chinese patients. Pharmacogenomics 2015; 16: 583-90.
155. Doke J. Grabit. Matlab Central http://www mathworks com/matlabcentral/fileexchange/7173 accessed 18/04/2016.

156. Yan Z, Caldwell GW, Jones WJ, Masucci JA. Cone voltage induced in-source dissociation of glucuronides in electrospray and implications in biological analyses. Rapid communications in mass spectrometry : RCM 2003; 17: 1433-42.
157. Higgins JP, Thompson SG. Quantifying heterogeneity in a meta-analysis. Statistics in medicine 2002; 21: 1539-58.
158. Higgins JPT, Thompson SG, Deeks JJ, Altman DG. Measuring inconsistency in meta-analyses. BMJ 2003; 327: 557-60.
159. Botton MR, Bandinelli E, Rohde LE, Amon LC, Hutz MH. Influence of genetic, biological and pharmacological factors on warfarin dose in a Southern Brazilian population of European ancestry. British journal of clinical pharmacology 2011; 72: 442-50.
160. Doi SA. Pharmacodynamic optimization of warfarin therapy II. American journal of therapeutics 2001; 8: 41-7.
161. Ekladious SMM, Issac MSM, Sharaf SAE-A, Abou-Youssef HS. Validation of a Proposed Warfarin Dosing Algorithm Based on the Genetic Make-Up of Egyptian Patients. Molecular diagnosis & therapy 2013; 17: 381-90.
162. Gong IY, Tirona RG, Schwarz UI, Crown N, Dresser GK, LaRue S, et al. Prospective evaluation of a pharmacogenetics-guided warfarin loading and maintenance dose regimen for initiation of therapy. Blood 2011; 118: 3163-71.
163. Lazo-Langner A, Monkman K, Kovacs MJ. Predicting warfarin maintenance dose in patients with venous thromboembolism based on the response to a standardized warfarin initiation nomogram. Journal of Thrombosis and Haemostasis 2009; 7: 1276-83.
164. Le Gal G, Carrier M, Tierney S, Majeed H, Rodger M, Wells PS. Prediction of the warfarin maintenance dose after completion of the 10 mg initiation nomogram: do we really need genotyping? Journal of Thrombosis and Haemostasis 2010; 8: 90-94.
165. Lenzini PA, Grice GR, Milligan PE, Dowd MB, Subherwal S, Deych E, et al. Laboratory and clinical outcomes of pharmacogenetic vs. clinical protocols for warfarin initiation in orthopedic patients. Journal of thrombosis and haemostasis 2008; 6: 1655-62.
166. Michaud V, Vanier MC, Brouillette D, Roy D, Verret L, Noel N, et al. Combination of phenotype assessments and CYP2C9-VKORC1 polymorphisms in the determination of warfarin dose requirements in heavily medicated patients. Clinical Pharmacology and Therapeutics 2008; 83: 740-48.
167. Pavani A, Naushad SM, Rupasree Y, Kumar TR, Malempati AR, Pinjala RK, et al. Optimization of warfarin dose by population-specific pharmacogenomic algorithm. The Pharmacogenomics Journal 2012; 12: 306-11.
168. Perini JA, Struchiner CJ, Silva-Assuncao E, Suarez-Kurtz G. Impact of CYP4F2 rs2108622 on the stable warfarin dose in an admixed patient cohort. Clinical pharmacology and therapeutics 2010; 87: 417-20.

169. Roper N, Storer B, Bona R, Fang M. Validation and comparison of pharmacogenetics-based warfarin dosing algorithms for application of pharmacogenetic testing. The Journal of molecular diagnostics : JMD 2010; 12: 283-91.
170. Santos PC, Marcatto LR, Duarte NE, Gadi Soares RA, Cassaro Strunz CM, Scanavacca M, et al. Development of a pharmacogenetic-based warfarin dosing algorithm and its performance in Brazilian patients: highlighting the importance of population-specific calibration. Pharmacogenomics 2015; 16: 865-76.
171. Schelleman H, Chen J, Chen Z, Christie J, Newcomb CW, Brensinger CM, et al. Dosing algorithms to predict warfarin maintenance dose in Caucasians and African Americans. Clinical pharmacology and therapeutics 2008; 84: 332-9.
172. Suriapranata IM, Tjong WY, Wang T, Utama A, Raharjo SB, Yuniadi Y, et al. Genetic factors associated with patient-specific warfarin dose in ethnic Indonesians. BMC medical genetics 2011; 12: 80.
173. Takahashi H, Wilkinson GR, Nutescu EA, Morita T, Ritchie MD, Scordo MG, et al. Different contributions of polymorphisms in VKORC1 and CYP2C9 to intra- and inter-population differences in maintenance dose of warfarin in Japanese, Caucasians and African-Americans. Pharmacogenetics and Genomics 2006; 16: 101-10.
174. Voora D, Koboldt DC, King CR, Lenzini PA, Eby CS, Porche-Sorbet R, et al. A polymorphism in the VKORC1 regulator calumenin predicts higher warfarin dose requirements in African Americans. Clin Pharmacol Ther 2010; 87: 445-51.
175. Wei M, Ye F, Xie D, Zhu Y, Zhu J, Tao Y, et al. A new algorithm to predict warfarin dose from polymorphisms of CYP4F2 , CYP2C9 and VKORC1 and clinical variables: derivation in Han Chinese patients with non valvular atrial fibrillation. Thromb Haemost 2012; 107: 1083-91.
176. Wells PS, Majeed H, Kassem S, Langlois N, Gin B, Clermont J, et al. A regression model to predict warfarin dose from clinical variables and polymorphisms in CYP2C9, CYP4F2, and VKORC1: Derivation in a sample with predominantly a history of venous thromboembolism. Thromb Res 2010; 125: e259-64.
177. Yoshizawa M, Hayashi H, Tashiro Y, Sakawa S, Moriwaki H, Akimoto T, et al. Effect of VKORC1 - 1639 G > A polymorphism, body weight, age, and serum albumin alterations on warfarin response in Japanese patients. Thrombosis Research 2009; 124: 161-66.
178. Zhu Y, Shennan M, Reynolds KK, Johnson NA, Herrnberger MR, Valdes Jr R, et al. Estimation of warfarin maintenance dose based on VKORC1 (-1639 G>A) and CYP2C9 genotypes. Clinical Chemistry 2007; 53: 1199-205.
179. Saleh MI, Alzubiedi S. Dosage Individualization of Warfarin Using Artificial Neural Networks. Molecular Diagnosis & Therapy 2014; 18: 371-9.

180. Haug KB, Sharikabad MN, Kringen MK, Narum S, Sjaatil ST, Johansen PW, et al. Warfarin dose and INR related to genotypes of CYP2C9 and VKORC1 in patients with myocardial infarction. Thrombosis journal 2008; 6: 7.
181. Harada T, Ariyoshi N, Shimura H, Sato Y, Yokoyama I, Takahashi K, et al. Application of Akaike information criterion to evaluate warfarin dosing algorithm. Thrombosis Research 2010; 126: 183-90.
182. Huang SW, Chen HS, Wang XQ, Huang L, Xu DL, Hu XJ, et al. Validation of VKORCI and CYP2C9 genotypes on interindividual warfarin maintenance dose: A prospective study in Chinese patients. Pharmacogenetics and Genomics 2009; 19: 226-34.
183. Wang M, Lang X, Cui S, Fei K, Zou L, Cao J, et al. Clinical application of pharmacogenetic-based warfarin-dosing algorithm in patients of Han nationality after rheumatic valve replacement: a randomized and controlled trial. International Journal of Medical Sciences 2012; 9: 472-9.
184. Kim HS, Lee SS, Oh M, Jang YJ, Kim EY, Han IY, et al. Effect of CYP2C9 and VKORC1 genotypes on early-phase and steady-state warfarin dosing in Korean patients with mechanical heart valve replacement. Pharmacogenetics and Genomics 2009; 19: 103-12.
185. Lu Y, Yang J, Zhang H, Yang J. Prediction of Warfarin Maintenance Dose in Han Chinese Patients Using a Mechanistic Model Based on Genetic and Non-Genetic Factors. Clinical Pharmacokinetics 2013; 52: 567-81.
186. Zhang H, Xue L, Qi C, et a. Effect of gene and clinical factors on the dose of warfarin [in Chinese]. China Pharmacy 2010; 21: 2049–52.
187. Tan SL, Li Z, Song GB, Liu LM, Zhang W, Peng J, et al. Development and comparison of a new personalized warfarin stable dose prediction algorithm in Chinese patients undergoing heart valve replacement. Die Pharmazie 2012; 67: 930-7.
188. Sasaki T, Tabuchi H, Higuchi S, Ieiri I. Warfarin-dosing algorithm based on a population pharmacokinetic/pharmacodynamic model combined with Bayesian forecasting. Pharmacogenomics 2009; 10: 1257-66.
189. Lei X, Guo Y, Sun J, Zhou H, Liu Y, Liang P, et al. Accuracy assessment of pharmacogenetic algorithms for warfarin dose prediction in Chinese patients. American Journal of Hematology 2012; 87: 541-44.
190. Wadelius M, Chen LY, Lindh JD, Eriksson N, Ghori MJR, Bumpstead S, et al. The largest prospective warfarin-treated cohort supports genetic forecasting. Blood 2009; 113: 784-92.
191. Solomon I, Maharshak N, Chechik G, Leibovici L, Lubetsky A, Halkin H, et al. Applying an artificial neural network to warfarin maintenance dose prediction. The Israel Medical Association journal : IMAJ 2004; 6: 732-5.
192. Pathare A, Al Khabori M, Alkindi S, Al Zadjali S, Misquith R, Khan H, et al. Warfarin pharmacogenetics: development of a dosing algorithm for Omani patients. J Hum Genet 2012; 57: 665-9.
193. Wu AHB, Wang P, Smith A, Haller C, Drake K, Linder M, et al. Dosing algorithm for warfarin using CYP2C9 and VKORC1 genotyping from a multi-ethnic population: Comparison with other equations. Pharmacogenomics 2008; 9: 169-78.

194. Francis B, Lane S, Pirmohamed M, Jorgensen A. A review of a priori regression models for warfarin maintenance dose prediction. PLoS One 2014; 9: e114896.
195. Hatch E, Wynne H, Avery P, Wadelius M, Kamali F. Application of a pharmacogenetic-based warfarin dosing algorithm derived from British patients to predict dose in Swedish patients. Journal of Thrombosis & Haemostasis 2008; 6: 1038-40.
196. Langley MR, Booker JK, Evans JP, McLeod HL, Weck KE. Validation of Clinical Testing for Warfarin Sensitivity: Comparison of CYP2C9-VKORC1 Genotyping Assays and Warfarin-Dosing Algorithms. The Journal of molecular diagnostics : JMD 2009; 11: 216-25.
197. Linder MW, Homme MB, Reynolds KK, Gage BF, Eby C, Silvestrov N, et al. Interactive Modeling for Ongoing Utility of Pharmacogenetic Diagnostic Testing: Application for Warfarin Therapy. Clinical chemistry 2009; 55: 1861-68.
198. CORRIGENDUM: Editorial. Clinical Pharmacology & Therapeutics 2008; 84: 430-30.
199. Shaw PB, Donovan JL, Tran MT, Lemon SC, Burgwinkle P, Gore J. Accuracy assessment of pharmacogenetically predictive warfarin dosing algorithms in patients of an academic medical center anticoagulation clinic. Journal of thrombosis and thrombolysis 2010; 30: 220-5.
200. Holford NHG, Sheiner LB. Understanding the dose-effect relationship: Clinical application of pharmacokinetic-pharmacodynamic models. Clinical Pharmacokinetics 1981; 6: 429-53.
201. Cosgun E, Limdi NA, Duarte CW. High-dimensional pharmacogenetic prediction of a continuous trait using machine learning techniques with application to warfarin dose prediction in African Americans. Bioinformatics 2011; 27: 1384-89.
202. Liu KE, Lo CL, Hu YH. Improvement of adequate use of warfarin for the elderly using decision tree-based approaches. Methods of Information in Medicine 2014; 53: 47-53.
203. Grossi E, Podda GM, Pugliano M, Gabba S, Verri A, Carpani G, et al. Prediction of optimal warfarin maintenance dose using advanced artificial neural networks. Pharmacogenomics 2014; 15: 29-37.
204. Cleveland WS. Robust Locally Weighted Regression and Smoothing Scatterplots. Journal of the American Statistical Association 1979; 74: 829-36.
205. Cleveland W. [LOWESS]: [A] [P]rogram for [S]moothing [S]catterplots by [R]obust [L]ocally [W]eighted [R]egression. The American Statistician 1981; 35.
206. Bland JM, Altman DG. Statistical methods for assessing agreement between two methods of clinical measurement. Lancet 1986; 1: 307-10.
207. Bland JM, Altman DG. Measuring agreement in method comparison studies. Statistical methods in medical research 1999; 8: 135-60.
208. Horng H, Spahn-Langguth H, Benet LZ. Mechanistic role of acyl glucuronides. In: Drug-Induced Liver Disease, 2013: 35-70.

209. Regan SL, Maggs JL, Hammond TG, Lambert C, Williams DP, Park BK. Acyl glucuronides: The good, the bad and the ugly. Biopharmaceutics and Drug Disposition 2010; 31: 367-95.
210. Stachulski AV. Chemistry and reactivity of acyl glucuronides. Current drug metabolism 2011; 12: 215-21.
211. Stachulski AV, Harding JR, Lindon JC, Maggs JL, Park BK, Wilson ID. Acyl glucuronides: Biological activity, chemical reactivity, and chemical synthesis. Journal of Medicinal Chemistry 2006; 49: 6931-45.
212. Dickinson RG, King AR. Studies on the reactivity of acyl glucuronides--II. Interaction of diflunisal acyl glucuronide and its isomers with human serum albumin in vitro. Biochemical pharmacology 1991; 42: 2301-6.
213. Spahn-Langguth H, Benet LZ. Acyl glucuronides revisited: is the glucuronidation process a toxification as well as a detoxification mechanism? Drug metabolism reviews 1992; 24: 5-47.
214. Eggers NJ, Doust K. Isolation and identification of probenecid acyl glucuronide. The Journal of pharmacy and pharmacology 1981; 33: 123-4.
215. Smith PC, Benet LZ. Characterization of the isomeric esters of zomepirac glucuronide by proton NMR. Drug metabolism and disposition: the biological fate of chemicals 1986; 14: 503-5.
216. Hansen-Møller J, Cornett C, Dalgaard L, Hansen SH. Isolation and identification of the rearrangement products of diflunisal 1-O-acyl glucuronide. Journal of Pharmaceutical and Biomedical Analysis 1988; 6: 229-40.
217. Xue YJ, Akinsanya JB, Raghavan N, Zhang D. Optimization to eliminate the interference of migration isomers for measuring 1-O-β-acyl glucuronide without extensive chromatographic separation. Rapid Communications in Mass Spectrometry 2008; 22: 109-20.
218. Faed EM. Properties of Acyl Glucuronides: Implications for Studies of the Pharmacokinetics and Metabolism of Acidic Drugs. Drug Metabolism Reviews 1984; 15: 1213-49.
219. Spahn-Langguth H, Dahms M, Hermening A. Acyl glucuronides: covalent binding and its potential relevance. Advances in experimental medicine and biology 1996; 387: 313-28.
220. Bailey MJ, Dickinson RG. Acyl glucuronide reactivity in perspective: Biological consequences. Chemico-Biological Interactions 2003; 145: 117-37.
221. Shipkova M, Armstrong VW, Oellerich M, Wieland E. Acyl glucuronide drug metabolites: Toxicological and analytical implications. Therapeutic Drug Monitoring 2003; 25: 1-16.
222. Schwartz MS, Desai RB, Bi S, Miller AR, Matuszewski BK. Determination of a prostaglandin D2 antagonist and its acyl glucuronide metabolite in human plasma by high performance liquid chromatography with tandem mass spectrometric detection--a lack of MS/MS selectivity between a glucuronide conjugate and a phase I metabolite. Journal of chromatography B, Analytical technologies in the biomedical and life sciences 2006; 837: 116-24.

223. Hermening A, Grafe AK, Baktir G, Mutschler E, Spahn-Langguth H. Gemfibrozil and its oxidative metabolites: quantification of aglycones, acyl glucuronides, and covalent adducts in samples from preclinical and clinical kinetic studies. Journal of chromatography B, Biomedical sciences and applications 2000; 741: 129-44.
224. Gous T, Couchman L, Patel JP, Paradzai C, Arya R, Flanagan RJ. Measurement of the direct oral anticoagulants apixaban, dabigatran, edoxaban, and rivaroxaban in human plasma using turbulent flow liquid chromatography with high-resolution mass spectrometry. Therapeutic Drug Monitoring 2014.
225. Delavenne X, Moracchini J, Laporte S, Mismetti P, Basset T. UPLC MS/MS assay for routine quantification of dabigatran - A direct thrombin inhibitor - In human plasma. Journal of Pharmaceutical and Biomedical Analysis 2012; 58: 152-56.
226. Korostelev M, Bihan K, Ferreol L, Tissot N, Hulot J-S, Funck-Brentano C, et al. Simultaneous determination of rivaroxaban and dabigatran levels in human plasma by high-performance liquid chromatography-tandem mass spectrometry. Journal of Pharmaceutical and Biomedical Analysis 2014.
227. Côté C, Lahaie M, Latour S, Bergeron M, Dicaire C, Savoie N, et al. Impact of methylation of acyl glucuronide metabolites on incurred sample reanalysis evaluation: ramiprilat case study. Bioanalysis 2011; 3: 951-65.
228. Silvestro L, Gheorghe M, Iordachescu A, Ciuca V, Tudoroniu A, Rizea Savu S, et al. Development and validation of an HPLC-MS/MS method to quantify clopidogrel acyl glucuronide, clopidogrel acid metabolite, and clopidogrel in plasma samples avoiding analyte back-conversion. Analytical and Bioanalytical Chemistry 2011; 401: 1023-34.
229. Andersen JV, Hansen SH. Simultaneous quantitative determination of naproxen, its metabolite 6-O-desmethylnaproxen and their five conjugates in plasma and urine samples by high-performance liquid chromatography on dynamically modified silica. Journal of chromatography 1992; 577: 325-33.
230. Khan S, Teitz DS, Jemal M. Kinetic Analysis by HPLC−Electrospray Mass Spectrometry of the pH-Dependent Acyl Migration and Solvolysis as the Decomposition Pathways of Ifetroban 1-O-Acyl Glucuronide. Analytical Chemistry 1998; 70: 1622-28.
231. Xue YJ, Simmons NJ, Liu J, Unger SE, Anderson DF, Jenkins RG. Separation of a BMS drug candidate and acyl glucuronide from seven glucuronide positional isomers in rat plasma via high-performance liquid chromatography with tandem mass spectrometric detection. Rapid communications in mass spectrometry : RCM 2006; 20: 1776-86.
232. Corcoran O, Mortensen RW, Hansen SH, Troke J, Nicholson JK. HPLC/1H NMR spectroscopic studies of the reactive alpha-1-O-acyl isomer formed during acyl migration of S-naproxen beta-1-O-acyl glucuronide. Chemical research in toxicology 2001; 14: 1363-70.
233. Farrant RD, Spraul M, Wilson ID, Nicholls AW, Nicholson JK, Lindon JC. Assignment of the 750 MHz 1H NMR resonances from a mixture of

transacylated ester glucuronic acid conjugates with the aid of oversampling and digital filtering during acquisition. Journal of pharmaceutical and biomedical analysis 1995; 13: 971-7.
234. Mortensen RW, Corcoran O, Cornett C, Sidelmann UG, Lindon JC, Nicholson JK, et al. S-naproxen-beta-1-O-acyl glucuronide degradation kinetic studies by stopped-flow high-performance liquid chromatography-1H NMR and high-performance liquid chromatography-UV. Drug metabolism and disposition: the biological fate of chemicals 2001; 29: 375-80.
235. Sidelmann UG, Lenz EM, Spraul M, Hofmann M, Troke J, Sanderson PN, et al. 750 MHz HPLC-NMR spectroscopic studies on the separation and characterization of the positional isomers of the glucuronides of 6,11-dihydro-11-oxodibenz[b,e]oxepin-2-acetic acid. Analytical chemistry 1996; 68: 106-10.
236. Lenz EM, Greatbanks D, Wilson ID, Spraul M, Hofmann M, Troke J, et al. Direct characterization of drug glucuronide isomers in human urine by HPLC-NMR spectroscopy: application to the positional isomers of 6,11-dihydro-11-oxodibenz[b,e]oxepin-2-acetic acid glucuronide. Analytical chemistry 1996; 68: 2832-7.
237. Ketola RA, Hakala KS. Direct analysis of glucuronides with liquid chromatography-mass spectrometric techniques and methods. Current drug metabolism 2010; 11: 561-82.
238. Liu DQ, Pereira T. Interference of a carbamoyl glucuronide metabolite in quantitative liquid chromatography/tandem mass spectrometry. Rapid communications in mass spectrometry : RCM 2002; 16: 142-6.
239. An G, Ruszaj DM, Morris ME. Interference of a sulfate conjugate in quantitative liquid chromatography/tandem mass spectrometry through in-source dissociation. Rapid communications in mass spectrometry : RCM 2010; 24: 1817-9.
240. Kadi AA, Hefnawy MM. Biological Fluids: Glucuronides from LC/MS. In: Encyclopedia of Chromatography, Third Edition: CRC Press, 2009: 203-09.
241. Wainhaus S. Acyl Glucuronides. In: Using Mass Spectrometry for Drug Metabolism Studies: CRC Press, 2004: 175-202.
242. Hartter S, Yamamura N, Stangier J, Reilly PA, Clemens A. Pharmacokinetics and pharmacodynamics in Japanese and Caucasian subjects after oral administration of dabigatran etexilate. Thrombosis and Haemostasis 2012; 107: 260-9.
243. Stangier J, Stähle H, Rathgen K, Roth W, Shakeri-Nejad K. Pharmacokinetics and pharmacodynamics of dabigatran etexilate, an oral direct thrombin inhibitor, are not affected by moderate hepatic impairment. Journal of Clinical Pharmacology 2008; 48: 1411-19.
244. Guidance for Industry, Bioanalytical Method Validation, US Department of Health and Human Services Food and Drug Administration, Center for Drug Evaluation and Research (CDER). 2001.
245. Schmitz EMH, Van Den Heuvel D, Boonen K, Van Dongen JLJ, Brunsveld L, Van De Kerkhof D. Determination of dabigatran, rivaroxaban and

apixaban using UPLC-MS/MS and comparison with coagulation assays for therapy monitoring. Nederlands Tijdschrift voor Klinische Chemie en Laboratoriumgeneeskunde 2013; 38: 142-44.
246. Stangier J, Stähle H, Rathgen K, Roth W, Reseski K, Körnicke T. Pharmacokinetics and pharmacodynamics of dabigatran etexilate, an oral direct thrombin inhibitor, with coadministration of digoxin. Journal of Clinical Pharmacology 2012; 52: 243-50.
247. Tan A, Jin W, Deng F, Hussain S, Musuku A, Massé R. Bioanalytical method development and validation using incurred samples-Simultaneous quantitation of ramipril and ramiprilat in human EDTA plasma by LC-MS/MS. Journal of Chromatography B: Analytical Technologies in the Biomedical and Life Sciences 2009; 877: 3673-80.
248. Stangier J, Rathgen K, Sthle H, Mazur D. Influence of renal impairment on the pharmacokinetics and pharmacodynamics of oral dabigatran etexilate: An open-label, parallel-group, single-centre study. Clinical Pharmacokinetics 2010; 49: 259-68.
249. Schmitz EMH, Boonen K, van den Heuvel DJA, van Dongen JLJ, Schellings MWM, Emmen JMA, et al. Determination of dabigatran, rivaroxaban and apixaban by ultra-performance liquid chromatography – tandem mass spectrometry (UPLC-MS/MS) and coagulation assays for therapy monitoring of novel direct oral anticoagulants. Journal of Thrombosis and Haemostasis 2014; 12: 1636-46.
250. Eisert WG, Hauel N, Stangier J, Wienen W, Clemens A, van Ryn J. Dabigatran: an oral novel potent reversible nonpeptide inhibitor of thrombin. Arteriosclerosis, thrombosis, and vascular biology 2010; 30: 1885-9.
251. Stangier J, Stahle H, Rathgen K, Fuhr R. Pharmacokinetics and pharmacodynamics of the direct oral thrombin inhibitor dabigatran in healthy elderly subjects. Clinical Pharmacokinetics 2008; 47: 47-59.
252. Stangier J, Clemens A. Pharmacology, pharmacokinetics, and pharmacodynamics of dabigatran etexilate, an oral direct thrombin inhibitor. Clinical and applied thrombosis/hemostasis : official journal of the International Academy of Clinical and Applied Thrombosis/Hemostasis 2009; 15 Suppl 1: 9S-16S.
253. Clemens A, Haertter S, Friedman J, Brueckmann M, Stangier J, van Ryn J, et al. Twice daily dosing of dabigatran for stroke prevention in atrial fibrillation: a pharmacokinetic justification. Current medical research and opinion 2012; 28: 195-201.
254. Chin PK, Vella-Brincat JW, Barclay ML, Begg EJ. Perspective on dabigatran etexilate dosing: why not follow standard pharmacological principles? British journal of clinical pharmacology 2012; 74: 734-40.
255. Powell JR. Are new oral anticoagulant dosing recommendations optimal for all patients? Jama 2015; 313: 1013-4.
256. Wright DF, Al-Sallami HS, Duffull SB. Is the dose of dabigatran really more predictable than warfarin? British journal of clinical pharmacology 2013; 76: 997-98.

257. Douxfils J, Mullier F, Dogné J-M. Dose tailoring of dabigatran etexilate: obvious or excessive? Expert Opinion on Drug Safety 2015; 14: 1283-89.
258. Chin PK. Which patients may benefit from dose adjustment of non-vitamin K antagonist oral anticoagulants? Seminars in thrombosis and hemostasis 2015; 41: 195-207.
259. Connolly SJ, Ezekowitz MD, Yusuf S, Reilly PA, Wallentin L. Newly Identified Events in the RE-LY Trial. New England Journal of Medicine 2010; 363: 1875-76.
260. Duffull SB, Wright DFB. What do we learn from repeated population analyses? British Journal of Clinical Pharmacology 2015; 79: 40-47.
261. Duffull SB, Wright DFB, Winter HR. Interpreting population pharmacokinetic-pharmacodynamic analyses - a clinical viewpoint. British Journal of Clinical Pharmacology 2011; 71: 807-14.
262. Hennig S, Norris R, Kirkpatrick CMJ. Target concentration intervention is needed for tobramycin dosing in paediatric patients with cystic fibrosis – a population pharmacokinetic study. British Journal of Clinical Pharmacology 2008; 65: 502-10.
263. Dansirikul C, Lehr T, Liesenfeld KH, Haertter S, Staab A. A combined pharmacometric analysis of dabigatran etexilate in healthy volunteers and patients with atrial fibrillation or undergoing orthopaedic surgery. Thrombosis and haemostasis 2012; 107: 775-85.
264. Liesenfeld KH, Lehr T, Dansirikul C, Reilly PA, Connolly SJ, Ezekowitz MD, et al. Population pharmacokinetic analysis of the oral thrombin inhibitor dabigatran etexilate in patients with non-valvular atrial fibrillation from the RE-LY trial. Journal of thrombosis and haemostasis : JTH 2011; 9: 2168-75.
265. Delavenne X, Ollier E, Basset T, Bertoletti L, Accassat S, Garcin A, et al. A semi-mechanistic absorption model to evaluate drug-drug interaction with dabigatran: application with clarithromycin. British journal of clinical pharmacology 2012.
266. Liesenfeld KH, Staab A, Härtter S, Formella S, Clemens A, Lehr T. Pharmacometric characterization of dabigatran hemodialysis. Clinical Pharmacokinetics 2013; 52: 453-62.
267. Troconiz IF, Tillmann C, Liesenfeld KH, Schafer HG, Stangier J. Population pharmacokinetic analysis of the new oral thrombin inhibitor dabigatran etexilate (BIBR 1048) in patients undergoing primary elective total hip replacement surgery. Journal of Clinical Pharmacology 2007; 47: 371-82.
268. Duffull SB, Aarons L. Development of a sequential linked pharmacokinetic and pharmacodynamic simulation model for ivabradine in healthy volunteers. European Journal of Pharmaceutical Sciences 2000; 10: 275-84.
269. Duffull SB, Chabaud S, Nony P, Laveille C, Girard P, Aarons L. A pharmacokinetic simulation model for ivabradine in healthy volunteers. European Journal of Pharmaceutical Sciences 2000; 10: 285-94.
270. Bloomfield C, Staatz CE, Unwin S, Hennig S. Assessing Predictive Performance of Published Population Pharmacokinetic Models of

Intravenous Tobramycin in Pediatric Patients. Antimicrobial agents and chemotherapy 2016; 60: 3407-14.
271. Zhao CY, Jiao Z, Mao JJ, Qiu XY. External evaluation of published population pharmacokinetic models of tacrolimus in adult renal transplant recipients. British journal of clinical pharmacology 2016; 81: 891-907.
272. Sherwin CM, Kiang TK, Spigarelli MG, Ensom MH. Fundamentals of population pharmacokinetic modelling: validation methods. Clinical pharmacokinetics 2012; 51: 573-90.
273. McDougall DA, Martin J, Playford EG, Green B. Determination of a suitable voriconazole pharmacokinetic model for personalised dosing. Journal of pharmacokinetics and pharmacodynamics 2016; 43: 165-77.
274. Eriksson BI, Dahl OE, Ahnfelt L, Kalebo P, Stangier J, Nehmiz G, et al. Dose escalating safety study of a new oral direct thrombin inhibitor, dabigatran etexilate, in patients undergoing total hip replacement: BISTRO I. Journal of thrombosis and haemostasis : JTH 2004; 2: 1573-80.
275. Nagashima R, O'Reilly RA, Levy G. Kinetics of pharmacologic effects in man: The anticoagulant action of warfarin. Clinical Pharmacology & Therapeutics 1969; 10: 22-35.
276. Sheiner LB. Computer-aided long-term anticoagulation therapy. Computers and biomedical research, an international journal 1969; 2: 507-18.
277. Xue L, Holford N, Ding X-l, Shen Z-y, Huang C-r, Zhang H, et al. Theory-based pharmacokinetics and pharmacodynamics of S- and R-warfarin and effects on international normalized ratio: influence of body size, composition and genotype in cardiac surgery patients. British Journal of Clinical Pharmacology 2017; 83: 823-35.
278. Chan E, McLachlan A, O'Reilly R, Rowland M. Stereochemical aspects of warfarin drug interactions: use of a combined pharmacokinetic-pharmacodynamic model. Clinical pharmacology and therapeutics 1994; 56: 286-94.
279. Saffian SM, Zhang M, Leong Chin PK, Jensen BP. Quantification of dabigatran and indirect quantification of dabigatran acylglucuronides in human plasma by LC-MS/MS. Bioanalysis 2015; 7: 957-66.
280. Kuhn J, Gripp T, Flieder T, Dittrich M, Hendig D, Busse J, et al. UPLC-MRM Mass Spectrometry Method for Measurement of the Coagulation Inhibitors Dabigatran and Rivaroxaban in Human Plasma and Its Comparison with Functional Assays. PloS one 2015; 10: e0145478.
281. Schmohl M, Gansser D, Moschetti V, Stangier J. Measurement of dabigatran plasma concentrations by calibrated thrombin clotting time in comparison to LC-MS/MS in human volunteers on dialysis. Thrombosis research 2015; 135: 532-6.
282. Baldelli S, Cattaneo D, Pignatelli P, Perrone V, Pastori D, Radice S, et al. Validation of an LC-MS/MS method for the simultaneous quantification of dabigatran, rivaroxaban and apixaban in human plasma. Bioanalysis 2016; 8: 275-83.

283. Schellings MWM, Boonen K, Schmitz EMH, Jonkers F, Van Den Heuvel DJ, Besselaar A, et al. Determination of dabigatran and rivaroxaban by ultra-performance liquid chromatography-tandem mass spectrometry and coagulation assays after major orthopaedic surgery. Thrombosis Research 2016; 139: 128-34.
284. Noguez JH, Ritchie JC. Quantitation of the Oral Anticoagulants Dabigatran, Rivaroxaban, Apixaban, and Warfarin in Plasma Using Ultra-Performance Liquid Chromatography with Tandem Mass Spectrometry (UPLC-MS/MS). Methods in molecular biology (Clifton, NJ) 2016; 1383: 21-7.
285. Karlsson MO, Lutsar I, Milligan PA. Population pharmacokinetic analysis of voriconazole plasma concentration data from pediatric studies. Antimicrobial agents and chemotherapy 2009; 53: 935-44.
286. Danhof M, de Jongh J, De Lange EC, Della Pasqua O, Ploeger BA, Voskuyl RA. Mechanism-based pharmacokinetic-pharmacodynamic modeling: biophase distribution, receptor theory, and dynamical systems analysis. Annual review of pharmacology and toxicology 2007; 47: 357-400.
287. Ooi QX, Wright DF, Tait RC, Isbister GK, Duffull SB. A Joint Model for Vitamin K-Dependent Clotting Factors and Anticoagulation Proteins. Clinical pharmacokinetics 2017.
288. Botton MR, Viola PP, Bandinelli E, Leiria TL, Rohde LE, Hutz MH. A new algorithm for weekly phenprocoumon dose variation in a southern Brazilian population: role for CYP2C9, CYP3A4/5 and VKORC1 genes polymorphisms. Basic & Clinical Pharmacology & Toxicology; 114: 323-9.
289. Good AC, Henz S. A clinical algorithm to predict the loading dose of phenprocoumon. Thrombosis Research; 120: 921-5.
290. Zhang Y, De Boer A, Verhoef TI, Van Der Meer FJM, Le Cessie S, Maitland-Van Der Zee AH, et al. Comparison of dosing algorithms for acenocoumarol and phenprocoumon using clinical factors with the standard care in the Netherlands. Thrombosis Research 2015; 136: 94-100.
291. Borobia AM, Lubomirov R, Ramirez E, Lorenzo A, Campos A, Munoz-Romo R, et al. An acenocoumarol dosing algorithm using clinical and pharmacogenetic data in Spanish patients with thromboembolic disease. PLoS ONE [Electronic Resource]; 7: e41360.
292. Cerezo-Manchado JJ, Rosafalco M, Anton AI, Perez-Andreu V, Garcia-Barbera N, Martinez AB, et al. Creating a genotype-based dosing algorithm for acenocoumarol steady dose. Thrombosis & Haemostasis; 109: 146-53.
293. Dimitrova-Karamfilova A, Tzveova R, Chilingirova N, Goranova T, Nachev G, Mitev V, et al. Acenocoumarol Pharmacogenetic Dosing Algorithms and Their Application in Two Bulgarian Patients with Low Anticoagulant Requirements. Biochemical Genetics; 53: 334-50.
294. Jimenez-Varo E, Canadas-Garre M, Garces-Robles V, Gutierrez-Pimentel MJ, Calleja-Hernandez MA. Extrapolation of acenocoumarol pharmacogenetic algorithms. Vascular Pharmacology; 74: 151-7.
295. Jimenez-Varo E, Canadas-Garre M, Gutierrez-Pimentel MJ, Calleja-Hernandez MA. Prediction of stable acenocoumarol dose by a pharmacogenetic algorithm. Pharmacogenetics and Genomics; 24: 501-13.

296. Krishna Kumar D, Shewade DG, Loriot MA, Beaune P, Sai Chandran BV, Balachander J, et al. An acenocoumarol dosing algorithm exploiting clinical and genetic factors in South Indian (Dravidian) population. European Journal of Clinical Pharmacology 2015; 71: 173-81.
297. Tong HY, Dávila-Fajardo CL, Borobia AM, Martínez-González LJ, Lubomirov R, León LMP, et al. A new pharmacogenetic algorithm to predict the most appropriate dosage of acenocoumarol for stable anticoagulation in a mixed Spanish population. PLoS ONE 2016; 11.
298. Chan NC, Coppens M, Hirsh J, Ginsberg JS, Weitz JI, Vanassche T, et al. Real-world variability in dabigatran levels in patients with atrial fibrillation. Journal of Thrombosis and Haemostasis 2015; 13: 353-59.
299. Pavani A, Naushad SM, Uma A, Kutala VK. Methodological issues in the development of a pharmacogenomic algorithm for warfarin dosing: comparison of two regression approaches. Pharmacogenomics 2014; 15: 7.
300. Khadzhynov D, Wagner F, Formella S, Wiegert E, Moschetti V, Slowinski T, et al. Effective elimination of dabigatran by haemodialysis. A phase I single-centre study in patients with end-stage renal disease. Thrombosis and haemostasis 2013; 109: 596-605.